EMERGING CONTAMINANTS: THEIR AVAILABILITY, TOXICITY AND REMOVAL BY HYBRID OZONATION-MEMBRANE FILTRATION

By

Alla Alpatova

A DISSERTATION

Submitted to
Michigan State University
in partial fulfillment of the requirements
for the degree of

DOCTOR OF PHILOSOPHY

Environmental Engineering

2010

ABSTRACT

EMERGING CONTAMINANTS: THEIR AVAILABILITY, TOXICITY AND REMOVAL BY HYBRID OZONATION-MEMBRANE FILTRATION

By

Alla Alpatova

There is an increasing public concern over the potential health effects and environment impact caused by emerging organic contaminants that enter natural aquatic systems as a result of various human activities. Emerging contaminants span a wide range of compounds, which were designed to offer improvements in different aspects of human life. Among this class of emerging pollutants carbon-based nanoparticles, are group of chemical compounds that attracts attention due to their unique chemical, physical and electronic properties. The wider application of carbon nanoparticles has been impeded by their low solubility in polar liquids and by their strong tendency to aggregate due to hydrophobic-hydrophobic interactions. Contradictory data on toxicity of carbon nanomaterials to eukaryotic and prokaryotic organisms may also affect public perception regarding these new chemicals. In this study the cytotoxicity and epigenetic toxicity of single-walled carbon nanotubes (SWCNTs) dispersed in water using a range of natural and synthetic dispersants and derivatized fullerene nanoparticles (nC_{60}) subjected to three treatment schemes (ozonation only, chlorination only, and sequential ozonation/chlorination) were evaluated by three independent methods: neutral red dye uptake and gap junction intercellular communication bioassays with rat liver epithelia cells (WB-F344 cell line) and colony forming units counting with *E. coli*. When the dispersant itself was non-toxic, no losses of *E. coli* and

WB-F344 viability upon their exposure to dispersed SWCNTs were observed. The cell membrane, lysosomes, and intercellular gap junction communication channels remained unaffected in the presence of nC$_{60}$ or its derivatives. No effect on the ability of *E. coli* to grow and form a colony was found after cells were added to nC$_{60}$ suspensions. Oxidized nC$_{60}$ aggregates were also characterized in terms of their morphology, size and surface charge and functionality. The formation of C-Cl bonds on the surface of chlorinated fullerenes was detected. This is an important finding as it demonstrates that carbon nanomaterials can potentially be precursors for chlorinated carbon-based disinfection by-products.

Pharmaceuticals are another class of emerging contaminants broadly used in human and veterinary medicine and in agriculture. In this study the hybrid ozonation – ceramic membrane filtration was evaluated for the removal of pharmaceutically active compounds and disinfection by-products precursors (DBPs) from surface waters with very different characteristics. This study demonstrated that under appropriate operating conditions the ozonation-ceramic membrane filtration could significantly improve water quality and reduce membrane fouling as compared to conventional filtration only. The concentration of model pharmaceuticals in permeate was reduced to below the detection limits. Significant reduction in total organic carbon, UV-254 absorbing compounds and DBPs formation potential was also achieved.

DEDICATION

To my grandparents

ACKNOWLEDGEMENTS

I would like to express my deep gratitude to my advisor Prof. Susan Masten. Her valuable research and moral support, patience, encouragement throughout my studies at Michigan State University were what made this dissertation possible.

I would like to thank to Dr. Melissa Baumann, Dr. Irene Xagoraraki and Dr. Evangeline Alocilja for serving in my dissertation committee and for supporting me through the hard times.

I am thankful to Dr. Simon Davies for his valuable suggestions and support during my research work.

My mom and dad receive my love for their support during my studies.

TABLE OF CONTENTS

LIST OF TABLES

LIST OF FIGURES

CHAPTER 1
INTRODUCTION

1.1. Motivation

There is an increasing public concern over the potential health effects and environment impact caused by emerging organic contaminants that enter natural aquatic systems as a result of various human activities. Emerging contaminants span a wide range of compounds, which were designed to offer improvements in different aspects of human life.

Among those carbon-based nanoparticles is a group of novel materials that attracts attention due to their unique chemical, physical and electronic properties. These chemicals wide suite of environmental applications ranging from sorbents to antimicrobial agents and sensors [1]. The advances in manufacturing of carbon-based nanomaterials have led to their growing production and consumption, and, as a consequence, have resulted in quick spread of these materials in environment, thus increasing their chances of entering drinking water supplies through manufacturing, improper handling or transportation spills. The wider application of carbon nanoparticles has been impeded by their low solubility in polar liquids and by the strong tendency to aggregate due to hydrophobic-hydrophobic interactions [2]. Dispersing of carbon nanoparticles and ensuring long-term stability in a liquid medium have proved especially challenging for aqueous systems. Additionally, due to their hydrophobic nature, carbon nanoparticles could affect the bioavailability and mobility of organic contaminants in terrestrial and aquatic ecosystems. Contradictory data on toxicity of carbon nanomaterials to eukaryotic and prokaryotic organisms may also affect public perception regarding these new chemicals. Understanding transformations pathways of carbon nanomaterials in aqueous systems will

provide important information in assessing their potential environmental risks and help in developing methods for their removal from drinking water supplies.

Pharmaceuticals are another class of emerging contaminants broadly used in human and veterinary medicine and in agriculture. The worldwide use of pharmaceuticals is high and is estimated in thousand tons per annum (e.g., the estimated total consumption of antibiotics is between 100,000-200,000 tons per annum [3]). Pharmaceutical residuals have been found in various aquatic compartments including industrial effluents [4-7], landfill leachate [8] and hospital effluents [9, 10], the influents to [9, 11-13] and effluents from [9, 10, 14] wastewater treatment plants, surface [15], ground [16] and drinking [17, 18] waters. A wide spectrum of adverse effects to human health and aquatic flora and fauna raises concern regarding their fate during drinking water treatment. As such, the development of advanced treatment processes for the removal of pharmaceuticals from water supplies is needed. The hybrid ozonation – ceramic membrane filtration could be viewed as a promising technology to remove emerging contaminants from waters with different characteristics. The advantage of this technology is that ozone is used in conjunction with membrane separation to oxidize refractory organic compounds and mitigate membrane fouling. The hydroxyl radicals formed during catalytic decomposition of ozone on the membrane surface are capable of oxidizing organic molecules which are concentrated there [19]. This leads to a reduction in the fouling layer thickness and permeate flux recovery [20]. As a result, significant improvements in water quality and the reduction of operational costs can be achieved.

***The objectives of this work were*:** 1) to develop methods to enhance the stability of SWCNTs and fullerenes C_{60} in aqueous media through surface modification by covalent attachment of

functional groups or non-covalent functionalization by natural and synthetic organic molecules; 2) to study the physicochemical properties of as-prepared and surface-modified carbon nanoparticles; 3) to evaluate the toxicity of as-prepared and surface-modified carbon nanoparticles by a range of bioassays with bacterial and mammalian cells; and 4) to investigate the use of hybrid ozonation-ceramic membrane filtration for the removal of pharmaceuticals from surface waters with very different characteristics.

SWCNTs were functionalized by a range dispersants of natural (natural organic matter (NOM), gum Arabic (GA), amylose) and synthetic (polyvinylpyrrolidone (PVP) and Triton X-100) origin, which bind to a nanotube surface non-covalently although through different physicochemical mechanisms. The water soluble fullerene nC$_{60}$ aggregates were prepared by direct dispersion of the as-received fullerene powder in ultrapure water. Dynamic light scattering, phase analysis light scattering, and UV-vis absorption were used to comprehensively examine the size, charge and concentration of the dispersed carbon nanoparticles. Additionally, x-ray photoelectron spectroscopy (XPS) was employed to determine the type and fraction of various functional groups present on the surface of nC$_{60}$ aggregates. The cyto- and epigenetic toxicity of nanoparticles was evaluated in a set of bioassays with bacterial and mammalian cell cultures, including general viability assay with *E. coli*, neutral red dye uptake (NRU) and gap junction intercellular communication bioassays with rat liver epithelial cell lines. Visual and fluorescent microscopy imaging were used to examine the morphology of the cells exposed to carbon nanoparticles.

The removal efficiency of two antibiotics, dicloxacillin and ceftazidime in hybrid ozonation-membrane filtration system was evaluated. These compounds represent the type of

pharmaceuticals found in surface waters [15] and have diverse mode of action against both g-positive and g-negative bacteria [21, 22]. System parameters, including permeate flux, transmembrane pressure, cross-flow velocity, dissolved ozone concentration and temperature were continuously monitored during each experiment. TOC, GC and HPLC techniques were used to routinely measure the water quality characteristics, including total organic carbon, disinfection byproducts formation potential (measured as concentration of trihalomethanes and haloacetic acids) and the concentration of pharmaceuticals.

1.2. Structure of the Dissertation

The dissertation consists of six chapters and two appendixes. *Chapter 1* includes motivation, objectives and techniques used in the study. *Chapters 2-4* cover experimental work.

Chapter 2 presents physicochemical characterizations, cyto- and epigenetic toxicity of SWCNTs suspensions dispersed in aqueous media via non-covalent functionalization. The chapter comprises a comprehensive literature review on the dispersion, long-term stability and toxicity of carbon nanotubes, materials and methods used in the work, and a discussion of the experimental results.

Chapter 3 presents the physicochemical properties, cyto- and epigenetic toxicity of fullerene nC$_{60}$ derivatives formed during ozonation and chlorination. A detailed relevant background information on the toxicity of nC$_{60}$ aggregates as a function of the preparation method is included, along with the materials and methods part, and discussion of the effect of chemical treatment of nC$_{60}$ aggregates on their particle size, surface functionality and toxicity.

Chapter 4 describes the removal of selected pharmaceuticals and disinfection by-products from surface waters in combined ozonation-ceramic membrane filtration process. The literature review covers the occurrence of pharmaceuticals and disinfection byproducts precursors in aquatic environments and the applicability of convention and advanced water treatment processes for their removal from drinking water supplies. The chapter also includes materials and methods and results and discussion sections.

Chapter 5 included a summary and conclusions drawn as a result of the work. The recommendations for future work are given in *Chapter 6*.

BIBLIOGRAPHY

BIBLIOGRAPHY

1. Mauter, M.S.; Elimelech, M. Environmental Applications of Carbon-Based Nanomaterials. *Environmental Science and Technology* (2008), **42**:16, 5843–5859.

2. Lin, Y.; Taylor, S.; Li, H.P.; Fernando, K.A.S.; Qu, L.W.; Wang, W.; Gu, L.R.; Zhou, B.; Sun, Y.P. Advances toward bioapplications of carbon nanotubes. *Journal of Material Chemistry* (2004), **14**:4, 527-541.

3. Wise, R. Antimicrobial resistance: priorities for action. *Journal of Antimicrobial Chemotherapy* (2002), **49**, 585-586.

4. Larsson, D.G.; de Pedro, C.; Paxeus, N. Effluent from drug manufactures contains extremely high levels of pharmaceuticals. *Journal of Hazardous Materials* (2007), **148**, 751-755.

5. Li, D.; Yang, M.; Hu, J.; Ren, L.; Zhang, Y.; Li, K. Determination and fate of oxytetracycline and related compounds in oxytetracycline production wastewater and the receiving river. *Environmental Toxicology and Chemistry* (2008), **27**:1, 80-86.

6. Li, D.; Yang, M.; Hu, J.; Zhang, Y.; Chang, H.; Jin, F. Determination of penicillin G and its degradation products in a penicillin production wastewater treatment plant and the receiving river. *Water Research* (2008), **42**:1-2, 307-317.

7. Qiting, J.; Xiheng, Z. Combination process of anaerobic digestion and ozonation technology for treating wastewater from antibiotic production. *Water Treatment* (1988), **3**, 285-291.

8. Metzger, J.W., *Drugs in municipal landfills and landfill leachates*, in *Pharmaceuticals in the Environment. Sources Fate Effects and Risks*, K. Kummerer, Editor. 2004, Springer: Berlin. 133-138.

9. Brown, K.D.; Kulis, J.; Thomson, B.; Chapman, T.H.; Mawhinney, D.B. Occurrence of antibiotics in hospital, residential, and dairy effluent, municipal wastewater, and the Rio Grande in New Mexico. *Science of the Total Environment* (2006), **366**, 772-83.

10. Thomas, K.V.; Dye, C.; Schlabach, M.; Langford, K.H. Source to sink tracking of selected human pharmaceuticals from two Oslo city hospitals and a wastewater treatment works. *Journal of Environmental Monitoring* (2007), **9**, 1410-1418.

11. Li, K.; Yediler, A.; Yang, M.; Schulte-Hostede, S.; Wong, M.H. Ozonation of oxytetracycline and toxicological assessment of its oxidation by-products. *Chemosphere* (2008), **72**, 473-478.

12. Gómez, M.J.; Martínez Bueno, M.J.; Lacorte, S.; Fernández-Alba, A.R.; Agüera, A. Pilot survey monitoring pharmaceuticals and related compounds in a sewage treatment plant located on the Mediterranean coast. *Chemosphere* (2007), **66**, 993-1002.

13. Tauxe-Wuersch, A.; De Alencastro, L.F.; Grandjean, D.; Tarradellas, J. Occurrence of several acidic drugs in sewage treatment plants in Switzerland and risk assessment. *Water Research* (2005), **39**, 1761-1772.

14. Verenitch, S.S.; Lowe, C.J.; Mazumder, A. Determination of acidic drugs and caffeine in municipal wastewaters and receiving waters by gas chromatography-ion trap tandem mass spectrometry. *Journal of Chromatography A* (2006), **1116**, 193-203.

15. Kolpin, D.W.; Furlong, E.T.; Meyer, M.T.; Thurman, E.M.; Zaugg, S.D.; Barber, L.B.; Buxton, H.T. Pharmaceuticals, hormones, and other organic wastewater contaminants in U.S. streams, 1999–2000: A national reconnaissance. *Environmetal Science and Technology* (2002), **36**:6, 1202-1211.

16. Sacher, F.; Gabriel, S.; Metzinger, M.; Stretz, A.; Wenz, M.; Lange, F.T.; Brauch, H.J.; Blankenhorn, I. Arzneimittelwirkstoffe im Grundwasser – Ergebnisse eines Monitoring-Programms in Baden-Württemberg (Active pharmaceutical ingredients in ground water – the results of a monitoring program in Baden-Württemberg (Germany)). *Vom Wasser* (2002), **99**, 183-196.

17. Heberer, T.; Stan, H.J. Determination of clofibric acid and N-(Phelylsulfonyl)-sacrosine in sewage, river and drinking water. *International Journal of Analytical Chemistry* (1997), **67**, 113-124.

18. Ye, Z.; Weinberg, H.S.; Meyer, M.T. Trace analysis of trimethoprim and sulfonamide, macrolide, quinolone, and tetracycline antibiotics in chlorinated drinking water using liquid chromatography electrospray tandem mass spectrometry. *Analytical Chemistry* (2007), **79**, 1135-1144.

19. Karnik, B.S.; Davies, S.H.; M.J., B.; S.J., M. The effects of combined ozonation and filtration on disinfection by-product formation. *Water Research* (2005), **39**, 2839-2850.

20. Karnik, B.S.; Davies, S.H.R.; Chen, K.C.; Jaglowski, D.R.; Baumann, M.J.; Masten, S.J. Effect of ozonation on the permeate flux of nanocrystalline ceramic membranes. *Water Research* (2005), **39**, 728-734.

21. Castle, S.S.; Enna, S.J.; David, B.B., *Dicloxacillin*, in *xPharm: The Comprehensive Pharmacology Reference*. 2007, Elsevier: New York. 1-5.

22. Castle, S.S.; Enna, S.J.; David, B.B., *Ceftazidime*, in *xPharm: The Comprehensive Pharmacology Reference*. 2007, Elsevier: New York. 1-5.

CHAPTER 2

SINGLE-WALLED CARBON NANOTUBES DISPERSED IN AQUEOUS MEDIA VIA NON-COVALENT FUNCTIONALIZATION: EFFECT OF DISPERSANT ON TOXICITY OF NANOTUBE SUSPENSIONS

2.1. Introduction

2.1.1. Dispersing of carbon nanotubes in aqueous media

The discovery [1] and subsequent extensive characterization of carbon nanotubes (CNTs) have revealed a class of materials with extraordinary electrical, mechanical, and thermal properties [2].

Recent efforts on the development of efficient and facile methods of dispersing CNTs in aqueous media have been focused on the hydrophilization of CNT with molecules that bind to the CNT surface non-covalently [3-22]. Such non-covalent functionalization has great promise as the modification-induced changes in the electronic and mechanical properties of CNTs are minimized [11]. Various surfactants [6, 12, 13], synthetic polymers (e.g., polyvinylpyrrolidone (PVP) [3, 7], poly(ethylene glycol) [14], polyphosphazene [15], natural organic matter (NOM) [9, 10, 23], biomolecules (e.g., proteins [16, 17], aminoacids [20], DNA [24]), and carbohydrates (e.g., cyclodextrines [21], amylose [8], starch [5], and GA [4] have been evaluated as dispersion agents (dispersants) for CNTs. Dispersion via non-covalent functionalization is based on the direct contact between a CNT and a dispersant molecule [12, 25]. Such modification of the CNT surface facilitates the disaggregation (i.e., debundling) of CNT bundles into smaller diameter

bundles [25] or even individual CNTs [9, 26] and leads to the stabilization of suspended CNTs via steric or electrostatic repulsion mechanisms or both.

The dispersion of CNTs in water has been enhanced by mixing [7, 9], sonication [4, 10, 27], or mixing followed by sonication [3, 5, 6, 12, 13, 26, 28]. These treatments were applied both in the absence [27] and in the presence of solubilizing agents: NOM [9, 10, 29], Triton X-100 [6], Triton X-405 [29], PVP-1300 [7], GA [4], and starch [5]. A three-step approach to solubilizing SWCNTs with amylose was suggested by Kim et al. [22]: dispersion of SWCNT in water by sonication followed by treatment with amylose in dimethylsulfoxide (DMSO)-H_2O mixture, followed by sonication allowing for molecularly controlled encapsulation of CNTs.

2.1.2. Stability of carbon nanotubes suspensions in water

Previous studies of the long-term changes in suspensions of dispersed CNTs have focused on monitoring changes in the concentration of suspended CNTs [9, 30-33]. By measuring UV-vis absorption at certain wavelength: 253 nm [32], 300 nm [34], 500 nm [27, 31, 34, 35], 530 nm [30], and 800 nm [9] the change in the concentration of suspended CNTs with time was determined.

Aqueous suspensions of non-functionalized CNTs are known to be unstable. There are considerable quantitative differences, however, in the reported stability data for non-functionalized CNTs. The concentration of unmodified multi-walled carbon nanotubes (MWCNTs) suspended in deionized water was reported to decline 86 % over 2 h in one study [30] and only 50% over 500 h in another study [32]. The suspensions of unmodified SWCNTs in

deionized water were found to completely precipitate after only 4 h [33].

It was found that non-covalent modification of CNT surface drastically improved the stability of CNT suspensions [9, 30-33]. The stability of the suspension of non-covalently functionalized CNTs was found to be a function of the type [9, 31] and concentration [29] of the dispersant, CNT length [30] and the presence of inorganic salts in the solution [23]. SWCNTs stabilized with oligothiophene-terminated poly(ethylene glycol) produced suspensions that were significantly more stable than CNTs dispersed in water with the aid of sodium dodecyl sulfate (SDS) and Pluronic F127 [31]. CNT suspensions in model Suwannee River NOM (SRNOM) solutions and in Suwannee River water were found to be considerably more stable than suspensions of CNTs dispersed in 1% aqueous solution of SDS [9]. Chappell et al. showed that the stability of MWCNTs dispersed using two types of humic acids, Triton X-405, Brij 35, and SDS was enhanced in dose-dependent manner [29]. In a study of the aggregation kinetics of MWCNTs in aquatic systems, Suwannee River humic acid was shown to significantly enhance stability of MWCNTs suspensions in the presence of monovalent and divalent salts [23]. While studying the stability of MWCNTs in water, Marsh and co-workers [30] observed that wrapping of the annealed CNTs with 1% SDS or charge doping increased their stability in the suspension; the authors demonstrated that shorter CNTs form more stable dispersions than longer CNTs of the same diameter. To date *there have been no systematic investigations that correlated long-term changes in size and charge of CNTs dispersed via non-covalently functionalized with the stability of the dispersion.*

2.1.3. Toxicity of carbon nanotubes

Toxicity of CNTs towards eukaryotic cells: Cytotoxicity. Most nanomaterial toxicity studies have been performed with mammalian cells, in particular on lung and skin cell cultures reflecting the understanding that the most likely routes of an organism's exposure to nanomaterials are respiratory and dermal contact. While the toxicity of CNTs was actively studied with respect to the type of the CNT (MWCNT versus SWCNT) [36-40], surface functionalization [41-44], CNT length [45-47], exposure dose [37, 38, 41, 42, 48-61], degree of purification [37, 40, 45, 51, 57, 58, 62], and degree of dispersion [63], only very limited information exists on the biocompatibility of CNTs as a function of surface coating. It is especially important to assess the toxicity of dispersed CNTs because of their increased mobility and potential to enter water supplies.

Several hypotheses have been put forth to explain the likely pathways of CNT toxicity: oxidative stress induced by the formation of reactive oxygen species (ROS) generated at the surface of CNTs [52, 60, 61] or the presence of residual catalyst, which is used during the CNT manufacturing process [39], physical contact between a CNT and a cell [55] or a combination of these factors [39] (also see SD, Section S.1.2). The dispersant used for the stabilization of CNTs in suspension was suggested as another possible cause of the observed nanotube toxicity [41].

In most studies of the toxicity of non-covalently functionalized CNTs the dispersants were surfactants. *In vivo* assessment of the toxicity of SWCNTs modified with Pluronic F108 administered intravenously to rabbits showed the absence of the acute toxicity [49]. Pluronic F-127-coated MWCNTs did not affect cell viability, apoptosis, and ROS formation in mouse and

human neuroblastoma cells [64], and mouse cerebral cortex [65]. In contrast, MWCNTs dispersed using Pluronic F68 caused cell death, changes in cell size and complexity, ROS production, interleukin-8 (IL-8) gene expression and nuclear factor (NF)-jB activation [61]. CNTs dispersed using Tween 80 were toxic to mesothelioma cells [63], led to an inflammation of murine allergic airway with augmented humoral immunity [66], and induced inflammatory and fibrotic responses when intracheally administrated to rats [46]. More ROS were observed upon exposure of human lung epithelial or primary bronchial epithelial cells to SWCNTs dispersed using dipalmitoylphosphatidylcholine, a major component of lung surfactant [67], as compared to dipalmitoylphosphatidylcholine-free samples. In contrast, low toxicity was observed in *in vivo* experiments when SWCNTs were dispersed using Tween 80 and intravenously injected into mice [60]. In another study, SWCNTs dispersed in 1% SDS aqueous solution showed no cytotoxicity with respect to the human alveolar epithelial cells [68]. CNTs dispersed using Pluronic PF-127 solution did not affect viability, apoptosis and ROS generation in the human neuroblastoma cells after 3 days of incubation; however, cell proliferation decreased as incubation time increased to two weeks [64]. In the only paper that mentioned the potential toxicity effect of the dispersant, the authors suggested that excess surfactant was responsible for the observed increase in toxicity; in this work, the controlled exposure of cells to 1% Pluronic F108 produced a 10% decrease in the cells viability [41].

Very little is known about the effect of non-covalent wrapping with dispersants other than surfactants on the biocompatibility of CNTs. In vitro cytotoxicity of CNTs wrapped with poly(methyl vinylketone) decorated with α-N-acetylgalactosamine [50], nano-1 peptide [69] and cholesterol-end-capped poly(2-methacryloyloxyethyl phosphorylcholine) [59] were examined

after their contact with human lung epithelial-like cells, normal skin fibroblasts and human umbilical vein endothelial cell line. No impact on cell growth and proliferation was demonstrated in all three cases. Cytotoxicity of GA-stabilized MWCNTs upon exposure to A549 cells was observed by LDH, XTT and MTT bioassays in [45]. Two possible reasons were accounted for this effect: (i) better availability of GA-stabilized MWCNTs and (ii) different intercellular accumulation pathway of GA-stabilized MWCNTs as compared to when carbon nanotubes were exposed in bundles.

Toxicity of CNTs towards eukaryotic cells: Genotoxicity and epigenetic toxicity. Most toxicological studies of CNTs focused on the evaluation of cytotoxicity [36-42, 45-55, 57-60, 62-67, 70-72]. However, genotoxicity [39, 53, 73-75] and epigenetic toxicity [76]; [77] are other possible causes of cell damage or other adverse effects. The genotoxicity of SWCNTs dispersed using fetal bovine serum at (5 to10) μg/mL concentration, with respect to primary mouse embryo fibroblasts was demonstrated using Comet assay [53]. In another recent study, CNTs (dispersed in BEGM cell culture medium and subjected to ultrasonication) induced a dose-dependent increase in DNA damage as indicated by Comet assay and caused a significant increase in micronucleated cells (micronucleus assay) in human bronchial epithelial cells [73]. Kang et al. observed high levels of stress-related gene products in *Escherichia coli* (*E. coli*) upon its exposure to CNTs, with the quantity and magnitude of expression being much higher in the presence of SWCNTs [39]; in this study CNTs were either deposited on a PVDF membrane surface or dispersed in saline solution. No mutagenic effect was observed in Salmonella microcosme test with baytubes® (high purity MWCNTs agglomerates, sonicated 10 min in deionized water [74] and in bacterial reverse mutation assay (Ames test) with Salmonella

typhimurium TA 98 and TA 100 strains and with *E. coli* WP2uvrA strain exposed to MWCNTs dispersed in DMSO [75]. *There have been no reports to date on the epigenetic toxicity of carbon nanomaterials.*

Toxicity of CNTs in prokaryotic cells. Most toxicity studies have focused on the effect of CNTs on mammalian cell lines. Only limited information exists on the cytotoxic effects of CNTs towards bacterial cells. Recently, antimicrobial activity of SWCNTs [39, 55, 72] and MWCNTs [39, 47, 72] either suspended in aqueous solution [39, 55] or deposited on the surface of a PVDF microfilter [39, 47, 55, 72] towards g-negative bacteria (*E. coli* and *Pseudomonas aeruginosa* [39, 47, 55, 72] and g-positive (*Staphylococcus epidermidis* and *Bacillus subtilis* [72]) bacteria was reported. It was suggested that membrane damage to the cells was caused by the direct physical contact between the CNT and cell [55] or by a combination of direct physical contact and oxidative stress [39]. No effect on the percentage of *E. coli* inactivation was observed upon exposure of SRNOM-stabilized SWCNTs as compared of SWCNTs dispersed in the absence of SRNOM [72]. Significant antimicrobial activity of CNTs composite films against *Staphylococcus aureus* and *Staphylococcus warneri* was reported in a separated study [78]. In contrast to the findings of above studies, *E. coli* growth and proliferation was not influenced when microchannel-structured MWCNTs scaffolds were immersed into the culture medium with the cells [71].

2.1.4. Effect of growth media on the toxicity of nanoparticles

The existing literature highlights the importance of the growth media in cytotoxicity testing and links the apparent cytotoxic effect of the nanomaterial to the salt and organic content of the

culture [79-81]. Lyon et al. [79] showed that in media with high salt content, the size of nC_{60} aggregates tends to increase as compared to that observed in low salt media. In another study, MWCNTs were found to stimulate growth of unicellular protozoan *Tetrahymena pyriformis* in growth medium, which contained proteose peptone, yeast extract and glucose; the increase in growth was attributed to the formation of peptone-MWCNTs conjugates, which were taken up by the microorganism [56]. While the aforementioned studies indicate that salt and organic composition of the medium, in which exposure studies are performed, may influence the interaction of CNTs with bacteria, *there have been no studies that comparatively evaluated CNT toxicity in growth media with different organic loadings and salt contents.*

2.1.5. The objectives and experimental approach

This study addressed some of the knowledge gaps identified above. Aqueous suspensions of SWCNTs functionalized by a range of non-covalently bound dispersants of natural (NOM, GA, amylose) and synthetic (PVP, Triton X-100) origin, were prepared and evaluated in terms of their physicochemical and toxicity properties. The study pursued the following objectives: (1) *to assess time-dependent cytotoxicity of non-covalently functionalized SWCNTs with respect to bacteria and mammalian cells as a function of dispersant type and growth media*. The effect of SWCNTs on *E. coli* was studied by measuring cell viability after 3 h, 24 h, and 48 h of exposure in three types of growth media with different organic loadings and salt contents. The cytotoxicity of dispersed SWCNTs towards mammalian cells was assessed in neutral red dye uptake (NDU) bioassay with rat liver epithelial cells after 30 min and 24 h of incubation; (2) *to assess time-dependent epigenetic toxicity of non-covalently functionalized SWCNTs as a function of dispersant type*. In this study, we evaluated epigenetic toxicity of the SWCNTs to rat liver

epithelial cells as a function of dispersant type in GJIC bioassay after 30 min and 24 h of incubation.

The set of chemically diverse dispersants was chosen based on their demonstrated effectiveness in solubilizing CNTs [4-6, 9, 10, 13, 26] and potential adverse effects [82-85]. NOM, GA and PVP have LD_{50} doses of (54.8 to 58.5) mg (intravenous administration in mice) (EMEA, 1999) 2,000 mg (oral administration in rats) [82] and 100,000 mg (oral administration in rats) [83] per kg of body weight, respectively. Amylose has been reported to be used in a colon-specific drug delivery due to its low toxicity and high biodegradability [84]. On the other hand, Triton X-100 was reported to be toxic to protozoan, fish, and mammalian cells [85].

Two batches of dispersed SWCNTs were prepared. The first batch was used to evaluate the viability of *E. coli* cells after their contact with dispersed SWCNTs by the quantification of colony forming units. To elucidate the effects of ionic and organic composition of the growth medium, the cytotoxicity of the SWCNTs suspended in three growth media of different organic and salt compositions was evaluated. First, in order to assess the acute cytotoxicity of dispersed SWCNTs, we conducted experiments in 0.1 M NaCl. Then, in order to investigate the effect of SWCNTs on the ability of *E. coli* form a colony over time, we employed three types of growth media: (i) LB medium with higher organic chemical and salt content, (ii) MD medium with low salt content and organic load, and (iii) 0.1 M NaCl solution. The second batch was used to evaluate cyto- and epigenetic toxicity of the dispersed SWCNTs against rat liver epithelial cells by the NDU and gap junction intercellular communication (GJIC) bioassays. The NDU assesses cell viability by measuring the accumulation of neutral red dye in lysosomes, which depends on

the cell's capacity to maintain pH gradients through the maintaining membrane integrity and production of ATP. The amount of dye incorporated by the cell is quantified spectrophotometrically [86]. The NDU bioassay has been used to assess cytotoxicity of CNTs [51]. The GJIC bioassay [86-89] utilizes the ability of epigenetic tumor promoters to alter level of GJIC [90, 91]. The degree of GJIC was quantified by measuring the distance (area) the fluorescent dye (≤ 1200 Da) travels between the cells after a given time. Both NDU and GJIC bioassays were carried out with WB-F344 rat liver epithelial cells exposed to dispersed SWCNTs for different periods of time. The WB-F344 cell line was chosen because these normal diploid rat liver epithelial cells have already used in numerous studies of cytotoxic or epigenetic effects [87] thus allowing us to have a comparative basis.

2.2. Materials and methods

2.2.1. Materials

SWCNTs (purity > 90%), produced by catalytic chemical vapor deposition, were obtained from Cheap Tubes, Inc (Brattleboro, VT) and used as received. The SWCNTs were used as obtained, allowing us to mimic what might occur in the environment. As indicated by the manufacturer, the SWCNTs had an inside diameter in the range of 0.8 nm to 1.6 nm, an outer diameter in the range of 1 nm to 2 nm and were 5 μm to 30 μm in length.

GA (approx. 250 kDa; a complex mixture of saccharides and glycoproteins obtained from the acacia tree), PVP (approx. 29 kDa), Triton X-100 (approx. 625 Da; polyethylene glycol p-(1,1,3,3-tetramethylbutyl)-phenyl ether) and amylose (molecular weight not specified; a polymeric form of glucose and a constituent of potato starch) were purchased from Sigma-

Aldrich (Milwaukee, WI). Suwannee River Natural Organic Matter (SRNOM) reverse osmosis isolation was obtained from International Humic Substances Society (St Paul, MN).

2.2.2. Dispersion procedures

Aqueous solutions of PVP, Triton X-100 were prepared by dissolving PVP (40 mg) and Triton X-100 (0.4 mL) in 40 mL of water and adjusting the pH of both solutions to 7 with 0.1 M HCl. The aqueous solution of GA was prepared by mixing 1g of GA in 50 mL of water and adjusting the pH of the mixture to 7 with 0.1 M HCl; this mixture was left to settle for 24 h and then 40 mL of supernatant was collected for use in the stability or toxicity studies. To prepare NOM solutions, two flasks of 40 mL of water, each containing 8 mg of NOM, were stirred for 24 h. Each solution was then filtered through a 0.22 μm filter under vacuum. The pH of one solution was kept at its original value (approx. 3.5) while the pH in another solution was adjusted to 7 with 0.1 M NaOH. SWCNTs were added to the above solutions to result in a 1 mg (SWCNT)/mL loading and were sonicated in Aquasonic 50T water bath (VWR Scientific Products Corp, West Chester, PA) for 20 min.

SWCNTs were dispersed with amylose based on modified version of the three-step approach reported by Kim et al. [22]. SWCNTs (40 mg) were sonicated in 25 mL of water (pH 7) at approximately 75 W for 5 min using Sonicator 3000 (Misonix, Inc., Farmingdale, NY) equipped with a microprobe. 100 mg of amylose in 6.28 mL of DMSO were prepared and added to the sonicated suspension of SWCNT in water so that the DMSO/water ratio was 20% by volume. The resulting mixture was sonicated for another 5 min in order to remove the excess amylose and DMSO. The suspension was sonicated, centrifuged and refilled with water four times. Following

the sonication, SWCNTs suspensions were divided into 12 mL aliquots and each aliquot was transferred into 15 mL centrifuge tube. After 24 h standing time, the top 4 mL of each suspension was withdrawn in order to be used in the stability or toxicity studies. Overall, two batches of dispersed SWCNT suspensions were prepared and were used, correspondingly, for 1) the general viability bioassay with *E. coli* and 2) NDU and GJIC bioassays.

2.2.3. Physicochemical characterization of SWCNT suspensions

UV-Vis spectrophotometry. The absorbance of SWCNT suspensions over the (200 to 800) nm wavelength range was measured over a period of four weeks (Multi-spec 1501, Shimadzu, Kyoto, Japan). For each type of SWCNT suspension prepared, the absorbance of SWCNT-free solution of the corresponding dispersant was used as a baseline.

Quantification of SWCNTs concentration in suspension. To determine the concentration of suspended SWCNTs, we first prepared a separate set of suspensions with ten-fold reduced SWCNT loading with respect to the CNT loading used in long-term stability and toxicity studies. By reducing the concentration of SWCNTs while keeping the same amount of dispersant (PVP, GA, NOM (pH 3.5 and 7), or Triton X-100) stable suspensions of fully dispersed (i.e., no precipitate observed) SWCNTs were produced. To measure the concentration of SWCNTs in suspension, four suspensions (with SWCNTs stabilized by PVP, NOM pH 3.5, NOM pH 7, and GA, respectively) with 10-fold reduced SWCNT content (0.1 g/L) were prepared using the same procedures as described in Section 3.2 and were subjected to sonication for 1 h (Sonicator 3000, Misonix, Inc., Farmingdale, NY) at (70 to 80) W. Since no settling of SWCNTs was observed over the short term following the application of this treatment, complete dispersion of SWCNTs

was assumed. UV-vis absorbance spectra were recorded at different dilutions and a calibration curve for absorption at 500 nm [27, 31, 34, 35, 92] as a function of concentration was constructed, and coefficient of molecular extinction, ε, was determined. This coefficient was used to determine the concentration of SWCNTs in suspensions used in toxicity experiments. SWCNT characteristics measured upon the preparation of CNT suspensions are given in Table 2.1.

Size and charge of dispersed single-walled carbon nanotubes. The effective hydrodynamic diameter and ζ-potential of suspended SWCNTs were determined after 1, 4, 7, 14, 21, and 28 days of settling. The size and charge were measured by dynamic light scattering (DLS) and phase analysis light scattering techniques, respectively (ZetaPALS, BI_MAS Option, Brookhaven Instrument Corp., Holtsville, NY).

2.2.4. Toxicity assessment: *E. coli* viability assay

Media preparation. Luria-Bertani (LB) growth medium was prepared according to the standard procedure [93]. Minimal Davis medium with 90% reduced potassium phosphate concentration (MD medium) was prepared [94]. 0.1 M NaCl solution was prepared by dissolving 9 g of NaCl in 1 L of water (pH 7) and autoclaving it for 15 min at 1 bar and 121 ºC. For the toxicity assessments, each component of LB, MD and NaCl media was prepared in 4-fold higher concentration as compared to original protocol and the aliquot part of the corresponding medium was added to SWCNTs suspension (as further described in "Quantification of cell viability" Section). Luria-Bertani Petri plates were prepared according to the published method [93].

Preparation of E. coli culture. E. coli K12 stock was prepared in glycerol and stored at -80 ºC. Prior to use, the stock was defrosted, and 30 mL of LB medium were inoculated with 5 μL of the stock. After overnight growth at 37 ºC, 5 μL of this suspension was spread onto LB agar plate and cultured at 37 ºC. Once distinct colonies were formed, the agar plate was transferred to the refrigerator and kept at 4 °C for up to one month. *E. coli* suspensions to be used in SWCNT cytotoxicity studies were prepared by scraping one colony from the surface of a Petri plate by aseptic loop and immersing the loop into 10 mL of LB or MD media in a 50 mL centrifuge tube. Tubes were placed on a shaker in an incubator 37 ºC for 12 h. When 0.1 M NaCl was used as an exposure medium in colony forming units bioassay, *E. coli* were first grown in the LB medium, centrifuged for 5 min at 2250 rpm and washed with 0.1 M NaCl as follows: the supernatant was decanted and replaced with an equal volume of 0.1 M NaCl, vortexed and resuspended by centrifugation. The washing procedure was repeated twice, presuming that after this treatment most of the remaining organic constituents of LB medium were removed from the *E. coli* suspension.

Quantification of cell viability. The SWCNTs suspension (1.425 mL), growth medium (475 μL) and 100 μL of the stock *E. coli* suspension were transferred into a 15 mL centrifuge tube and incubated under gentle shaking at 37 °C. Samples were taken after 3, 24, and 48 h and a series of dilutions (10^4 to 10^6) was prepared for each sample. Five samples of 10 μL and 20 μL from each dilution were placed onto an agar plate and incubated at 37 °C until distinct colonies developed. Colony forming units (CFU)/1 mL were calculated for each sample.

Table 2.1. Effective hydrodynamic diameter, ζ-potential, polydispersity and concentration of the dispersed SWCNTs as a function of dispersant type. All parameters were measured upon 24 hours of the preparation.

Type of dispersant	Effective hydrodynamic diameter, nm		ζ-potential, mV		Polydispersity		Concentration, mg/L	
	Batch 1	*Batch 2*	*Batch 1*	*Batch 2*	*Batch 1*	*Batch 2*	*Batch 1*	*Batch 2*
NOM pH 3.5	323.4±5.9	350.9±8.1	-44.8±1.1	-42.3±1.0	0.268	0.264	86.10	95.82
NOM pH 7.0	323.5±8.3	321.2±6.7	-51.0±1.2	-45.6±1.3	0.257	0.263	59.70	56.31
PVP	350.0±9.4	321.4±6.2	-14.3±0.6	-13.8±1.7	0.267	0.270	117.10	108.60
GA	892.4±15.2	905.8±46.7	-23.8±0.9	-23.1±0.9	0.282	0.281	174.80	200.57
Triton X-100	252.3±22.5	232.8±4.0	-24.3±0.8	-23.9±1.0	0.263	0.300	132.20	150.44
Amylose	non-available	685.5±32.7	-35.0±0.9	-15.3±0.9	non-available	0.269	non-available	non-available

Each experiment was run in triplicates with negative (bacterial suspension with the corresponding amount of ultrapure water) and vehicle (solution of the corresponding dispersant) controls, herein called vehicle control I and vehicle control II, respectively. The results are reported as a fraction of control (FOC) ± standard deviation (STD), calculated as the ratio of the average number of colonies grown after *E. coli* exposure to SWCNTs suspensions or vehicle control II to the average number of colonies grown in vehicle control I plates.

2.2.5. Toxicity assessment: Neutral red dye uptake bioassay

For the NDU bioassay we adapted a published procedure [86, 88, 89]. A solution (0.015 w/v) of neutral red dye (3-amino-7-(dimethylamino)-2-methylphenazine hydrochloride) in D-medium was incubated at 37 °C for 2 h and filtered through a 0.22 µm syringe filter (Millipore Corp., New Bedford, MA) to remove undissolved dye and ensure sterile conditions. Confluent WB-F344 cells were exposed to 500 µL of each of SWCNTs suspension and incubated at 37 °C for 30 min and 24 h under gentle shaking in a humidified atmosphere containing 5% CO_2. After cells were exposed to SWCNTs, the exposure medium was removed by aspiration and the cells were washed with 1 mL of phosphate saline buffer (PBS). Following washing, 2 mL of the neutral red dye solution per plate was added and the cells were incubated for 1 h at 37 °C in the humidified atmosphere containing 5% CO_2. Upon incubation, the cells were rinsed three times with PBS, and 2 mL of aqueous solution containing 1% acetic acid and 50% ethanol was added to each plate to lyse the cells. 1.5 mL of the lysate was transported into 2 mL microcentrifuge tube and the optical density was recorded at 540 nm using a Beckman DU 7400 diode array

detector (Beckman Instruments, Inc., Schaumburg, IL). The background absorbance was measured at 690 nm and then subtracted from the original absorbance. Each experiment was conducted in triplicates. The neutral red dye uptake was reported as the FOC (absorption of neutral red in the chemically treated sample divided by the absorption of neutral red in the nontreated control I sample). FOC values of 1.0 indicates non-cytotoxic response while FOC values < 0.8 indicate that less dye was absorbed by cells and that chemical is cytotoxic at that dose [88, 95].

2.2.6. Toxicity assessment: Gap junction intercellular communication bioassay

The principles of GJIC bioassay were originally described in [86] and further developed in [87-89]. SWCNTs suspensions (500 μL) were introduced to the cell culture plates with confluent WB-F344 cells and incubated for 30 min and 24 h at 37 ^{0}C in humidified atmosphere containing 5% CO_2 under gentle shaking. Then, cells were washed with PBS solution and 1 mL of 0.05% solution of Lucifer yellow fluorescent dye in PBS buffer was added to each plate. Three different scrapes were made on the bottom of a cell culture plate using a surgical steel scalpel blade. The dye was absorbed through the monolayer of confluent cells. The transfer of dye through gap junctions lasted 3 min, followed by a thorough rinse with PBS solution to remove extracellular dye. Cells were fixed with 0.5 mL of 4% formalin solution in PBS. The migration of the dye in the cells was observed at 200X magnification using a Nikon epifluorescence microscope equipped with a Nikon Cool Snap EZ CCD camera and the images were digitally acquired using a Nikon NIS-Elements F2.2 imaging system. The fluorescence area of the dye migration from the scrape line was quantified using Image J 1.40g (a public domain Java image processing program, http://rsbweb.nih.gov/ij/index.html). Each experiment was performed in duplicate with

same controls as in the NDU bioassay. Data are reported as the FOC, which is the ratio of the area of dye spread in the chemically treated sample to the area of dye spread in the vehicle control I samples. A FOC value of 1.0 corresponds to full communication between cells, FOC values of (0.5 to 0.9) represent partial GJIF inhibition, (0.3 to 0.5) values correspond to significant inhibition of the GJIF and values < 0.3 denote complete inhibition of the GJIC [89]. Student's t-tests at 95% confidence interval were run for all three bioassays to determine whether the difference between the results obtained in the control I plates and the results in the tested plates were significant.

The concentrations of SWCNTs upon addition to suspension of cells in the general *E. coli* viability bioassay, and in NDU and GJIC bioassays are reported in Table 2.1.

2.3. Results and discussion

2.3.1. General viability bioassay with *E. coli* (prokaryotic)

Immediately after *E. coli* cells were exposed to SWCNTs suspended in growth medium as well as after 3 h of exposure, no SWCNT aggregation was visually observed (Table 2.2) in experiments with all three types of the media - 0.1 M NaCl, MD (medium with lower salt organics content) and LB (medium with higher salt and organics content). After 24 h of incubation, limited precipitation was observed for all SWCNT suspensions in LB and MD media. After 48 h of incubation more precipitation occurred in each type of media.

Table 2.2. Effect of the nutrient medium on the aggregation state of the dispersed SWCNTs. "+" means that aggregation of SWCNTs has been observed in corresponding medium and that *E. coli* growth has occurred in each tested suspension. "-" means that no aggregation was observed upon 3 hrs of exposure of *E. coli* to the dispersed SWCNTs in the corresponding medium.

MEDIUM TYPE	AGGREGATION				*E. COLI* GROWTH		
	0 hrs	3 hrs	*24 hrs*	*48 hrs*	*3 hrs*	*24 hrs*	*48 hrs*
LB	-	-	+	+	+	+	+
MD	-	-	+	+	+	+	+
0.1M NaCl	-	-	non-available	non-available	+	non-available	non-available

No inhibition of *E. coli* colony forming ability was observed after 3 h of incubation with amylose-, NOM-, GA- and PVP-stabilized SWCNTs in 0.1 M NaCl (Figure 2.2). The FOC values did not decline in any of these samples and no significant difference in the influence on CFU counts was found between dispersed SWCNTs and solutions of corresponding dispersants. When the bacteria suspension was brought in contact with Triton X-100-stabilized SWCNTs, approximately 25% loss of the cell viability was measured as compared to vehicle control I samples. However, there was no statistical difference between FOC of Triton-stabilized SWCNTs and the control (solution of Triton X-100 only). It remains unclear if the observed cytotoxicity of the these suspensions was due to i) SWCNTs stabilized by Triton X-100 or ii) the residual "free" (i.e. not associated with suspended SWCNTs) Triton X-100 potentially present in the solution or iii) the combined effect of both Triton X-100/SWCNT and dissolved Triton X-100. The complete separation of the Triton X-100/SWCNT and dissolved Triton X-100 could not be accomplished using centrifugation. Even for very long centrifugation times, the supernatant had grayish color indicating that some fraction of SWCNTs was not removed.

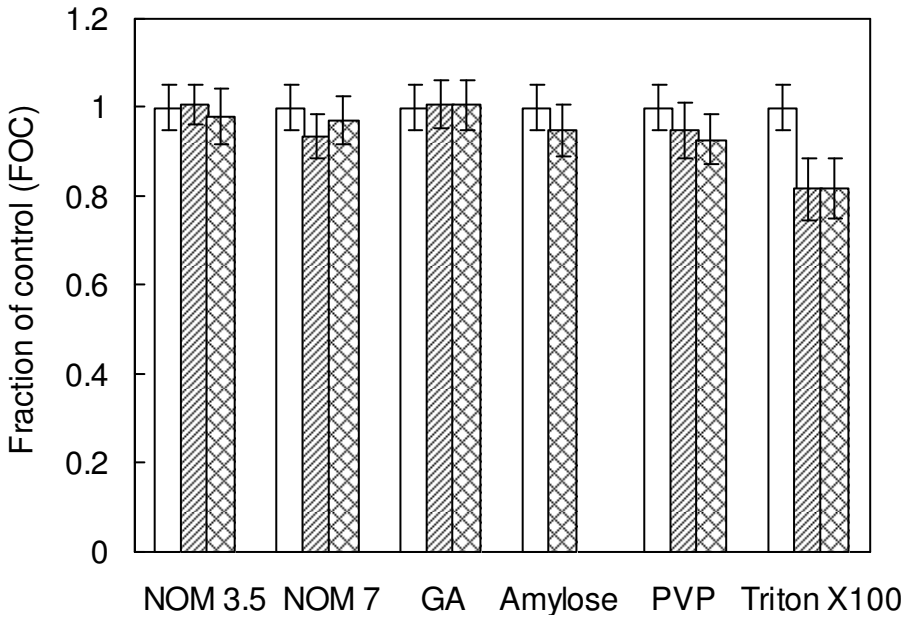

Figure 2.1. Viability of *E. coli* in 0.1M NaCl. Exposure time: 3 h. Open, hatched and cross-hatched bars correspond to control I, control II and dispersed SWCNTs. In the case of amylose ultrapure water was used as control.

The ability of *E. coli* to grow and to form colonies in the presence of amylose-, GA-, PVP-, and NOM-stabilized SWCNTs in LB medium mimicked both control samples regardless of the contact time (Figure 2.2). On the contrary, 21 and 18 % mortality rates after 3 h of incubation were observed for *E. coli* in Triton X-100/SWCNTs suspension and Triton X-100 solution, respectively. After 24 h of contact, the number of colonies grown on the Petri plates decreased by 30% when bacteria were in contact with Triton X-100-stabilized SWCNTs and by 27% when bacteria were in Triton X-100 only solution as compared to vehicle control I plates. As the exposure time increased to 48 h, *E. coli* resumed its growth; with FOC of both Triton X-100 suspensions approaching values for vehicle control I sample.

When dispersed SWCNTs were tested in MD medium, no losses in cell viability for amylose-, GA-, PVP- and NOM-stabilized SWCNTs were measured (Figure 2.3). In the case of Triton X-100 suspensions, the reduction in *E. coli* survival was observed after 3 h of exposure; comparable losses of the *E. coli* viability were also observed for both Triton X-100-stabilized SWCNTs and the Triton X-100 only solution. However, after 24 h of exposure, fewer *E. coli* colonies were observed on Petri plates from suspensions of Triton X-100-stabilized SWCNTs and Triton X-100 solution only (vehicle control II) (33 and 44%, respectively). As the incubation time increased to 48 h, bacterial CFU counts in the presence of both Triton X-100 samples increased and approached that of vehicle control I samples. As was previously mentioned, the exposure of Triton X-100-stabilized SWCNTs to MD medium for 24 h resulted in formation of large flake-like aggregates, which settled out of the suspension. It is possible that this low salt medium induced specific interactions between bacterial cells and Triton X-100-coated SWCNTs, which were suppressed in the medium having a higher ionic strength. This led to a larger decrease in *E. coli* viability in these samples in comparison with the losses in Triton X-100 solution only. Damaged or dead cell attached to the SWCNTs aggregates and formed debris at the bottom of the testing tubes. The simultaneous effect of bacterial and nanoparticles settling out of the solution has been previously described [96] where the response of *Shewanella oneidensis* to C_{60}-NH_2 nanoparticles was studied.

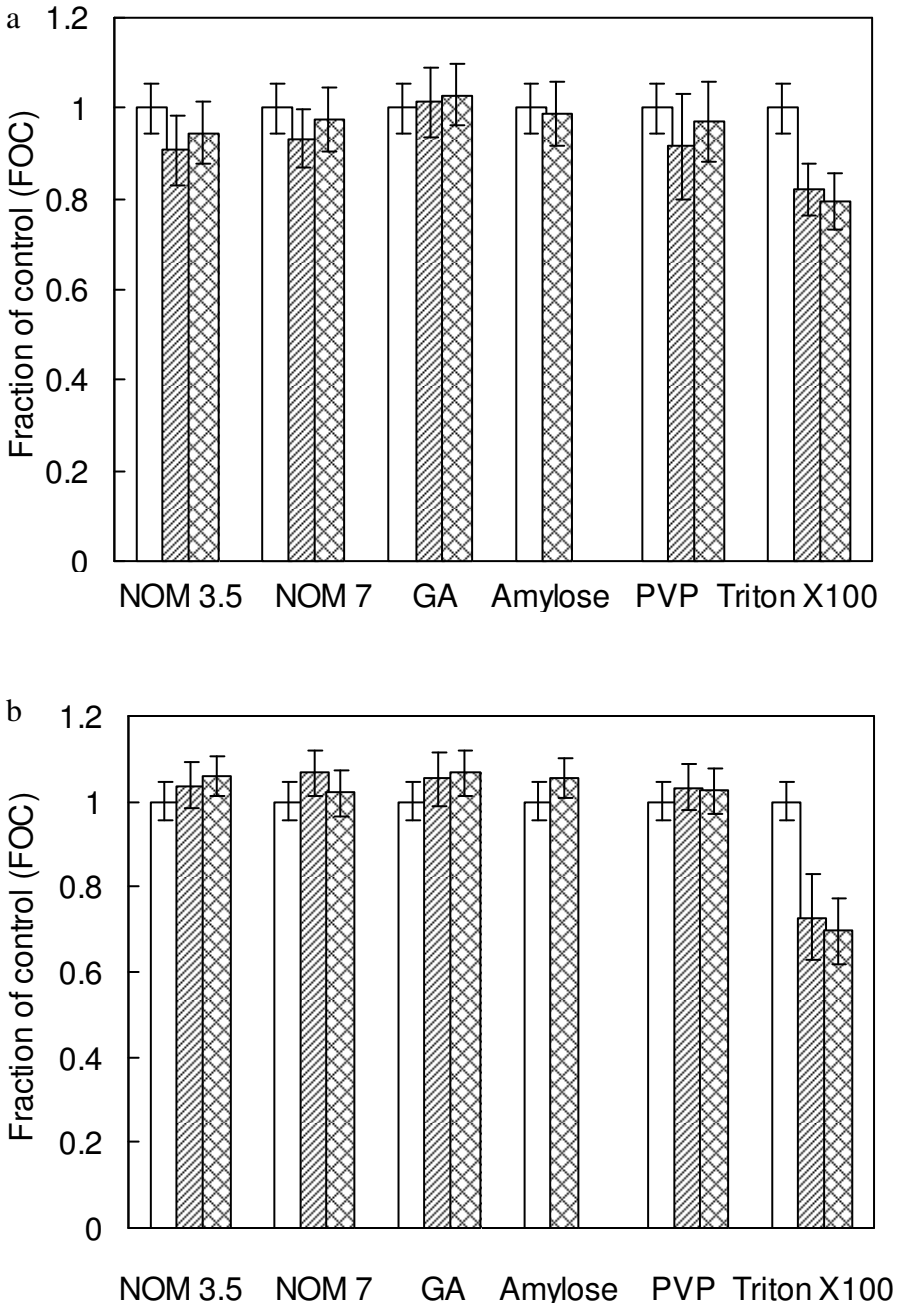

Figure 2.2. Viability of *E. coli* in LB medium. Exposure time: (a) 3 h, (b) 48 h, (c) 48 h. Open, hatched and cross-hatched bars correspond to control I, control II and dispersed SWCNTs. In the case of amylose ultrapure water was used as control.

Figure 2.2 (cont'd).

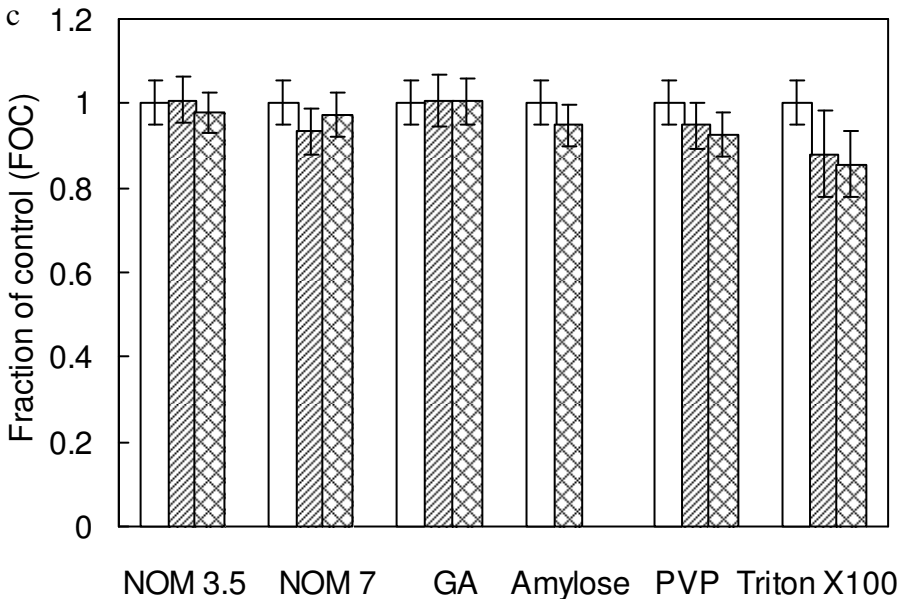

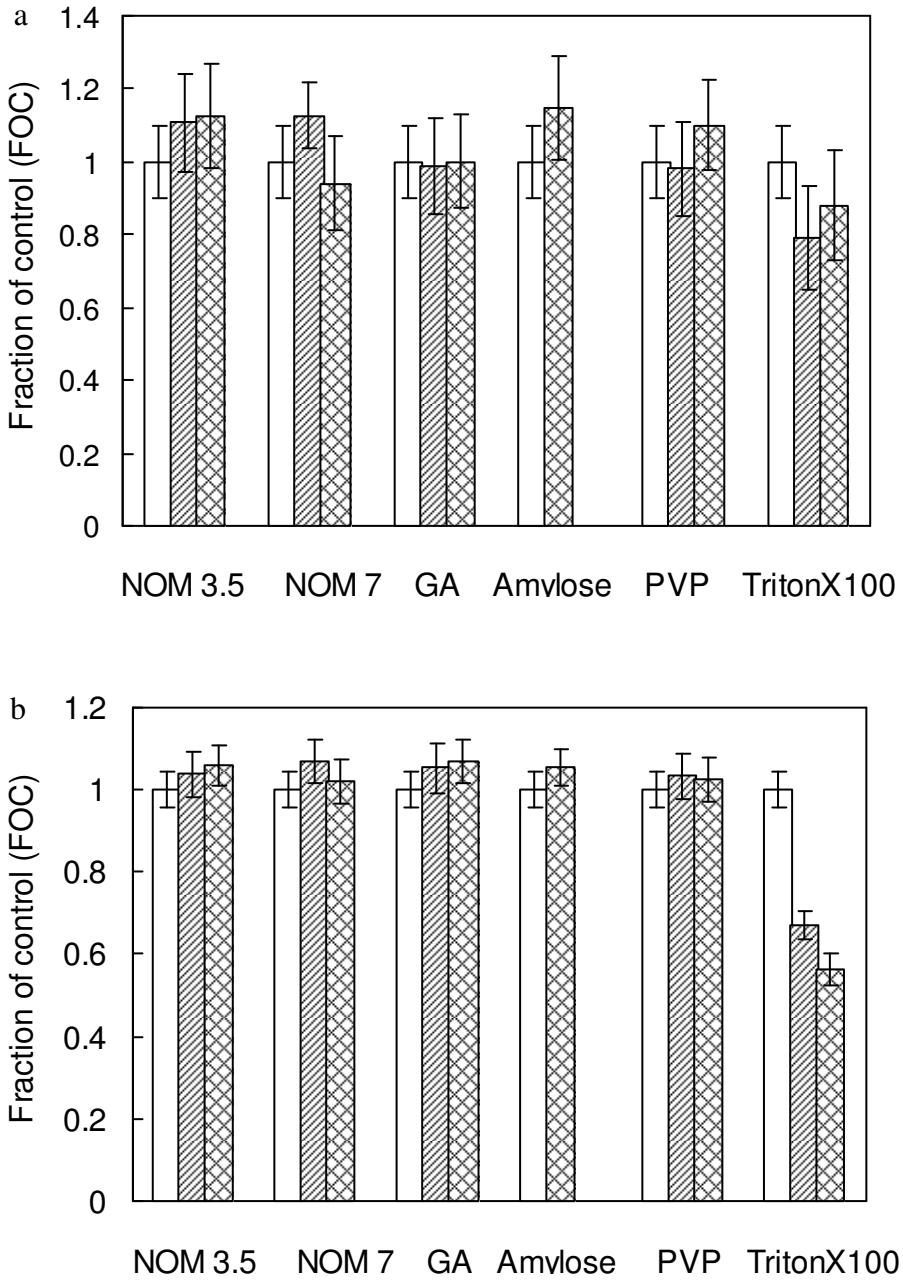

Figure 2.3. Viability of *E. coli* in MD medium. Exposure time: (a) 3 h, (b) 48 h, (c) 48 h. Open, hatched and cross-hatched bars correspond to control I, control II and dispersed SWCNTs. In the case of amylose ultrapure water was used as control.

Figure 2.3 (cont'd).

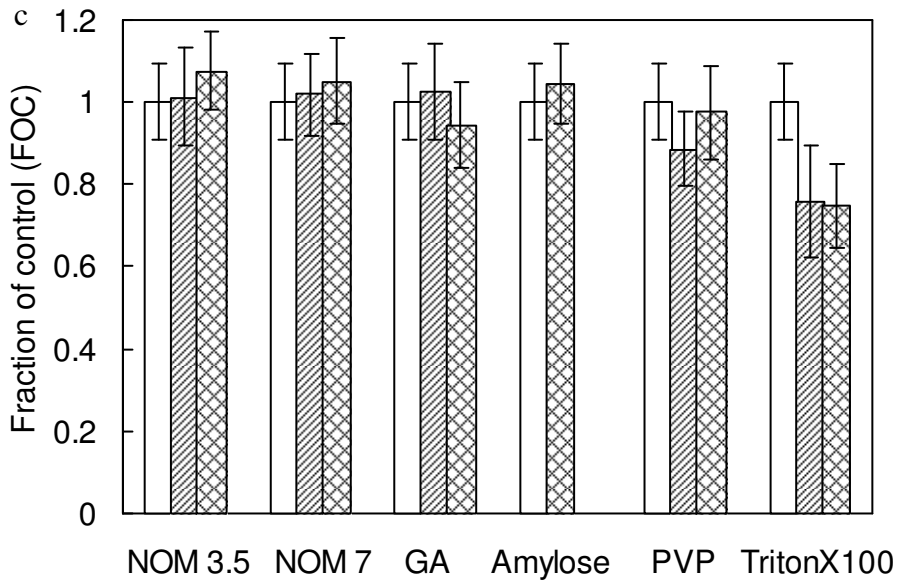

The fact that we observed inhibition of *E. coli* viability after 24 h of exposure in MD medium and did not observed this effect in LB medium highlights the importance of growth medium in cytotoxicity testing. Similarly, *E. coli* exposure to SWCNTs, stabilized with amylose, GA, PVP and NOM (both pH) did not affect CFU counts in any of the three media pointing to the importance of the dispersant in the assessments of biocompatibility of CNTs.

2.3.2. Neutral red dye uptake bioassay on eukaryotic cells

The assessment of cytotoxicity was determined by the viable uptake of neutral red into F344-WB rat liver epithelial cells. Nonviable cells lack the ability to absorb this dye. Results (Figure 2.4) indicated that SWCNTs dispersed using NOM (pH 3.5), NOM (pH 7), GA, amylose and PVP were not cytotoxic. However, Triton X-100 detergent induced a significant cytotoxic effect independent of SWCNTs. This latter observation can also be seen under phase contrast

microscopy of cells treated with Triton X-100 for 30 min (Figure 2.5). The morphology of the cells drastically changed from that of the normal control cells, in which the cells became clearer due to loss of most cytosolic contents, except for the cell nuclei. After a 24 h treatment with Triton X-100, the cells completely detached or solubilized from the culture plates.

2.3.3. Gap junction intercellular communication bioassay on eukaryotic cells

A representative fluorescent micrograph of the GJIC assay after treatment with (NOM + SWCNTs) is shown in Figure 6. The migration of the fluorescent dye through several cell layers is an indicator that the gap junction channels are open. After WB-F344 cells were incubated with dispersed SWCNTs suspensions for (1) 30 min and (2) 24 h, there was no significant affect on GJIC for all suspensions tested (Figure 2.6).

Due to Triton-stabilized SWCNTs being cytotoxic, GJIC was not measured in cells exposed this mixture.Also, when cells were examined under phase contrast, no changes in size and shape of the individual cells were detected (Fig.6). Hence, it can be concluded that under these experimental conditions WB-F344 cells exposed to dispersed SWCNTs retain normal intercellular communication irrespective of the applied treatment.

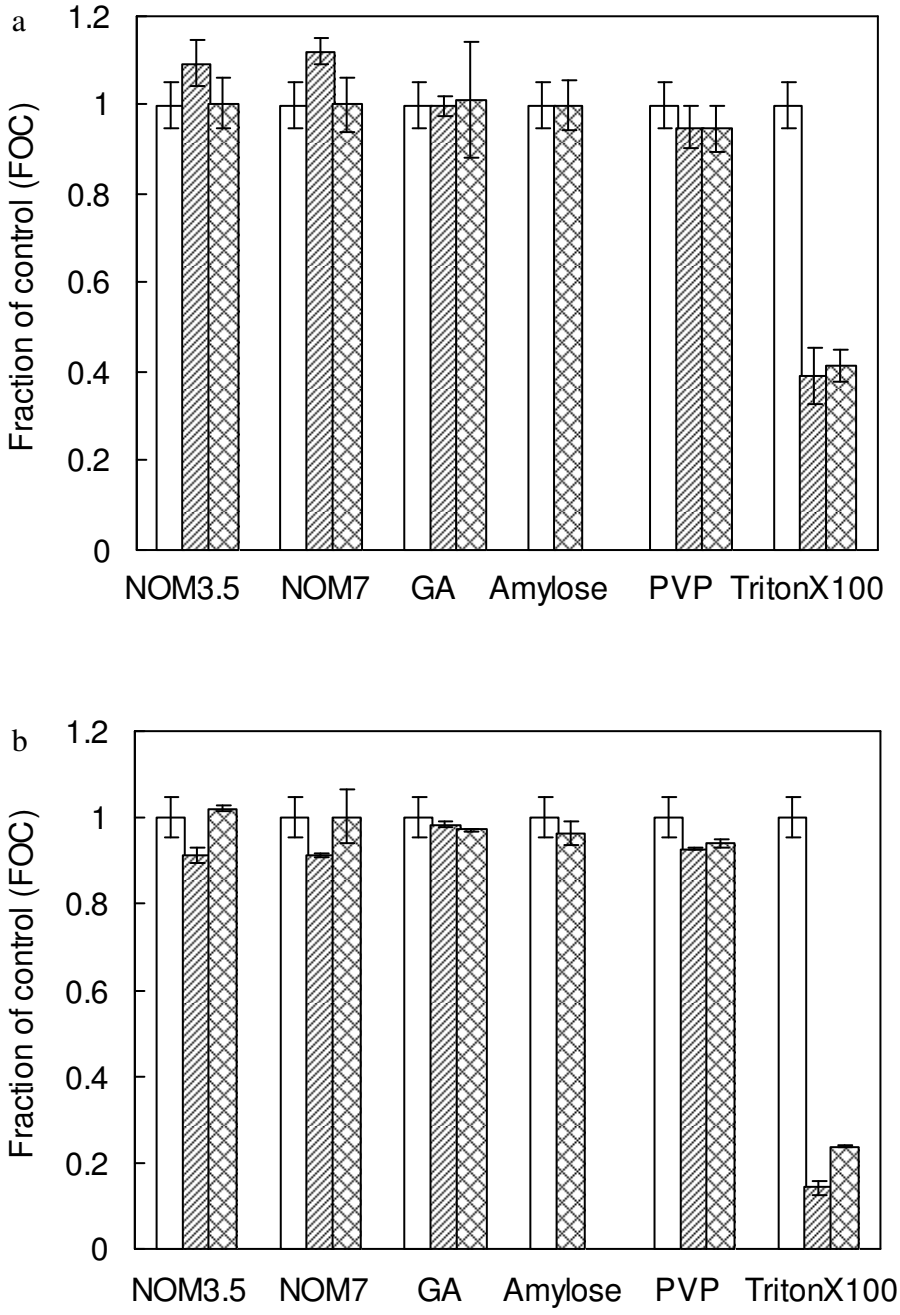

Figure 2.4. Neutral red dye uptake by WB-F344 cells as a function of dispersant type (a- 30 min, b - 24 hrs of exposure). Open, hatched and cross-hatched bars correspond to control I, control II and dispersed SWCNTs. In the case of amylose control I and control II were ultrapure water.

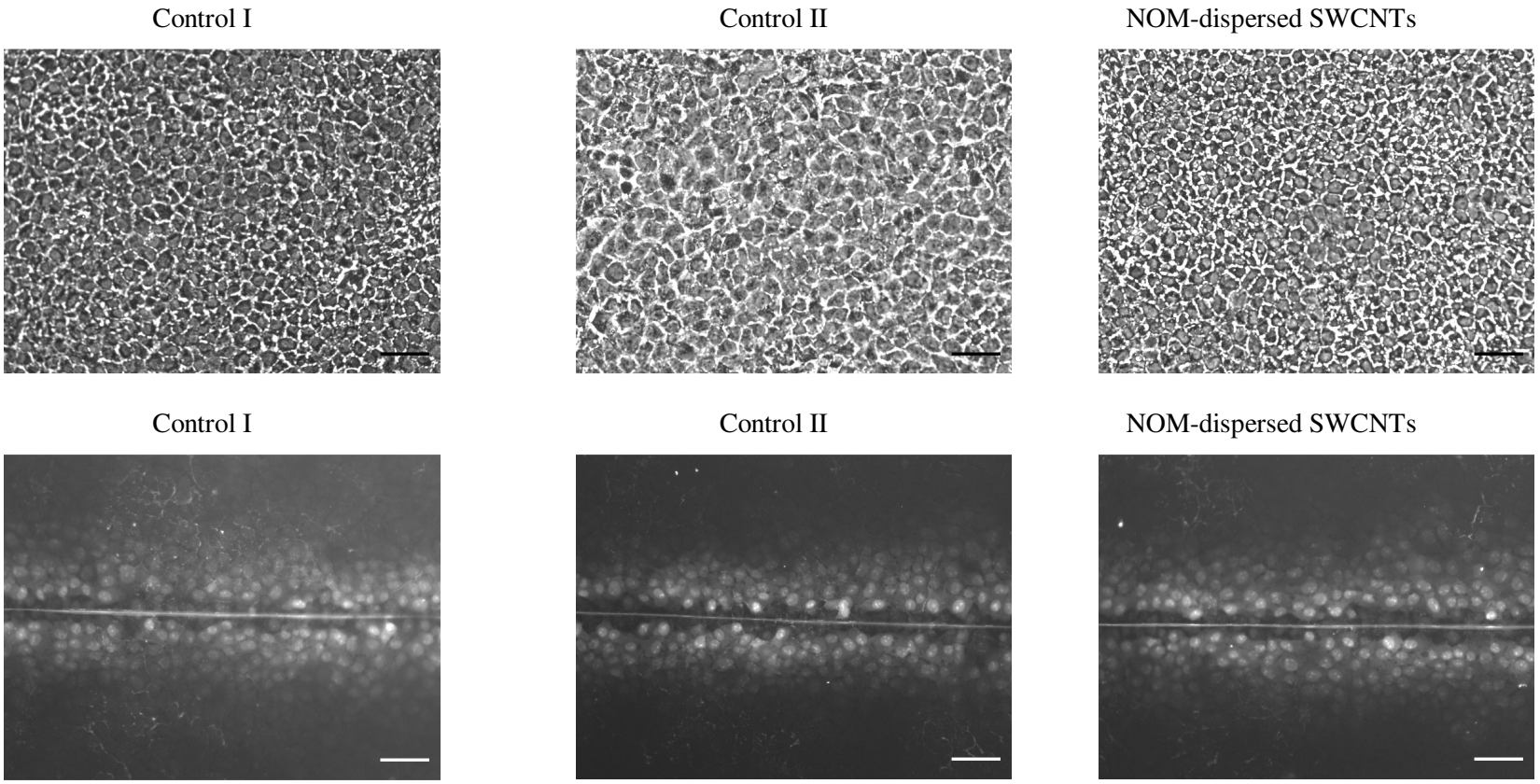

Figure 2.5. Representative phase contrast (upper row) and UV epifluorescent (bottom row) images of WB-F344 cells incubated with 500 µL of H_2O (vehicle control I), 500 µL of SRNOM pH 3.5 (vehicle control II) and 500 µL of SRNOM-solubilized SWCNTs (pH 3.5). Bright dots correspond to cells that absorb the dye; the absorption is indicative of cellular health. All images were taken at 200x magnification. Scale bar is 50 µm.

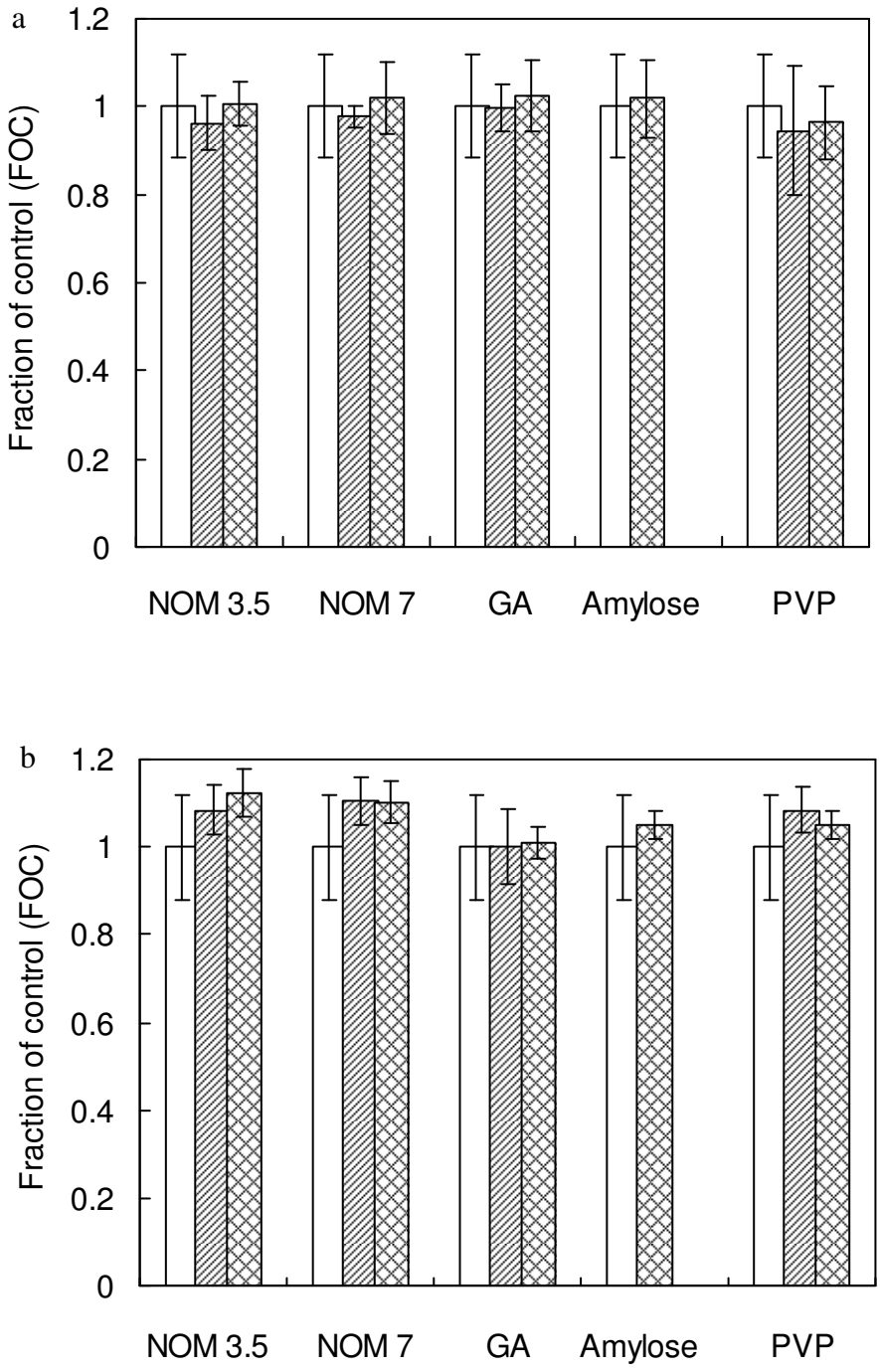

Figure 2.6. GJIC in WB-F344 cells as a function of dispersant type (a - 30 min, b - 24 hrs of exposure). Open, hatched and cross-hatched bars correspond to control I, control II and dispersed SWCNTs. In the case of amylose control I and control II were ultrapure water.

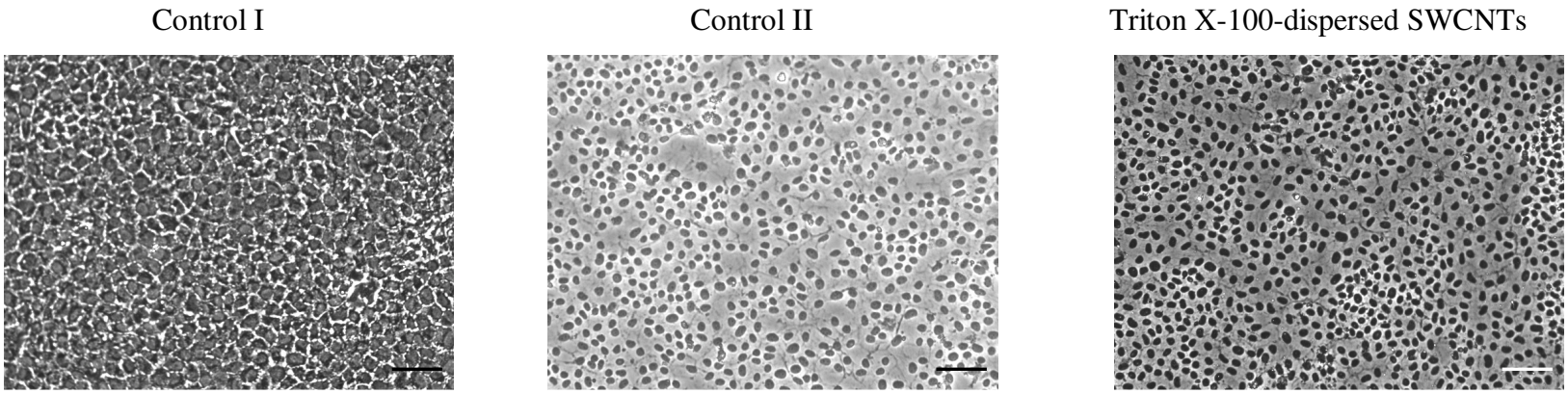

Figure 2.7. Representative phase contrast images of WB-F344 cells incubated with 500 μL of H_2O (vehicle control I), 500 μL of Triton X-100 (vehicle control II) and 500 μL of Triton X-100-solubilizeda SWCNTs. Black dots observed in vehicle control II and Triton X-100-solubilized SWCNTs samples correspond to dead WB-F344 cells. All images were taken at 200x magnification. Scale bar is 50 μm.

BIBLIOGRAPHY

BIBLIOGRAPHY

1. Iijima, S. Helical Microtubules of Graphitic Carbon. *Nature* (1991), **354**:6348, 56-58.

2. Tasis, D.; Tagmatarchis, N.; Bianco, A.; Prato, M. Chemistry of carbon nanotubes. *106* (2006), **3**, 1105–1136.

3. O'Connell, M.J.; Boul, P.J.; Ericson, L.M.; Huffman, C.; Wang, Y.; Haroz, E. Reversible water-solubilization of single-walled carbon nanotubes by polymer wrapping. *Chemical Physical Letters* (2001), **342**, 265–271.

4. Bandyopadhyaya, R.; Nativ-Roth, E.; Regev, O.; Yerushalmi-Rozen, R. Stabilization of individual carbon nanotubes in aqueous solutions. *Nano Letters* (2002), **2**:1, 25-28.

5. Star, A.; Steuerman, D.W.; Heath, J.R.; Stoddart, J.F. Starched carbon nanotubes. *Angewandte Chemie International Edition* (2002), **41**:14, 2508-2512.

6. Islam, M.F.; Rojas, E.; Bergey, D.M.; Johnson, A.T.; Yodh, A.G. High weight fraction surfactant solubilization of single-wall carbon nanotubes in water. *Nano Letters* (2003), **3**:2, 269–273.

7. Didenko, V.V.; Moore, V.C.; Baskin, D.S.; Smalley, R.E. Visualization of individual single-walled carbon nanotubes by fluorescent polymer wrapping. *Nano Letters* (2005), **5**:8, 1563-1567.

8. Bonnet, P., Albertini, D.; Bizot, H.; Bernard, A.; Chauvet, O. Amylose/SWNT composites: From solution to film – synthesis, characterization and properties. *Composite Science and Technology* (2007), **67**, 817–821.

9. Hyung, H.; Fortner, J.D.; Hughes, J.B.; Kim, J.H. Natural organic matter stabilizes carbon nanotubes in the aqueous phase. *Environmental Science and Technology* (2007), **41**:1, 179-184.

10. Liu, Y.Q.; Gao, L.; Zheng, S. Debundling of single-walled carbon nanotubes by using natural polyelectrolytes. *Nanotechnology* (2007), **18**:36, 365702.

11. Yang, Z.; Chen, X.H.; Chen, C.S. Noncovalent-wrapped sidewall multi-walled carbon nanotubes functionalization with polyimide. *Polymer Composites* (2007), **28**:1, 36-41.

12. Grossiord, N.; P., S.; J., M.; E., K.C. Determination of the surface coverage of exfoliated carbon nanotubes by surfactant molecules in aqueous solution. *Langmuir* (2007), **23**, 3646-3653.

13. Moore, V.C.; Strano, M.S.; Haroz, E.H.; Hauge, R.H.; Smalley, R.E.; Schmidt, J.; Talmon, Y. Individually suspended single-walled carbon nanotubes in various surfactants. *Nano Letters* (2003), **3**:10, 1379-1382.

14. Vaisman, L.; Marom, G.; Wagner, H.D. Dispersions of surface-modified carbon nanotubes in water-soluble and water-insoluble polymers. *Advanced Functional Materials* (2006), **16**:3, 357-363.

15. Park, H.J.; Heo, H.Y.; Lee, S.C.; Park, M.; Lee, S.-S.; Kim, J.; Chang, J.Y. Dispersion of single-walled carbon nanotubes in water with polyphosphazene polyelectrolyte. *Journal of Inorganic and Organometallic Polymers and Materials* (2006), **16**:4, 1574-1443.

16. Karajanagi, S.S.; Yang, H.C.; Asuri, P.; Sellitto, E.; Dordick, J.S.; Kane, R.S. Protein-assisted solubilization of single-walled carbon nanotubes. *Langmuir* (2006), **22**:4, 1392-1395.

17. Zong, S.; Cao, Y.; Jua, H. Direct electron transfer of hemoglobin Immobilized in multiwalled carbon nanotubes enhanced grafted collagen matrix for electrocatalytic detection of hydrogen peroxide. *Electroanalysis* (2007), **19**:7-8, 841-846.

18. Nepal, D.; Geckeler, K.E. pH-sensitive dispersion and debundling of single-walled carbon nanotubes: Lysozyme as a tool. *Small* (2006), **2**:3, 406-412.

19. Wang, Y.; Iqbal, Z.; Malhotra, S.V. Functionalization of carbon nanotubes with amines and enzymes. *Chemical Physics Letters* (2005), **402**, 96-101.

20. Georgakilas, V.; Tagmatarchis, N.; Pantarotto, D.; Bianco, A.; Briand, J.-P.; Prato, M. Amino acid functionalisation of water soluble carbon nanotubes. *Chemical Communications* (2002), 3050–3051.

21. Dodziuk, H.; Ejchart, A.; Anczewski, W.; Ueda, H.; Krinichnaya, E.; Dolgonosa, G.; Kutner, W. Water solubilization, determination of the number of different types of single-

wall carbon nanotubes and their partial separation with respect to diameters by complexation with h-cyclodextrin. *Chemical Communications* (2003), 986–987.

22. Kim, O.-K.; Je, J.; Baldwin, J.W.; Kooi, S.; Pehrsson, P.E.; Buckley, L.J. Solubilization of single-wall carbon nanotubes by supramolecular encapsulation of helical amylose. *Journal of American Chemical Society* (2004), **125**, 4426 - 4427.

23. Saleh, N.D.; Pfefferle, L.D.; Elimelech, M. Aggregation kinetics of multiwalled carbon nanotubes in aquatic systems: measurements and environmental implications. *Environmental Science and Technology* (2009), **42**:21, 7963–7969.

24. Enyashin, A.N.; Gemming, S.; Seifert, G. DNA-wrapped carbon nanotubes. *Nanotechnology* (2007), **18**, 245702.

25. Liu, J.; Rinzler, A.G.; Dai, H.J.; Hafner, J.H.; Bradley, R.K.; Boul, P.J.; Lu, A.; Iverson, T.; Shelimov, K.; Huffman, C.B.; Rodriguez-Macias, F.; Shon, Y.S.; Lee, T.R.; Colbert, D.T.; Smalley, R.E. Fullerene pipes. *Science* (1998), **280**:5367, 1253-1256.

26. O'Connell, M.J.; Bachilo, S.M.; Huffman, C.B.; Moore, V.C.; Strano, M.S.; Haroz, E.H.; Rialon, K.L.; Boul, P.J.; Noon, W.H.; Kittrell, C.; Ma, J.; Hauge, R.H.; Weisman, R.B.; Smalley, R.E. Band Gap Fluorescence from Individual Single-Walled Carbon Nanotubes. *Science* (2002), **297**, 593-596.

27. Salzmann, C.G.; Chu, B.T.T.; Tobias, G.; Llewellyn, S.A.; Green, M.L.H. Quantitative assessment of carbon nanotube dispersions by Raman spectroscopy. *Carbon* (2007), **45**:5, 907-912.

28. McDonald, T.J.; Engtrakul, C.; Jones, M.; Rumbles, G.; Heben, M.J. Kinetics of PL Quenching during Single-Walled Carbon Nanotube Rebundling and Diameter-Dependent Surfactant Interactions. *The Journal of Physical Chemistry B* (2006), **110**, 25339-25346.

29. Chappell, M.A.; George, A.J.; Dontsova, K.M.; Porter, B.E.; Price, C.L.; Zhou, P.; Morikawa, E.; Kennedy, A.J.; Steevens, J.A. Surfactive stabilization of multi-walled carbon nanotube dispersions with dissolved humic substances. *Environmental Pollution* (2009), **157**, 1081–1087.

30. Marsh, D.H.; Rance, G.A.; Zaka, M.H.; Whitby, R.J.; Khlobystov, A.N. Comparison of the stability of multiwalled carbon nanotube dispersions in water. *Physical Chemistry Chemical Physics* (2007), **9**:40, 5490-5496.

31. Lee, J.U.; Huh, J.; Kim, K.H.; Park, C.; Jo, W.H. Aqueous suspension of carbon nanotubes via non-covalent functionalization with oligothiophene-terminated poly(ethylene glycol). *Carbon* (2007), **45**, 1051-1057.

32. Jiang, J.; Gao, L. Production of aqueous colloidal dispersions of carbon nanotubes *Journal of Colloid and Interface Science* (2003), **260**, 89-94

33. Tseng, C.-H.; Wang, C.-C.; Chen, C.-Y. Modification of multi-walled carbon nanotubes by plasma treatment and further use as templates for growth of CdS nanocrystals. *Nanotechnology* (2006), **17**, 5602-5612.

34. Sinani, V.A.; Gheith, M.K.; Yaroslavov, A.A.; Rakhnyanskaya, A.A.; Sun, K.; Mamedov, A.A.; Wicksted, J.P.; Kotov, N.A. Aqueous dispersions of single-wall and multiwall carbon nanotubes with designed amphiphilic polycations. *Journal of the American Chemical Society* (2005), **127**:10, 3463-3472.

35. Bahr, J.L.; Mickelson, E.D.; Bronikovski, M.J.; Smalley, R.E.; Tour, J.M. Dissolution of small diameter single-wall carbon nanotubes in organic solvents. *Chemical Communications* (2001), 193-194.

36. Jia, G.; Wang, H.; Yan, L.; Wang, X.; Pei, R.; Yan, T.; Zhao, Y.; Guo, X. Cytotoxicity of carbon nanomaterials: single-wall nanotube, multi-wall nanotube, and fullerene. *Environmental Science and Technology* (2005), **39**, 1378–1383.

37. Murr, L.E.; Garza, K.M.; Soto, K.F.; Carrasco, A.; Powell, T.G.; Ramirez, D.A.; Cuererro, P.A.; Lopez, D.A.; Venzor, J. Cytotoxicity assessment of some carbon nanotubes and related carbon nanoparticle aggregates and the implications for anthropogenic carbon nanotube aggregates in the environment. *International Journal of Environmental Research and Public Health* (2005), **2**, 31-42.

38. Ding, L.H.; Stilwell, J.; Zhang, T.T.; Elboudware, J.O.; Jiang, H.J.; Selegue, J.P.; Cooke, P.A.; Gray, J.W.; Chen, F.F. Molecular characterization of the cytotoxic mechanism of multiwall carbon nanotubes and nanoonions on human skin fibroblast. *Nano Letters* (2005), **5**, 2448–2464.

39. Kang, S.; Herzberg, M.; Rodrigues, D.F.; Elimelech, M. Antibacterial effects of carbon nanotubes: size does matter! *Langmuir* (2008), **24**:13, 6409-6413.

40. Soto, K.F.; Carrasco, A.; Powell, T.G.; Garza, K.M.; Murr, L.E. Comparative in vitro cytotoxicity assessment of some manufactured nanoparticulate materials characterized by transmission electron microscopy. *Journal of Nanoparticle Research* (2005), **7**, 145-169.

41. Sayes, C.M.; Liang, F.; Hudsona, J.L.; Mendeza, J.; Guob, W.; Beach, J.M.; Moore, V.C.; Doyle, C.D.; West, J.L.; Billups, W.E.; Ausmanb, K.D.; Colvin, V.L. Functionalization density dependence of single-walled carbon nanotubes cytotoxicity in vitro. *Toxicology Letters* (2006), **161**:135–142.

42. Yu, B.Z.; Yang, J.S.; Li, W.X. In vitro capability of multi-walled carbon nanotubes modified with gonadotrophin releasing hormone on killing cancer cells. *Carbon* (2007), **45**:10, 1921-1927.

43. Yun, Y.; Dong, Z.; Tan, Z.; Schulz, M.J.; Shanov, V. Fibroblast cell behavior on chemically functionalized carbon nanomaterials. *Materials Science and Engineering C* (2009), **29**, 719–725.

44. Meng, J.; Yanga, M.; Song, L.; Kong, H.; Wang, C.Y.; Wang, R.; Wang, C.; Xie, S.S.; Xua, H.Y. Concentration control of carbon nanotubes in aqueous solution and its influence on the growth behavior of fibroblasts. *Colloids and Surfaces B: Biointerfaces* (2009), **71**, 148–153.

45. Simon-Deckers, A.; Gouget, B.; Mayne-L'Hermiteb, M.; Herlin-Boimeb, N.; Reynaudb, C.; Carrièrea, M. In vitro investigation of oxide nanoparticle and carbon nanotube toxicity and intracellular accumulation in A549 human pneumocytes. *Toxicology* (2008), **253**, 137-146.

46. Muller, J.; Huaux, F.; Moreau, N.; Misson, P.; Heilier, J.-F.; Delos, M.; Arras, M.; Fonseca, A.; Nagy, J.B.; Lison, D. Respiratory toxicity of multi-wall carbon nanotubes. *Toxicology and Applied Pharmacology* (2005), **207**:31, 221–231.

47. Kang, S.; Mauter, M.S.; Elimelech, M. Physicochemical determinants of multiwalled carbon nanotube bacterial cytotoxicity. *Environmental Science and Technology* (2008), **42**:19, 7528-7534.

48. Pulskamp, K.; Worle-Knirsch, J.M.; Hennrich, F.; Kern, K.; Krug, H.F. Human lung epithelial cells show biphasic oxidative burst after single-walled carbon nanotube contact. *Carbon* (2007), **45**, 2241–2249.

49. Cherukuri, P.; Gannon, C.J.; Leeuw, T.K.; Schmidt, H.K.; Smalley, R.E.; Curley, S.A.; Weisman, R.B. Mammalian pharmacokinetics of carbon nanotubes using intrinsic near-infrared fluorescence. *Proceedings of the National Academy of Sciences* (2006), **103**, 18882–18886.

50. Chen, X.; Tam, U.C.; Czlapinski, J.L.; Lee, G.S.; Rabuka, D.; Zettl, A.; Bertozzi, C.R. Interfacing carbon nanotubes with living cells. *Journal of the American Chemical Society* (2006), **128**, 6292-6293.

51. Flahaut, E.; Durrieu, M.C.; Remy-Zolghadri, M.; Bareille, R.; Baquey, C. Investigation of the cytotoxicity of CCVD carbon nanotubes towards human umbilical vein endothelial cells. *Carbon* (2006), **44**:6, 1093-1099.

52. Manna, S.K.; Sarkar, S.; Barr, J.; Wise, K.; Barrera, E.V.; Jejelowo, O.; Rice-Ficht, A.; Ramesh, G.T. Single-walled carbon nanotube induces oxidative stress and activates nuclear transcription factor-kB in human keratinocytes. *Nano Letters* (2005), **5**, 1676–1684.

53. Yang, H.; Liu, C.; Yang, D.; Zhanga, H.; Xia, Z. Comparative study of cytotoxicity, oxidative stress and genotoxicity induced by four typical nanomaterials: the role of particle size, shape and composition. *Journal of Applied Toxicology* (2009), **29**, 69–78.

54. Patlolla, A.; Tchounwou, P. Multiwalled carbon nanotube-induce cytotoxicity, genotoxicity and apoptosis in normal human dermal fibroblast cells. *Environmental and Molecular Mutagenesis* (2007), **48**:7, 563-563.

55. Kang, S.; Pinault, M.; Pfefferle, L.D.; Elimelech, M. Single-walled carbon nanotubes exhibit strong antimicrobial activity. *Langmuir* (2007), **23**:17, 8670–8673.

56. Zhu, Y.; Ran, T.; Li, Y.; Guo, J.; Li, W. Dependence of the cytotoxicity of multi-walled carbon nanotubes on the culture medium. *Nanotechnology* (2006), **16**, 4668–4674.

57. Shvedova, A.A.; Castranova, V.; Kisin, E.R.; Schwegler-Berry, D.; Murray, A.R.; Gandelsmann, V. Exposure to carbon nanotube material: assessment of nanotube cytotoxicity using human keratinocyte cells. *Journal of Toxicology and Environmental Health, Part A* (2003), **24**:1909–1926.

58. Elias, A.L.; Carrero-Sanchez, J.C.; Terrones, H.; Endo, M.; Laclette, H.P.; Mauricio, M. Viability studies of pure carbon- and nitrogen-doped nanotubes with *Entamoeba*

Histolytica: from amoebicidal to biocompatible structures. *Small* (2007), **3**:10, 1723 – 1729.

59. Xu, F.-M.; Xu, J.-P.; Ji, J.; Shen, J.-C. A novel biomimetic polymer as amphiphilic surfactant for soluble and biocompatible carbon nanotubes (CNTs). *Colloids and Surfaces B: Biointerfaces* (2008), **67**, 67–72.

60. Yang, S.-T.; Wang, X.; Jia, G.; Guc, Y.; Wang, T.; Nie, H.; Ge, C.; Wang, H.; Liu, Y. Long-term accumulation and low toxicity of single-walled carbon nanotubes in intravenously exposed mice. *Toxicology Letters 181 (2008)* (2008), **181**, 182–189.

61. Ye, S.-F.; Wu, Y.-H.; Hou, Z.-Q.; Zhang, Q.-Q. ROS and NF-jB are involved in upregulation of IL-8 in A549 cells exposed to multi-walled carbon nanotubes. *Biochemical and Biophysical Research Communications* (2009), **379**, 643–648.

62. Fiorito, S.; Serafino, A.; Andreola, F.; Bernier, P. Effects of fullerenes and single-wall carbone nanotubes on murine and human macrophages. *Carbon* (2006), **44**, 1100–1105.

63. Wick, P.; Manser, P.; Limbach, L.K.; Dettlaff-Weglikowskab, U.; Krumeich, F.; Roth, S.; Stark, W.J.; Bruinink, A. The degree and kind of agglomeration affect carbon nanotube cytotoxicity. *Toxicology Letters* (2007), **168**, 121-131.

64. Vittorio, O.; Raffa, V.; Cuschieri, A. Influence of purity and surface oxidation on cytotoxicity of multi-wall carbon nanotubes with human neuroblastoma cells. *Nanomedicine: Nanotechnology, Biology, and Medicine* (2009), **accepted**.

65. Bardi, G.; Tognini, P.; Ciofani, G.; Raffa, V.; Costa, M.; Pizzorusso, T. Pluronic-coated carbon nanotubes do not induce degeneration of cortical neurons in vivo and in vitro. *Nanomedicine: Nanotechnology, Biology, and Medicine* (2009), **5**, 96–104.

66. Inoue, K.-i.; Koike, E.; Yanagisawa, R.; Hirano, S.; Nishikawa, M.; Takano, H. Effects of multi-walled carbon nanotubes on a murine allergic airway inflammation model. *Toxicology and Applied Pharmacology* (2009), **237** 3, 306-316.

67. Herzog, E.; Byrne, H.J.; Davoren, M.; Casey, A.; Duschl, A.; Oostingh, G.J. Dispersion medium modulates oxidative stress response of human lung epithelial cells upon exposure to carbon nanomaterial samples. *Toxicology and Applied Pharmacology* (2009), **236**, 276–281.

68. Wörle-Knirsch, J.M.; Pulskamp, K.; Krug, H.F. Oops they did it again! Carbon nanotubes hoax scientists in viability assays. *Nano Letters* (2006), **6**:6, 1261-1268.

69. Chin, S.F.; Baughman, R.H.; Dalton, A.B.; Diekmann, G.R.; Draper, R.K.; Mikoryak, C.; Musselman, I.H.; Poenitzsch, V.Z.; Xie, H.; Pantano, P. Amphiphilic helical peptide enhances the uptake of single-walled carbon nanotubes by living cells. *Experimental Biology and Medicine* (2007), **232**:9, 1236–1244.

70. Monteiro-Riviere, N.A.; Nemanich, R.J.; Inman, A.O.; Wang, Y.Y.; Riviere, J.E. Multi-walled carbon nanotube interactions with human epidermal keratmocytes. *Toxicology Letters* (2005), **155**, 377–384.

71. Gutie´rrez, M.C.; Garcıa-Carvajal, Z.Y.; Hortiguela, M.J.; Yuste, L.; Rojo, F.; Ferrer, M.L.; Monte, F. Biocompatible MWCNT scaffolds for immobilization and proliferation of *E. coli. Journal of Materials Chemistry* (2007), **17**, 2992–2995.

72. Kang, S.; Mauter, M.S.; Elimelech, M. Microbial cytotoxicity of carbon-based nanomaterials: implications for river water and wastewater effluent. *Environmental Science and Technology* (2009), **43**:7, 2648–2653.

73. Lindberg, H.K.; Falck, G.C.-M.; Suhonen, S.; Vippola, M.; Vanhalab, E.; Catalána, J.; Savolainena, K.; Norppa, H. Genotoxicity of nanomaterials: DNA damage and micronuclei induced by carbon nanotubes and graphite nanofibres in human bronchial epithelial cells in vitro. *Toxicology Letters* (2009), **186**, 166–173.

74. Wirnitzer, U.; Herbold, B.; Voetz, M.; Ragot, J. Studies on the in vitro genotoxicity of baytubes®, agglomerates of engineered multi-walled carbon-nanotubes (MWCNT). *Toxicology Letters* (2009), **186**, 160–165.

75. Di Sotto, A.; Chiaretti, M.; Carru, G.A.; Bellucci, S.; Mazzantia, G. Multi-walled carbon nanotubes: Lack of mutagenic activity in the bacterial reverse mutation assay. *Toxicology Letters* (2009), **184**, 192–197.

76. Upham, B.L.; Masten, S.J.; Lochwood, B.R.; Trosko, J.E. Nongenotoxic effects of polycyclic aromatic hydrocarbons and their ozonation by-products on the intercellular communication of rat liver epithelial cells. *Fundamental and Applied Toxicology* (1994), **23**, 470-475.

77. Trosko, J.E.; Chang, C.-C.; Upham, B.; Wilson, M. Epigenetic toxicology as toxicant-induced changes in intracellular signalling leading to altered gap junctional intercellular communication. *Toxicology Letters* (1998), **102-103**, 71-78.

78. Narayan, R.J.; Berry, C.J.; Brigmon, R.L. Structural and biological properties of carbon nanotube composite films. *Materials Science and Engineering: B* (2005), **123**:123-129.

79. Lyon, D.Y.; Fortner, J.D.; Sayes, C.M.; Colvin, V.L.; Hughes, J.B. Bacterial cell association and antimicrobial activity of a C_{60} water suspension. *Environmental Toxicology and Chemistry* (2005), **24**, 2757–2762.

80. Thill, A.; Zeyons, O.; Spalla, O.; Chauvat, F.; Rose, J.; Auffan, M.; Flank, A.M. Cytotoxicity of CeO_2 nanoparticles for Escherichia coli. Physico-chemical insight of the cytotoxicity mechanism. *Environmental Science and Technology* (2006), **40**:19, 6151-6156.

81. Tong, Z.; Bischoff, M.; Nies, L.; Applegate, B.; Turco, R. Impact of fullerene (C_{60}) on a soil microbial community. *Environmental Science and Technology* (2007), **41**, 2985–2991.

82. Schmitt, D.; Tran, N.; Riefler, S.; Jacoby, J.; Merkel, D.; Marone, P.; Naouli, N. Toxicologic evaluation of modified gum acacia: mutagenicity, acute and subchronic toxicity. *Food and Chemical Toxicology* (2008), **46**, 1048–1054.

83. Burnette, L.W. A review of the physiological properties of PVP. *Proceedings of the Scientific Section of the Toilet Goods Association* (1960), **38**, 1-4.

84. Chourasia, M.K.; Jain, S.K. Polysaccharides for colon targeted drug delivery. *Drug Delivery* (2004), **11**:2, 129–148.

85. Dayeh, V.R.; Chow, S.L.; Schirmer, K.; Lynn, D.H.; Bols, N.C. Evaluating the toxicity of Triton X-100 to protozoan, fish, and mammalian cells using fluorescent dyes as indicators of cell viability. *Ecotoxicology and Environmental Safety* (2004), **57**:3, 375–382.

86. Borenfreund, E.; Puerner, J.A. Toxicology determined in vitro by morphological alterations and neutral red absorption. *Toxicology Letters* (1985), **24**, 119-124.

87. Herner, H.A.; Trosko, J.E.; Masten, S.J. The Epigenetic Toxicity of Pyrene and Related Ozonation Byproducts Containing an Aldehyde Functional Group. *Environmental Science and Technology* (2001), **35**:17, 3576-3583.

88. Satoh, A.Y.; Trosco, J.E.; Masten, S.J. Epigenetic toxicity of hydroxylated biphenyls and hydroxylated polychlorinated biphenyls on normal rat liver epithelial cells. *Environmental Science and Technology* (2003), **37**, 2727-2733.

89. Weis, L.M.; Rummel, A.M.; Masten, S.J.; Trosko, J.E.; Upham, B.L. Bay or baylike regions of polycyclic aromatic hydrocarbons were potent inhibitors of gap junctional intercellular communication *Environmental Health Perspectives* (1998), **106**:1, 17-22.

90. Trosko, J.E.; Chang, B.V.; Madhucar, J.E.; Klauning, J.E. Chemical, Oncogene, and growth factor inhibition of gap junctional intercellular communication: an alternative hypothesis to carcinogenesis. *Pathobiology* (1991), **58**, 265-278.

91. Yamasaki, Y. Gap junctional intercellular communication and carcinogenesis. *Carcinogenesis* (1990), **11**, 1051-1058.

92. Huang, W.J.; Taylor, S.; Fu, K.F.; Lin, Y.; Zhang, D.H.; Hanks, T.W.; Rao, A.M.; Sun, Y.P. Attaching proteins to carbon nanotubes via diimide-activated amidation. *Nano Letters* (2002), **2**:4, 311-314.

93. Atlas, R.M. Handbook of microbiological media. 1993, Boka Raton: CRC Press.

94. Fortner, J.D.; Lyon, D.Y.; Sayes, C.M.; Boyd, A.M.; Falkner, J.C.; Hotze, E.M.; Alemany, L.B.; Tao, Y.J.; Guo, W.; Ausman, K.D.; Colvin, V.L.; Hughes, J.B. C_{60} in water: nanocrystal formation and microbial response. *Environmental Science and Technology* (2005), **39**:11, 4307-4316.

95. El-Fouly, M.H.; Trosko, J.E.; Chang, C.C. Scrape-loading and dye transfer: a rapid and simple technique to study gap junctional intercellular communications. *Experimental Cell Research* (1987), **168**, 422-430.

96. Tang, Y.J.; Ashcroft, J.M.; Chen, D.; Min, G.; Kim, C.-H.; Murkhejee, B.; Larabell, C.; Keasling, J.D.; Chen, F.F. Charge-associated effects of fullerene derivatives on microbial structural integrity and central metabolism. *Nano Letters* (2007), **7**:3, 754-760.

CHAPTER 3

PHYSICOCHEMICAL PROPERTIES AND TOXICITY OF FULLERENE nC$_{60}$ DERIVATIVES FORMED DURING OZONATION AND CHLORINATION

3.1. Introduction

3.1.1. Toxicity of nC$_{60}$ aggregates

The fullerene molecule, which has numerous potential uses in electronic, optical and separation systems [1-3], is highly reactive and is able to participate in the reactions of nucleophilic and electrophilic substitution [4], to form transitional complexes with metals [5] and is photosensitive [6]. Different methods have been reported for the production of water soluble fullerene aggregates nC$_{60}$: prolonged mixing/sonication of pristine fullerene with water [7-14]; solvent exchange with organic solvents (tetrahydrofuran (THF), ethanol, toluene, polyvinylpyrrolidone (PVP) or toluene/trichloromethane/PVP) following by its extraction from the suspension by rotor evaporation, boiling or by purging nitrogen gas [7-9, 12, 13, 15-22]; ultrasonication in toluene [8, 9, 23], water/sodium dodecylsulfate [24] or sulfuric/nitric acids mixture [25]; solubilization through complex formation with cyclodextrin [26] or liposomes [27].

The toxicity of nC$_{60}$ aggregates has been systematically examined in a number of studies [7, 10-17, 20-22, 24, 28-48], and the main findings are summarized in Table 3.1. The toxicity was found to depend on many factors including preparation method [7, 12, 13, 35, 41], surface chemistry [20, 29, 31, 33, 40, 43, 44], biological model (*in vitro* versus *in vivo*) [13, 31], and the cell [15, 16, 33, 36, 40, 43] or organism type [28, 35].

nC_{60} aggregates prepared by the solvent exchange method are considered to be more toxic as compared to solvent-free *n*C_{60} based on *in vivo* [20] and *in vitro* [7, 12, 22, 41] bioassays. When THF was used as an intermediate solvent, THF/*n*C_{60} aggregates were responsible for the loss of the membrane integrity in human dermal fibroblast cells, human liver carcinoma cells and neuronal human astrocyte cells [30] and mouse fibrosarcoma cells, rat and human glioma cells [42]. By conducting *in vitro* toxicity testing with a range of mammalian cell lines (human dermal fibroblasts, mouse fibrosarkoma and melanoma cells) and applying mathematical modeling, Markovich et al. [7] ranked *n*C_{60} aggregates by their ability to cause cell necrosis in the following order: THF-derived *n*C_{60} (THF/*n*C_{60}) > ethanol-derived *n*C_{60} (EtOH/*n*C_{60}) > *n*C_{60} solubilized without any organic solvent (aqu/*n*C_{60}). Similar results were reported by Spohn et al. [13] by using human epithelial cells. Levi et al [37] found that *n*C_{60} aggregates prepared by mixing with water, did not affect human epithelial cells while THF/*n*C_{60} aggregates caused acute toxicity. However, when potential by-products from THF/*n*C_{60} formation were removed from the system by washing, THF/*n*C_{60} had no longer adverse effects on the cells. Water-soluble fullerene aggregates, prepared with toluene as an intermediate solvent (Tol/*n*C_{60}), did not suppress the life cycle of human epithelial and human liver carcinoma cells.

nC$_{60}$ aggregates, prepared without using intermediate solvents, exhibited significantly lower or no toxicity to a range of aquatic species as compared to solvent-derived aggregates. No toxic effects were observed in benthic *Hyalella aztecaat* at concentrations up to 0.7 mg/L, marine harpacticoid copepods at concentrations up to 2.25 mg/L and fathead minnow and Japanese medaka at 0.05 mg/L of nC$_{60}$ [10]. In contrast, THF/nC$_{60}$ aggregates were cytotoxic towards fathead minnow (100% mortality after 6-18 hrs of exposure to 0.5 mg/L of THF/nC$_{60}$) [35], zebrafish (pericardial edema, delay in embryo and larval development and hatching rate after exposure to 1.5 mg/L of THF/nC$_{60}$ [34]) and *Daphnia* species (LC$_{50}$ = 0.46 mg/L after 48 hrs of exposure [38] and significant mortality at 5 mg/L [20]). No toxic effects were observed upon exposure of *Ceriodaphnia dubia* (> 3 mg/L, [11]) and *Daphnia magna* (24 mg/L) to washed THF/nC$_{60}$ [13].

The cytotoxicity of nC$_{60}$ aggregates towards bacterial cells was assessed in a number of bioassays [12, 14-16, 22, 24, 32, 36, 39-41, 43]. In all studies but one, THF/nC$_{60}$ was found to significantly affect the viability of microbial cells. For example, THF/nC$_{60}$ aggregates inhibited the growth of *B. subtilis* (0.4 mg/L [43], 0.5-0.75 mg/L [36] and 1.5-3 mg/L [40]); *E. coli* ($\geq$ 0.4 mg/L [43] and 0.5-1 mg/L [40]), and *P. putida* (0.25-0.5 mg/L [36]). However, one recent study reported that THF/nC$_{60}$ exposed to a soil microbial community did not significantly affect its structure and function [32]. The difference in toxicity effects between aggregates formed with and without THF as a solubilizing aide was attributed to the synergetic effects between the

residual THF and nC$_{60}$ [24] or to the formation of THF hydroperoxide and other reaction by-products during the preparation of THF/nC$_{60}$ [13, 22]. When aggregates were produced by the solvent-assisted technique in which solvents other than THF were used (i.e., ethanol/methanol mixture or o-xylene) as a solubilizing aide, an anaerobic microbial community was not affected over several months of observation [39].

When comparing the toxicity of aqueous versus solvent-assisted aggregates towards bacterial cells, less toxicity to *E. coli* [12, 14, 24] or *B. subtilus* [41] was observed in the case of aqu/nC$_{60}$ as compared to THF/nC$_{60}$ [12, 41] or PVP/nC$_{60}$ [12]. Interestingly, aqu/nC$_{60}$ obtained by direct mixing of pristine fullerene with water were toxic upon addition to *E. coli* [14], while aqu/nC$_{60}$ produced through grinding/sonication procedure and exposed to *E. coli* resulted in no inhibition of cell growth [24].

Table 3.1. Toxicity of fullerene aggregates to different organisms.

Fullerene type	Concentration range tested	Organism type	Effect	Reference
Toxicity to bacterial cells				
-THF/*n*C_{60} -$C_{60}(OH)_{22-24}$	0.04-4 mg/L (THF/*n*C_{60}) 5 mg/L ($C_{60}(OH)_{22-24}$)	*E. coli* *B. subtilus*	-No growth for both bacteria at > 0.4 mg/L in MD medium -$C_{60}(OH)_{22-24}$: no significant toxicity	[43]
-THF/*n*C_{60} -$C_{60}(OH)_{22-24}$	*n*C_{60}: 0.04-7.5 mg/L $C_{60}(OH)_{22-24}$: 5 mg/L	*E. coli* *B. subtilus* *V. fisheri*	-THF/*n*C_{60}: MIC: 0.5-1 mg/L (*E. coli)* and 1.5-3 mg/L (*B. subtilus*) MBC: 1.5-3 mg/l (*E. coli*) and 2-4 mg/L (*B. subtilus*) EC_{50}: 1.08 *mg/L* (*V. fisheri*) -$C_{60}(OH)_{22-24}$: no toxic effects	[40]
-aqu/*n*C_{60}: grinding followed by sonication	5 mg/L	*E. coli*	-Growth curves for aqu/*n*C_{60} and control samples (no aqu/*n*C_{60}) were within the experimental error	[24]

Table 3.1 (cont'd)

-THF/C_{60} -Tol/*n*C_{60} -aqu/*n*C_{60}: stirring with water -PVP/C_{60}	n/a	*B. subtilus*	-THF/C_{60}: MIC: 0.09±0.01 mg/L -Tol/*n*C_{60}: MIC: 0.7±0.3 mg/L -aqu/*n*C_{60}: MIC: 0.5±0.13 mg/L -PVP/C_{60}: MIC: 0.95±0.35 mg/L	[41]
-THF/C_{60}	0.01-0.5 mg/L (*P.putida*) 0.01-0.5 mg/L (*B.subtilus*)	*P. putida* *B .subtilus*	-MIC (*B.subtilus*): 0.5-0.75 mg/L -MIC (*P.putida*): 0.25-0.5 mg/L	[36]
-C_{60}-OH, C_{60}-COOH and C_{60}-NH_2: solvent exchange with toluene -as-received C_{60}	20 mg/L (C60) 20-80 mg/L (C_{60}-OH and C_{60}-COOH) 1-80 mg/L (C60-NH2)	*E. coli* *S. oneidensis*	-C_{60}, C_{60}-OH and C_{60}-COOH did not significantly inhibit bacterial growth -C_{60}-NH_2 strongly inhibited bacterial growth	[33]
-as-received C_{60} -THF/*n*C_{60}	1000 µg/g soil (C_{60}) 1 µg/g soil (THF/ *n*C_{60})	*Surface soil microcosm*	-Both C_{60} and THF/*n*C_{60} did not show toxic effects	[32]
-THF/*n*C_{60}	10 mg/L	*E. coli* *B. subtilis*	Exerts ROS-independent oxidative stress to bacterial cells	[16]
-THF/*n*C_{60}	5 mg/L	*E. coli* *B. subtilis*	*E. coli*: cells integrity was not compromised, no changes in membrane potential *B. subtilis*: changes in membrane potential	[15]

Table 3.1 (cont'd)

-as-received fullerene dissolved in o-xylene following by solvent evaporation and coating	0.027 and 1.4 mg/L	Anaerobic wastewater treatment sludge	-C_{60} did not have significant impact on the anaerobic community for a period of few months	[39]
-THF/*n*C_{60} -PVP/*n*C_{60} aqu/*n*C_{60}: stirring with water	140 µM	*E. coli*	THF/*n*C_{60}: cytotoxic PVP/*n*C_{60}: no cytotoxicity aqu/*n*C_{60}: no cytotoxicity	[12]
-aqu/*n*C_{60}: stirring with water	0.36-1.46 mg of total carbon/L	*E. coli* *V. fisheri*	-EC_{50}: 0.82 mg of total carbon/L after 30 min of exposure to *V. fisheri* -Inhibited growth and respiratory activity of *E. coli*	[14]
-THF/*n*C_{60} washed with water	0-10 mg/L	*E. coli*	-Ozonated C_{60} up to 10 mg/L did not cause significant growth inhibition or inactivation E.coli in the absence either oxygen or light - Ozonated C_{60} up to 10 mg/L inactivated *E. coli* in the presence of both oxygen and light	[48]

Table 3.1 (cont'd)

-aqu/nC_{60}: stirring with Suwannee River water	n/a	*Ceriodaphnia Dubia MetPLATE^{TM} test with E. coli*	No toxicity at > 3 mg/L	[11]
A set of cationic and anionic fullerene derivatives	n/a	*E. coli* MS-2 bacteriophage	-Anionic derivatives did not inhibit *E. coli* growth in the dark -Cationic derivative was cytotoxic to *E. coli* at 140 μM and MS-2 bacteriophage at 50 μM	[46]
-THF/nC_{60} washed with water	0.03-2 mg/L	*E. coli*	Toxicity of nC_{60} aggregates strongly depended on the number of washings: MIC (1 washing): 0.03 mg/L; MIC (12 washing): 1 mg/L	[22]
Toxicity to aquatic organisms				
-aqu/nC_{60}: stirring with water	0-5 mg/L (*Daphnia magna*) 7 mg/L (*Hyalella azteca*) 22.5 mg/L (*Coppercod*:) 0.5 mg/L (*Pimephales promelas* and *Ozyzias latipes*)	*A set of aquatic organisms*	-*Daphnia magna* 21 day exposure test: delay in molting and reducing off spring production at 2.5 mg/L -*Hyalella azte*ca: no acute toxicity at 7 ppm -Coppercod: treated animals did not respond differently from control group -*Ozyzias latipes and Pimephales promelas*: no acute toxicity for up to 96 h	[28]

Table 3.1 (cont'd)

-aqu/nC$_{60}$: sonication with water -THF/nC$_{60}$	0.2-9 mg/L (aqu/nC$_{60}$) 40-880 µg/L (THF/nC$_{60}$)	*Daphnia magna*	- aqu/nC$_{60}$: LC$_{50}$ 7.9 mg/L - THF/nC$_{60}$: LC$_{50}$ 460 µg/L	[38]
-THF/nC$_{60}$	0.5 mg/L	Juvenile Largemouth Bass	Lipid peroxidation in brains of fish at 0.5 mg/L after 48 h of exposure	[10]
- THF/nC$_{60}$ - aqu/nC$_{60}$: stirring with water	0-2000 µg/L (THF/nC$_{60}$) 0-35 mg/L (aqu/nC$_{60}$)	*Daphnia magna, Pimephales promelas*	-*Daphnia magna* 48 h LC$_{50}$ is 0.8 ppm for THF/nC$_{60}$ and is >35 mg/L for aqu/nC$_{60}$ -*Pimephales promelas*:100% mortality between 6 and 18 h for THF/nC$_{60}$ and no obvious effects after 48 h THF/nC$_{60}$	[35]
-C$_{60}$ and C$_{60}$(OH)$_{24}$ were sonicated in dimethyl sulfoxide	50-300 µg/L	*Embryonic zebrafish*	-C$_{60}$ induced mortality, fin malformation and pericardial edema under in both light and dark conditions -C$_{60}$ depleted glutathione -stress response genes were up-regulated following the exposure to C$_{60}$	[44]

Table 3.1 (cont'd)

- THF/nC$_{60}$ -aqu/nC$_{60}$: stirring with moderately hard reconstituted water -C$_{60}$(OH)$_{24}$ -C$_{60}$-C$_{70}$Hx	0-500 mg/L	*Daphnia pulex*	-Acute toxicity at 500 mg/L upon exposure to all types of nC$_{60}$, with THF/nC$_{60}$ causing the highest mortality -Production of toxicity biomarkers glutaqthione-S-transferase and catalase was significant at concentrations below 100 mg/L	[20]
-Tween80/nC$_{60}$: bead milling with Tween80	4.3-4.6 mg/L	*Cyprinos Carpio*	No lipid peroxidation in *Cyprinos Carpio* brain after 48 h of exposure	[45]
- THF/nC$_{60}$ washed with water -aqu/nC$_{60}$: stirring with water	0-24 mg/L	*Daphnia magna* Human lung epithelial cells	-No acute toxicity to *Daphnia magna* after 48 h of contact for both nC$_{60}$ types -No influence on ROS induction by both fullerene types	[13]

[1]MIC - minimum inhibitory concentration, [2]MBC - minimum bacteriostatic concentration

Oxidative stress to a living cell exerted by nC$_{60}$ aggregates, was suggested as a possible mechanism of fullerene toxicity to eukaryotic [7, 13, 28-30, 42, 44] and prokaryotic [12, 15, 16, 22] cells. For the eukaryotic cell, the observed toxicity was attributed to the formation of reactive oxygen species (ROS), which caused lipid peroxidation [28-30], altered key response genes [44] and led to the ROS-associated mitohondrical dysfunction followed by cell necrosis [7, 42]. However, while studying the photoactivity of fullerene aggregates, Brunet et al. [12] did not observe a correlation between the ROS production and antibacterial activity for the nC$_{60}$ aggregates, prepared by mixing with water, solvent exchange with THF and encapsulated with PVP [12]. ROS-independent oxidative stress caused by direct contact between the fullerene nanoparticle and the bacterial cell, resulted in protein oxidation in the cell membrane, was also suggested to explain the cytotoxicity of fullerene aggregates [12, 15, 16].

To date, most of toxicological studies on nC$_{60}$ aggregates were focused on the evaluation of their cytotoxic effects. Genotoxicity and epigenetic toxicity are important factors in evaluating carcinogenic potency of a chemical. While the first phase of carcinogenesis (tumor initiation) usually requires a genotoxic/mutagenic agent [49, 50], the second phase (tumor promotion) needs an epigenetic tumor promoter [50, 51]. The genotoxicity of nC$_{60}$ was studied by several researches [17, 21, 44]. Dhawan et al. [17] reported that nC$_{60}$ aggregates, prepared by two methods (extended mixing with water and solvent exchange with ethanol), were genotoxic to human lymphocytes at concentrations as low as 12 μg/L. Liang et al. [21] showed that nC$_{60}$ prepared by solvent exchange with toluene/$CHCl_3$/PVP could disrupt DNA replication *in vitro*

by binding to DNA and changing the conformation of DNA templates. Alteration in gene expression of several key stress response genes upon exposure of embryonic zebrafish to fullerene dispersed in dimethylsulfoxide was observed [44]. No studies into epigenetic toxicity of the fullerene molecule have been reported.

3.1.2. Oxidation of nC$_{60}$ aggregates

Fullerene could potentially enter water supply systems making it susceptible to oxidation or chlorination during disinfection. Like naturally occurring organic matter (NOM) which reacts with disinfectants to produce toxic byproducts [52-57], the fullerene molecule, which also consists of carbon atoms, may also react to form its own set of disinfection byproducts. The reaction of fullerene with ozone has been studied in both organic (e.g, carbon tetrachloride [58, 59] and toluene [60]) and in aqueous media [61]. The reaction between ozone and water soluble fullerene aggregates in water was found to follow a general second order reaction [62] and resulted in the formation of water soluble fullerene oxides with repeating hydroxyl and hemiketal functionalities [61]. Due to the strong electron-attractive nature of the fullerene molecule [4], the chlorination of fullerenes has been previously achieved only under extreme conditions [63-65].

Although the toxicity of nC$_{60}$ aggregates has been broadly investigated, there is lack of systematic investigations of the potential adverse effects of nC$_{60}$ byproducts formed during ozonation and chlorination processes, or the combination of both. Recently, Cho et al. [48] demonstrated that THF/nC$_{60}$ ozonated at CT value of 150 mg/L/min were neither directly antibacterial nor bactericidal to *E. coli* at concentrations up to 10 mg/L.

3.1.3. The objectives and experimental approach.

The objectives of our research were (1) to evaluate the physicochemical properties of nC$_{60}$ aggregates, formed during treatment with ozone and chlorine and (2) to evaluate if cyto- and epigenetic toxicity of the derivatized aggregates would be altered as compared to as-prepared nC$_{60}$.

Four batches of nC$_{60}$ suspensions were prepared and subjected to the oxidation schemes as is described in Figure 3.1. *The first batch* was used to assess cytotoxicity of nC$_{60}$ aggregates in a dose-response manner as a function of the applied ozone dose and reaction time. *The second and third batches* were used to investigate the physicochemical properties (UV-vis adsorption, aggregate size and ζ-potential) and cyto- and epigenetic toxicity of nC$_{60}$ aggregates as a function of applied chlorine/ozone dose and reaction time. *The fourth batch* was used to investigate the effect of oxidation processes on the surface functionality (type and amount of functional groups) of nC$_{60}$ aggregates.

In our study we employed the general viability bioassay with *E. coli* and NRU bioassay with WB-F344 rat liver epithelia cells to evaluate the cytotoxicity of as-prepared and oxidized nC$_{60}$ aggregates to prokaryotic and eukaryotic cells, respectively.

The general viability bioassay with *E. coli* is a microbial bioassay that investigates the ability of bacteria to grow and form a colony in the presence of a chemical [66]. *E. coli* was used widely

in the past to evaluate the toxicity of fullerene and its derivatives [12, 14-16, 22, 24, 33, 40, 43]. A number of standard nutrient media to maintain *E.coli*, varied in organic and electrolyte content, have been recommended [67]. Several researches found significant loss of nC_{60} toxicity where the bioassay was performed in a medium with higher ionic strength. The loss in toxicity is believed to be due to enhanced aggregation of nC_{60} [40, 43]. Further, the organic constituents of the nutrient medium could possibly interact with nC_{60} aggregates and alter their toxicity. Hence, in this study three types of media (Luria-Bertani (LB), Minimal Davis (MD) and 0.1 M NaCl) with different in ionic strength and organic content were employed to comprehensively evaluate the cytotoxicity of nC_{60} aggregates to *E. coli.*

The NDU measures cell integrity based on the fact that normal cells in culture readily absorb and retain the dye. When the cell membrane or the lysosomes inside the cell are damaged by an irritating chemical, the dye will be lost through the leaky membrane and its amount can be quantified [68].

The epigenetic toxicity of as-prepared and oxidized nC_{60} aggregates was evaluated in WB-F344 rat liver epithelia cells by using a specific nongenotoxic assay that measures changes in the gap junction intercellular communications [69]. GJIC measurements are based on the scrape loading/dye transferring technique; more detailed information can be found elsewhere [68, 70-72]. The bioassay was conducted at concentrations of nC_{60} and its derivatives that did not cause cytotoxicity as determined by the NDU. This was done because cytotoxicity can mimic some

physiological responses by inducing compensatory hyperplasia, which simulates, in part, noncytotoxic mitogenesis [71].

3.2. Materials and methods

3.2.1. Materials

Powdered fullerene (>99%) was purchased from Materials Research Electronics Corporation (Tuscon, AZ). Formaldehyde solution (37%), calcium chloride, magnesium chloride, sodium chloride, potassium phosphate monobasic, potassium phosphate dibasic, sodium citrate, sodium bisulphate and glucose were purchased from JT Baker (Phillipsburg, NJ). Neutral red dye (3-amino-7-(dimethylamino)-2-methylphenazine hydrochloride), acetic acid, glacial, magnesium sulfate heptahydrate, ammonium sulfate were received from Sigma-Aldrich (Milwaukee, WI). Ethyl alcohol, anhydrous was purchased from Pharmco Products Inc. (Brookfield, CT). Bacto™ yeast extract, Bacto™ tryptrone and Bacto™ agar were obtained from Difco Laboratories (Sparks, MD). Dilithium salt of Lucifer yellow dye was purchased from Molecular Probes Inc. (Eugene, OR). Fetal bovine serum and gentamicin were obtained from Gibco Laboratories (Grand Island, NY).

The ultrapure water used in the entire set of experiments was supplied by a commercial ultrapure water system (Lab Five, USFilter Corp., Hazel Park, MI) equipped with a terminal 0.2 µm capsule microfilter (PolyCap, Whatman Plc., Sanford, ME).

3.2.2. Production of nC_{60} suspensions

nC_{60} suspensions were produced by modifying the procedure described by Deguchi et al. [24]. As-received fullerene powder (500 mg) was ground in the jar grinder (Model # 764AVW, U.S. Stoneware, Ohio, USA) with two zirconium oxide balls as grinding medium and then transferred to a glass bottle with 500 mL of ultra-pure water and sonicated in an Aquasonic 50T water bath (VWR Scientific Products Corp, West Chester, PA) for 7 days. The suspension was then filtered through the 0.45 μm microfilter (Millipore Corp, New Bedford, MA) and diluted to a final concentration of 7.5 mg/L with ultrapure water.

3.2.3. Quantification of nC_{60} in suspensions

The concentrations of nC_{60} aggregates were measured by the method described by Dhawan et al. [17]**.** The suspension (30 mL) was transferred into 250 mL round-bottom flask and heated in a water bath at 70 ^{o}C until the water was fully evaporated. The dry deposit was redissolved in 5 mL of toluene and sonicated in an Aquasonic 50T water bath (VWR Scientific Products Corp, West Chester, PA) for 1 hour. The UV-vis absorption spectra of the fullerene solution in toluene were recorded using a photodiode array spectrophotometer (Multi-spec 1501, Shimadzu, Kyoto, Japan). Calibration standards for C_{60} in toluene in the range of (0.4-26.6 mg/L) were prepared by the sequential dilution of the sample with the highest concentration.

3.2.4. Oxidation schemes

Gaseous ozone was produced from pure oxygen gas (99.99% purity, Airgas Inc., MI) using an ozone generator (Model # OZ2PCS, Ozotech Inc, Yreca, CA). In the first oxidation scheme, an ozone solution was prepared by bubbling ozone gas through the ultrapure water. The concentration of dissolved ozone was measured by ozone microsensor (AMT Analysenmesstechnik GmbH, Rostock, Germany). A suspension of as-prepared nC$_{60}$ suspension was diluted to 0.2, 3.6, 5 or 7.5 mg/L and spiked with the ozone solution to result in an initial dissolved ozone concentration of 0.36 mg/L in each vial. After the desired time (2 or 33 min), the samples were purged with the ultrapure nitrogen gas to strip any residual ozone. The dissolved ozone concentration and exposure times were chosen to simulate the EPA CT values of 0.72 and 12 min·mg/L which are required for 3 log deactivation of *Giardia* cysts and *Cryptosporidium* at 20 ^{o}C, accordingly [73]. In the second oxidation scheme, ozone gas at a gas-phase concentration of 5 g/m^{3} was bubbled through 250 mL of 7.5 mg/L as-prepared nC$_{60}$ suspension. The reaction chamber was placed on the magnetic stirrer (Model # PC-510, Corning Inc., Lowell, MA) and the suspension was mixed using the stir bar. The volumetric flow rate of ozone gas was set at 1039±50 mL/min with a direct reading flow meter (Model EW-32033-10, Cole-Parmer**,** Vernon Hills, Il) and the ozone gas-phase concentration was measured with an ozone gas monitor (Model # 450H, Teledyne Instruments, City of Industry, CA). Approximately 2.5 mL of the suspension was collected every 30 min through the stopcock positioned in the lower part of the reaction vessel and the absorption spectra were recorded by using a photodiode array spectrophotometer (Multi-spec 1501, Shimadzu, Kyoto, Japan). The oxidation reaction was allowed to proceed until the absorbance at 346 nm had decreased by 25, 50, 75 or 90%.

Following ozonation, the suspensions were dosed with an aliquot of standardized sodium hypochloride stock solution to result in a chlorine dose of 6.8 or 68 mg (Cl_2)/L and allowed to react for 10 or 100 min depending on the treatment scheme. At the desired time, the residual chlorine was quenched by addition of 0.1M sodium bisulfite. The stock hypochlorite solution was standardized according to the method 4500-Cl.B. [74]. Chlorine dosing solution was prepared according to the method 5710B [74].

3.2.5. Physicochemical characterizations of *n*C_{60} suspensions

The XPS technique was employed to evaluate surface functionality of *n*C_{60} aggregates treated according to scheme 2C. XPS spectra were recorded on a Perkin Elmer Phi 5400 ESCA system with a magnesium Ka X-ray source. Samples were analyzed at pressures between 10^{-9} and 10^{-8} Torr with a pass energy of 29.35 eV, take-off angle of 45° and spot size of 250 mm^2. Atomic concentrations were determined using previously determined sensitivity factors. All peaks were referenced to the signature C1s peak for adventitious carbon at 284.6 eV. Multipack software package (Physical Electronics, Eden Prairie, MN) was used to curve fit the obtained XPS elemental peaks. Samples for the XPS analysis were prepared by depositing *n*C_{60} aggregates on the surface of a polymeric membrane during filtration in a stainless dead-end filtration cell (HP 4750, Sterlitech Corp., Kent, WA) at a pressure of 120 psi. The deposited material was air dried at room temperature (20 $^{o}C \pm 2$). To avoid possible losses of *n*C_{60} from the suspensions treated at higher ozone dosages, a set of membranes with progressively decreasing molecular weight cut off (nanofiltration membranes NF90 and NF270 and reverse osmosis membrane BW30-365,

Dow Film Tech, Milwaukee, WI) was used. The type of membrane used in each of the experiments is listed in Table 3.2. Two tailed Student's t-test at 95% CI was used to test the significance of the data obtained during XPS analysis of nC$_{60}$ samples with the regard of treatment type.

The effective diameter and ζ-potential of nC$_{60}$ aggregates treated according to schemes 2A and 2B, were measured by dynamic light scattering and phase analysis light scattering techniques in a ZetaPALS unit (Brookhaven Instrument Corp., Holtsville, NY).

The absorbance spectra of nC$_{60}$ suspensions, treated according to scheme 2B, were recorded by Multi-Spec 1501 UV-vis photodiode array spectrophotometer (Shimadzu, Kyoto, Japan) with in the 180-800 nm spectral range with 3 nm resolution.

Table 3.2. Membranes used in preparation nC$_{60}$ samples for the XPS analysis.

Type of the nC$_{60}$ suspension	Type of membrane	Molecular weight cut-off, Da
As-prepared nC$_{60}$ suspension	NF-270	400
0% ozonated and then dosed with 68 mg (Cl_2)/L and allowed to react for 100 min	NF-270	
25% ozonated and then dosed with 68 mg (Cl_2)/L and allowed to react for 100 min	NF-270	
50% ozonated and then dosed with 68 mg (Cl_2)/L and allowed to react for 100 min	N-90	200
75% ozonated and then dosed with 68 mg (Cl_2)/L and allowed to react for 100 min	BW-30-365	100-200
90% ozonated and then dosed with 68 mg (Cl_2)/L and allowed to react for 100 min	BW-30-365	

3.2.6. Toxicity assessment: *E.coli* viability bioassay

E.coli viability bioassay of nC_{60} suspensions treated according to schemes 1, 2A and 2B was performed according to the procedure described by Alpatova et al. [75]. Briefly, 1.425 µL of each tested nC_{60} suspension, 475 µL of the culture medium and 100 µL of *E.coli* stock were transferred into 15 mL centrifuge tubes (Corning Inc, Corning, NY) and incubated at 37 ^{o}C. A bacterial suspension in ultrapure water served as vehicle control. Samples were taken after 3 or 24 hrs, sequentially diluted and plated on agar plates. The exposure times used in this work to evaluate the viability of *E. coli* were chosen based on typical exposure times reported elsewhere [75]. Each experiment was run in triplicate. The results are reported as a fraction of control (FOC) ± standard deviation (SD), calculated as the average number of colonies grown after *E. coli* exposure to nC_{60} suspensions divided by the average number of colonies grown in the vehicle control samples.

3.2.7. Toxicity assessment: Neutral red dye uptake bioassay

The NDU bioassay of nC_{60} suspensions treated according to scheme 2B was, performed as described by Alpatova et al. [75]. WB-F344 rat liver epithelial cells were exposed to 500 µL of each of nC_{60} suspension or to 500 µL of ultrapure water (vehicle control) and incubated at 37 ^{o}C for 30 min and 24 h. A 30 min and 24 h exposure times were chosen based on exposure times reported in [75]. The optical density of the lysate was recorded at 540 nm on a Beckman DU 7400 diode array detector (Beckman Instruments, Inc., Schaumburg, IL) with the background absorbance taken at 690 nm. The results from the NRDU bioassay are reported as the (FOC) ±

SD (absorption from the sample treated with nC_{60} suspension divided by the absorption of the vehicle control sample). FOC values of 1.0 mean that the cells maintained their integrity while FOC values < 0.8 mean that cell integrity was not retained and nC_{60} suspensions were cytotoxic at the concentration studied.

3.2.8. Toxicity assessment: Gap junction intercellular communication bioassay

The GJIC bioassay of nC_{60} suspensions, treated according to scheme 2B, was adopted from Alpatova et al. [75]. nC_{60} suspensions (200 or 500 µL) or the same volumes of ultrapure water (vehicle controls) were added to the confluent WB-F344 cells and the plates were incubated for 30 min and 24 hrs at 37 ^{o}C. A 30 min and 24 h exposure times were chosen based on exposure times reported in [75]. Lucifer yellow fluorescent dye (1 mL) was introduced into the cells with three different scrapes through the monolayer of confluent cells using a sterile surgical steel scalpel blade. Data are reported as a fraction of the dye spread in treated sample as compared to that observed in the vehicle control (ultrapure water only) (FOC) ± SD at 95% CI. According to [70, 72], FOC values of 1.0, (0.5-0.9), (0.3-0.5) and <0.3 correspond to full communication between cells, partial GJIC inhibition, significant inhibition and complete inhibition of the GJIC, respectively.

The two-tailed Student's t-test was used to determine if the differences in the results obtained in the vehicle control plates and the results in the tested plates were statistically significant at 95% CI.

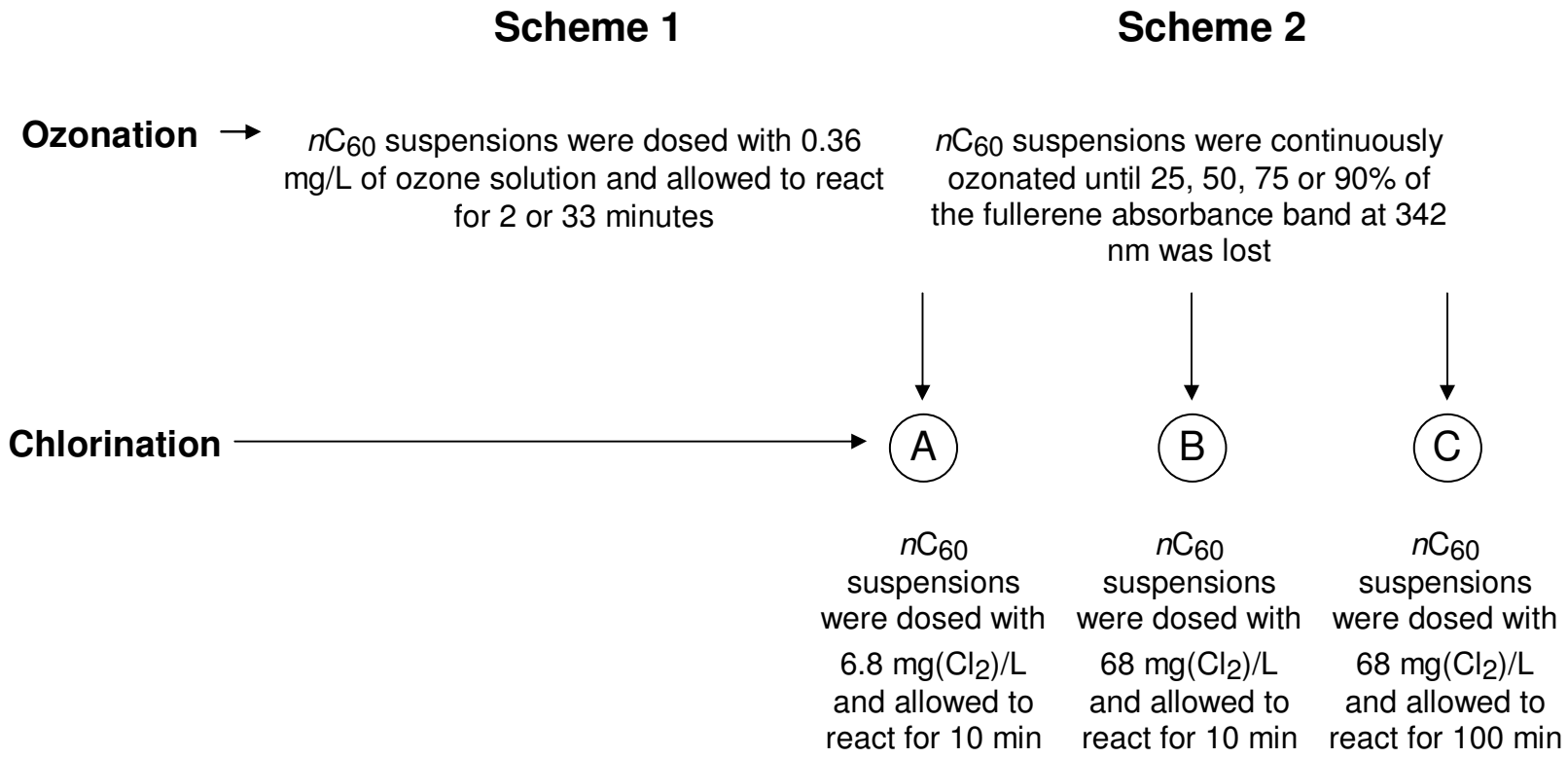

Figure 3.1. nC_{60} treatment schemes.

3.3. Results and discussion

3.3.1. XPS characterization of nC$_{60}$ aggregates

XPS analysis has been used to identify and provide rough quantification of the amount of functional groups formed as a result of chemical treatment of nC$_{60}$ suspensions according to Scheme 2C. In general, when a sample is subjected to XPS, the depth to which beam of X-rays penetrate a sample would depend on the type of material (usually 5-8 nm), the X-ray energy, and the sample geometry [76]. Given the method used to prepare nC$_{60}$ samples, we expect their surface to be rough and heterogeneous. As such, this is hard to predict on how deep the beam of X-rays penetrates the nC$_{60}$ samples. Since fullerene was the only carbon source expected to exist in the nC$_{60}$ samples, the covalent bonds detected in our samples were assumed to originate from the interactions between the carbon atoms which comprise the fullerene shell (i.e. fullerene surface) and O and Cl atoms.

Taking into consideration that the chlorination procedure is associated with the addition of a range of chemical compounds including sodium hypochlorite, NaOCl; potassium dihydrogen phosphate, KH_2PO_3; sodium hydroxide, NaOH; and sodium bisulfate, $NaHSO_3$; a number of elements were expected to be present in the XPS spectra of each individual nC$_{60}$ sample. The examination of the XPS spectra of nC$_{60}$ aggregates revealed the existence of multiple peaks with different characteristic binding energies (E_b). For illustrative purposes, a representative full XPS

spectrum of one of nC_{60} samples (nC_{60} chlorinated at an initial chlorine concentration of 68 mg (Cl_2)/L and allowed to react for 100 min is shown in Figure 3.2.

In order to identify the species, detected during the XPS measurements, each nC_{60} spectrum was first curve-fitted following by assigning the detected peak to an individual atom by matching the measured and referenced E_b. We divided the elements found in the nC_{60} samples into two groups. The first group included P, N, S, K, Na and Si and the second group included C, O and Cl, with O and Cl which are expected to form covalent bonds with C.

3.3.1.1. Identification of the atoms found in the XPS spectra

The following nine elements have been identified in the nC_{60} samples: C, O, Cl, P, N, S, K, Na and Si. The atomic concentrations (%) of each element detected in nC_{60} sample as a function of treatment type are presented in Table 3.3.

The first group comprises atoms which were not expected to be associated with the carbon atoms and were likely to be present in nC_{60} samples due to the addition of the various chemicals to the nC_{60} suspensions during the chlorination process (e.g., P, S, K and Na) or as a contamination (e.g., N and Si). The rejection of NaCl by NF-270, NF-90, and BW-30 membranes was reported to be 40%, 85% and 99%, respectively [77, 78]. Although the determination of the rejection of the individual ions in the nC_{60} suspensions is beyond the scope of this study, it was assumed that

along with Na^+, the membranes used to deposit the nC_{60} aggregates, also reject K^+, SO_4^{2-}, SO_3^{2-} and PO_4^{3-} ions due to larger ion sizes. To confirm this, we have first determined the bonding state of each element in the first group, and then have suggested the form in which this element might be present in the nC_{60} sample by matching the calculated E_b with the E_b characteristic for the bond of this atom to another atom, found in a nC_{60} sample. Calculated and referenced E_b values or the Group 1 atoms are summarized in Table 3.4.

The P(2p) peak was observed at an E_b range of 132.9-133.34 eV. The P atom bonded to O as PO_3^{3-} has an E_b of 132.9-133.5 eV [79]. Taking into account that the P(2p) peak was detected in the chlorinated only and in the sequentially ozonated/chlorinated nC_{60} samples (Table 3.3) and not in the as-prepared nC_{60} samples, we have attributed the presence of the P(2p) peak to phosphate contamination originating from the addition of KH_2PO_3 during chlorination.

The N(1s) peak lies at an E_b range of 399.2-400.6 eV. The referenced N^o peak lies at 400.8 eV [80]. Given that the N(1s) peak was found in the XPS spectra of all nC_{60} samples (Table 3.3) and that no nitrogen-containing compounds were added to the nC_{60} suspensions, we have attributed this peak to the adsorption of N_2 onto fullerene during its manufacturing or storage.

The S(2p) peak in nC_{60} samples appears at an E_b range of 167.5-169.2 eV. The S(2p) peak was detected for only the chlorinated and consecutively ozonated/chlorinated samples and for as-prepared samples from the Replicate 2 (Table 3.3). The range of binding energies of highly oxidized sulfur compounds were reported to be 167.7-170.0 eV (depending on the sulfur oxidation state) [81] and 169.1 eV (SO_4^{2-}) [82]. $NaHSO_3$ was added to the suspensions, reacting with free chlorine to form SO_4^{2-} ions according to the following reaction:

$$NaHSO_3 + NaOCl \rightarrow NaHSO_4 + NaCl$$

By comparing the calculated and referenced binding energies of sulfur, the sulfur peak found in nC_{60} samples was able to be attributed to sulfur atoms bonded to oxygen as SO_3^{2-} or SO_4^{2-}. The S(2p) peak measured in as-prepared nC_{60} samples from the Replicate 2 (and which $NaHSO_3$ was not added) are believed to result from an experimental error.

The range of measured binding energies of K(2p) in nC_{60} samples lie between 292.6 and 293.1 eV and were detected in chlorinated only and sequentially ozonated/chlorinated samples (Table 3.3). Potassium, K, bonded to chlorine Cl as KCl has a reported E_b of 292.8 [82] (the sample KCl was prepared by deposition from water-alcohol solution to form a dense layer) or 293.6 [83]. The binding energies of Cl(2p) found in the nC_{60} samples are presented in Table 3.5. Curve-fitting of the Cl(2p) peak revealed the presence of two Cl forms, with each form comprised of doublets. The Cl moiety with the lower E_b has a range of E_b of 197.5–199.6 eV, depending on the sample type. After comparing binding energies of K(2p) and the Cl component

with the lower E_b, it is clear that the K in the nC_{60} samples is bonded to Cl as KCl. Also, taking into consideration that no K(2p) peak has been found in non-chlorinated nC_{60} samples (which have not received KH_2PO_3 treatment), we have assumed that the presence of a K(2p) peak in nC_{60} samples resulted from the KH_2PO_3 addition to the nC_{60} suspensions during the chlorination step.

The Na(1s) peak in the nC_{60} samples lies at an E_b range between 1070.0 and 1071.6 eV. This peak was detected in all chlorinated samples and in the as-prepared samples from Replicate 2 (Table 3.3). The referenced E_b values of Na(1s) bonded as Na_3PO_4 or NaCl are 1071.1 and 1071.6 eV, respectively [82]. The referenced E_b of Cl in NaCl is 198.60 eV [82]. By matching the binding energies of Na(1s) and Cl(2p), it is evident that Na in the nC_{60} samples is consistent with that of Na bonded to Cl as NaCl. Since the reference E_b of Na(1s) bonded as Na_3PO_4 lies in the range of the measured Na(1s) binding energies, a portion of the Na^+ ions may also be associated with PO_4^{3-} ions. Since sodium was not expected to be present in the as-prepared samples and it has not been found in the as-prepared Replicate 1 nC_{60} samples, the Na(1s) peaks in the Replicate 2 samples were attributed to experimental error arising from the fact that the sodium borosilicate glassware used in this study was subjected to acid wash with 0.1M HCl which may have resulted in sodium leaching.

The Si(2p) peak in nC_{60} samples was identified at an E_b range of 100.5-103.0 eV in all nC_{60} Replicate 1 samples, while no Si(2p) peak was found in the Replicate 2 nC_{60} samples (Table 3.3). The elemental Si(2p) peak lies at an E_b of 99.3 eV [82], Si(2p) bonded to C as SiC lies at an E_b of 102.0 eV and Si(2p) bonded to O as SiO_2 lies at a E_b range of 103.3-103.7 eV [84].The C(1s) peak for C bonded to Si has a binding energy E_b of 282.7 eV [84]. Spectral deconvolution of the C(1s) peak in Replicate 1 nC_{60} samples has not revealed peaks with binding energies which consistent with the C-Si bond. In a personal conversation with the fullerene powder supplier (Materials Research Electronic Corporation, Tuscon, AZ) it has been revealed that the fullerene powder may contain some Si impurities [85]. Therefore, we assumed that the Si detected in nC_{60} samples was due to elemental Si or SiO_2 contamination.

Curve fitting of the C(1s) peak has resulted in a number of distinct carbon peaks with a range of E_b between 282.1 and 289.2 eV (Table 3.6). For illustrative purposes, Figure 3.3 shows a representative C(1s) spectrum and peak deconvolution of nC_{60} aggregates, chlorinated at an initial chlorine concentration of 68 mg (Cl_2)/L and 100 min reaction time. Spectral deconvolution of the C(1s) peak has revealed the existence of non-functionalized carbon moieties, where one carbon atom is linked to another carbon atom, and functionalized carbon moieties, where carbon is bonded to other atoms. The C(1s) peak with an E_b range of 284.62-284.86 eV (depending on the sample type) corresponds to the underivatized C as C-C with a referenced E_b of 285.0 eV [86]. The E_b of C(1s), which shifted in the direction of increasing E_b,

has been assigned to the functionalized carbon moieties. The C(1s) peak with an E_b range of 286.28-286.60 eV (depending on the sample type) has been attributed to C linked to O as C-OH (referenced E_b is 286.6 eV [86]). The C(1s) peak with an E_b range of 287.3-288.2 eV has been identified as C bonded to O as carbonyl (referenced E_b of 288.0 eV [86]). The C(1s) peak with E_b of 288.73-289.23 eV has been assigned as C bonded to O as carboxyl (reference E_b of 288.9 eV [86]).

The C portion of the C-Cl bond was also expected to be present in the C(1s) spectrum of the chlorinated nC$_{60}$ samples. The reference E_b range of C-Cl is 286.30±0.8 eV (the theoretical position of the C-Cl bond in the C(1s) spectrum is shown by the dotted line in Figure 3.3). However, the C-Cl peak was not differentiated on the C(1s) spectrum during the peak deconvolution procedure, likely due to the significantly lower chlorine atomic concentration, as compared to the oxygen atomic concentration (see Table 3.4). This might have led to spreading of C-Cl peak between the more intense C-O peaks.

Some C(1s) Replicate 2 peaks (namely, both the chlorinated only and the 25% ozonated/chlorinated along with one 90% ozonated/chlorinated nC$_{60}$ sample) contained a peak with an E_b at approximately 282 eV. We were not able to assign these C(1s) peaks and assume that these peaks resulted from X-ray beam imaging off the sample which picked up carbon from the sample holder or the tape.

The O(1s) spectrum of nC_{60} samples was fit by two components and the relative binding energies which correspond to each compound are presented in Table 3.6 as a function of treatment type. Component 1 with an E_b range of 531.3-531.9 eV was attributed to the carbonyl moiety which lies at an E_b of 531.5 eV [76]. The second component, with an E_b range of 532.7-533.1 eV was referenced to oxygen in the C-OH group. The C-OH in an aromatic ring lies at E_b of 533.64 eV [76]. An example of a typical O(1s) XPS spectrum and peak deconvolution of nC_{60} chlorinated at an initial chlorine concentration of 68 mg (Cl_2)/L and reacted for 100 min is shown in Figure 3.4.

The amount of hydroxyl, carbonyl and carboxyl groups on the nC_{60} surface can be estimated based on the areas of the corresponding C(1s) and O(1s) peaks. The percent of hydroxyl functionalities was calculated by multiplying the atomic concentration of oxygen by the peak area which corresponds to the OH group in the nC_{60} sample. The percent of carbonyl groups was calculated by multiplying the atomic concentration of carbon by the peak area which corresponds to the carbonyl group in the nC_{60} sample. The percent of the carboxyl groups was calculated by multiplying the carbon atomic concentration by the C(1s) peak area which corresponds to the E_b of the carboxylic group. The quantity of hydroxyl, carbonyl and carboxyl functional groups were calculated for each nC_{60} sample and the results reported in Table 3.6.

Curve-fitting of the Cl(2p) peak revealed the presence of two Cl forms, with each form comprised of doublets. An example of a Cl(2p) XPS spectrum and peak deconvolution of an $n$$C_{60}$ chlorinated at an initial chlorine concentration of 68 mg (Cl_2)/L and reacted for 100 min is shown in Figure 3.5. The binding energies of the Cl(2p) bond found in the $n$$C_{60}$ samples are summarized in Table 3.6. The reported binding energies, E_b, are 198.4 and 198.6 eV for Cl(2p) as NaCl and KCl, correspondingly [82]. Based on the referenced E_b, we attribute the fitted E_b range of 197.5-199.6 eV to the Cl component that is bonded to the alkali metals (K and Na) present in the $n$$C_{60}$ samples as a result of chlorination. The referenced E_b for Cl(2p) as Cl-C is 200.60±0.2 eV [87]. A comparison between the reported E_b and the measured E_b range of 200.1-202.4 eV allows us to conclude that Cl(2p) peaks with the E_b range of 200.1-202.4 eV correspond to Cl(2p) atoms covalently bonded to C atoms as Cl-C.

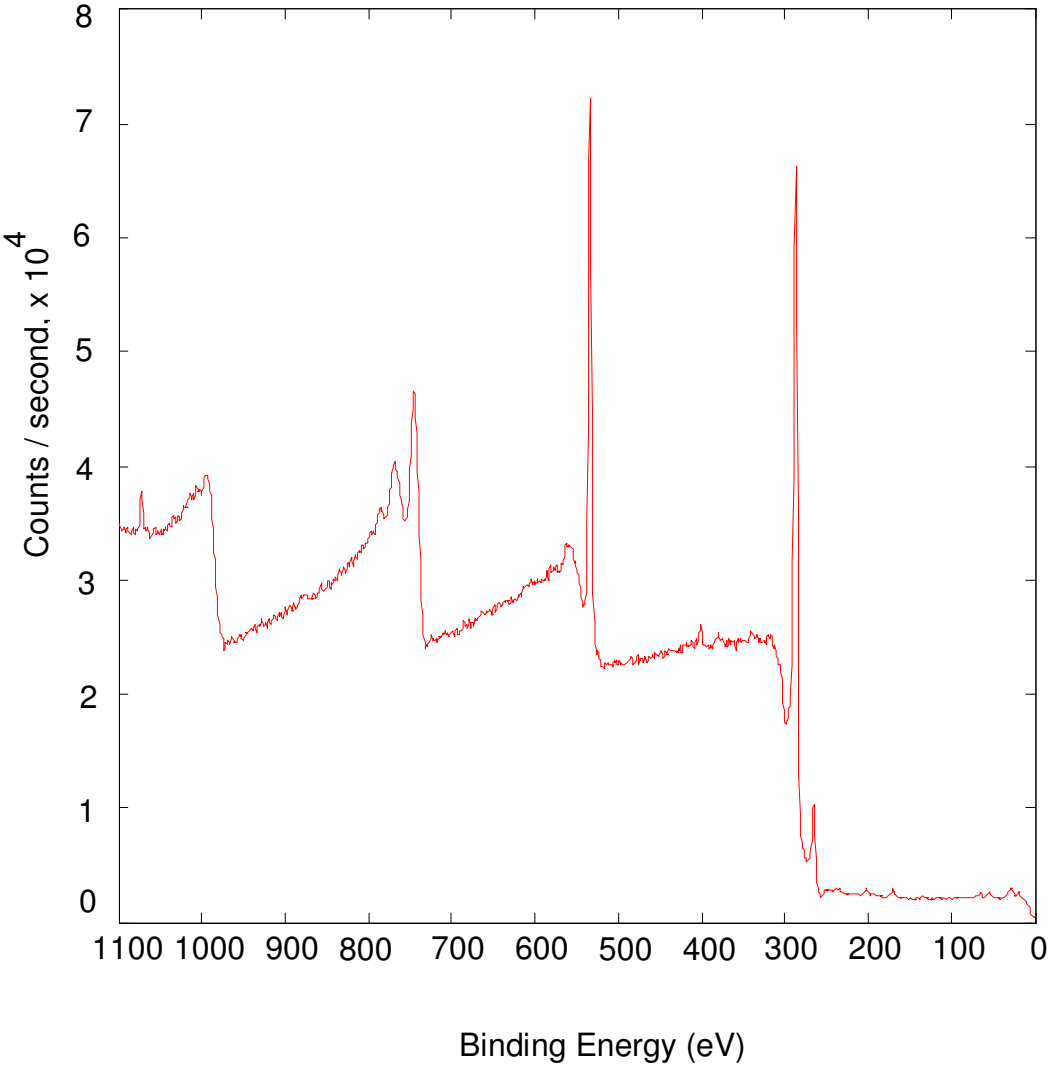

Figure 3.2. A representative full XPS of nC$_{60}$ chlorinated at initial chlorine concentration of 68 mg (Cl_2)/L and allowed to react for 100 min. For interpretation of the references to color in this all other figures, the reader is reffered to the electronic version of this dissertation.

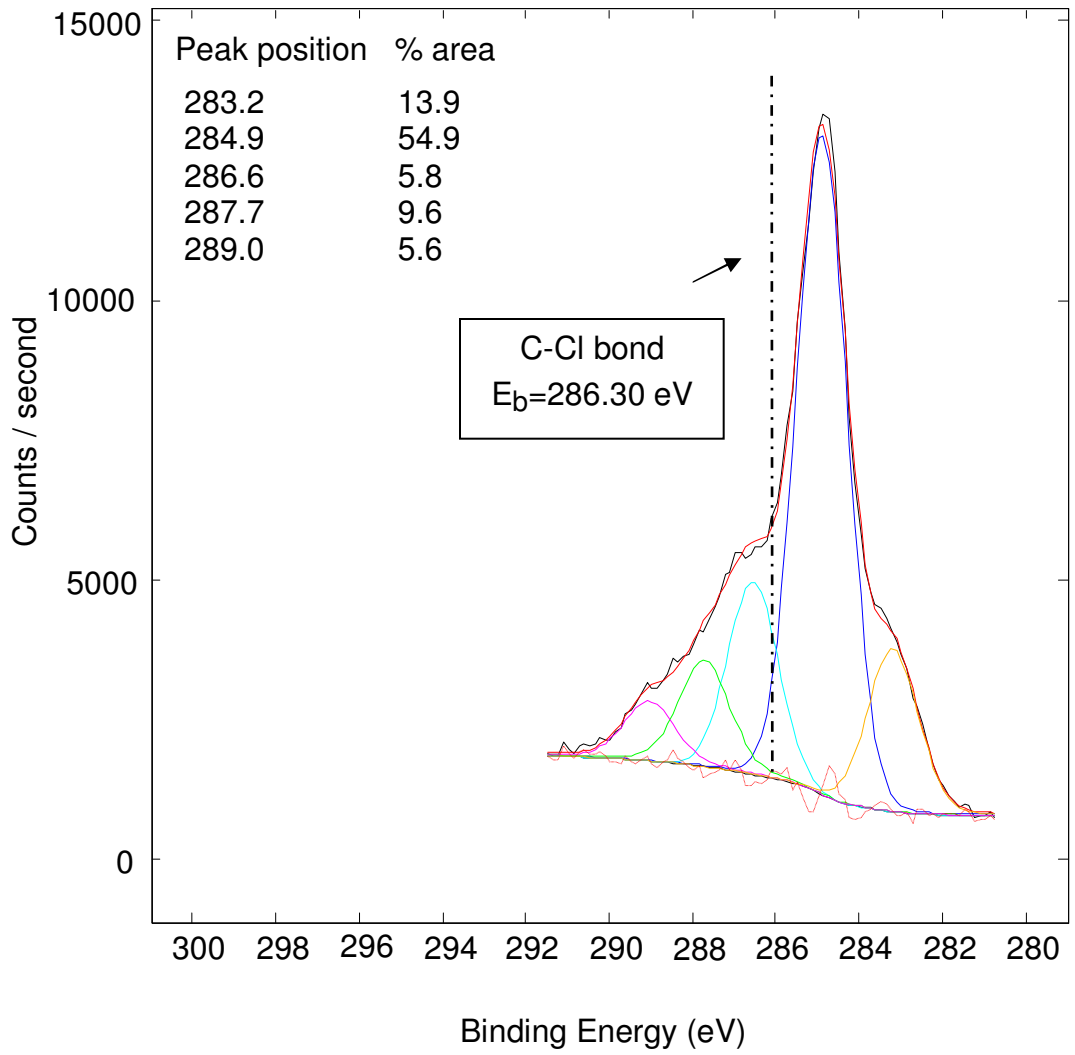

Figure 3.3. A representative high-resolution spectrum and peak deconvolution of C(1s) of nC$_{60}$ chlorinated at initial chlorine concentration of 68 mg (Cl_2)/L and allowed to react for 100 min.

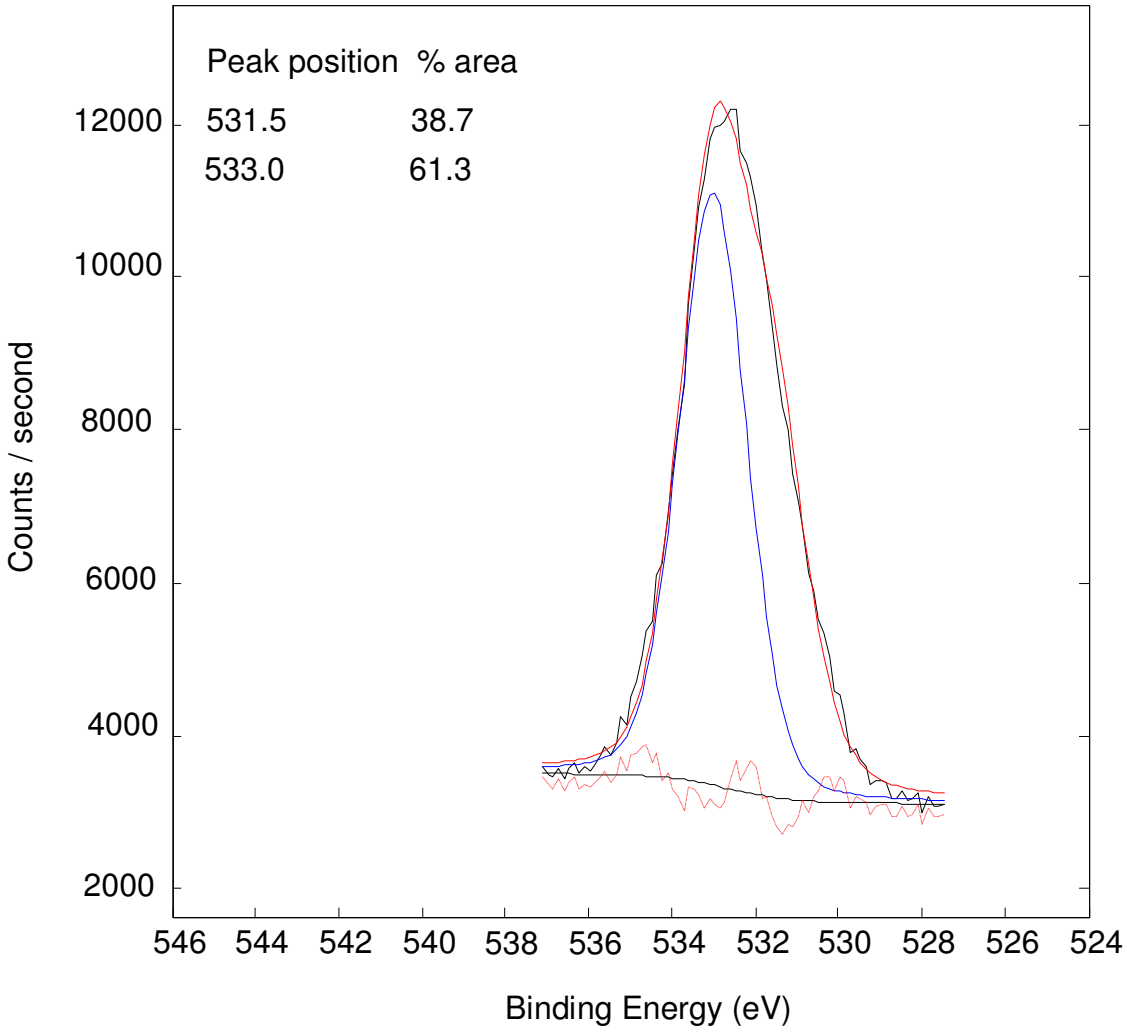

Figure 3.4. A representative peak deconvolution of O(2s) of nC$_{60}$ chlorinated at initial chlorine concentration of 68 mg (Cl_2)/L and allowed to react for 100 min.

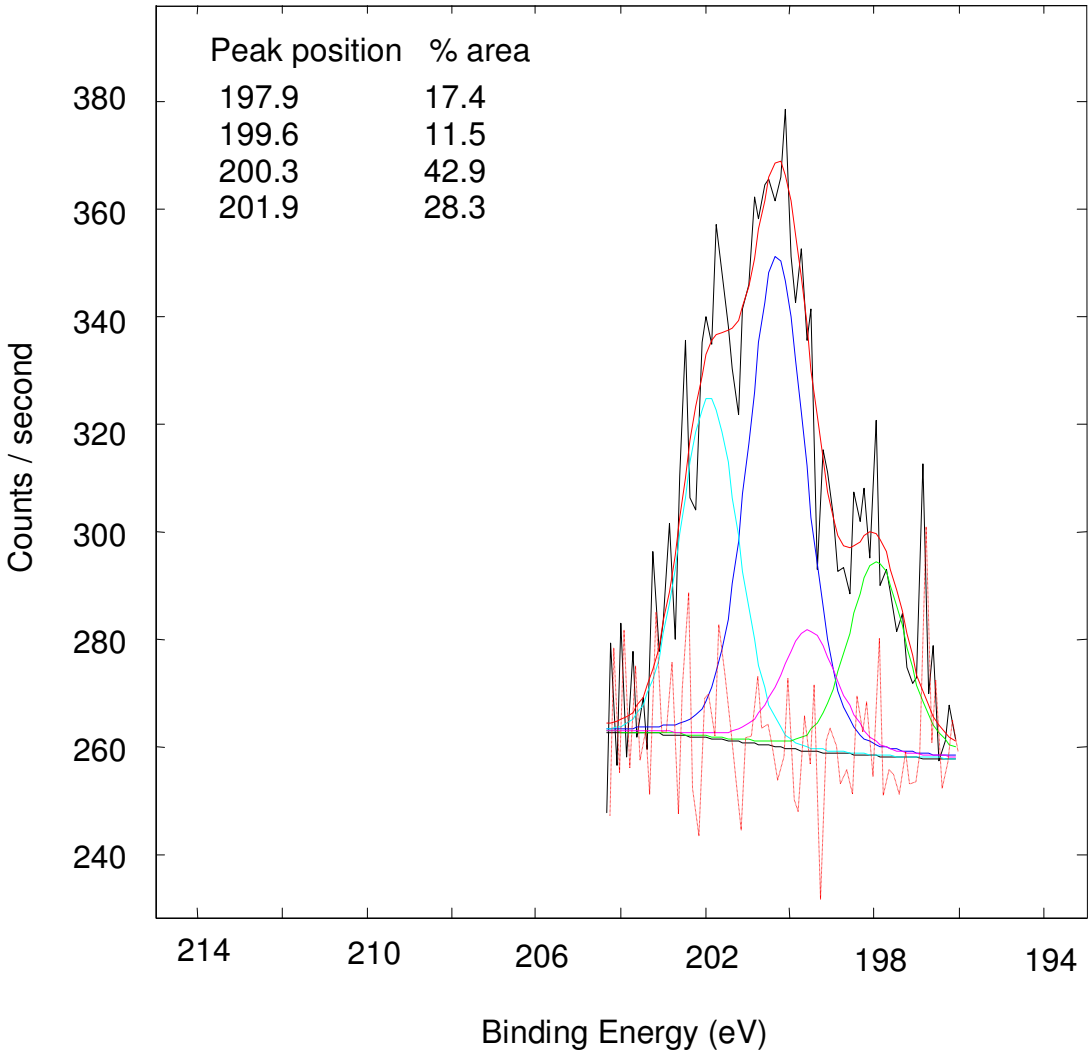

Figure 3.5. A representative peak deconvolution of Cl(2p) of nC$_{60}$ chlorinated at initial chlorine concentration of 68 mg (Cl_2)/L and allowed to react for 100 min.

Table 3.3. Atomic concentration (in %) of an individual atoms identified in nC$_{60}$ samples as a function of treatment type.

Sample type	Atomic concentration of an individual atom, %								
	C	O	Si	N	S	Cl	Na	K	P
As-prepared									
Replicate 1, Coupon 1	80.8	17.4	0.3	1.4	0	0	0	0	0
Replicate 1, Coupon 2	80.7	17.6	0.3	1.4	0	0	0	0	0
Replicate 2, Coupon 1	77.6	20.8	0	1.3	0.2	0.1	0	0	0
Replicate 2, Coupon 2	75.9	21.9	0	1.9	0.3	0.1	0	0	0
Chlorinated only									
Replicate 1, Coupon 1	69.8	25.3	0.1	1.7	0.3	0.2	2.0	0.34	0.3
Replicate 1, Coupon 2	69.6	24.3	0.2	1.7	0.6	0.4	2.4	0.2	0.6
Replicate 2, Coupon 1	69.7	25.2	0	1.7	0.5	0.4	1.8	0.5	0.3
Replicate 2, Coupon 2	72.5	23.3	0	1.5	0.5	0.3	1.3	0.23	0.3
25%/chlorinated									
Replicate 1, Coupon 1	63.1	26.8	0.2	6.0	0.4	0.3	1.7	1.1	0.3
Replicate 1, Coupon 2	64.1	26.7	0.3	5.6	0.4	0.3	1.1	1.1	0.4
Replicate 2, Coupon 1	54.1	34.4	0	1.9	1.9	0.9	3.5	2.7	0.7
Replicate 2, Coupon 2	66.8	26.6	0	2.6	0.5	0.4	2.4	0.3	0.5

Table 3.3 (cont'd)

50%/chlorinated									
Replicate 1, Coupon 1	61.9	27.7	0.4	3.9	0.4	0.2	2.7	1.6	1.3
Replicate 1, Coupon 2	60.3	29.0	0.6	4.3	0.4	0.2	2.3	1.6	1.2
Replicate 2, Coupon 1	63.5	28.6	0	3.2	0.5	0.3	1.9	1.2	0.7
Replicate 2, Coupon 2	63.1	29.1	0	2.9	0.5	0.3	2.3	1.1	0.8
75%/chlorinated									
Replicate 1, Coupon 1	60.4	28.5	1.5	4.4	0.4	0.5	1.7	1.3	1.7
Replicate 1, Coupon 2	61.7	27.2	1.5	3.8	0.6	0.5	1.8	1.4	1.5
Replicate 2, Coupon 1	56.3	32.3	0	2.3	0.6	0.3	5.0	1.1	2.0
Replicate 2, Coupon 2	60.6	30.2	0	4.4	0.7	0.4	2.0	1.2	0.8
90%/chlorinated									
Replicate 1, Coupon 1	57.7	31.9	1.3	2.9	0.6	0.2	2.4	1.2	1.9
Replicate 1, Coupon 2	42.2	40.6	1.2	2.4	0.6	0.4	4.5	2.9	5.4
Replicate 2, Coupon 2	55.9	33.8	0	5.1	0.6	0.2	1.5	1.8	1.1
Replicate 2, Coupon 2	59.4	31.5	0	4.4	0.5	0.2	1.9	0.8	1.4

Table 3.4. Binding energies (E_b) of atoms found in nC_{60} samples.

Atom	Referenced E_b, eV	Treatment type	Replicate 1		Replicate 2	
			Coupon 1	Coupon 2	Coupon 1	Coupon 2
P as PO_4^{3-}	132.9-133.5 [79]	As-prepared	no peak	no peak	no peak	no peak
		Chlorinated only	132.9	133.4	133.7	133.2
		25%/chlorinated	133.4	133.4	133.9	133.7
		50%/chlorinated	133.2	133.2	133.8	133.7
		75%/chlorinated	133.2	133.1	133.5	133.5
		90%/chlorinated	133.5	133.5	133.9	133.1
N as N^o	400.8 [80]	As-prepared	400.6	399.2	400.4	400.9
		Chlorinated only	400.3	400.1	399.8	400.1
		25%/chlorinated	400.1	400.1	400.9	400.4
		50%/chlorinated	400.2	400.2	400.3	400.3
		75%/chlorinated	400.2	399.9	400.4	399.8
		90%/chlorinated	399.9	400.2	399.6	400.1

Table 3.4 (cont'd).

S in oxidized state S as SO_4^{2-}	167.48-169.18 [81] 169.1 [82]	As-prepared	no peak	no peak	168.2	168.2
		Chlorinated only	n/a	168.1	167.9	168.2
		25%/chlorinated	167.9	168.9	168.9	168.7
		50%/chlorinated	169.2	167.9	168.5	168.5
		75%/chlorinated	n/a	167.9	168.6	168.3
		90%/chlorinated	168.1	167.5	167.9	169.1
K as KCl	292.8 [82] 293.6 [83]	as prepared	no peak	no peak	no peak	no peak
		Chlorinated only	293.1	293.1	292.9	292.9
		25%/chlorinated	292.9	293.1	292.9	293.0
		50%/chlorinated	292.9	292.9	293.0	293.0
		75%/chlorinated	292.9	292.6	292.9	292.9
		90%/chlorinated	292.8	292.7	292.9	292.6
Na as Na_3PO_4 Na as NaCl	1071.1 1071.6 [82]	As-prepared	no peak	no peak	1071.5	1070.00
		Chlorinated only	1071.6	1071.5	1071.7	1071.4
		25%/chlorinated	1071.1	1071.5	1071.9	1071. 8
		50%/chlorinated	1071.3	1071.4	1071.1	1071.4
		75%/chlorinated	1071.4	1071.3	1071.7	1071.6
		90%/chlorinated	1071.4	1071.2	1071.5	1071.1

Table 3.4 (cont'd).

Si^o Si as SiC Si as SiO_2	99.3 102.0 103.3-103.7 [84]	As-prepared	wide peak between 100.5 and 103.0 eV	wide peak between 100.5 and 103 eV	no peak	no peak
		Chlorinated only			no peak	no peak
		25%/chlorinated			no peak	no peak
		50%/chlorinated			no peak	no peak
		75%/chlorinated			no peak	no peak
		90%/chlorinated			no peak	no peak

Table 3.5. Referenced binding energies (E_b) of C, O and Cl atoms in different functional groups.

Atom	Binding energy, E_b, eV	Type of group	Reference
C(1s)	282.7	C-Si	[84]
	285.0	C-C (graphite)	[86]
	286.6	C-OH (hydroxyl)	
	288.0	COH (carbonyl)	
	288.9	COOH (carboxyl)	
	286.30±0.8	C-Cl	[87]
O(1s)	531.25	Aromatic C=O	[76]
	533.64	Aromatic C-OH	
Cl(2p)	200.60±0.2	Cl-C	[87]
	198.4	Cl in KCl	[82]
	198.6	Cl in NaCl	

3.3.1.2. Changes in nC$_{60}$ surface chemistry as a result of treatment with ozone and chlorine

Our experiments were aimed at evaluating the effect of sequential ozonation/chlorination on the surface chemistry of nC$_{60}$ aggregates. We hypothesized that the oxidation treatment applied in our work would alter the elemental composition of the nC$_{60}$ aggregates and change their surface functionality. Also, we were specifically interested in finding evidence of chlorine attachment to the fullerene cage resulting from the ozonation/chlorination of nC$_{60}$ suspensions. The identification and quantification of bonds present in nC$_{60}$ samples and the type and amount of these functional groups have been successfully studied by employing XPS. As it is seen in Figure 3.6a, the atomic concentration of carbon in nC$_{60}$ samples, calculated after curve fitting of the C(1s) peak, decreased when the nC$_{60}$ samples were subjected to ozonation. At a 95% confidence interval, there was a statistically significant difference in carbon content among as-prepared,

chlorinated only and ozonated (at 25- 90%) and then chlorinated nC$_{60}$ aggregates, but no difference was found among the ozonated/chlorinated nC$_{60}$ samples. For example, the atomic concentration of carbon in the as-prepared nC$_{60}$ sample was measured at 78.8±2.4%, while the carbon content of the 90% ozonated/chlorinated nC$_{60}$ sample was 53.8±7.8%. From Figure 3.6a, one can observe that the general trend is decreasing carbon content with an increasing degree of ozonation. The decrease in the amount of carbon in nC$_{60}$ samples could be attributed to the mineralization of the carbon during ozonation. Although the total organic carbon was not measured in this study, the disappearance of fullerene was observed by monitoring the characteristic fullerene absorbance at 246 nm during ozonation. Visual examination of nC$_{60}$ suspensions showed progressive changes in color from brown (in the case of an as-prepared suspension) to straw (in the case of a suspension ozonated at 90%). While the atomic carbon concentration in nC$_{60}$ samples decreased with increasing degree of oxidation, the amount of derivatized carbon in nC$_{60}$ samples gradually increased as ozonation progressed (Figure 3.6b).

While the underivatized carbon prevailed over the derivatized carbon forms with a ratio of 0.42±0.06 (1 derivatized carbon atom per 2.5 underivatized carbon atoms) in the as-prepared nC$_{60}$ samples, the amount of underivatized carbon atoms significantly decreased resulting in a ratio of 0.95±0.29 (1 derivatized carbon atom per 1 underivatized carbon atom) in the 90% ozonated/chlorinated nC$_{60}$ samples.

Table 3.6. Percentage of O- and C-containing functional groups in nC_{60} samples as a function of treatment type.

Treatment type	C, %	E_b, eV	% of the peak area	O, %	E_b, eV	% of the area	OH, %	COH, %	COOH, %	ΣO, %	Cl, %	E_b, eV	% of the area	Cl-C, %
Replicate 1, Coupon 1														
As-prepared	80.8	284.8	76.2	17.4	531.8	22.5	13.4	4.9	3.7	22.1	0	0	0	0
		286.4	13.1											
		287.4	6.2		532.9	77.5								
		288.7	4.6											
Chlorinated only	69.8	284.9	68.7	25.3	531.5	33.12	16.9	6.3	3.0	26.12	0.3	197.9	33.4	44.6
		286.6	18.1									199.5	22.0	
		287.9	8.9		532.9	66.8						200.6	26.9	
		288.1	4.3									202.2	17.7	
25%/ chlorinated	63.1	284.8	60.7	26.7	531.4	53.3	12.6	0	10.23	22.7	0.3	197.8	24.8	58.9
		286.5	22.5									199.4	16.3	
		288.2	16.3		532.8	46.7						200.5	35.5	
												202.1	23.4	
50%/ chlorinated	65.9	284.8	65.9	27.7	531.4	49.3	14.0	7.89	2.7	24.6	0.2	197.8	35.4	41.3
		286.4	18.1									199.4	23.4	
		287.9	11.9		533.0	50.7						200.4	24.9	
		288.0	4.1									201.9	16.4	

Table 3.6 (cont'd).

75%/ chlorinated	60.4	284.8	67.7	28.5	531.3	50.9	13.9	0	7.3	21.2	0.5	197.7	37.1	38.5
		286.4	20.3									199.3	24.5	
		288.1	12.1		532.7	49.0						200.3	23.2	
												201.9	15.3	
90%/ chlorinated	57.7	284.7	63.9	31.9	531.3	44.7	17.7	0	5.3	23.0	0.4	197.9	44.6	25.9
		286.3	26.8									199.5	29.5	
		288.1	9.3		532.7	55.4						200.8	15.6	
												202.4	10.3	
Replicate 1, Coupon 2														
As-prepared	80.7	284.86	75.1	17.6	531.9	32.2	11.9	5.2	2.6	19.8	0	0	0	0
		286.55	15.2											
		287.94	6.5		533.0	67.8								
		289.15	3.2											
Chlorinated only	69.6	284.82	69.9	24.3	531.4	36.7	15.4	6.1	1.9	23.4	0.4	197.8	35.4	41.3
		286.39	18.5									199.4	23.4	
		287.41	8.8		532.8	63.4						200.4	24.9	
		288.73	2.8									201.9	16.4	
25%/ chlorinated	64.1	284.78	60.8	26.7	531.5	54.2	12.2	9.5	1.8	23.6	0.3	197.5	30.5	49.3
		286.36	21.6									199.3	20.1	
		288.03	14.9		532.9	45.9						200.5	29.7	
		289.23	2.8									202.1	19.6	

Table 3.6 (cont'd).

50%/ chlorinated	60.30	284.8	63.7	29.0	531.4	47.9	15.1	8.1	1.4	24.6	0.2	197.8	32.9	45.3
		286.5	20.5									199.4	21.8	
		288.1	13.5		532.8	52.1						200.5	27.3	
		289.2	2.3									202.1	18.0	
75%/ chlorinated	61.73	284.7	69.1	27.2	531.3	51.9	13.1	6.5	0.9	20.6	0.5	197.9	37.3	38.0
		286.3	18.9									199.4	24.6	
		287.9	10.5		532.7	48.1						200.1	22.9	
		288.2	1.6									201.7	15.1	
90%/ chlorinated	42.19	284.7	65.9	27.2	531.2	50.5	13.5	3.1	0	16.6	0.2	197.9	49.6	17.7
		286.1	26.6									199.5	32.7	
		287.9	7.4		532.6	49.5						200.2	10.6	
		288.2	0									201.8	7.0	
Replicate 2, Coupon 1														
As-prepared	77.64	284.8	69.9	20.8	531.9	35.1	13.5	6.3	4.9	24.7	0.1	n/a	n/a	n/a
		286.4	15.6											
		287.7	8.1		533.1	64.9								
		289.0	6.3											
Chlorinated only	69.69	284.9	68.7	25.3	531.4	26.9	18.5	6.0	4.0	28.5	0.4	197.8	23.8	60.5
		286.6	16.9									199.4	15.7	
		287.9	8.6		532.8	73.1						200.4	36.4	
		289.1	5.8									202.0	24.1	

Table 3.6 (cont'd).

25%/ chlorinated	54.1	282.0	7.1	34.4	531.4	43.9	19.3	11.0	0	30.3	0.9	198.2	31.9	47.1
		284.7	58.7									199.8	21.1	
		286.4	20.4		532.8	56.1						200.2	28.3	
		288.2	13.9									201.8	18.7	
50%/ chlorinated	63.5	284.9	66.2	28.6	531.4	39.7	17.3	0	8.2	25.5	0.3	197.9	27.7	50.8
												199.6	18.3	
		286.6	20.9		532.9	60.3						200.3	32.6	
		288.3	12.9									201.9	21.5	
75%/ chlorinated	56.3	284.8	63.8	32.3	531.3	41.5	18.9	0	7.6	26.5	0.3	197.8	36.8	47.7
		286.5	22.8									199.4	24.3	
		288.3	13.5		532.8	58.5						200.3	23.4	
												201.9	15.4	
90%/ chlorinated	55.9	284.6	47.2	33.8	531.2	41.0	19.9	11.2	0	31.1	0.2	197.8	30.9	49.7
		286.1	32.9									199.4	20.4	
		287.9	19.9		532.5	58.9						200.6	29.3	
												202.2	19.3	
Replicate 2, Coupon 2														
As-prepared	75.9	284.8	70.5	21.9	531.9	30.4	15.2	5.4	4.4	25.1	0.1	n/a		n/a
		286.5	16.5											
		288.9	7.2		533.0	69.6								
		289.0	5.8											

Table 3.6 (cont'd).

Chlorinated only	72.5	283.2	13.9	23.3	531.5	38.7	14.3	11.5	6.9	32.7	0.3	197.9	17.4	71.2
		284.9	54.9									199.6	11.5	
		286.6	15.8		533.0	61.3						200.3	42.9	
		287.7	9.6									201.9	28.3	
25%/ chlorinated	66.8	282.9	9.6	26.6	531.5	45.9	14.4	11.9	7.4	33.7	0.4	197.9	25.8	57.2
		284.8	55.4									199.5	17.0	
		286.5	17.9		532.9	54.1						200.4	34.4	
		287.9	11.0									201.9	22.7	
		289.0	6.0											
50%/ chlorinated	63.1	284.8	63.5	29.1	531.5	44.9	16.0	7.3	3.8	27.1	0.3	197.9	29.7	50.2
		286.5	18.9									199.5	19.6	
		287.9	11.6		533.0	55.1						200.5	30.6	
		289.1	6.0									202.1	20.2	
75%/ chlorinated	60.6	284.8	58.6	30.2	531.3	47.5	15.9	7.6	1.8	25.3	0.4	198.0	36.3	47.9
		286.4	25.9									199.6	23.9	
		288.0	12.6		532.9	52.5						200.4	23.9	
		289.0	2.9									202.0	15.7	
90%/ chlorinated	59.4	282.6	12.4	31.6	531.4	44.6	14.2	6.9	2.1	23.4	0.2	197.8	29.0	50.4
		284.8	44.9									199.4	19.1	
		286.4	27.4		532.9	55.4						200.2	31.2	
		288.0	11.7									201.8	20.6	
		289.1	3.5											

Since the presence of Cl-C bonds in chlorinated nC$_{60}$ samples was confirmed by XPS measurements, one could assume that, along with C-O bonds, derivatized carbon should also exist as C-Cl. However, as it was mentioned above, the C-Cl peak was not identified in the XPS spectrum of nC$_{60}$ samples due to the significantly lower atomic concentration of chlorine as compared to oxygen, and weak C-Cl peak was hidden by the strong C-O peak during curve-fitting.

The atomic concentration of oxygen on the nC$_{60}$ surface increased when nC$_{60}$ samples were treated with ozone (Figure 3.7a). Statistically significant differences in the oxygen content were observed between the non-ozonated and the 25-90% ozonated/chlorinated nC$_{60}$ samples. No statistically significant differences in O-content were found when comparing sequentially ozonated/chlorinated nC$_{60}$ samples as a function of ozonation degree. Thus, the atomic concentration of carbon in as-prepared and 90% ozonated/chlorinated nC$_{60}$ samples was 19.4±2.3 and 31.1±2.8%, accordingly. Even though the differences in the peak areas of O(1s) were not statistically significant in the case of ozonated/chlorinated nC$_{60}$ samples, there may be a trend towards the increase in oxygen peak area with the increase in degree of ozonation.

Three types of O-containing functional groups (hydroxyl, carboxyl and carbonyl) were identified on the surface of the as-prepared and sequentially ozonated/chlorinated nC$_{60}$ aggregates (Table 3.6). The O-containing functional groups detected on the surface of as-prepared nC$_{60}$ were

presumably formed through the adsorption of hydroxyl radicals or hydrolysis [88]. This is consistent with Chen et al. [89] who reported a considerable increase in the oxygen content from 1.2 to 3.7% after 40 days of stirring fullerene powder into water.

The percentage of carbonyl and carboxyl groups in nC$_{60}$ samples was calculated by multiplying the atomic concentration of C by the area of the corresponding C(1s) peak. As it is seen from Figure 3.7a, that was no statistically significant difference in amount of oxygen calculated according to two different methods. When the values of O-containing functional groups in each sample were added, they matched the O-values obtained from the area of O(1s) peak for the ozonated/chlorinated nC$_{60}$ samples.

As shown in Figure 3.7b, the fraction of oxygen present as hydroxyl groups (representing monooxidized carbon) prevailed over carboxyl and carbonyl groups (representing dioxygenated carbon forms) for the as-prepared samples. The fraction decreased during ozonation. The ratio of [carboxyl+carbonyl] to [hydroxyl] groups was 0.4±0.1 in as-prepared nC$_{60}$ samples and increased to 0.8±0.1 in 90% ozonated/chlorinated nC$_{60}$ samples. This is in good agreement with the data reported for C$_{60}$ subjected to ozonation in toluene, where after ozonation the C$_{60}$ cage was opened and comprised of carboxylic and ketone groups [90]. When nC$_{60}$ was ozonated in an aqueous phase, highly oxidized fullerene oxides with repeating hydroxyl and hemiketal functionalities were suggested as reaction products [61]. Student's t-test performed at a 95% CI, aimed at testing difference in the fraction of hydroxyl and carbonyl functionalities as a function

of treatment type, revealed significant differences between the non-ozonated (as prepared and chlorinated) nC$_{60}$ samples and sequentially ozonated/chlorinated nC$_{60}$ samples, but no difference among sequentially ozonated/chlorinated nC$_{60}$ samples. As discussed above, similar results have been obtained after testing for differences in oxygen atomic concentration in nC$_{60}$ samples with regard to treatment type.

Based on the XPS analysis of nC$_{60}$ samples, the presence of Cl bonded as Cl-C was directly confirmed by the appearance of Cl(2p) peaks with binding energy corresponding to Cl-C. The percentage of the Cl-C bonds as a function of applied treatment was calculated by multiplying the chlorine atomic concentration by the Cl(2p) peak areas with the E_b that corresponds to the Cl-C bond, where the data are presented in Table 3.6. There was no statistically significant difference in the amount of Cl attached to C among treatments. Nonetheless, as it is shown in Figure 3.8, the amount of Cl bonded to C decreases with increasing ozone dose. Chlorination of carbon-rich NOM is known to lead to the formation of a wide range of halogenated compounds that are toxic to humans and aquatic life. When NOM is subjected to ozonation, the concentration of disinfection by-products also decreases. For example, Galapate et al. [91] shown that ozonation of Minaga Reservoir water led to the reduction of THMs by 43% as compared to the non-ozonated water. Although it has been reported that fullerene does not readily react with chlorine (i.e., by action of ICl on C_{60} dissolved in organic solvents) [63], or direct reaction of solid fullerene and chlorine at low (-35 ^{o}C) [64] or high (+250 ÷ +400 ^{o}C) [65] temperatures, the presence of C-Cl bonds on nC$_{60}$ after their ozonation/chlorination by NaOCl at

ambient temperature demonstrates that these carbon nanoparticles can be potential precursors for chlorinated carbon-based disinfection by-products.

3.3.2. Optical characteristics of nC_{60} aggregates

UV-vis absorption spectra of nC_{60} suspensions subjected to treatment by Scheme 2B are shown on Figure 3.9. The absorption spectra of as-prepared nC_{60} contained two narrower absorption bands at 270 nm and 246 nm and a broad band between 400 nm and 550 nm. The absorption peak observed at 242 nm is an inherent characteristic of the colloidal fullerene [88]. The broadband that appeared in long-wave region is evidence of the presence of donor-acceptor complexes between nC_{60} and the unshared electron pair of O_2 in water molecule, i.e., the more hydrated the fullerene molecule, the more pronounced this band would be [8, 88]. The absorption spectrum of as-prepared nC_{60} suspension progressively lost its characteristic absorbance as ozonation proceeded, with almost complete disappearance of all peaks at the highest ozone dose applied. Consistent with that observed by Fortner et al. [61], the alteration in the molecular structure of nC_{60} is apparent based on the loss of the characteristics $^1T_{1u}$-^1A_g transition peaks at 450, 340 and 260 nm.

Sequential ozonation/chlorination of the nC_{60} suspensions did not produce new bands in the wavelength range studied. The position of the main characteristic peaks of nC_{60} remained unchanged for all chlorinated suspensions and the presence of C-Cl bonds did not alter the

absorbance spectra of the suspensions. However, the pairwise comparison of the absorbance bands of ozonated and ozonated at the same ozone dose and then chlorinated nC_{60} samples revealed that the addition of Cl atom to the fullerene cage decreased the intensity of the absorbance peaks at 270 and 246 nm of the chlorinated nC_{60}. This decrease can be attributed to the addition of Cl atom to the fullerene cage [92]. Comparison of Figures 3.8 and 3.10 suggests that the decrease in the percentage of C-Cl bonds as a result of nC_{60} ozonation is correlated with the decrease in absorbance at 346 and 270 nm.

3.3.3. ζ – potential of nC_{60} aggregates

As electrophoretic mobility measurements have indicated, all nC_{60} suspensions tested in this study, were negatively charged with the ζ – potential measuring in the range from -2.3±1.8 mV to -39.1±3.2 mV regardless of the treatment scheme (Figure 3.10). The surface charge of the as-prepared nC_{60} suspension (-44.6±1 mV) was more negative than that reported for nC_{60} suspensions produced by solvent exchange technique (-9 mV at pH 5-6 in toluene [92], -30 mV in THF [19] and -31.6 mV in ethanol [17]), but close to ζ – potential of nC_{60} suspension produced by extended mixing with water (-30 mV at pH 7 after two weeks mixing [32], -38 mV at pH 7 after several weeks of mixing [8] and -44.5 mV after 11 months of mixing [17] and greater than -30 mV after 111 days of extended mixing [93]). When nC_{60} suspensions were subjected to ozonation only, the ζ – potential of the oxidized nC_{60} did not change significantly until the absorbance at 342 nm has decreased by 75%. When the nC_{60} absorbance at 346 nm

had decreased by 90%; the ζ – potential decreased to -28.81±1.1 mV. With the increase in the degree of ozonation, nC$_{60}$ undergoes a transformation to hemiketal arrangement through the formation of primary ozonides and closed epoxides [52]. These intermediates accumulated in the suspension, thus changing the ζ – potential. In the case of consecutively ozonated/chlorinated nC$_{60}$ suspensions, the ζ – potential became more positive with increasing degree of ozonation for both applied chlorine doses: from -36.9 ± 1.4 mV to -2.3±1.8 mV at 6.8 mg (Cl_2)/L (reaction time 10 min) and from -37.9±2.7 to -8.7±0.6 mV for 68 mg (Cl_2)/L (reaction time10 min). The observed trend is more pronounced for fullerene particles ozonated such that their absorbance at 346 nm decreased by >50%.

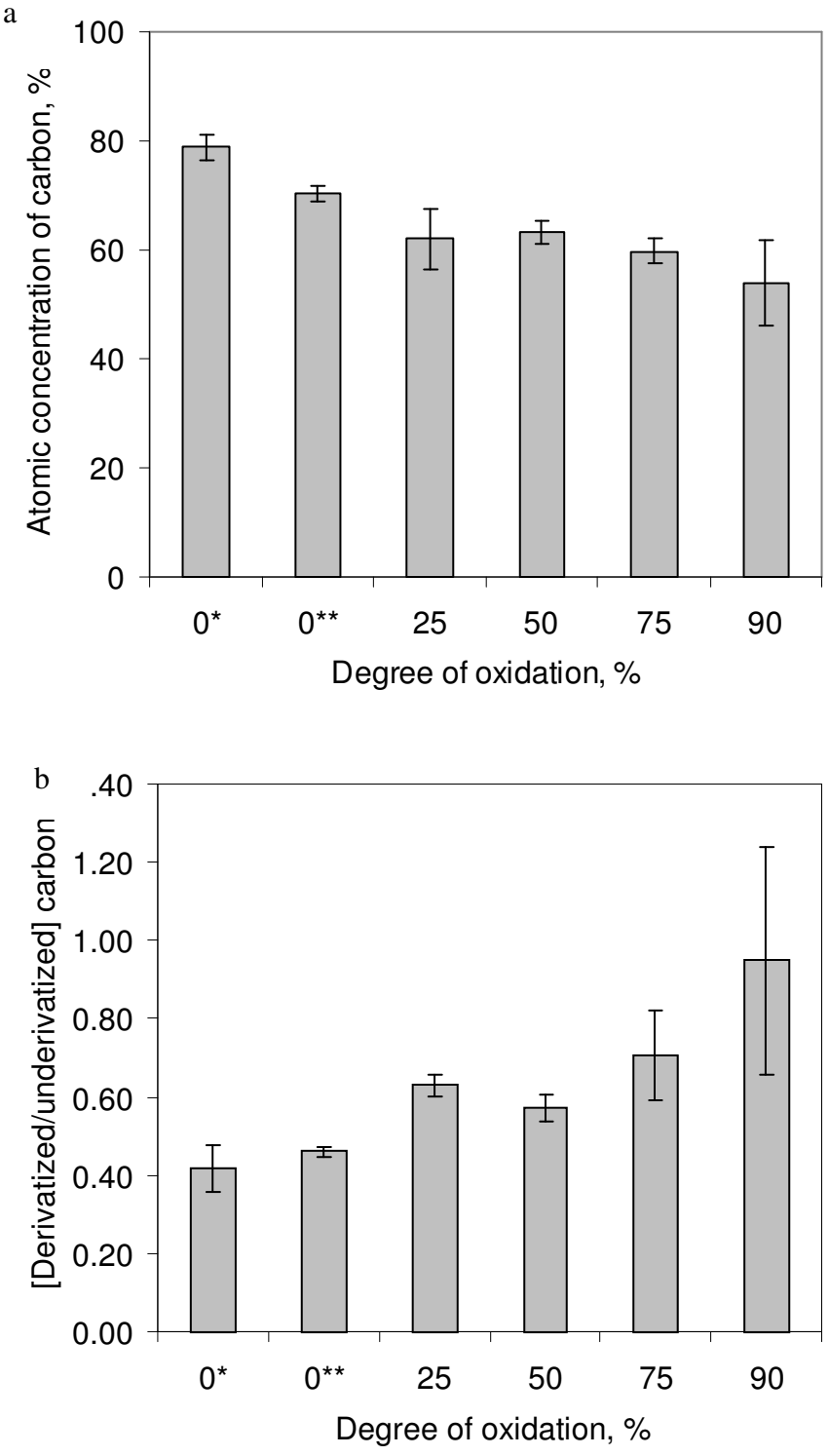

Figure 3.6. Atomic concentration of carbon in % (a) and ratio of derivatized to underivatized carbon (b) in nC$_{60}$ samples as a function of treatment type. * - as prepared nC$_{60}$, ** - chlorinated only nC$_{60}$.

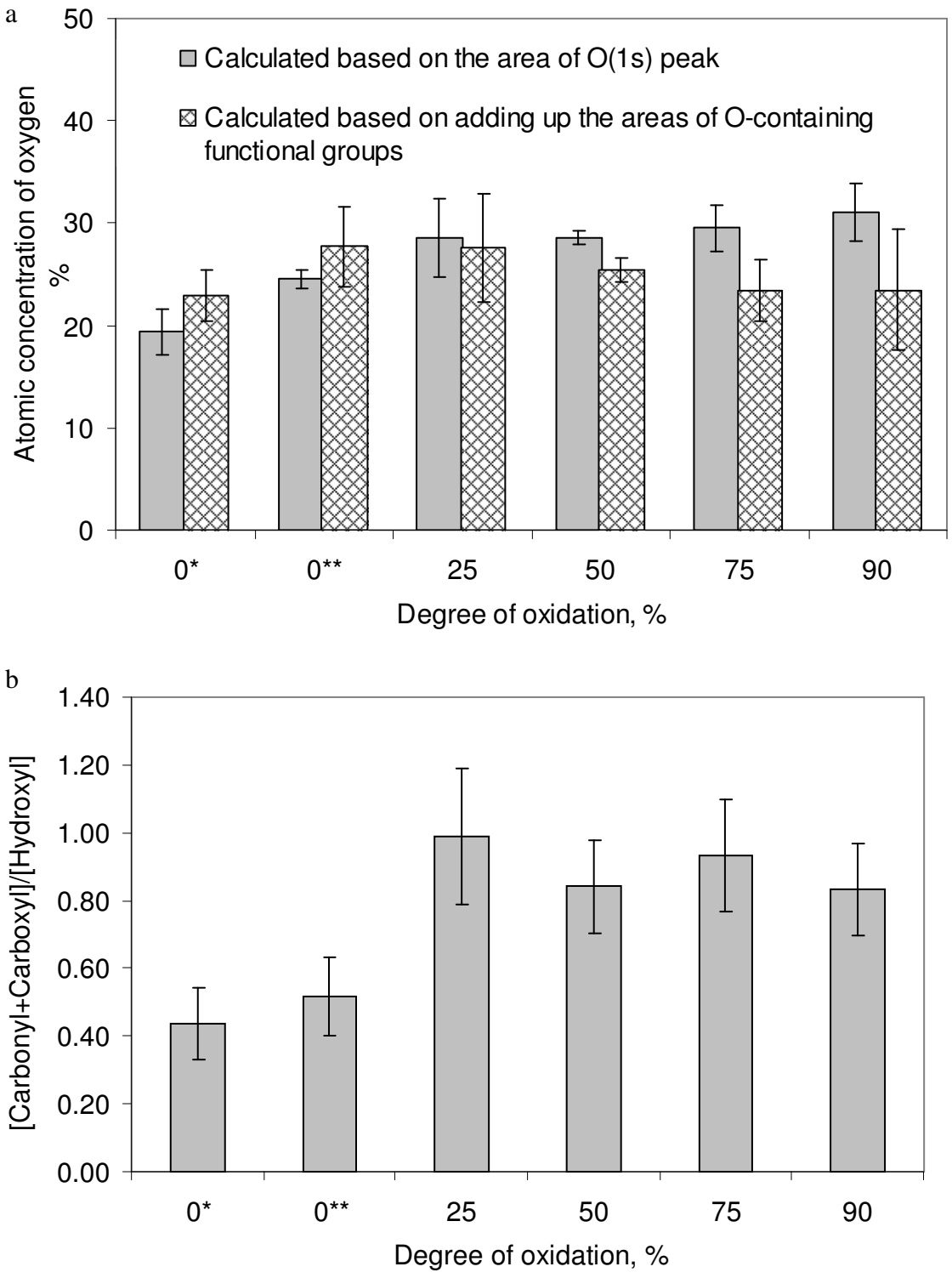

Figure 3.7. Atomic concentration of oxygen in % (a) and ratio of [carbonyl + carboxyl] to [hydroxyl] functional groups (b) in nC$_{60}$ samples as a function of treatment type. * - as prepared nC$_{60}$, ** - chlorinated only nC$_{60}$.

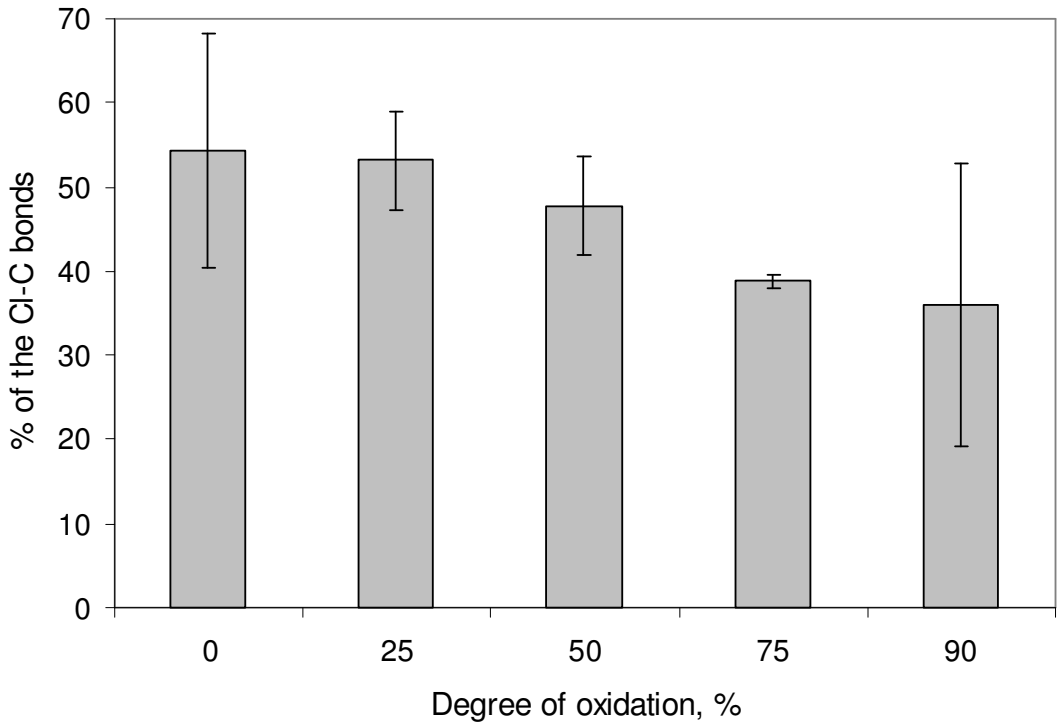

Figure 3.8. Percentage of the Cl-Cl bonds measured in chlorinated nC$_{60}$ samples as a function of treatment type.

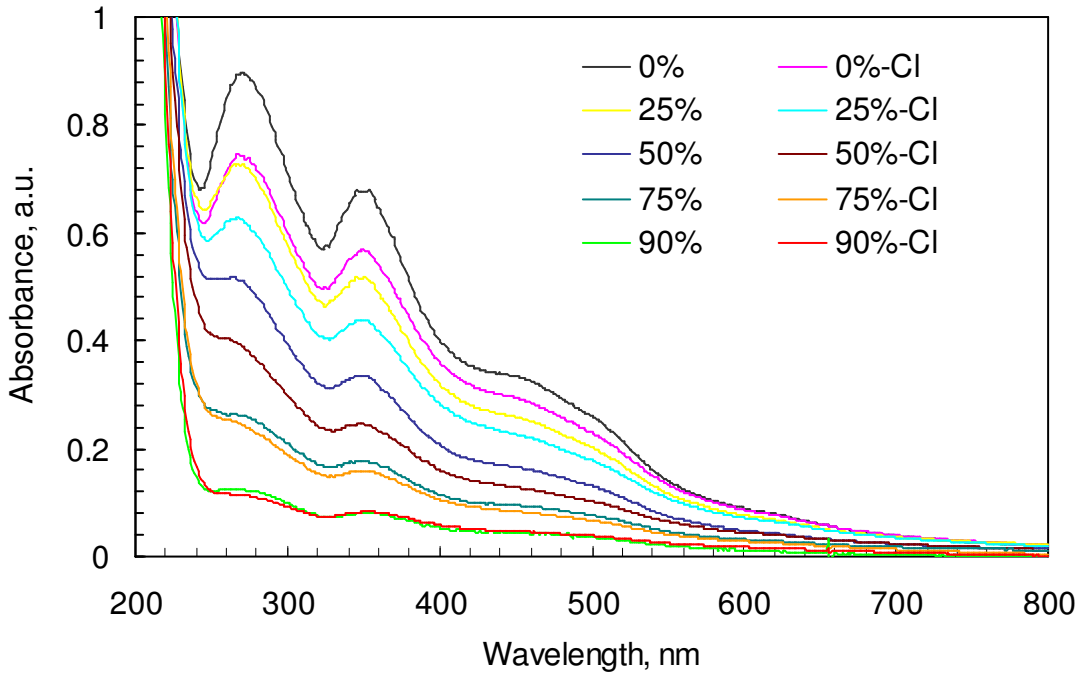

Figure 3.9. Absorbance spectra of nC_{60} suspensions that were ozonated until the absorbance at 346 nm has decreased by 25, 50, 75 or 90% (denoted as X%) and nC_{60} suspensions that were ozonated until the absorbance at 346 nm had decreased by 25, 50, 75 or 90% and then chlorinated at initial chlorine concentration of 68 mg (Cl_2)/L and allowed to react for 10 min (denoted as X%-Cl). Degree of oxidation is measured as a % decrease in the absorbance at 342 nm upon treatment with ozone. Spectra were taken in phosphate buffer at pH 7.

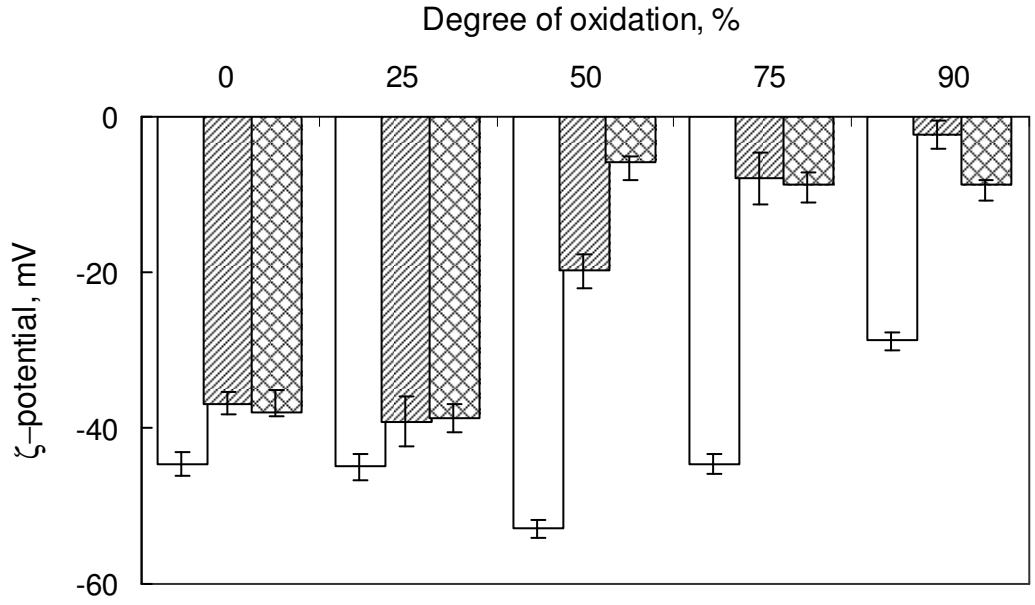

Figure 3.10. ζ-potential of nC$_{60}$ aggregates. Open bars correspond to suspensions ozonated until the absorbance at 346 nm has decreased by 25, 50, 75 or 90%; hatched bars correspond to suspensions ozonated and then chlorinated at a chlorine dose of 6.8 mg (Cl_2)/L and allowed to react for 10 min; cross-hatched bars correspond to suspensions ozonated and then chlorinated at a chlorine dose of 68 mg (Cl_2)/L and allowed to react for 10 min. Degree of oxidation is measured as a % decrease in the absorbance at 346 nm upon treatment with ozone.

3.3.4. General viability bioassay with *E. coli* (prokaryotic cells)

As shown in Figure 3.11, the exposure of as-prepared nC$_{60}$ suspensions in LB and MD media did not suppress bacterial growth, which is consistent with previously observed *E. coli* responce to 5 mg/L of nC$_{60}$ suspension prepared by a similar technique to that used in our work [24]. The derivatized nC$_{60}$ also did not significantly influence *E. coli* growth in either of studied nutrient medi, regardless of the applied ozone dose. As XPS measurements have indicated, the ozonation of nC$_{60}$ suspensions has led to an increasing in O content. In general, derivatized fullerenes such

as C_{60}-COOH (*25*) and C_3, $C_{60}(OH)_{24}$, $Na^{+}_{2-3}[C_{60}O_{7-9}(OH)_{12-15}]^{(2-3)-}$ which bear O-containing hydrophilic functional groups, are considered to be less toxic to microorganisms and eukaryotic cells than non-derivatized C_{60} [33]. This is in good agreement with our findings, where oxidized nC_{60} suspensions were found to be nontoxic to bacterial cells.

As discussed previously, sequential ozonation/chlorination of nC_{60} suspensions led to the formation of chlorinated fullerene byproducts. To investigate the cytotoxic effects of these oxidized nC_{60} aggregates, we evaluated the ability of *E. coli* to grow and form a colony as a function of treatment type, exposure time and nutrient media.

The acute toxicity to *E. coli* of ozonated only and consecutively ozonated/chlorinated nC_{60} aggregates formed after a reaction time of 10 min, with initial chlorine concentrations of 6.8 and 68 mg/L, was measured after 3 hours of contact in 0.1M NaCl. As it can be seen from Figure 3.12, *E. coli* viability was not affected in any of the tested suspensions. At a 95% confidence interval, there was no significant difference in number of colonies grown on the agar plates between vehicle control (a bacterial suspension in ultrapure water), the as-prepared and the treated nC_{60}. Also, no statistically significant difference in the toxicity resulting from the two different chlorine doses was found.

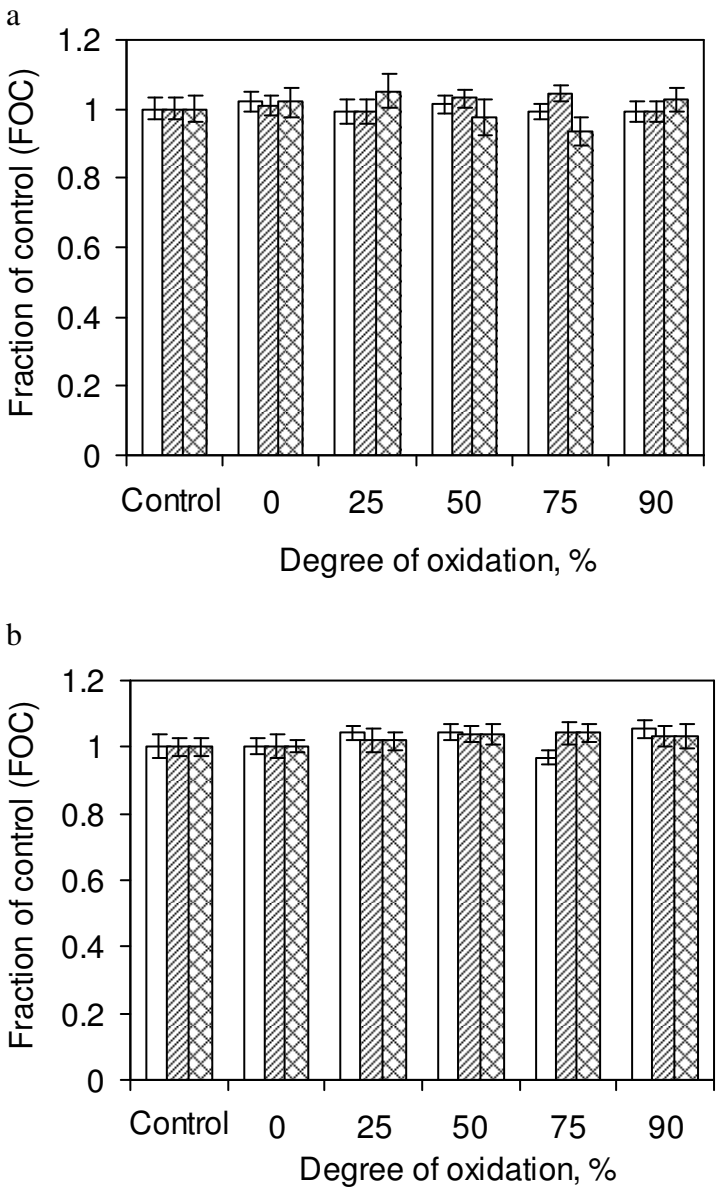

Figure 3.11. *E. coli* viability after 24 hours of incubation with nC_{60} treated according to the scheme 1 in MD (a) and LB (b) media. Open bars correspond to as-prepared suspensions; hatched bars correspond to suspensions, dosed with 0.36 mg/L of ozone solutions and allowed to react for 2 min; cross-hatched bars correspond to suspensions, dosed with 0.36 mg/L of ozone solutions and allowed to react for 33 min. Control samples: bacterial suspensions treated with the equal volume of ultrapure water.

Cytotoxicity tests, performed in LB medium, were aimed at evaluating the effect of oxidized nC$_{60}$ on *E. coli* as a function of exposure time. Figure 3.13 shows the results from these experiments, where Figures (a) and (b) represent the FOC (fraction of control, the average number of colonies grown after *E. coli* exposure to nC$_{60}$ suspensions divided by the average number of colonies grown in the vehicle control samples) upon exposure to nC$_{60}$ suspensions after 3 and 24 hours of contact, respectively. Similar to the previous experiments in 0.1 M NaCl, no reduction in *E. coli* growth upon addition of any type of nC$_{60}$ suspensions was observed at both tested exposure times.

The results from these experiments indicate that the addition of C-Cl bonds to the fullerene cage from the chlorination reaction, did not lead to an increase in cytotoxicity of these oxidized fullerenes.

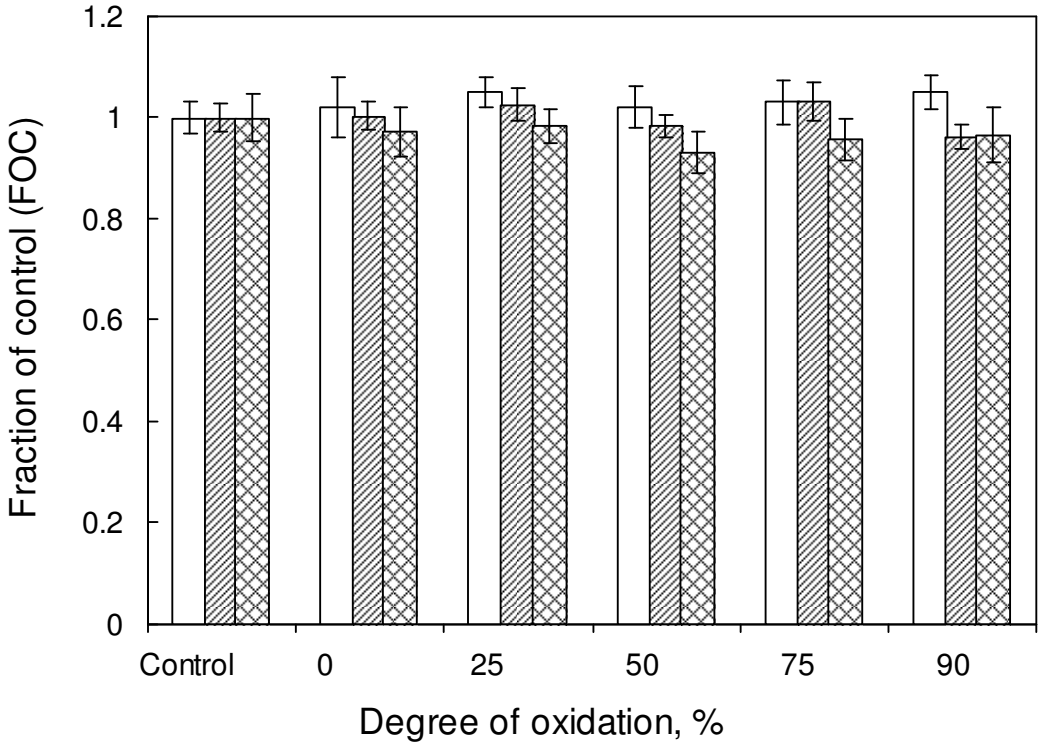

Figure 3.12. *E.coli* viability after 3 hours of incubation with nC$_{60}$ in 0.1M NaCl. Open bars correspond to nC$_{60}$ aggregates ozonated until the absorbance at 342 nm has decreased by 25, 50, 75 or 90%; hatched bars correspond to suspensions ozonated and then chlorinated at a chlorine dose of 6.8 mg (Cl_2)/L and allowed to react for 10 min; cross-hatched bars correspond to suspensions ozonated and then chlorinated at a chlorine dose of 68 mg (Cl_2)/L and allowed to react for 10 min. Degree of oxidation is measured as a % decrease in the absorbance at 346 nm upon treatment with ozone. Control samples: bacterial suspensions treated with equal volume of the ultrapure water.

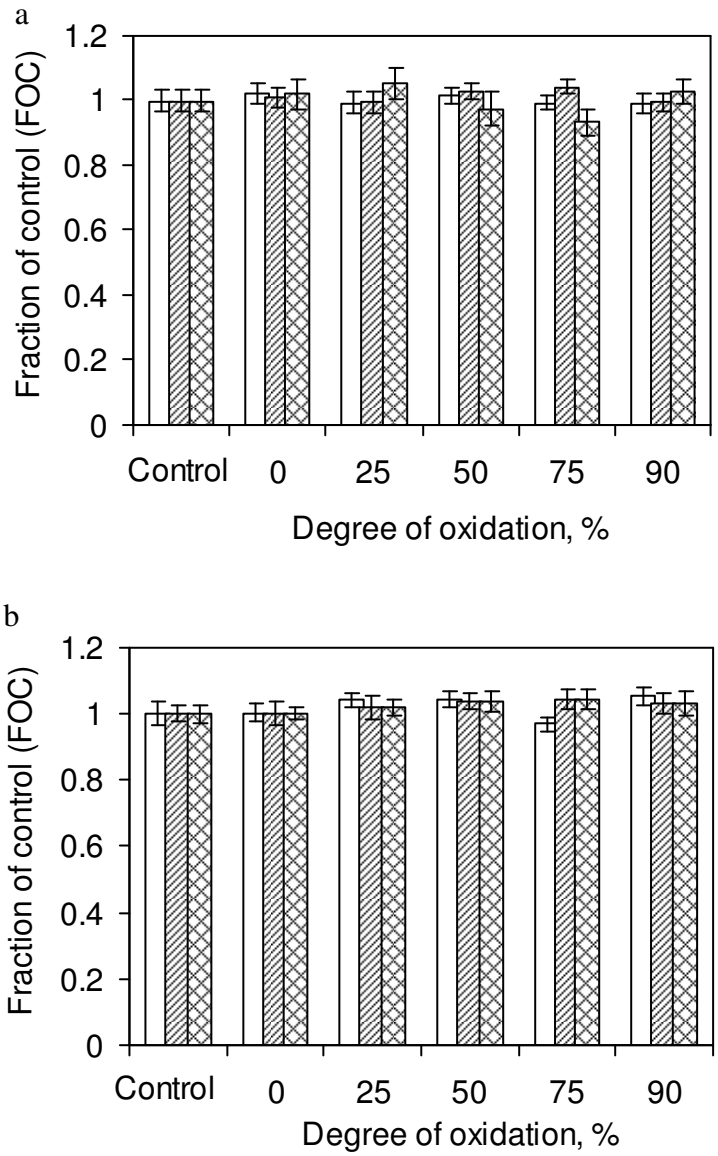

Figure 3.13. *E. coli* viability after 3 (a) and 24 (b) hours of incubation with nC$_{60}$ in LB medium. Open bars correspond to nC$_{60}$ aggregates ozonated until the absorbance at 346 nm has decreased by 25, 50, 75 or 90%; hatched bars correspond to suspensions ozonated and then chlorinated at a chlorine dose of 6.8 mg (Cl_2)/L and allowed to react for 10 min; cross-hatched bars correspond to suspensions ozonated and then chlorinated at a chlorine dose of 68 mg (Cl_2)/L and allowed to react for 10 min. Degree of oxidation is measured as a % decrease in the absorbance at 346 nm upon treatment with ozone. Control samples: bacterial suspensions treated with equal volume of the ultrapure water.

3.3.5 Neutral red dye uptake (NDU) bioassay on eukaryotic cells

In general, prokaryotic cells are considered to be less sensitive to the stress caused by nanoparticles than eukaryotic cells, perhaps due to thicker cell walls and a robust cell metabolism. In this study, we investigated the cytotoxicity of the nC$_{60}$ suspensions towards WB-F344 cells by employing NDU bioassay. This method allows for measurement of the cell integrity and is an indicator of the cell viability. In our experiments, confluent WB-F344 cells were dosed with 500 μL of each nC$_{60}$ suspension for 30 min and 24 hrs. This dose (equivalent to 1:4 dilution of the culture medium) was selected as the maximum dose because of the concern that further increases in the volume added would dilute the culture medium to the extent that it would affect cell growth. The results from these tests are shown in Figure 3.14. Cytotoxicity was not observed for the as-prepared nC$_{60}$ suspension, and ozonated/chlorinated suspensions. The FOC values oscillated around 1.00 (range from 0.94 ± 0.01 to 1.06 ± 0.03). The incubation time did not statistically significantly influence the cytotoxicity. This implies that the cell membrane was able to maintain its integrity during the treatment period, and the amount of the neutral red dye incorporated by the treated cells is compatible with that taken up by the vehicle control samples treated with an equal volume of water. These results are in agreement with the study by Lyon et al. [15], where *E.coli* cells maintained the cell integrity upon exposure to THF/nC$_{60}$.

Optical microscopy was used to observe cell morphology. No changes were observed and the cells remained adhered to the surface of the Petri dish. For illustrative purposes, Figure 3.15 shows typical light and UV epifluorescent images of the WB-F344 cells exposed to vehicle control and the treated nC$_{60}$ suspensions.

3.3.6. Gap junction intercellular communication (GJIC) bioassay on eukaryotic cells

The potential of nC$_{60}$ aggregates for epigenetic toxicity was evaluated using the GJIC bioassay. The effect of as-prepared, ozonated and consecutively ozonated/chlorinated nC$_{60}$ suspensions on the GJIC was studied for two different nC$_{60}$ doses, 200 and 500 μL, and for incubation times of 30 min and 24 h for each dose. The results from these experiments are shown in Figure 3.16. No reduction of a GJIC was measured for any of the parameters studied. All computed FOC values were found to be greater than 0.9, which indicates full communication between the cells. Epifluoescent images of WB-F344 cells (Figure 3.15c, d) show that the spread of Lucifer yellow dye spread did not change after exposure to nC$_{60}$ aggregates. Additionally, no changes in WB-F344 cell morphology were observed under visible light (Figure 15a, b).

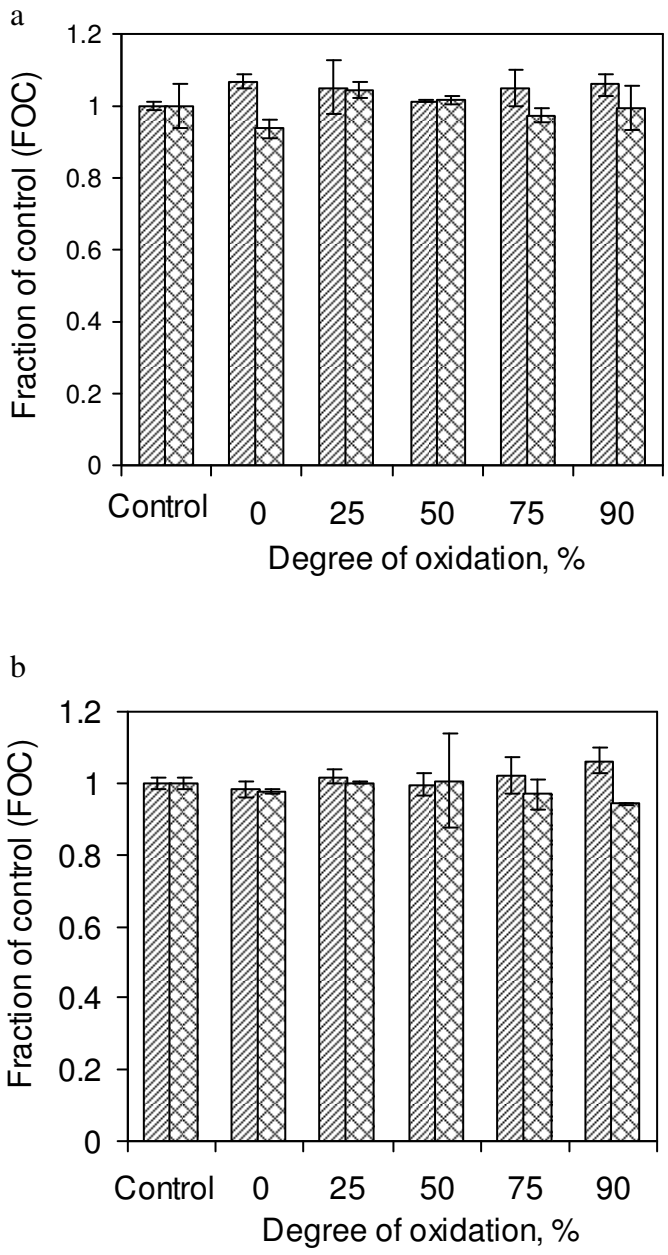

Figure 3.14. Neutral red dye uptake by WB-F344 cells after they were dosed with 500 μL of *n*C_{60} aggregates ozonated until the absorbance at 346 nm has decreased by 25, 50, 75 or 90% (a) and ozonated and then chlorinated at chlorine dose of 68 mg (Cl_2)/L and allowed to react for 10 min (b). Hatched and cross-hatched bars correspond to 3 and 24 hrs of incubation, respectively. Degree of oxidation is measured as a % decrease in the absorbance at 346 nm upon treatment with ozone. Control samples: bacterial suspensions treated with equal volume of the ultrapure water.

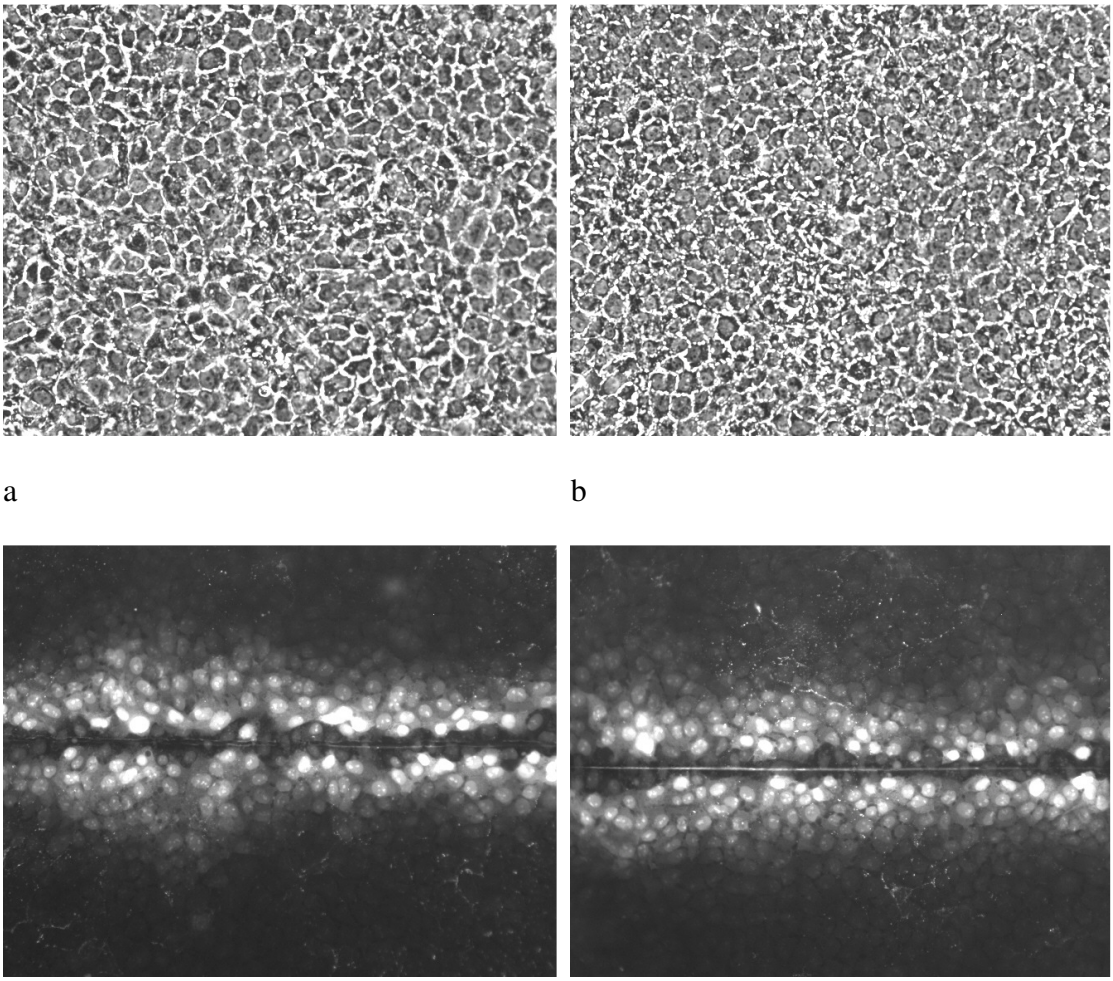

a b

c d

Figure 3.15. Representative phase contrast (a) and UV epifluorescent (c) images of WB-F344 cells incubated with 500 μL of H_2O (control) for 24 hrs. Representative phase contrast (b) and UV epifluorescent (d) images of WB-F344 cells incubated with ozonated until the absorbance at 346 nm has decreased by 90% and then chlorinated at chlorine dose of 68 mg (Cl_2)/L and allowed to react for 10 min (b). All images were taken at 200x magnification.

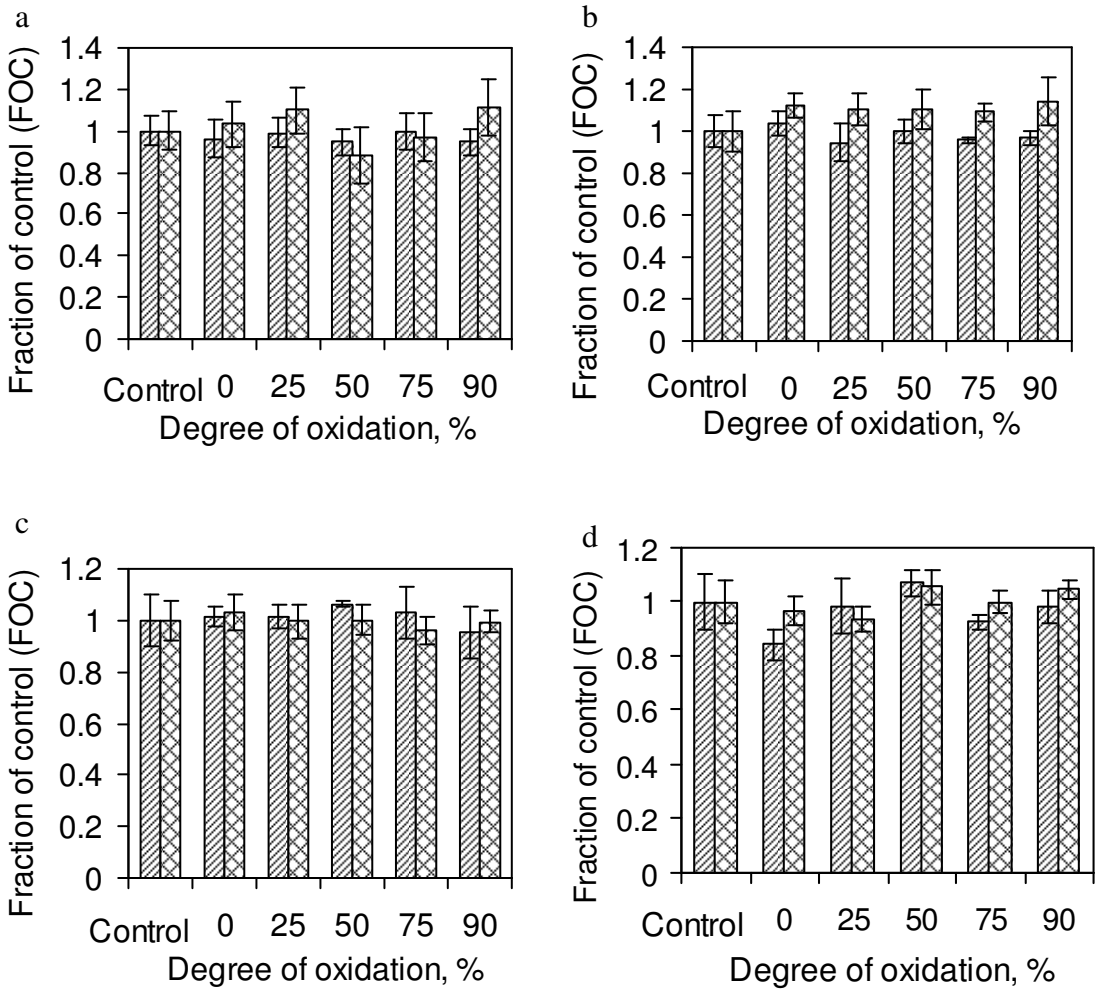

Figure 3.16. GJIC in WB-F344 cells as a function of the applied dose of nC_{60} and exposure time (a – 30 min, suspensions ozonated until the absorbance at 346 nm has decreased by 25, 50, 75 or 90%; b – 30 min, suspensions ozonated and then chlorinated at chlorine dose of 68 mg (Cl_2)/L and allowed to react for 10 min; c – 24 hours, suspensions ozonated until the absorbance at 346 nm has decreased by 25, 50, 75 or 90%; d – 24 hours, suspensions ozonated and then chlorinated at chlorine dose of 68 mg (Cl_2)/L and allowed to react for 10 min). Hatched and cross-hatched bars correspond to 200 and 500 μL of each of nC_{60} suspension, respectively. Degree of oxidation is measured as a % decrease in the absorbance at 346 nm upon treatment with ozone. Control samples: bacterial suspensions treated with equal volume of the ultrapure water.

BIBLIOGRAPHY

BIBLIOGRAPHY

1. Wang, S.; Yang, J.; Li, Y.; Lin, H.; Guo, Z.; Xiao, S.; Shi, Z.; Zhu, D.; Woo, H.-S.; Carroll, D.L.; Kee, I.-S.; Lee, J.-H. Composites of C_{60} based polyphenylene vinylene dyes and conjugated polymer for polymer light-emitting devices. *Applied Physics Letters* (2002), **80**, 3847-3849.

2. Cravino, A.; Sariciftci, N.S. Double-cable polymers for fullerene based organic optoelectronic applications. *Journal of Materials Chemistry* (2002), **12**, 1931-1943.

3. Guihen, E.; Glennon, J.D. Nanoparticles in separation science - recent developments. *Analytical Letters* (2003), **36**, 3309-3336.

4. Taylor, R.; Walton, D. The chemistry of fullerenes. *Nature* (1993), **363**, 685-693.

5. Forro, L.; Mihaly, L. Electronic properties of dopped fullerenes. *Reports on Progress in Physics* (2001), **64**, 649-699.

6. Arbogast, J.W.; Darmanyan, A.P.; Foote, C.S.; Rubin, Y.; Diederich, F.N.; Alvarez, M.M.; Anz, S.J.; Whetten, R.L. Photophysical properties of C_{60}. *Journal of Physical Chemistry* (1991), **95**, 11-12.

7. Markovic, Z.; Todorovic-Markovic, B.; Kleut, D.; Nikolic, N.; Vranjes-Djuric, S.; Misirkic, M.; Vucicevic, L.; Janjetovic, K.; Isakovic, A.; Harhaji, L.; Babic-Stojic, B.; Dramicanin, M.; Trajkovic, V. The mechanism of cell-damaging reactive oxygen generation by colloidal fullerenes. *Biomaterials* (2007), **28**, 5437-5448.

8. Brant, J.; Lecoanet, H.; Hotze, M.; Wiesner, M. Comparison of electrokinetic properties of colloidal fullerenes (n-C_{60}) formed using two procedures. *Environmental Science and Technology* (2005), **39**, 6343-6351.

9. Brant, J.A.; Labille, J.; Bottero, J.-Y.; Wiesner, M.R. Characterizing the impact of preparation method on fullerene cluster structure and chemistry. *Langmuir* (2006), **22**, 3878-3885.

10. Oberdorster, E.; Zhu, S.; Blickley, T.M.; McClellan-Green, P.; Haasch, M.L. Ecotoxicology of carbon-based engineered nanoparticles: effects of fullerene (C_{60}) on aquatic organisms. *Carbon* (2006), **44**, 1112-1120.

11. Gao, J.; Youn, S.; Hovsepyan, A.; Llaneza, V.L.; Wang, Y.; Bitton, G.; Bonzongo, J.-C.C. Dispersion and toxicity of selected manufactured nanomaterials in natural river water samples: Effects of water chemical composition. *Environmental Science and Technology* (2009), **43**:9, 3322-3328.

12. Brunet, L.; Lyon, D.Y.; Hotze, E.M.; Alvarez, P.J.J.; Wiesner, M.R. Comparative photoactivity and antibacterial properties of C_{60} fullerenes and titanium dioxide nanoparticles. *Environmental Science and Technology* (2009), **43**, 4355-4360.

13. Spohn, P.; Hirsch, C.; Hasler, F.; Bruinink, A.; Krug, H.F.; Wick, P. C_{60} fullerene: A powerful antioxidant or a damaging agent? The importance of an in-depth material characterization prior to toxicity assays. *Environmental Pollution* (2009), **157**, 1134-1139.

14. Chae, S.-R.; Wang, S.; Hendren, Z.D.; Wiesner, M.R.; Watanabe, Y.; Gunsch, C.K. Effects of fullerene nanoparticles on *Escherichia coli* K12 respiratory activity in aqueous suspension and potential use for membrane biofouling control. *Journal of Membrane Science* (2009), **329**, 68-74.

15. Lyon, D.Y.; Pedro J.J. Alvarez, P.J.J.J. Fullerene water suspension ($n$$C_{60}$) exerts antibacterial effects via ROS-independent protein oxidation *Environmental Science and Technology* (2008), **41**:21, 8127-8132.

16. Lyon, D.Y.; Brunet, L.; Hinkal, G.W.; Wiesner, M.R.; Alvarez, P.J.J. Antibacterial activity of fullerene water suspensions ($n$$C_{60}$) is not due to ROS-mediated damage. *Nano Letters* (2008), **8**:5, 1539-1543.

17. Dhawan, A.; Taurozzi, J.S.; Pandey, A.K.; Shan, W.; Miller, S.M.; Hashsham, S.A.; Tarabara, V.V. Stable colloidal dispersion of C_{60} fullerenes in water: evidence for genotoxicity. *Environmental Science and Technology* (2006), **40**, 7394-7401.

18. Deguchi, S.; Alargova, R.G.; Tsujii, K. Stable dispersions of fullerenes, C_{60} and C_{70} in water. Preparation and characterization. *Langmuir* (2001), **17**, 6013-6017.

19. Jamakoshi, Y.N.; Yagami, T.; Fukuhara, K.; Sueyoshi, S.; Miyata, N. Solubilization of fullerenes into water with polyvinylpyrrolidone applicable to biological tests. *Journal of Chemical Society* (1994), **4**, 517-518.

20. Klaper, R.; Crago, J.; Barr, J.; Arndt, D.; Setyowati, K.; Chen, J. Toxicity biomarker expression in daphnids exposed to manufactured nanoparticles: Changes in toxicity with functionalization. *Environmental Pollution* (2009), **157**, 1152-1156.

21. Liang, Y.; Luo, F.; Lin, Y.; Zhou, Q.F.; Jiang, G. C_{60} affects DNA replication *in vitro* by decreasing the melting temperature of DNA templates. *Carbon* (2009), **47**, 1457-1465.

22. Zhang, B.; Cho, M.; Fortner, J.D.; Lee, J.; Huang, C.-H.; Hughes, J.B.; Kim, J.-H. Delineating oxidative processes of aqueous C_{60} preparations: role of THF peroxide. *Environmental Science and Technology* (2009), **43**:1, 108-113.

23. Ko, W.-B.; Heo, J.-Y.; Nam, J.-H.; Lee, K.-B. Synthesis of a water-soluble fullerene [C_{60}] under ultrasonication. *Ultrasonics* (2004), **41**, 727-730.

24. Deguchi, S.; Mukai, S.-A.; Tsudonne, M.; Horikoshi, K. Facile generation of fullerene nanoparticles by hand-grinding. *Advanced Materials* (2006), **18**, 729-732.

25. Avdeev, M.V.; Khokhryakov, A.A.; Tropin, T.V.; Andrievsky, G.V.; Klochkov, V.K.; Derevyanchenko, L.I.; Rosta, L.; Garamus, V.M.; Priezzhev, V.B.; Korobov, M.V.; Aksenov, V.L. Structural features of molecular-colloidal solutions of C_{60} fullerenes in water by small-angle neutron scattering. *Langmuir* (2004), **20**, 4363-4368.

26. Andersson, T.; Nilsson, K.; Sundahl, M.; Westman, G.; Wennerstorm, O. C_{60} embedded in gamma-cyclodextrin – a water soluble fullerene. *Chemical Communications* (1992), 604-608.

27. Hungerbuhler, H.G.; Guldi, D.M.; Asmus, K.-D. Incorporaion of C_{60} into artificial lipid membranes *Journal of the American Chemical Society* (1993), **115**, 3386-3387.

28. Oberdörster, E. Manufactured nanomaterials (Fullerenes, C_{60}) induce oxidative stress in the brain of Juvenile Largemouth Bass. *Environmental Health Perspectives* (2004), **112**, 1058-1062.

29. Sayes, C.M.; Fortner, J.D.; Guo, W.; Lyon, D.; Boyd, A.M.; Ausman, K.D.; Tao, Y.J.; Sitharaman, B.; Wilson, L.J.; Hughes, J.B.; West, J.L.; Colvin, V.L. The differential cytotoxicity of water-soluble fullerenes. *Nano Letters* (2004), **4**:10, 1881-1887.

30. Sayes, C.M.; Gobin, A.M.; Ausman, K.D.; Mendez, J.; West, J.L.; Colvin, V.L. Nano-C_{60} cytotoxicity is due to lipid peroxidation. *Biomaterials* (2005), **26**, 7587-7595.

31. Sayes, C.M.; Marchione, A.A.; Reed, K.L.; Warheit, D.B. Comparative pulmonary toxicity assessments of C_{60} water suspensions in rats: few differences in fullerene toxicity in vivo in contrast to in vitro profiles. *Nano Letters* (2007), **7**:8, 2399-2406.

32. Tong, Z.; Bischoff, M.; Nies, L.; Applegate, B.; Turco, R. Impact of fullerene (C_{60}) on a soil microbial community. *Environmental Science and Technology* (2007), **41**, 2985-2991.

33. Tang, Y.J.; Ashcroft, J.M.; Chen, D.; Min, G.; Kim, C.-H.; Murkhejee, B.; Larabell, C.; Keasling, J.D.; Chen, F.F. Charge-associated effects of fullerene derivatives on microbial structural integrity and central metabolism. *Nano Letters* (2007), **7**:3, 754-760.

34. Zhu, X.; Zhu, L.; Li, Y.; Duan, Z.; Chen, Z.W.; Alvarez, P.J. Developmental toxicity in toxicity in zebrafish (*Danio Rerio*) embtyos after exposure to manufactured nanomaterials: buckminsterfullerene aggregates ($n$$C_{60}$) and fullerol. *Environmental Toxicology and Chemistry* (2007), **26**, 976-979.

35. Zhu, S.; Oberdorster, E.; Haasch, M.L. Toxicity of an engineered nanoparticle (fullerene, C_{60}) in two aquatic species, Daphnia and fathead minnow. *Marine Environmental Research* (2006), **62**, S5-S9.

36. Fang, J.; Lyon, D.; Weisner, M.; Dong, J.; Alvarez, P.J.J. Effect of fullerene water suspension on bacterial phospholipids and membrane phase behaviour. *Environmental Science and Technology* (2007), **41**, 2636-2642.

37. Levi, N.; Hantgan, R.R.; Lively, M.O.; Carroll, D.L.; Prasad, G.L. Fullerenes: detection of intracellular photoluminescence and lack of cytotoxic effects. *Journal of Nanobiotechnology* (2006), **4**, 1-11.

38. Lovern, S.; Klaper, R. Daphnia magna mortality when exposed to titanium dioxide and fullerene (C_{60}) nanoparticles. *Environmental Toxicology and Chemistry* (2006), **26**, 1132-1137.

39. Nyberg, L.; Turco, R.F.; Nies, L. Assessing the impact of nanomaterials on anaerobic microbial communities *Environmental Science and Technology* (2008), **42**:6, 938-1943.

40. Lyon, D.Y.; Fortner, J.D.; Sayes, C.M.; Colvin, V.L.; Hughes, J.B. Bacterial cell association and antimicrobial activity of a C_{60} water suspension. *Environmental Toxicology and Chemistry* (2005), **24**, 2757-2762.

41. Lyon, D.; Adams, L.K.; Falkner, J.; Alvares, P.J. Antibacterial activity of fullerene water suspensions: effects of preparation method and particle size. *Environmental Science and Technology* (2006), **40**, 4361-4366.

42. Isakovic, A.; Markovic, Z.; Todorovic-Markovic, B.; Nikolic, N.; Vranjes-Djuric, S.; Mirkovic, M.; Dramicanin, M.; Harhaji, L.; Raicevic, N.; Nikolic, Z.; Trajkovic, V. Distinct cytotoxic mechanisms of pristine versus hydroxylated fullerene. *Toxicological Sciences* (2006), **91**, 173-183.

43. Fortner, J.D.; Lyon, D.Y.; Sayes, C.M.; Boyd, A.M.; Falkner, J.C.; Hotze, E.M.; Alemany, L.B.; Tao, Y.J.; Guo, W.; Ausman, K.D.; Colvin, V.L.; Hughes, J.B. C_{60} in water: nanocrystal formation and microbial response. *Environmental Science and Technology* (2005), **39**:11, 4307-4316.

44. Usenko, C.Y.; Harper, S.L.; Tanguay, R.L. Fullerene C_{60} exposure elicits an oxidative stress response in embryonic zebrafish. *Toxicology and Applied Pharmacology* (2008), **229**, 44–55.

45. Shinohara, N.; Matsumoto, T.; Gamo, M.; Miyauchi, A.; Endo, S.; Yonezama, Y.; Nakanishi, J. Is lipid peroxidation induced by the aqueous suspension of fullerene C_{60} nanoparticles in the brains of *Cyprinus carpio*? *Environmental Science and Technology* (2009), **43**, 948-953.

46. Lee, J.; Mackeev, Y.; Cho, M.; Li, D.; Kim, J.-S.; Wilson, L.J.; Alvarez, P.J. Photochemical and antimicrobial properties of novel C_{60} derivatives in aqueous systems. *Environmental Science and Technology* (2009), **43**, 6604-6610.

47. Jia, G.; Wang, H.; Yan, L.; Wang, X.; Pei, R.; Yan, T.; Zhao, Y.; Guo, X. Cytotoxicity of carbon nanomaterials: single-wall nanotube, multi-wall nanotube, and fullerene. *Environmental Science and Technology* (2005), **35**, 1378-1383.

48. Cho, M.; Fortner, J.D.; Huges, J.B.; Kim, J.-H. *Escherichia coli* inactivation by water-soluble, ozonated C_{60} derivative: kinetics and mechanisms. *Environmental Science and Technology* (2009), **43**:19, 7410-7415.

49. Cooper, G.M., *Classification and development of neoplasms*, in *Elements of Human Cancer*. 1992, Jones and Bartlett Publishers: Boston, MA. 15-30

50. Harris, C.C. Chemical and physical carcinogenesis: advances and perspectives for the 1990s. *Canser Research* (1991), **51**, 5023s-5044s.

51. Boyd, J.A.; Barrett, J.C. Genetic and cellular basis of multistep carcinogenesis. *Pharmacology and Therapeutics* (1990), **46**, 469-486. .

52. Jonson, J.D.; Jensen J.N. 1986. THM and TOX formation: routes, rates and precursors. *Journal of the American Water Works Association* (1986), **78**, 156-162.

53. Richardson, S.D., *Drinking water disinfection by-products. Ecyclopedia of environmental analysis and remediation*, R.A. Meyers, Editor. 1998, Wiley: NY. 1398-1421.

54. Minear, R.A.; Amy, G.L. Disinfection by-products in water treatment: the chemistry of their formation and control. 1996, NY: Lewis Publishers.

55. Upham, B.L.; Boddy, B.; Xing, X.; Trosko, J.; Masten, S.J. Nongeneotoxic effects of selected pesticides and their disinfection by-products on gap junctional intercellular communication *Ozone Science and Engineering* (1997), **19**, 351-369.

56. Koivusalo, M.; Jaakola, J.J.K.; Vartiainen, T. Drinkig water mutagenicity in past exposure assessment of the studies on drinking water and cancer: application and evaluation in Finland. *Environmental Research* (1994), **64**, 90-101.

57. Betts, K. Growing concern about disinfection by-products. *Environmental Science and technology* (1998), **32**, 546A-548A.

58. Razumovskii, S.D.; Bylgakov, R.G.; Nevyadovskii, E.Y. Kinetics and stoichiometry of the reaction of ozone with fullerene C_{60} in a CCl_4 solution. *Kinetics and Catalysis* (2003), **44**:2, 229-232.

59. Cataldo, F.; Ori, O. Ozone reaction with C_{60} fullerene. A stydy on the antiozonant activity of C_{60} fullerene in dienic rubber. *Polymer Degradation and Stability* (1995), **48**, 291-296.

60. Davydov, V.Y.; Filatova, G.N.; Knipovich, O.M.; Lunin, V.V. Study of the kinetics of fullerenes ozonolysis. *Proceedings of the Electrochemical Society* (1996), **96**:10, 1295-1306.

61. Fortner, J.D.; Kim, D.-I.; Boyd, A.M.; Falkner, J.C.; Moran, S.; Colvin, V.L.; Huges, J.B.; Kim, J.-H. Reaction of water-stable C_{60} aggregates with ozone. *Environmental Science and Technology* (2007), **41**, 7497-7502.

62. Anachkov, M.P.; Cataldo, F.; Rakovsky, S.K. Reaction kinetics of C_{60} fullerene ozonation. *Fullerenes, Nanotubes, and carbon nanostructures* (2003), **11**:2, 95-103.

63. Birkett, p.R.; Avent, A.G.; Darwish, A.D.; Kroto, H.W.; Taylor, R.; Walton, D.R.M. Preparation and ^{13}C NMR spectroscopic characterization of $C_{60}Cl_6$. *Journal of the Chemical Society, Chemical Communications* (1993), 1230-1232.

64. Tebbe, F.N.; Becker, J.Y.; Chase, D.B.; Firment, L.E.; Holler, E.R.; Malone, B.S.; Krusic, P.J.; Wasserman, E. Multiple, reversible chlorination of C_{60}. *Journal of the American Chemical Society* (1991), **113**, 9900-9901.

65. Olah, G.A.; Bucsi, I.; Lambert, C.; Aniszfeld, R.; Trivedi, N.J.; Sensharma, D.K.; Prakash, G.K.S. Chlorination and bromination of fullerenes. Nucleophilic methoxylation of polychlorofullerenes and their aluminum trichloride catalyzed Friedel-Crafts reaction with aromatics to polyarylfullerenes. *Journal of the American Chemical Society* (1991), **113**, 9385-9387.

66. Thill, A.; Zeyons, O.; Spalla, O.; Chauvat, F.; Rose, J.; Auffan, M.; Flank, A.M. Cytotoxicity of CeO_2 nanoparticles for *Escherichia Coli*. Physico-chemical insight of the cytotoxicity mechanism *Environmental Science and Technology* (2006), **40**:19, 6151–6156.

67. Atlas, R.M. Handbook of Microbiological Media. 1993, Boka Raton: CRC Press.

68. Borenfreund, E.; Puerner, J.A. Toxicology determined in vitro by morphological alterations and neutral red absorption. *Toxicology Letters* (1985), **24**, 119-124.

69. El-Fouly, M.H.; Trosko, J.E.; Chang, C.C. Scrape-loading and dye transfer: a rapid and simple technique to study gap junctional intercellular communications. *Experimental Cell Research* (1987), **168**, 422-430.

70. Weis, L.M.; Rummel, A.M.; Masten, S.J.; Trosko, J.E.; Upham, B.L. Bay or baylike regions of polycyclic aromatic hydrocarbons were potent inhibitors of gap junctional intercellular communication *Environmental Health Perspectives* (1998), **106**:1, 17-22.

71. Satoh, A.Y.; Trosco, J.; Masten, S.J. Epigenetic toxicity of hydroxylated biphenyls and hydroxylated polychlorinated biphenyls on normal rat liver epithelial cells. *Environmental Science and Technology* (2003), **37**, 2727-2733.

72. Herner, H.A.; Trosko, J.E.; Masten, S.J. The epigenetic toxicity of pyrene and related ozonation byproducts containing an aldehyde functional group. *Environmental Science and Technology* (2001), **35**:17, 3576-3583.

73. *EPA Guidance Manual, Appendix B. Ct Tables, LT1ESWTR Disinfection Profiling and benchmarking*, W. U.S. EPA, DC., Editor. 2003.

74. Clesceri, L.S.; Greenberg, A.E.; Eaton, A.D. Standard methods for examinations of water and wastewater. 20th ed. 1998: American Public Health Association.

75. Alpatova, A.L.; Shan, W.; Babica, P.; Upham, B.L.; Rogensues, A.R.; Masten, S.J.; Drown, E.; Mohanty, A.K.; Alocilja, E.C.; Tarabara, V.V. Single-walled carbon nanotubes dispersed in aqueous media via non-covalent functionalization: Effect of dispersant on the stability, cytotoxicity, and epigenetic toxicity of nanotube suspensions. *Water Research* **44**:2, 505-520.

76. Briggs, D.; Beamson, G. XPS studies of the oxygen 1s and 2s levels in a wide range of functional groups. *Analytical Chemistry* (1993), **65**, 1517-1523.

77. Ngiem, L.; Schafer, A.; Elimelech, M. Removal of natural hormones by nanofiltration membranes: measurement, modeling, and mechanisms. *Environmental Science and Technology* (2004), **38**, 1888-1896.

78. *Dow Water and Process Solutions*, http://www.dow.com/liquidseps/prod/bw30_440i.htm.

79. Jørgensen, S.; Anton Horst, J.A.; Dyrlie, O.; Larring, Y.; Ræder, H.; Norby, T. XPS surface analyses of $LaPO_4$ ceramics prepared by precipitation with or without excess of PO_4^{3-}. *Surface and Interface Analysis* (2001), **34**, 306–310.

80. Baltrusaitis, J.; Jayaweera, P.M.; Grassiana, V.H. XPS study of nitrogen dioxide adsorption on metal oxide particle surfaces under different environmental conditions. *Physical Chemistry Chemical Physics* (2009), **11**, 8295–8305.

81. Coena, M.C.; Keller, B.; Groening, P.; Schlapbach, L. Functionalization of graphite, glassy carbon, and polymer surfaces with highly oxidized sulfur species by plasma treatments. *Journal of Applied Physics* (2002), **92**:9, 5077-5083.

82. Briggs, D.; Seah, M.P. Practical surface analysis. 2 ed. Vol. 1. 1990: Willey.

83. Stoch, J.; Ladecka, M. An XPS study of the KCl surface oxidation in oxygen glow discharge. *Applied Surface Science* (1988), **31**:4, 426-436.

84. Baumann, M.J. PhD Dissertation, Cape Western University, 1987.

85. Alpatova, A.L., *Personal communication with the sales representative of Materials Research Electronic Corporation*. 2010: East Lansing.

86. Clark, D.T.; Thomas, H.R. Applications of ESCA to polymer chemistry. XVII. Systematic investigation of the core levels of simple homopolymers. *Journal of Polymer Science: Polymer Chemistry Edition* (1978), **16**:4, 791-820.

87. Papirer, E.; Lacroix, R.; Donnet, J.-B.; Nanse, G.; Fioux, P. XPS study of the halogenation of carbon black - Part 2. Chlorination. *Carbon* (1995), **1**, 63-72.

88. Andrievsky, G.V.; Klochkov, V.K.; Bordyuh, A.B.; Dovbeshko, G.I. Comparative analysis of two aqueous-colloidal solutions of C_{60} fullerene with help of FTIR reflectance and UV-Vis spectroscopy. *Chemical Physics Letters* (2002), **364**, 8-17.

89. Chen, K.L.; Elimelech, M. Relating colloidal stability of fullerene (C_{60}) nanoparticles to nanoparticle charge and electrokinetic properties. *Environmental Science and Technology* (2009), **43**, 7270-7276.

90. Cataldo, F.; Heymann, D. A study of polymeric products formed by C_{60} and C_{70} fullerene ozonation. *Polymer Degradation and Stability* (2000), **70**, 237-243.

91. Galapate, R.P.; Baes, A.U.; Okada, M. Transformation of Dissolved Organic Matter During Ozonation: Effects on Trihalomethane Formation Potential. *Water Research* (2001), **35**:9, 2201-2206.

92. Mchedlov-Petrossyan, N.O.; Klochkov, V.K.; Andrievsky, G.V. Colloidal dispersions of fullerene C_{60} in water: some properties and regularities of coagulation by electrolytes. *Journal of the Chemical Society, Faraday Transactions articles* (1997), **93**:24, 4343-4346.

93. Ma, X.; Bouchard, D. Formation of aqueous suspensions of fullerenes *Environmental Science and Technology* (2009), **43**:2, 330-336.

CHAPTER 4

REMOVAL OF SELECTED PHARMACEUTICALS AND DISINFECTION BY-PRODUCTS FROM SURFACE WATERS BY HYBRIX OZONATION-CERAMIC MEMBRANE FILTRATION PROCESS

4.1. Introduction

4.1.1. Pharmaceuticals as emerging contaminants

Pharmaceutically active compounds are often complex molecules with a wide range of physicochemical properties and biological activity. Due to advances in the analytical techniques used to identify and quantify these compounds in environmental samples, pharmaceuticals can now be detected in upper ng/L to µg/L concentration range and thus are often referred as micropollutants [1, 2].

The production and application patterns of any specific drug significantly vary from country to country due to different consumption levels, legislation, and accessibility of an individual pharmaceutical to the public. For example, the antibiotic vancomycin is used widely in the USA, while in Germany this compound is used only when other treatments are inefficient due to microbial resistance [3]. Streptomycin, a bacteriocide and fungicide, is banned in Germany [2]. Some pharmaceuticals can be sold over-the-counter in some countries, while in others they are available only by prescription.

Pharmaceuticals are released into the environment predominantly via human or animal excretion (in their native form or as an active metabolites) through the sewage system and into the influent

of wastewater treatment plants [4, 5]. Other sources include household disposal of unused medicines via sinks/toilets or via waste collection [6], disposal of pharmaceuticals that have been used during medical therapy [7], agricultural run off [4] and effluent from pharmaceutical production plants [3].

Having been designed to exert a certain physiological effect on humans, animals, or plants, pharmaceuticals are chemically stable, often persistent to biological degradation and accumulate in aquatic and terrestrial ecosystems [4, 8]. When released into the environment, these compounds affect physiological processes in lower animals (e.g., renal failure in the vulture caused by diclofenac residuals [9], reproductive dysfunction in fish due to the long-term exposure to estrogenic compounds [10-12], chronic effects to freshwater invertebrates caused by diazepam, digoxin and amlodipine [13]). There is evidence that some pharmaceuticals (e.g, cyclophoshamide and ifosfamide) may increase the risk of cancer in humans [14]. Antibiotics facilitate the development of antibiotic-resistant microorganisms by affecting the microorganism genome (e.g., tetracycline-resistant *E. coli* [15]). Furthermore, when a pharmaceutical co-exists in a mixture with other pharmaceuticals, the toxicity of such mixture follows the concept of "concentration addition", where the effects of compounds of each compounds are additive. For example, Cleuvers et al. [16] found that mixture of the anti-inflammatory drugs diclofenac, ibuprofen, naproxen and acetylsalicylic acid was toxic to *Daphnia magna* and algae at concentrations where a single compound exhibited no or little toxicity. Degradation products of an individual pharmaceutical may also be toxic and contribute to the overall toxicity of the mixture [17].

The toxicity of an individual pharmaceutical depends on the applied dose and the mode of action. Webb et al. [18] evaluated the risk from exposure of humans to different types of pharmaceuticals via drinking water. The authors found that antidepressants, antibacterials and antipsycholitics were the most toxic among other chemicals studied. As a result of these and other studies, regulatory agencies are undertaking action towards determining human risks from the presence of pharmaceuticals in drinking water. According to the European Commission draft guidelines, the authorization for a human use medicinal product should be accompanied by an environmental risk assessment [19]. The U.S. Food and Drug Administration requires manufacturers to provide an environmental assessment report when the expected concentration of the active ingredient of the pharmaceutical in the aquatic environment exceeds 1 µg/L [20]. In addition, amendments to the Food Quality Protection Act (Bill number P.L. 104-170) and to the Safe Water Drinking Act (Bill number S.1316) have authorized the U.S. Environmental Protection Agency (EPA) to monitor all substances for their potential ability to disrupt endocrine systems in any organism where drinking water and food could be contaminated. However, due to the wide range of pharmaceuticals produced and the absence of standardized analytical methods for their identification and quantification, no pharmaceutical is presently regulated in U.S. drinking water.

The efficiency of removal of pharmaceutical compounds in wastewater treatment processes varies significantly, but in general is quite low. Conventional waste water treatment plants only partially remove selected pharmaceuticals (e.g., 26% for sulfamethazine, sulfamethoxazole, sulfathiazole and trimethoprim [21]; 29% for carmazepine [22]; 67% for sulfamethoxazole [23]). While studying the removal of 28 human and veterinary antibiotics in a conventional wastewater

treatment plant, Watkinson et al. [24] found that most of contaminants were still detected in final effluents in the low µg/L range. Consequently, if these contaminants are not completely eliminated during waste water treatment, they may reach surface and ground waters, and as a result, impose a risk to aquatic and terrestrial flora and fauna.

4.1.2. Occurrence of pharmaceuticals in the aquatic environments

Mompelat et al. [5] reviewed the occurrence and fate of pharmaceutical products and their by-products from the source to drinking water. The authors reported that about 160 pharmaceutical products and 30 of their by-products were studied in relation to their occurrence in aquatic compartments, fate in the environment, or fate and elimination during wastewater or drinking water treatment. Pharmaceuticals from various prescription classes including analgesics, antibiotics, anti-epileptics, anti-rheumatics, β-blockers, chemotherapeutics, steroid hormones, antacids, oral antidiabetics, antineoplastics, antihypertensives, antidepressants, ansiolitics, blood lipid lowering agents, non-steroidal anti-inflammatory drugs (NSAID) were detected in the environment [6, 7]. The most common therapeutic classes detected in waters were NSAIDs (16%), antibiotics (15%), blood lipid lowering agents (12%) and sex hormones (9%).

To date, the highest concentrations of pharmaceutical compounds in water (50 -100 mg/L of oxytetracycline) have been measured in effluents from drug-production facilities in China [25, 26]. In Europe, twenty different compounds have been detected in effluents from Oslo city hospitals with paracetamol, ciprofloxacin and trimethoprim having the highest detected concentrations of 1.36, 0.054 and 0.015 mg/L, respectively [27]. In general, the concentration of pharmaceutically active compounds in water gradually decreases from industrial effluents to

aquatic environments. For example, the concentration of ofloxacin, a fluoroquinolone antibiotic, was found to be 3550, 410, 110 and below detection limits in hospital effluents, wastewater treatment plant influent and effluent, and in the Rio Grande River, respectively [28].

The presence of pharmaceutical residuals in natural waters in waters from many countries including USA [8, 29], UK [30, 31], Switzerland [32], Germany [7, 33], Denmark [34], Australia [35], Mexico [28], Brazil [36], South Korea [37] has been well-documented. Among different types of pharmaceuticals studied, NSAIDs were measured in surface and ground waters at highest concentrations. Acetaminophen was found in 24% of the USA streams sampled with the concentrations from below detection limits to 10 µg/L [8]. Ibuprofen, another NSAID, was detected in 10% of the U.S. streams tested at 1 µg/L [8]) and in two stormwater channels in the UK at concentrations of up to 0.93 µg/L [31]. Blood pressure lowering agents such as clofibric acid, fenofibric acid and gemfibrozil were found in the microgram concentration range in surface and ground waters around the world [33, 36, 38, 39].

The occurrence of antibiotics in natural waters has been intensively investigated in a number of studies [8, 40-43]. These includes penicillins (e.g., 48 ng/L of piperacillin in surface water in Germany [40]), makrolides (e.g., 1700 ng/L of erythromythcin and 560 ng/L of roxithromycin in the USA [8] and Germany [41] surface waters, respectively), chinolones (e.g., up to 26.2 ng/L of ciprofloxacin in Italian surface waters [42]), sulfonamides (e.g., sulfamexazol up to 163 and 410 ng/L in German surface and ground waters, respectively [43]), tetracyclines (e.g.,690 ng/L of tetracycline in the U.S. streams [8]).

The detected concentrations of a pharmaceutical in the natural water may differ from country to country. Carbamazepine, a neuroactive compound, was measured widely in surface waters in Germany at concentrations above 1 µg/L [33], whereas its average concentration in the U.S. rivers was only 60 ng/L [44].

4.1.3. Removal of pharmaceuticals by conventional drinking water treatment processes

The efficiency of pharmaceutical removal in conventional drinking water treatment processes such as coagulation/flocculation/sedimantation [33, 37, 45] and sand/bank filtration [7, 37, 46, 47] has been investigated at the bench-scale/pilot level [33, 45-47] and at operating water-treatment plants [7, 33, 37]. Westerhoff et al. [45] studied the removal of 62 endocrine-disruptors, pharmaceuticals and personal care products spiked with concentrations of 10-250 ng/L into three types of natural waters and one model water containing an NOM isolate. It was found that coagulation with aluminum sulfate and ferric chloride coagulants removed <25% of the target chemicals. For most of the studied compounds, no difference in the removal efficiency as a function of water composition or compound's concentration was observed. However, the removal efficiency increased with increasing k_{ow}, likely due to their increased adsorption onto suspended sediment particulates. Treatment with lime softening achieved comparable removal efficiencies as compared to coagulation, which was attributed to the same removal mechanism. Similar results, where coagulation was found to be inefficient for the removal of a suite of pharmaceuticals and endocrine disruptors from drinking waters from two different water treatment plants, were reported by Kim et al. [37]. Ternes et al. [33] studied the removal of four selected pharmaceuticals (benzafibrate, clofibric acid, carbamazepine and diclofenac) using sand

filtration and coagulation with ferric chloride. No significant removal of pharmaceuticals was observed by either method.

Bank filtration, a water treatment process where surface water is filtered through the sediments and then collected in the wells, has been also tested for its efficacy in removing pharmaceutically active compounds. Heberer et al. [7] found that bezafibrate and clofibric acid were effectively removed during bank filtration whereas bezabibrate, carbamazepine, clofibric acid, diclofenac, primidone, propyphenazone were still detected in wells. In a study by Massmann et al. [46], the behavior of phenazone-type pharmaceuticals during bank filtration was investigated with regard to hydrodynamic conditions. The authors found that while almost complete removal of pharmaceuticals was achieved during aerobic sand filtration in the waterworks, the studied compounds were more persistent under anoxic conditions. The effect of filtration velocity on the removal of phenazone-type pharmaceuticals originating from the effluent of a former pharmaceutical production plant was investigated by Zuehlke et al. [47]. The reduction in the filtration velocity from 5 m/h to 2 m/h resulted in improved removal of phenazone, propythenazone and their methabolites, while other metabolites were highly persistent during filtration regardless the velocity and contact time.

4.1.4. Removal of pharmaceuticals by membrane filtration

Membrane filtration has been examined widely for the removal of pharmaceuticals from synthetic [48-59], natural [55-57, 60, 61] and wastewaters [54, 57, 59, 61]. The effect of membrane (morphology, porosity, charge, hydrophobicity) and solute characteristics (structure,

molecular weight, polarity) [48-53, 58] and solution chemistry [53-59, 61] on the rejection of pharmaceuticals has been investigated.

Removal mechanisms. It was found that the rejection of pharmaceuticals was greatly affected by the physicochemical properties of the membrane and the pharmaceutical. Yoon et al. [49] showed that hydrophobic adsorption and size exclusion mechanisms were the predominant cause for the retention of a range of pharmaceuticals and endocrine disrupting compounds by a nanofiltration (NF) membrane, while the ultrafiltration (UF) membrane rejected hydrophobic compounds due to hydrophobic/hydrophobic interactions between membrane surface and solute molecule. Similarly, Kimura et al. [48] observed that negatively charged pharmaceuticals were rejected at efficiencies >90% on NF and reverse osmosis (RO) membranes. On the contrary, the rejection of neutral compounds was lower (<90%) and depended on the molecular size of the compound. Rajenovic et al. [60] showed that acetaminophen, hydrochlorothiazide, propyphenazone and glibenclamize in their neutral form were removed by size exclusion, and their rejection (44.8-85%) was lower as compared to the removal of the anions, ketoprofen, diclofenac and sulfamethoxazole (>95%). The effect of membrane material on the rejection of selected pharmaceuticals by RO membranes was investigated [50]. Authors found that the rejections were in the range of 57-91%, depending on the membrane and compound type. Size exclusion was the main rejection mechanism in the case of the polyamide membrane, while rejection was based on the compound's polarity during filtration on a cellulose acetate membrane. The rejection of pharmaceuticals also depended on a membrane pore size. As shown in [62], the retention of sulfamethoxazole, carbamazepine, and ibuprofen by tighter NF membranes resulted from size exclusion, while the combination of the electrostatic repulsion and

size exclusion resulted in rejection on a loose NF membrane. In another study, Shafer et al. [52] suggested that the combination of size exclusion and adsorption was responsible for the removal of the hormone estrone from its aqueous solutions by NF/RO membranes. The adsorption of pharmaceutically active compounds and hormones by polymeric membranes was proposed to be a primary mechanism for the rejection in a number of studies [51, 56, 57, 63-65]. Nghiem et al. [65] suggested that diffusion of a micropollutant into the polymeric matrix depended on the molecule size, hydrogen bonding between micropollutant and membrane functional groups, and hydrophobic/hydrophobic interactions. By conducting a set of batch experiments to determine the adsorption/desortion of estrone to hollow fiber membranes in $NaHCO_3$/NaCl solution, Chang et al. [51] found that about 14% of estrone was released into an electrolyte solution after equilibrium in the system had been reached. When the fresh portion of electrolyte solution was added to the system, estrone desorption further increased by 4%. By relating these results to the membrane filtration, the authors suggested that concentration of estrone in the permeate would be a function of the amount of estrone accumulated on the membrane surface. As such, estrone rejection will decrease when the surface concentration reaches equilibrium with the influent concentration, leading to estrone molecules passing through the membrane into permeate; when the estrone surface concentration is lower than that of influent, estrone will desorb into permeate, resulting in negative rejection. This is important finding because it implies that pharmaceuticals could first accumulate on the membrane surface and then desorb during backwashing and membrane cleaning, or during operation as the concentration of estrone in the feed increases.

The effect of physicochemical properties of a pharmaceutical. The physicochemical properties of the micropollutant molecule affects its separation on the membrane surface. It was reported that

the retention of pharmaceuticals on the polymeric membrane as a function of pH was affected by the compound's pK_a [58, 59, 62], dipole moment [62] and K_{ow} [56]. The removal of three types of pharmaceuticals (ibuprofen, sulfamethoxazole and carbamazepine) with very different characteristics was investigated [62]. The rejection of sulfamethoxazole (pK_{a1}=1.7, pK_{a2}=5.6-5.7) followed a sigmoid shape coincident with the species distribution, when pH increased from 3.5 to 10, whereas the rejection of carbamazepine (pK_a=2.7) was relatively stable over the pH range studied. Additionally, the rejection of sulfamethoxazole in its neutral form was greater than that for carbamazepine despite the higher molecular weight of carbamazepine. The authors suggested that the observed effect was due to the higher dipole moment of the carbamazepine molecule as compared to that of the sulfamethoxazole molecule (D = 3.6 and 5.4, respectively). The attraction between the polar moieties of the membrane and a molecule with greater dipole moment causes the molecule to be directed towards the membrane pore. The rejection of ibuprofen (pK_a = 4.8-4.9) where lower when this compound was in its neural form because of the adsorption to the membrane surface. In a similar fashion, the rejection of estrone by the UF membrane mirrored the pH distribution of estrone species, with higher rejections observed at pH values less than the estrone pK_a (pK_a = 10.4) when the molecule was ionized [58]. On the contrary, the retention of pharmaceuticals without acidic functional groups did not depend on the solution pH. Thus, the rejection of prophylphenazone and carbamazepine did not change when the pH was increased from 3 to 9, whereas the rejection of pharmaceuticals which had acidic groups in their structure, was greatly influenced by pH [59].

In the study by Comerton et al. [56], the adsorption of 22 endocrine disruptors and pharmaceuticals was well-correlated with their K_{ow} and the pure water permeability of the membrane, and moderately correlated with their solubility in water. Similarly, antibiotics and hormones with more negative log K_{ow} were more strongly adsorbed on the membrane surface as compared to those with positive log K_{ow} [53]. Thus, almost 80% of chlorotetracylcine (log K_{ow} = -0.62) and 50% of doxcycline (log K_{ow} = -0.02) were adsorbed on the membrane surface while only 22-46% of the studied hormones with positive log K_{ow} values were adsorbed during the filtration experiments.

The effect of NOM. The presence of NOM in the feed water was found to have a significant effect on the rejection of different types of pharmaceuticals by polymeric membranes [53-57, 61, 66]. The effect of the membrane type on estrone rejection in the presence of three types of NOM (natural water, Suwannee River fulvic acid and secondary wastewater effluent, all having the same TOC value of 10 mg/L) by several commercially available polymer membranes was investigated in [61]. The adsorption of estrone in natural water and secondary wastewater effluent was similar, but lower than that in fulvic acid. The authors suggested that low molecular weight compounds contained in fulvic acid suspensions may facilitate the transport of estrone through the membrane. However, no clear correlation between the adsorption and rejection of estrone was observed and the presence of organic material in the solution had only a slight effect on the rejection of estrone by polymeric membranes. In the follow up study the removal of estrone was investigated in three different water matrixes (pure background electrolyte, secondary effluent and water spiked with NOM) and with three commercially available

polymeric membranes [54]. The TOC of the synthetic water was selected to be similar to that of secondary influent (10 mg/L). The rejection of estrone was enhanced by the presence of NOM due to its binding to organic material, and the relative increase in rejection was higher in the case of water spiked with NOM than in secondary effluent which contains organic material of lower molecular weight. The authors attributed this effect to better retention of NOM molecules as compared to that with secondary effluent.

Koyuncu et al. [53] suggested that the formation of macromolecular complexes between a hormone and NOM molecule led to enhanced removal of several hormones (estradiol, estrone and testosterone) in the presence of NOM. The adsorption of estrone and 17β-estradiol to natural particles was also observed by Schafer et al. [55]. During filtration of activated sludge, which had been spiked with estrone, through a UF membrane, the biomass provided a filtration layer, which enhanced the rejection of estrone. Comerton et al. [56, 57] found that that were a significant difference in the rejection of acetaminophen, gemfibrozil and carbamazepine from two different waters, Lake Ontario water and membrane bioreactor effluent on NF membrane. They also reported that the rejection of pharmaceuticals was greater from filtered lake water than from the raw lake water. Mascaoui et al. [66] determined the K_{OW} of a number of pharmaceuticals and endocrine disrupting compounds into isolated river colloidal NOM and suggested a linear relationship between the pharmaceutical's partitioning coefficient normalized to colloidal carbon content and log K_{ow}. Based on the result of the previous studies, the rejection of a pharmaceutical during membrane filtration is a complex process and strongly depends on the membrane pore size and pharmaceutical-organic molecule interactions in the solution.

The effect of ionic strength. The effect of ionic strength on the rejection of pharmaceuticals by polymeric membranes was studied [53, 57, 58]. Schafer et al. [58] evaluated the rejection of estrone as a function of electrolyte type and concentration. Two opposite effects were observed: estrone removal deteriorated with increasing NaCl concentration up to 100 mM. On the contrary, in the presence of $CaCl_2$, increasing the electrolyte concentration from 5 to 100 mM resulted in a slight increase in estrone rejection. The authors suggested that the electrostatic interactions between the estrone molecules and the membrane surface in the presence of NaCl (i.e., lowering the membrane charge due to shielding effect and reducing the apparent molecule size of molecule) led to the decrease in its rejection by the membrane. The increase in the rejection in the presence of Ca^{2+} ions was attributed to the bridge formation between the estrone molecule and the membrane surface, facilitated by Ca^{2+} ions. Similarly, lower estrone rejection was observed in the presence of 10 mM NaCl as compared to pure hormone solution and 10 mM $CaCl_2$ [53]. On the contrary, a decrease in the rejection of acetaminophen was observed with the tight NF membrane in the presence of Ca^{2+} ions in the effluent from a membrane bioreactor [57]. The authors attributed the observed effect to the interference compound-organic matter complex formation by Ca^{2+} ions.

Based on the reported studies, membrane filtration was more effective in removing pharmaceuticals than conventional drinking water processes. However, given, that membrane filtration is simply a physical separation of a solute from the aqueous phase; the retained pharmaceuticals will accumulate on the retentate side of the membrane, and cause problems in

terms of brine disposal. Additionally, the secondary contamination of surface waters with pharmaceuticals followed their discharge with effluents from membrane treatment plants is also possible.

4.1.5. Removal of pharmaceuticals by ozonation

Due to its high oxidation potential (E_{ox}^{o} = 2.07 V), ozone, O_3, has been effectively used for disinfection and the removal of taste and odor causing substances, disinfection by-products and refractory organic compounds [67]. The removal efficacy of ozone strongly depends on the contaminant structure, oxidant dose and water matrix (pH, alkalinity, NOM content, etc) [68-70]. In aqueous solutions ozone reacts with various organic compounds through two main pathways: by direct reaction with molecular ozone or through the indirect reaction of radical species (including the hydroxyl (·OH) radical) formed during decomposition of the O_3 molecule in water [71]. Molecular ozone is more selective and attacks double bonds and aromatic molecules with electron donor groups (mainly amines and phenols), while the ·OH radical is less selective and reacts with most organic molecules [68, 71]. The efficiency of pharmaceutical removal by ozonation has been studied with regard to pharmaceutical type [33, 45, 72, 73], ozone dose [72] and water matrix [45, 72] in laboratory bench trials [33, 45], and at a water treatment plant [33, 37]. Broseus et al. [72] investigated the elimination of 16 pharmaceuticals, endocrine disrupting compounds and pesticides from two different types of surface waters by ozonation. The authors found that ozonation at CT value of about 2 mg·min/L resulted in the removal of over 80% of the compounds targeted. Pharmaceuticals and hormones which contained phenolic or amino functional groups were not detected or detected at trace levels in the ozonated samples. Similarly, Westerhoff et al. [45] found that steroids containing phenolic (estradiol,

ethynylestradiol, or estrone) and amino (e.g., acetaminophen) moieties were oxidized to greater extent (>80%) than those with no aromatic ring or phenolic groups (e.g., androsterone, 88%, progesterone, 91%, and testosterone, 90%). The efficiency of ozonation of compound, containing electron-withdrawing functional groups such as carboxylic or chlorine functional groups, was also less (ibuprofen, 80%, diazepam, 81%) as compared to compounds bearing electron-donating functional groups. Ozonation of compounds, containing electron-withdrawing functional groups also required higher ozone dosages as compared to those containing electron-donating moieties. Thus, Ternes et al. [33] showed that the removal of 90% diclofenac and carbamazepine (both containing amino groups) was achieved upon addition of 0.5 mg/L of O_3, whereas 50% reduction in concentration of bezafibrate (containing carboxylic group) required the addition of 1.5 mg/L of O_3, and no significant removal of clofibric acid which contains two electron-withdrawing groups (chlorine and keton) occured at an ozone dose of 3 mg/L.

Additionally, the application of ozone could lead to the formation of by-products which still had biological activity [74] or were even more toxic than the parent compounds [75].

4.1.6. Removal of pharmaceuticals by catalytic chemical oxidation

Catalytic oxidation, based on the generation of free radicals to destruct the targeted pollutants, is a promising technology in water treatment [76]. The most common radical that is generated during the catalytic oxidation is the ·OH radical. The ·OH radical is a powerful and nonselective oxidant (E^{o}_{ox} = 2.72 V) that can react with most organic compounds [77]. One way to utilize the catalytic chemical oxidation is to couple ozone with another compound that promotes ozone

decomposition and, as a result, facilitates the formation of ·OH radicals. For example, the addition of hydrogen peroxide prior to ozonation improved the oxidation of contrast media by 12-23% [73] and a range of endocrine disrupting agents and personal care products by 5-15% [45] as compared to ozone alone. An oxidizing power of ozone could also be improved by performing ozonation in the presence of metal ions or oxides, which facilitate the formation of ·OH radicals from ozone decomposition [78-80]. For example, catalytic ozonation of salicylic acid in the presence of MnO_2 resulted in 87% oxidation as compared to ozonation alone (48% conversion degree) [81]. When salicylic acid was subjected to catalytical ozonation on Al_2O_3, it has also resulted in a higher degree of mineralization as compared to ozonation [78]. Enhanced mineralization of paracetamol (85%) in the presence of Cu^{2+} or Fe^{3+} ions was also observed [79].

Taking into consideration that conventional water treatment processes have limited efficacy in removing many pharmaceuticals from drinking water supplies, catalytic ozone oxidation is an attractive alternative to conventional drinking water processes for simultaneous removal of pharmaceuticals and DBPs precursors from natural waters. Kasprzyk-Horden et al. [80] showed that catalytic ozonation of NOM on Al_2O_3 support also resulted in significant reduction in the concentration of DBPs and biodegradable organic carbon. Karnik et al. [82] found that ozonation - ceramic membrane filtration of natural water resulted in a reduction of up to 50% of dissolved organic carbon concentration and the formation of partially oxidized compounds from NOM that were less reactive with chlorine, decreasing the concentration of total trihalomethanes and haloacetic acids by up to 80% and 65%, respectively. Membrane fouling was reduced due to the

reaction of ozone or secondary oxidants such as ·OH radicals with NOM deposited on the membrane surface [83]. Metal oxides (Al_2O_3, ZrO_2, and TiO_2), which are commonly used to fabricate ceramic membranes [84], facilitate the formation of ·OH radicals through catalytic decomposition of ozone on their surface. Ceramic membranes, which were used in the above studies, have many advantages over polymeric membranes as they are thermally, chemically stable, have longer lifetimes [84, 85], and are ozone resistant [82, 83, 86-88]. The presence of ·OH radicals in the system was confirmed by using salicylic acid as a radical probe [89].

4.1.7. The objectives and experimental approach

The goal of this study was to demonstrate that the application of the hybrid ozonation-ceramic membrane filtration system would facilitate efficient removal of model pharmaceuticals and DBPs precursors from surface waters of very different characteristics. The oxidation of pharmaceuticals and DBPs precursors on the surface of membranes was expected because of the catalytic properties of TiO_2, which form the separation layer on the ceramic membrane. TiO_2 has the capacity to adsorb the superoxide ion O_2^-, which promotes the decomposition of ozone into free radicals [90, 91].

The *objectives* of the study were as follows: (1) to investigate the efficiency of removal of model pharmaceuticals from surface waters in hybrid ozonation-membrane filtration process; (2) to evaluate the disinfection by-products formation potential (DBPFP, namely, TTHMs and HAAs) of the permeate resulting from hybrid ozonation-membrane filtration as compared to that from

membrane filtration alone; and (3) to investigate the effect of ozone on the flux recovery during ozonation-membrane filtration of surface waters with different chemical composition.

As a result, the following hypotheses were tested in this study:

(1) the extent of flux recovery during hybrid ozonation-membrane filtration would depend on the water matrix content such as TOC and alkalinity;
(2) the removal efficiency of model pharmaceuticals, TOC, UV-254 and disinfection byproducts by hybrid ozonation-membrane filtration will be higher than by the membrane filtration alone;
(3) the removal efficiency of model pharmaceuticals, TOC, UV-254 and disinfection byproducts by hybrid ozonation-membrane filtration would depend on the water matrix content such as TOC and alkalinity.

The goal and objectives of the study were achieved by varying the following experimental conditions: (1) type of the applied treatment (hybrid ozonation-membrane filtration and membrane filtration alone); (2) type of surface water and (3) type of model compound.

Model compounds. The removal efficiency of two antibiotics, dicloxacillin and ceftazidime in the hybrid ozonation-membrane filtration system was evaluated. These compounds represent type of antibiotics found in surface waters [8] and have diverse mode of action against both gram-positive and gram-negative bacteria [92, 93]. Dicloxacillin is an oral, semisynthetic penicillinase-resistant penicillin used primarily for the treatment of skin and skin structure

infections, upper respiratory tract infections, and as follow-up therapy after intravenous treatment for osteomyelitis [92]. Ceftazidime is a parenteral, third-generation cephalosporin antibiotic that is administered by intravenous or intramuscular injection [93]. Ceftazidime is used for the treatment of meningitis, lower respiratory infections, febrile neutropenic events, urinary tract infections, pelvic inflammatory disease, and skin and skin structure infections. Importantly, both compounds contain one or more heterocyclic functional groups and other nitrogenous moieties and are expected to be resistant to ozonation.

4.2. Materials and methods

4.2.1. Materials

Dicloxacillin, ceftazidime, sodium hypochlorite, acetonitrile and N,N-methyl-*p*-phenylene diamine were received from Sigma-Aldrich (Milwaukee, WI). EPA 552 Halogenated Acetic Acids Mix (2000 µg/mL) was obtained from Supelco (Bellefonte, PA) and 501 Trihalomethane Mix (200 µg/mL) was purchased from Restek (Bellefonte, PA). Potassium phosphate monobasic, potassium phosphate dibasic, sodium bisulphate, sodium hydroxide and HPLC grade water and phosphoric acid were purchased from JT Baker (Phillipsburg, NJ). All chemicals were of analytical grade.

The ultrapure water used for the membrane cleaning and system flushing, was supplied by a commercial ultrapure water system (Lab Five, USFilter Corp., Hazel Park, MI) equipped with a terminal 0.2 µm capsule microfilter (PolyCap, Whatman Plc., Sanford, ME).

4.2.2. Hybrid ozonation-membrane filtration system

The hybrid ozonation-membrane filtration set up consisted of an ozone injection system, membrane module, recirculation pump, reservoir, ozone injection system, and data acquisition system (Figure 4.1). The required cross-flow velocity and transmembrane pressure (TMP) were achieved with recirculation pump (Gear Pump Drive, Micropump®, Cole Parmer Inc., Vernon Hills, IL) and a back pressure regulator (Swagelok®, Salon, OH). The system was operated in a total (permeate and retentate) recycling mode in which the permeate was recycled using a peristaltic pump (Masterflex®, Cole Parmer Inc., Vernon Hills, IL) into a 5 L feed tank on a 40 min interval. Temperature, crossflow velocity TMP and permeate flux during the filtration experiments were recorded every 60 seconds using LabView data acquisition system (National Instruments, Austin, TX).

Ozone was generated using a high-pressure ozone generator (Atlas Series, Absolute Ozone® Generator, Absolute System Inc., Edmonton, Canada) from ultrapure oxygen gas. Prior to be fed into the ozone generator, oxygen was dried using a moisture trap containing anhydrous calcium sulfate (21001, Drierite Co., OH, USA). The gas pressure was maintained at 0.2-0.3 bar higher than the TMP to facilitate ozone injection into the feed line. The ozone concentration in the gas phase was measured by an ozone gas monitor (Model 450H, Teledyne Instruments, City of Industry, CA) and the dissolved ozone concentration in the retentate in the recirculation loop was continuously monitored using an amperometric ozone microsensor (AMT Analysenmesstechnik GmbH, Rostock, Germany). The operating conditions for the hybrid ozonation-membrane filtration are summarized in Table 4.1.

Table 4.1. Operating conditions for the hybrid ozonation-membrane filtration system.

Ozonation:	
Ozone gas-phase concentration (mg/L):	5±0.5-30±0.5
Volumetric ozone-gas flow rate (mL/min):	40±0.5
Ozone inlet pressure (bar):	2.5±0.1
Membrane filtration:	
TMP (bar):	2.1±0.1
Volumetric cross-flow rate (mL/min):	0.55±0.05
Temp. (^{o}C):	24±1
Feed volume (L):	1 or 1.2

4.2.3. Ceramic membrane

A tubular ceramic UF membrane (Inside CéRAM, TAMI North America, Saint-Laurent, Québec, Canada) with a nominal molecular weight cut-off (MWCO) of 1 kDa, inner diameter of 0.1 cm and active length of 25 cm was used in all filtration tests. The support and the separation layer of this membrane are composed of α-Al_2O_3 and TiO_2, respectively. The membrane has seven channels and a total filtering surface area of 131.9 cm^2. The membrane was placed in stainless-steel holder (TAMI North America, St. Laurent, Québec, Canada).

Prior to first use the bare ceramic membrane was cleaned by soaking the membrane in 0.1 N sodium hydroxide (NaOH) solution for 12 h. The membrane was then rinsed with ultrapure water for at least 3 hrs and the initial clean water flux was measured. Prior to each filtration experiment, the clean water flux was measured again for 10-15 min to ensure that membrane permeability was not changed significantly. The fouled membrane was cleaned with ultrapure

water in the same conditions as during ozonation-membrane filtration experiments until the original clean water flux was restored.

4.2.4. Water sources

Three types of surface waters with very different chemical composition were used in this study. Both Lake Huron and Huron River are source waters for local Michigan water treatment plants (WTPs). Lake Lansing is a borderline eutrophic lake and is used currently as a recreatioal lake. All samples were collected during December 2009 in five gallon carboys, pre-filtered through the 0.5-μm ceramic cartridge microfilter (Doulton USA, Southfield, MI) and stored at 4 ^{o}C for further usage. Selected water quality characteristics of the tested waters are shown in Table 4.2. Waters were spiked with an aliquot of freshly prepared stock pharmaceuticals solutions to result in a concentration range of 1.5 mg/L of each antibiotic in the feed water.

To study the efficiency of model antibiotic removal in the absence of NOM, the model pharmaceuticals were spiked at a concentration of 1.5 mg/L into 10 mM of sodium bicarbonate ($NaHCO_3$) solution at pH 8.50.

4.2.5. Water quality analysis

Total TTHMs and HAAs. Water samples were dosed with sodium hypochlorite at a concentration that ensured the residual free chlorine concentration in the range of 0.5–3 mg/L after 48 h incubation in dark at room temperature. Upon completion of the reaction, residual chlorine was quenched by adding sodium bisulfate. The concentration of free chlorine in solution was determined by standard colorimetric method with N,N-methyl-*p*-phenylene diamine [94].

Table 4.2. Water quality characteristics.

Water source	Lake Huron	Huron River	Lake Lansing
Location of the sampling point	Saginaw WTP	Ann Arbor WTP	Boat ramp, Lake Lansing Park-South
[1]Alkalinity (mg/L as $CaCO_3$)	75.00±2	239.00±3	150.00±3
[2]Turbidity (NTU)	0.60	0.95	0.52
[1]TOC (mg/L)	2.05±0.02	5.89±0.06	11.39±0.03
[1]UV-254	0.027±0.01	0.161±0.01	0.254±0.01
[1]Conductivity, µS/cm	201.30	731.00	345.00
[1]pH	8.19±0.05	8.50±0.05	7.70±0.05
[1]Ca^{2+}, mg/L	16.50±0.5	44.50±0.5	28.00±0.5
[1]Mg^{2+}, mg/L	7.00±0.5	18.00±0.5	11.50±0.5
$SUVA_{254}$ (L/mg/m)	1.3	2.7	2.2

[1]Measured after pre-filtration.
[2]Measured before pre-filtration.

TTHMs compounds in water (chloroform ($CHCl_3$), bromodichloromethane ($CHBrCl_2$), dibromochloromethane ($CHBr_2Cl$), and bromoform ($CHBr_3$)) were extracted from water by hexane and analyzed by gas chromatography (Standard Method 5710)

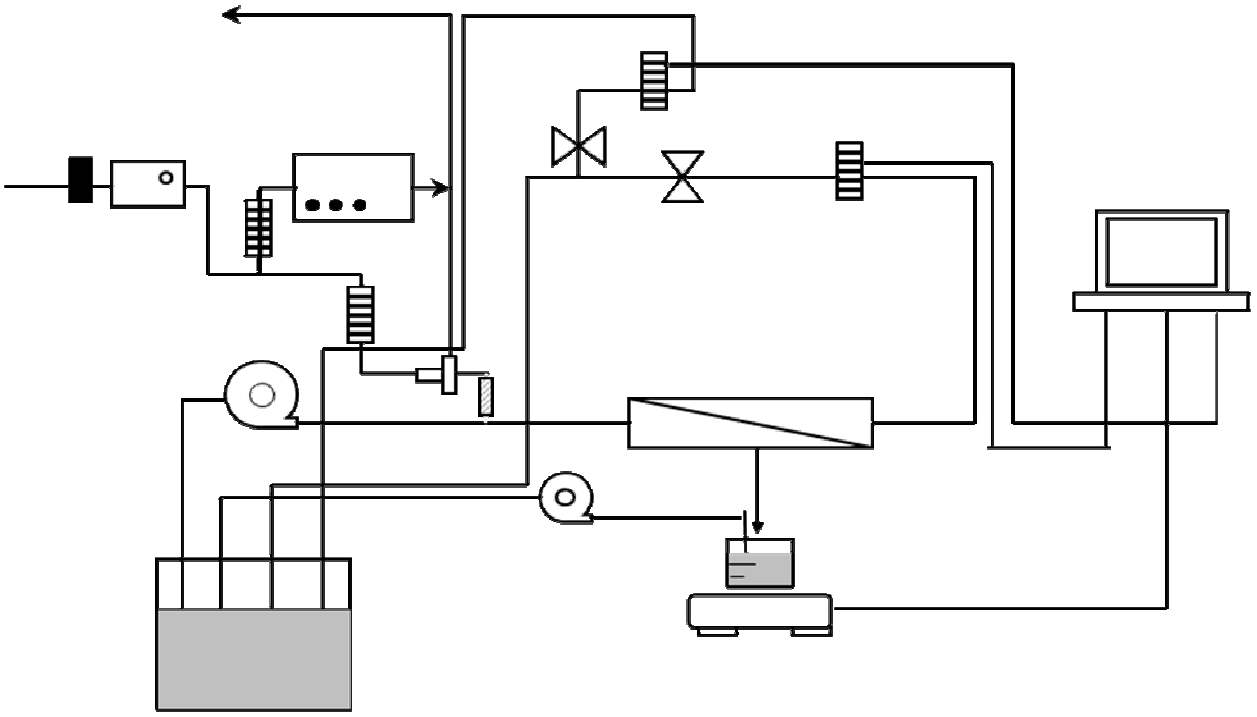

Figure 4.1. Schematic of the hybrid ozonation – membrane filtration system.

[94]. A Perkin Elmer Autosystem gas chromatograph (Perkin Elmer Instruments, Shelton, CT) equipped with an electron capture detector (ECD), an auto-sampler, and a 30 m × 0.25 mm ID, 1 μm DB-625ms column (J&W Scientific, Folsom, CA) was used for the analysis. The oven temperature was ramped from 50 to 150 ^{o}C at a rate of 10 °*C*/min. The flow rate of the carrier gas (N_2) was 12.0 mL/min. The injector and detector temperatures were 275 and 350 ^{o}C, respectively.

SDS haloacetic acids (monobromoacetic acid (MBAA), dichloroacetic acid (MCAA), dichloroacetic acid (DCAA), trichloroacetic acid (TCAA), and dibromoacetic acid (DBAA)) were extracted and derivatized according to the EPA method 552.3 [95]. The concentration of each HAA was determined by gas chromatography. A Perkin Elmer Autosystem gas chromatograph (Perkin Elmer Instrumens, Shelton, CT) equipped with an ECD, an autosampler, and a 30 m × 0.32 mm ID, 3 μm DB-5 column (J&W Scientific, Folosom, CA) was used for the analysis. The oven temperature was programmed to hold for 15 min at 40 ^{o}C, then increased to 75 ^{o}C at a rate of 5 ^{o}C/min and held for 5 min. The carrier gas flow rate (nitrogen) was 10 mL/min with the injector and detector temperature set to 200 ^{o}C and 260 ^{o}C, respectively.

TOC and UV-254. The TOC concentration was measured using a TOC analyzer (Model 1010 Analyzer, OI Analytical, College Station, TX). The UV absorbance at 254 nm was measured by means of a UV spectrophotometer (Spectronic Genesys 5, Milton Roy Inc., Ivyland, PA) using a 1 cm quartz cell.

4.2.6. Concentration of the model pharmaceuticals

The physicochemical characteristics of antibiotics used in this study are shown in Table 4.3. The concentrations of antibiotics in the feed and permeate were measured using high-performance liquid chromatography (HPLC). The system consisted of Perkin Elmer Instruments (PEI) (Shelton, CT) Binary LC 250 pump, PEI Diode Array detector 235C, PEI series 200 autosampler and Discovery C18 HPLC column (25 cm x 4.6 mm, 5 µm) (Supelco, Bellefonte, PA). The HPLC operating conditions are presented in Table 4.4.

Table 4.3. Selected characteristics of the antibiotics used in this study.

Common name	Dicloxacillin	Ceftazedime
Type	[1]β-lactam penicillin	[2]β-lactam cephalosporin
Action	[1]Treatment of skin and upper respiratory tract infections	[2]Treatment of meningitis, lower respiratory tract, urinary tract and skin infections
Chemical formula	$C_{19}H_{17}Cl_2N_3O_5S$	$C_{22}H_{22}N_6O_7S_2$
MW, g/mole	470	547
[3]Molecular volume, cm^3	7.81E-22	9.60E-22
[4]$\log K_{ow}$	2.912 (3.861)	-1.602 (-1.361)
[4]Water solubility at 25 ^oC, mg/L	3.625	396.2
[4]Estimated removal in Sewage Treatment, %	5	1.85

[1][92]; [2][93]; [3]estimated according to [96]; [4][97].

Table 4.4. HPLC operating conditions.

Parameter	Dicloxacillin	Ceftazidime
Mobile phase	30% acetonitrile and 70% of 0.1% H_3PO_4	70% acetonitrile and 30% of 0.1% H_3PO_4
Flow rate (mL/min)	1	1
Detection wavelength (nm)	210	245
Injection volume (μL)	120	15
Retention time (min)	4.30	2.74
Run time (min)	6.50	4.50

4.3. Results and Discussion

4.3.1. Effect of type of water on the permeate flux

Figure 4.2 shows the changes in permeate flux during ozonation-ceramic membrane filtration of the studied waters as a function of water type. The results are presented as a normalized permeate flux (J/J_{in}) versus filtration time, where J_{in} is a permeate flux at a time t = 0 h, and J is a permeate flux at a time t. Two types of filtration experiments were conducted for each type of the water: membrane filtration with no gas injection into the system, and membrane filtration with the injection of gaseous ozone into the system. The concentration of ozone in gaseous phase during ozonation-membrane filtration experiments was chosen based on TOC of the feed.

As it is seen from Figure 4.2, the most significant flux decline was observed during the filtration of Lake Lansing (LL) water (approximately 56% of the initial permeate flux) as compared to Huron River (61% of the initial permeate flux) and Lake Huron (83% of the initial permeate flux). The extent to which the permeate flux declines during membrane filtration increased with

increasing TOC in the feed water. This effect can be attributed to thicker fouling layer formed on the membrane surface during the filtration of waters with higher concentration of NOM. This is consistent with the finding of Nystrom et al. [98], where a greater flux decline was observed during the filtration of synthetic water with a greater concentration of humic acids. This finding suggests that the inorganic fraction of the feed water which is more abundant in Huron River water as compared to Lake Huron and LL waters (see Table 4.2), also contributes to the permeate flux decline. No difference in the degree of flux decline was observed during filtration of as-received feed water and feed water spiked with pharmaceuticals for all studied waters (Figure 4.2). One possible explanation is that concentration of model pharmaceuticals was not sufficient to affect membrane fouling.

When tested waters were subjected to ozonation–membrane filtration, flux recovery greatly depended on the applied ozone gas-phase concentration. As can be seen in Figure 4.2 a, no flux recovery was observed when LL water was dosed with 5 g/m^3 of gaseous ozone. However, when the same water was subjected to ozonation-membrane filtration at 20 g/m^3 of gas-phase ozone, the permeate flux fully recovered after 10 h of filtration regardless of the presence of pharmaceuticals in the feed.

The effect of ozone gas-phase concentration on the flux recovery during filtration off Huron River water was studied at three different ozone dosages (5, 15 and 30 g/m^3) and at two different pHs (7.00 and 8.50). As Figure 4.2b shows, when the feed water was spiked with model pharmaceuticals and subjected to ozonation-membrane filtration, it only slightly improved the

permeate flux as compared to membrane filtration only (approximately 61, 64, 67 and 68% of the initial flux after 7 h of filtration period for 0, 5, 15 and 30 g/m^3 of gaseous ozone respectively). While prolonged filtration of as-received Huron River water resulted in some flux recovery (approximately 79% of the initial flux) after 12 h of operation, this was accompanied by an intermittent flux behavior (Figure 4.2b). The visual observations of the permeate collection vessel showed that beginning from approximately 3 h of filtration there were periods with no permeate flowing from the permeate line followed by the periods when the permeate flux was higher than average. As a result, the normalized flux points which correspond to ozonation-filtration experiments with as-received water are scattered. However, if two neighbor flux points (the highest and the lowest fluxes) were averaged, this would have resulted in the straight line. One possible explanation to this phenomenon is the scale formation within the tubes that collect permeate. Table 4.5 represents the Langelier saturation index (LSI) of studied waters. The LSI index depends on water quality characteristics, including temperature, pH, calcium hardness and alkalinity. The Huron River water has the lowest LSI among all three waters (-0.90). The LSI index below (-0.5) is an indicator that the water is supersaturated and tends to precipitate $CaCO_3$. We hypothesis that the scaling formed on the inner walls of the tubing that connect the membrane housing with permeate collecting vessel, could block the permeate flow. As a result, permeate which passes through the membrane, would accumulate within the membrane housing. At certain point in time the permeate pressure would overcome the scale resistance and the scale would be flushed out, resuming permeate delivery to the collecting vessel. The fact that this effect was observed only in the case of as-received water and was not observed during the filtration of the feed spiked with pharmaceuticals could be attributed to the specific interactions between Ca^{2+} and organic matter presented in the feed water.

The permeate flux recovery was greater in the case of LL water than Huron River water despite the higher TOC value of LL water (11.39±0.03 and 5.89±0.06 mg C/L, accordingly), lower ozone dose (20 and 30 g/m^3, respectively) and shorter filtration time (10 and 12 h, accordingly). This suggests that water matrix constituents other than TOC (e.g., alkalinity) could also control the efficiency of the ozonation-membrane filtration process. It is known that carbonate ions are scavengers of $^{\cdot}$OH radicals. The alkalinity of Huron River water is ca 1.6 times higher than that of LL water (239.00±3 and 150.00±3 mg $CaCO_3$/L, respectively).

Table 4.5. The Langelier saturation index (LSI).

Type of water	Lake Huron	Huron River	Lake Lansing
LSI	+0.10	-0.90	-0.21

Table 4.6. Average dissolved ozone concentration in the retentate.

Type of water	Lake Huron	Huron River	Huron River	Lake Lansing
Ozone dosage, g/m^3	5	30 (pH 7.00)	30 (pH 8.50)	20
[1]Dissolved ozone consentration, mg O_3/L	1.60±0.61	0.35±0.01	0.39±0.05	0.43±0.07

[1]Measured during the last 30 min of experiment.

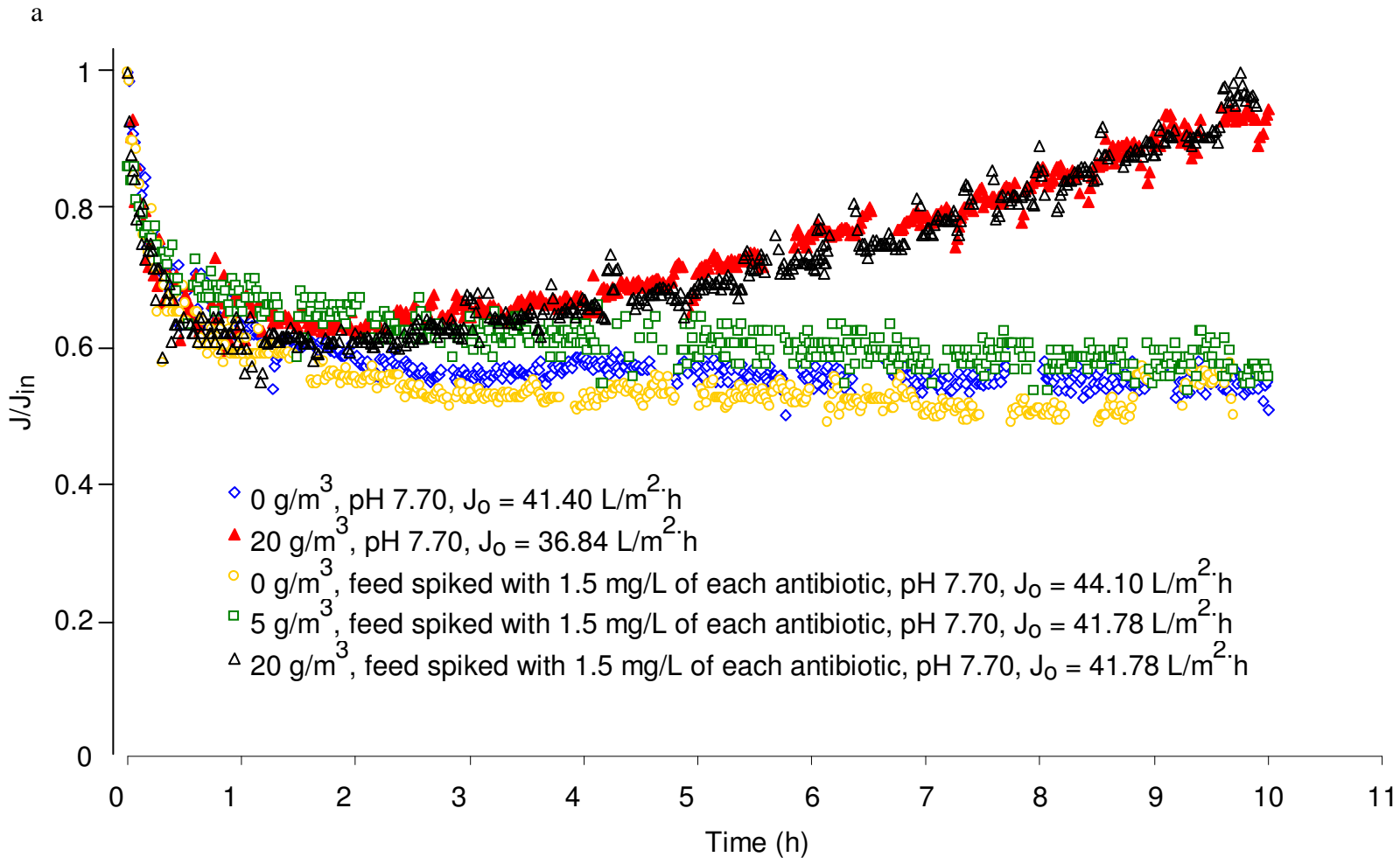

Figure 4.2. Transient permeate flow during filtration of LL (a), Huron River (b) and Lake Huron (c) waters as a function of treatment type. Conditions: 1 kDa uncoated membrane; raw water was spiked with 1.5 mg/L of each antibiotic, TMP = 2.1±0.1 bar, cross flow velocity = 0.55±0.05 m/s, ozone gas flow rate 40 mL/min.

Figure 4.2 (cont'd).

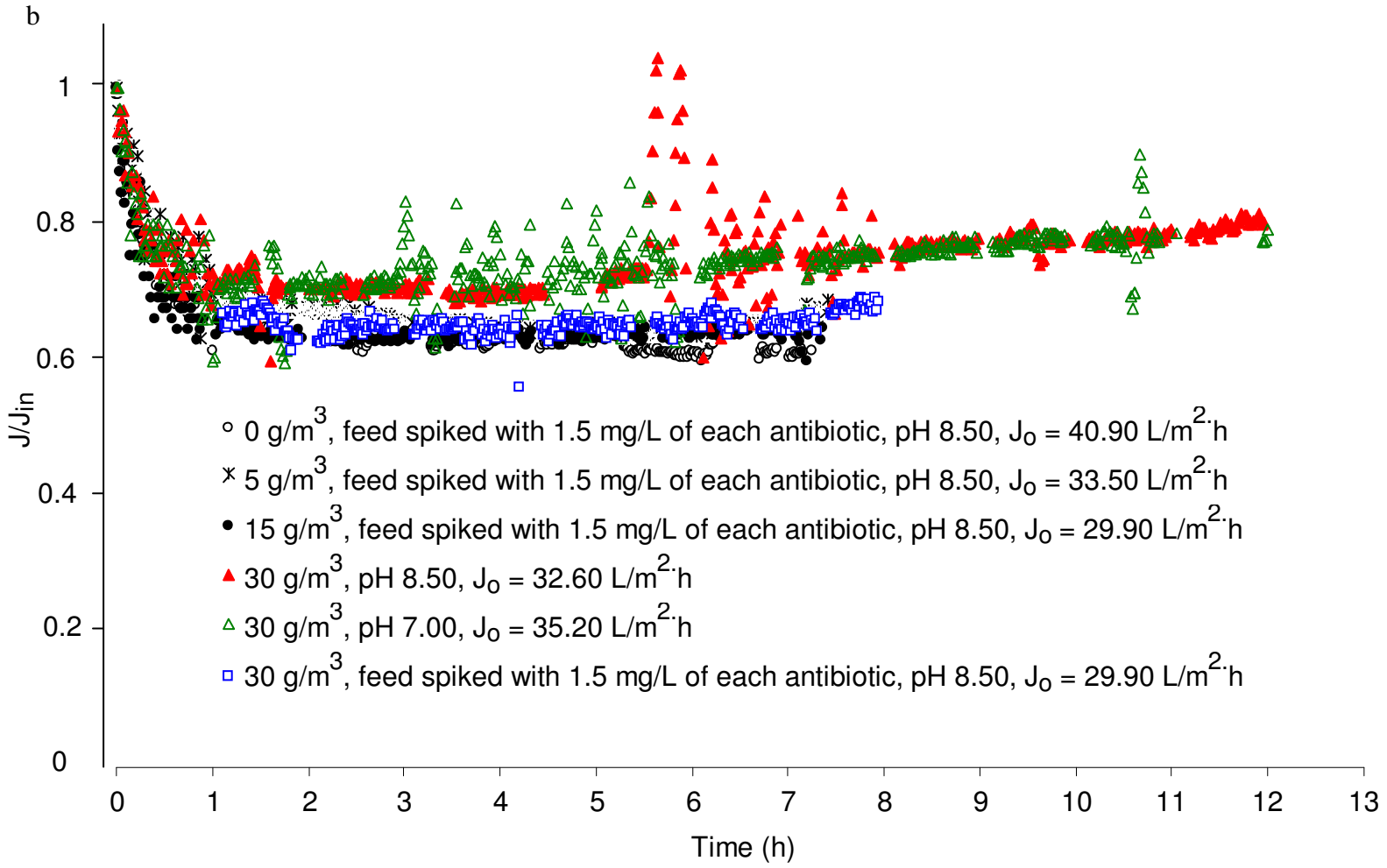

Figure 4.2 (cont'd).

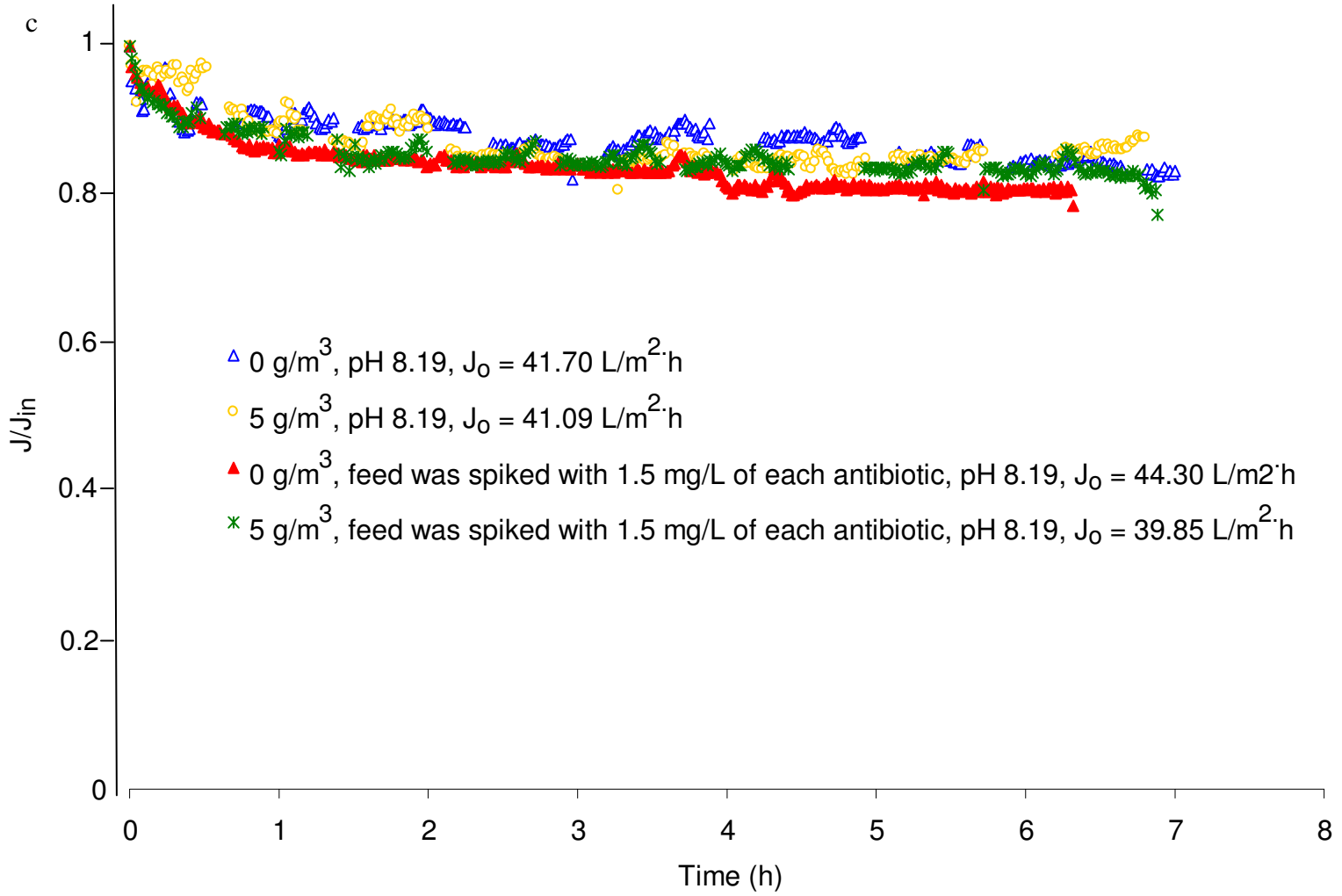

Hence, it likely that during ozonation-membrane of Huron River more ˙OH radicals are scavenged from the membrane surface due to their reaction with the carbonate ions presented in water. This will decrease the rate of ozone decomposition and, as a consequence, "stabilize" ozone. This is consistent with the average concentrations of dissolved ozone in the retentate line measured during the last 30 min of each experiment (0.35±0.01 and 0.43±0.07 mg O_3/L for LL and Huron River waters, accordingly). The difference between the dissolved ozone concentrations in two waters was statistically insignificant, which is an evidence of the higher ozone demand of Huron River water. To reduce the scavenging capacity of carbonate ions, the pH of the feed water was decreased to 7.00. However, at it is seen on Figure 4.2b, this adjustment did not change the permeate flux pattern as compared to observed at pH 8.50. Also, the dissolved ozone concentration of 0.39±0.05 mg O_3/L did not statistically differ from that measured at pH 8.50 (0.35±0.01 mg O_3/L).

No permeate flux recovery was observed during the ozonation-membrane filtration of Lake Huron at 5 g/m^3 of gas-phase ozone within the duration of experiment (7 h) (Figure 4.2c). Taking into consideration the smallest percentage of the initial flux decline, as well as low TOC and intermediate alkalinity of this water, it is likely that the increase of ozonation time would result in the full flux recovery.

4.3.2. The removal of model pharmaceuticals during hybrid ozonation-membrane filtration

As it is shown in Figure 4.3, the removal of model pharmaceuticals was greater during ozonation-membrane filtration as compared to that of membrane filtration alone in all tested

waters, and the ozone dose, required for the complete oxidation of the model pharmaceuticals depended on water type. While 99.90% removal of dicloxacilline and cefrazidime was achieved in TOC-free water (10 mM $NaHCO_3$) and Lake Huron water at gas-phase ozone concentration of 5 g/m^3, only 40.0±0.1 and 91.2±1.1% of dicloxacilline and 64.3±0.01 and 87.9±0.4% of ceftazidime were removed from Huron River and LL waters, respectively. The removal of model pharmaceuticals from the waters should be correlated with the TOC and alkalinity of the corresponding water. The NOM and pharmaceuticals are concurrently oxidized during the ozonation-membrane filtration. Since the TOC of Lake Huron water is the least among three tested waters (Table 4.2), it would require less ozone to oxidize NOM. As a consequence, the efficiency of pharmaceutical removal during ozonation-membrane filtration of Lake Huron water is higher as compared to that of Huron River and LL waters. The higher alkalinity observed in Huron River water would likely lead to decreasing scavenging of $^{\cdot}OH$ radicals, which would result in lower efficiency of pharmaceutical removal from this water as compared to Lake Huron and LL waters. Thus, higher ozone dosages (15 and 20 g/m^3) will be required to completely remove model pharmaceuticals from Huron River and LL waters, correspondingly.

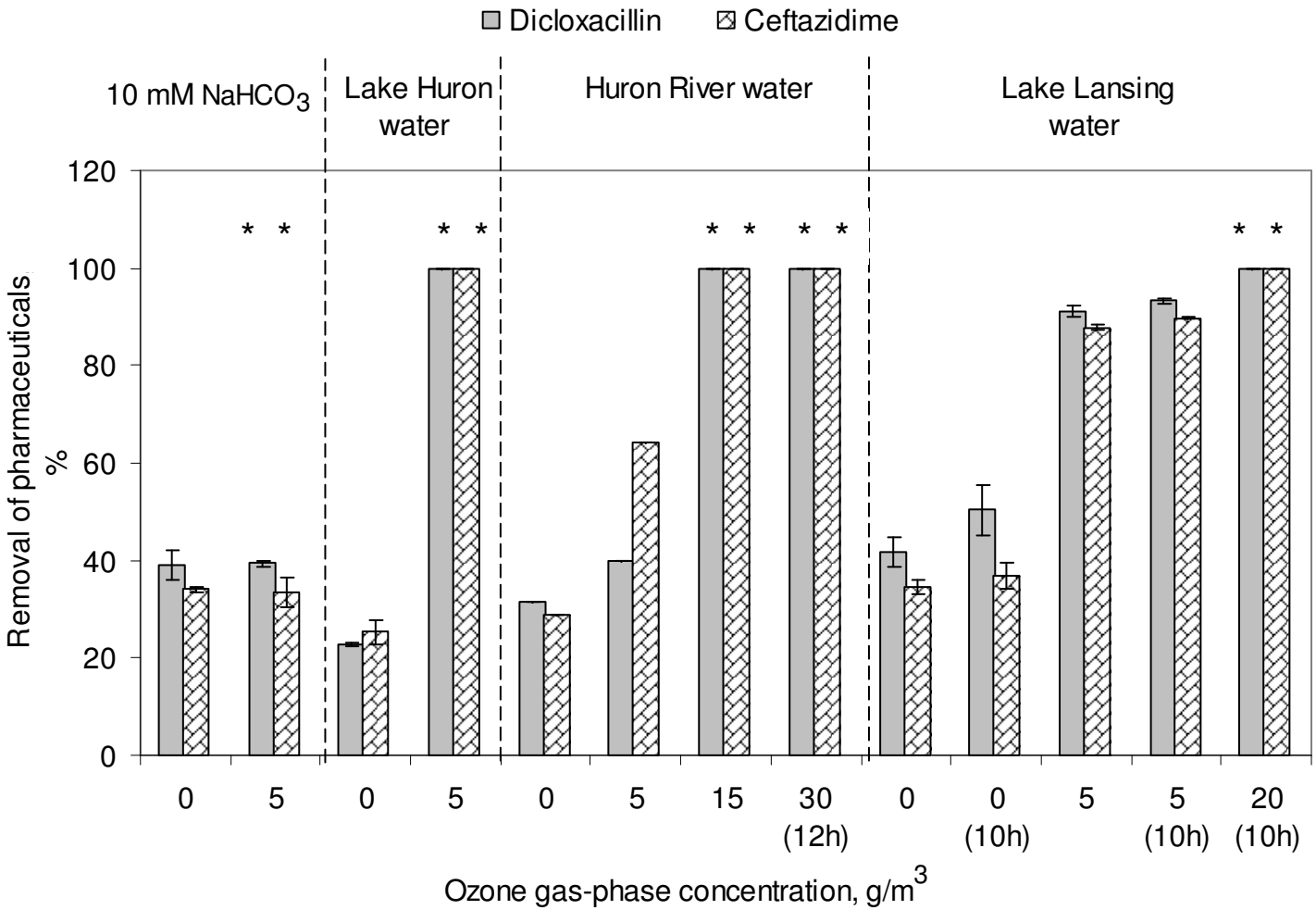

Figure 4.3. Effect of ozone gas-phase concentration on antibiotics removal during hybrid ozonation-membrane filtration. Conditions: 1 kDa uncoated membrane; raw water was spiked with 1.5 mg/L of each antibiotic, TMP = 2.1±0.1 bar, cross flow velocity = 0.55±0.05 m/s, ozone gas flow rate 40 mL/min. * concentration of antibiotic in permeate decreased below the detection level. Since experiments with Huron River water were done once, no error bars are shown. The samples for the HPLC/UV analysis were taken after 7 h of filtration unless the sampling time is indicated in brackets.

4.3.3. The removal of model pharmaceuticals during membrane filtration

When experiments were performed in the conventional filtration regime, the rejection of pharmaceuticals strongly depended on the water matrix. The rejections from NOM-free water (10 mM $NaHCO_3$) were 39.05±3.07 and 34.06±0.48% for dicloxacilline and ceftazidime, accordingly. Given that the molecular weights of the modeled pharmaceuticals were less than the MWCO of 1 kDa ceramic membrane, one could expect that the rejection of pharmaceuticals from their pure solutions by membrane would be much less than the measured values. The observed rejections suggest that the rejection of modeled pharmaceuticals by ceramic membranes was not due to the size exclusion, but rather adsorption or electrostatic repulsion (or their combination). The combination of electrostatic repulsion and size exclusion [62] and combination of size exclusion and adsorption [52] contributed to the rejection of a range of pharmaceuticals by loose NF membranes. In our experiments, at a given experimental conditions, both membrane surface and modeled pharmaceuticals are expected to be negatively charged therefore electrostatic repulsion may be the dominant rejection mechanism of dicloxacilline and ceftazidime on the 1 kDa ceramic UF membrane.

The rejection of spiked pharmaceuticals was less in Lake Huron water as compared to Huron River and LL waters (Figure 4.3). After 7 h of filtration the rejection of dicloxacilline were 22.7±0.4, 31.6, 41.8±3.04 and 42.21±3.0%, for Lake Huron, Huron River and LL waters, respectively; and the rejections of ceftazidime were 25.3±2.3, 29.0, 35.10±1.59 and 34.6±1.6% for Lake Huron, Huron River and LL waters, accordingly. In Figure 4.4a, the removal efficiency of model pharmaceuticals was plotted as a function of the feed water TOC. It appears that the rejection of pharmaceuticals increases with the increasing TOC concentration for these specific

waters. This finding is consistent with the study by Agbekodo et al. [99] who reported an increase in atrazine and simazine retention by an NF membrane as a function of NOM concentration.

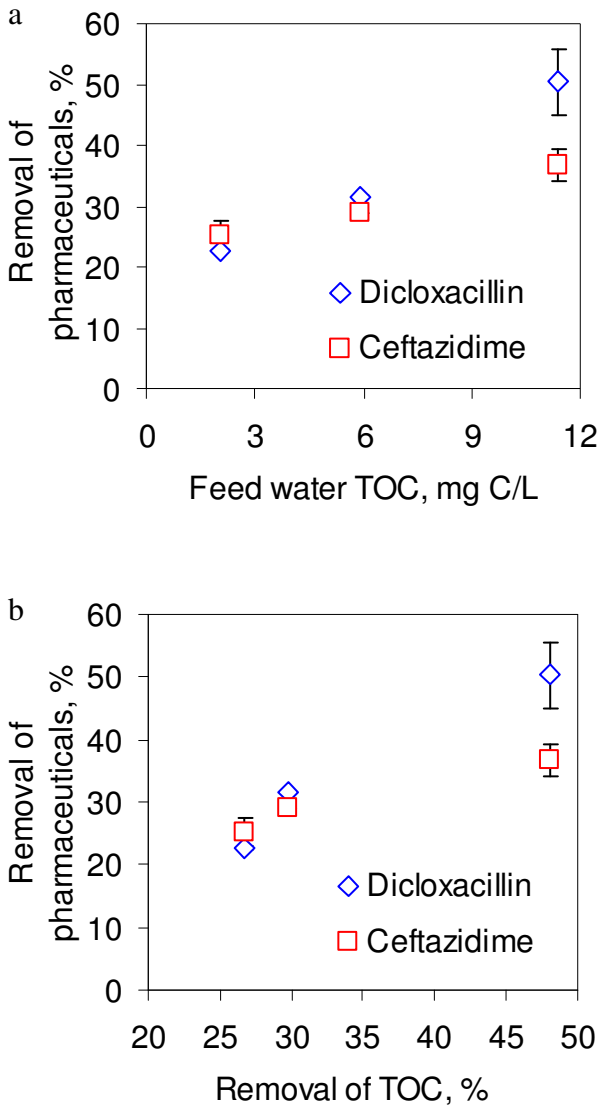

Figure 4.4. Removal of the pharmaceuticals as a function of TOC during membrane filtration only. Conditions: 1 kDa uncoated membrane; raw water was spiked with 1.5 mg/L of each pharmaceutical, TMP = 2.1±0.1 bar, cross flow velocity = 0.55±0.05 m/s, ozone gas flow rate 40 mL/min.

The rejection of model pharmaceuticals from the NOM-free water (10 mM $NaHCO_3$) solution was greater than that observed in Lake Huron water. The effect of NOM size on the rejection of dicloxacilline and ceftazidime could explain for this effect. The model pharmaceuticals may adsorb to NOM molecules present in the feed. If NOM molecules are smaller than the pore size, the pharmaceuticals would pass through the membrane pores, and their rejection would be less as compared to that observed in the NOM-free water. Nghiem et al. [54] observed that the rejection of estrone was greater from waters which contain larger molecular weight NOM. However, as it is seen from Figure 4.4b, the increase in water TOC would be resulted in an increase in the rejection of the pharmaceuticals. The observed correlation can be attributed to the formation of a fouling layer, which serves as an additional separation layer preventing organic molecules from passing through the membrane. As it was discussed previously, membrane fouling increased with increasing in feed TOC. As a consequence, better retention of pharmaceuticals would be observed from waters which facilitate the formation of a thicker fouling layer on the membrane surface.

The effect of pharmaceutical on its rejection during filtration experiments was also found to depend on water type. No statistically significant difference at 95% CI, was observed in the removal of dicloxacilline as compared to ceftazidime from NOM-free water (10 mM $NaHCO_3$) solution and Lake Huron water. On the contrary, a statistically significant difference between the rejections of dicloxacilline and ceftazidime rejections was observed in LL water. This may be explained by the specific interactions of dicloxacilline with the constituents of LL water. Since experiments with Huron River water were done once, the statistical analysis of effect of pharmaceuticals on their rejection during filtration of Huron River water was not conducted.

4.3.4. The removal of TOC and UV-254 absorbing compounds during membrane filtration and hybrid ozonation-membrane filtration

The removal of TOC and UV-254 absorbing compounds was evaluated with regard to the type of feed water and applied ozone dosage (Figures 4.5-4.7). As it is shown in Figure 4.5, greater TOC and UV-254 removals were achieved from waters with higher TOC concentration with both membrane filtration and hybrid ozonation-membrane filtration for both as-received water and water spiked with the model pharmaceuticals. The enhanced TOC removal during membrane filtration of LL water as compared to that of Huron River and Lake Huron waters could be attributed to the formation of the fouling layer on the membrane surface which would retain NOM molecules. The ozonation-membrane filtration enhanced the removal of TOC and UV-254 as compared to membrane filtration only, but extent it did so depended on the type of water. At an ozone dose of 5 g/m^3 both parameters followed the order: Lake Huron water < Huron River water < LL water. Given that Lake Huron water had the highest applied ozone dose per 1 mg of TOC/L ratio, one would expect that ozonation-membrane filtration would result in more effective TOC and UV-254 removals as compared to Huron River and LL waters. One possible explanation to this phenomenon is as follows. The hydraulic retention time of water in Lake Huron is 21 years [100]. As such, Lake Huron water would have the "oldest", i.e., the most recalcitrant organic material, which would be more resistant to oxidation as compared to that of Huron River and LL waters. Yavich et al. [101] found that biodegradation of Lake Erie water (hydraulic retention time is 2.7 years [100]) did not result in a reduction of organic carbon, whereas the concentration of organic carbon in Huron River and LL waters was reduced from 6.4 to approximately 5.25 and from 10.2 to approximately 5.2 mg/L, respectively. These results

point out that the studied waters are distinct not only in the amount of TOC content, but also in the amount of the recalcitrant organic material which is resistant to oxidation.

To study the effect of ozone dose on the extent of TOC and UV-254 removal, Huron River and LL waters were subjected to hybrid ozonation-membrane filtration at different ozone gas-phase concentrations. As it is seen in Figure 4.7a, the increase in ozone gas-phase concentration from 5 to 15 g/m^3 had little effect on the degree of TOC removal from Huron River water spiked with the model pharmaceuticals (30.53±0.08 and 32.03±0.02% for 5 and 15 g/m^3 gas-phase ozone, accordingly), and a further increase in ozone gas-phase concentration to 30 g/m^3 only slightly improved the removal of TOC (42.01±0.02%). Similarly, when the applied ozone dosage was increased 4 fold from 5 to 20 g/m^3, the efficiency of TOC removal from LL water spiked with model pharmaceuticals, increased only from 50.53±6.66 to 66.42±1.92% (Figure 4.6b). These results are consistent with the study by Karnik et al. [82] who found that increase of ozone dose from 1.5 to 10 g/m^3 did not lead to significant increase in the removal of dissolved organic carbon from LL water on a 15 kDa ceramic membrane. This was attributed to the conversion of larger NOM molecules into smaller ones as a result of their oxidation by ozone. As a result, the smaller molecules can freely pass through the membrane and the efficiency of TOC removal does not increase significantly.

a

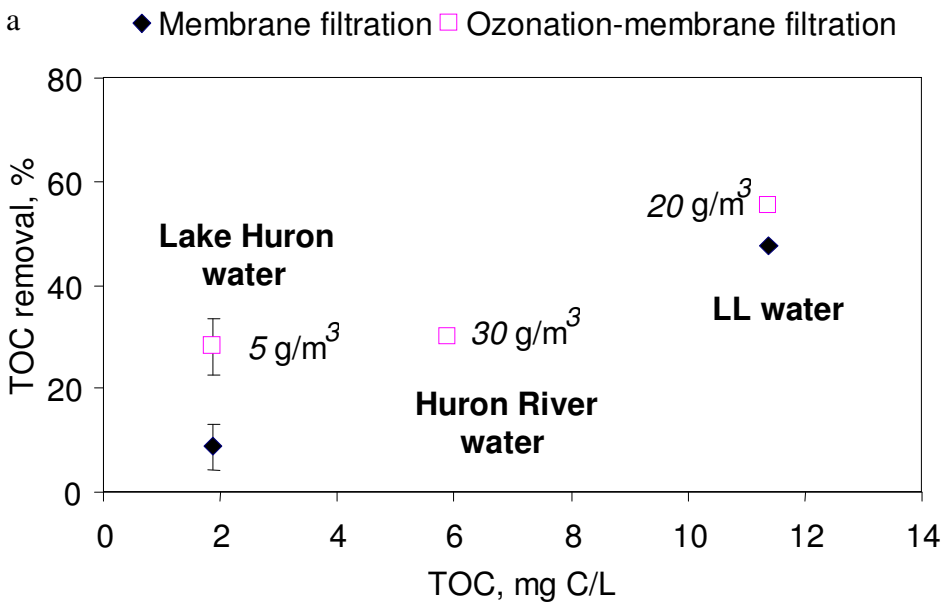

b

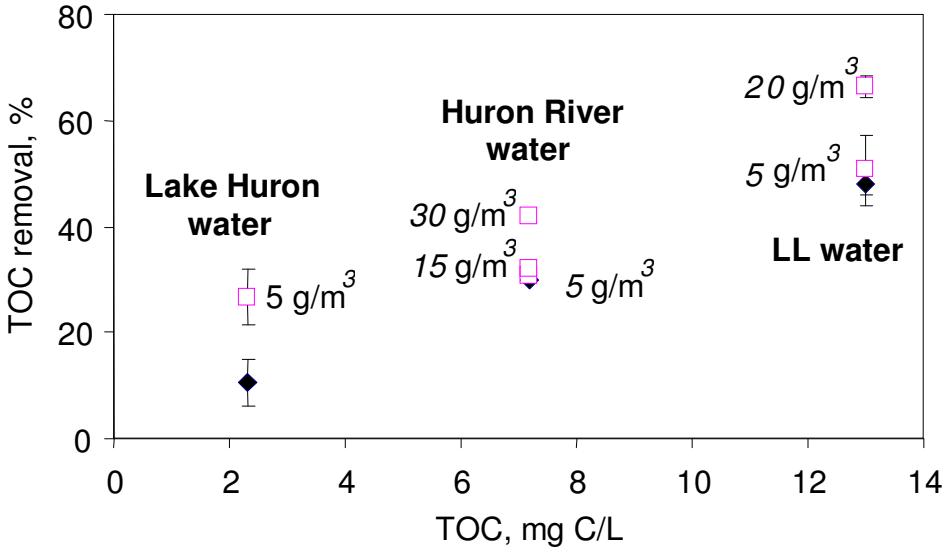

Figure 4.5. TOC removal (%) as a function of the initial water TOC (a - as-received feed, b - feed water, spiked with 1.5 mg/L of each antibiotic). Conditions: 1 kDa uncoated membrane; raw water was spiked with 1.5 mg/L of each pharmaceutical, TMP = 2.1±0.1 bar, cross flow velocity = 0.55±0.05 m/s, ozone gas flow rate 40 mL/min.

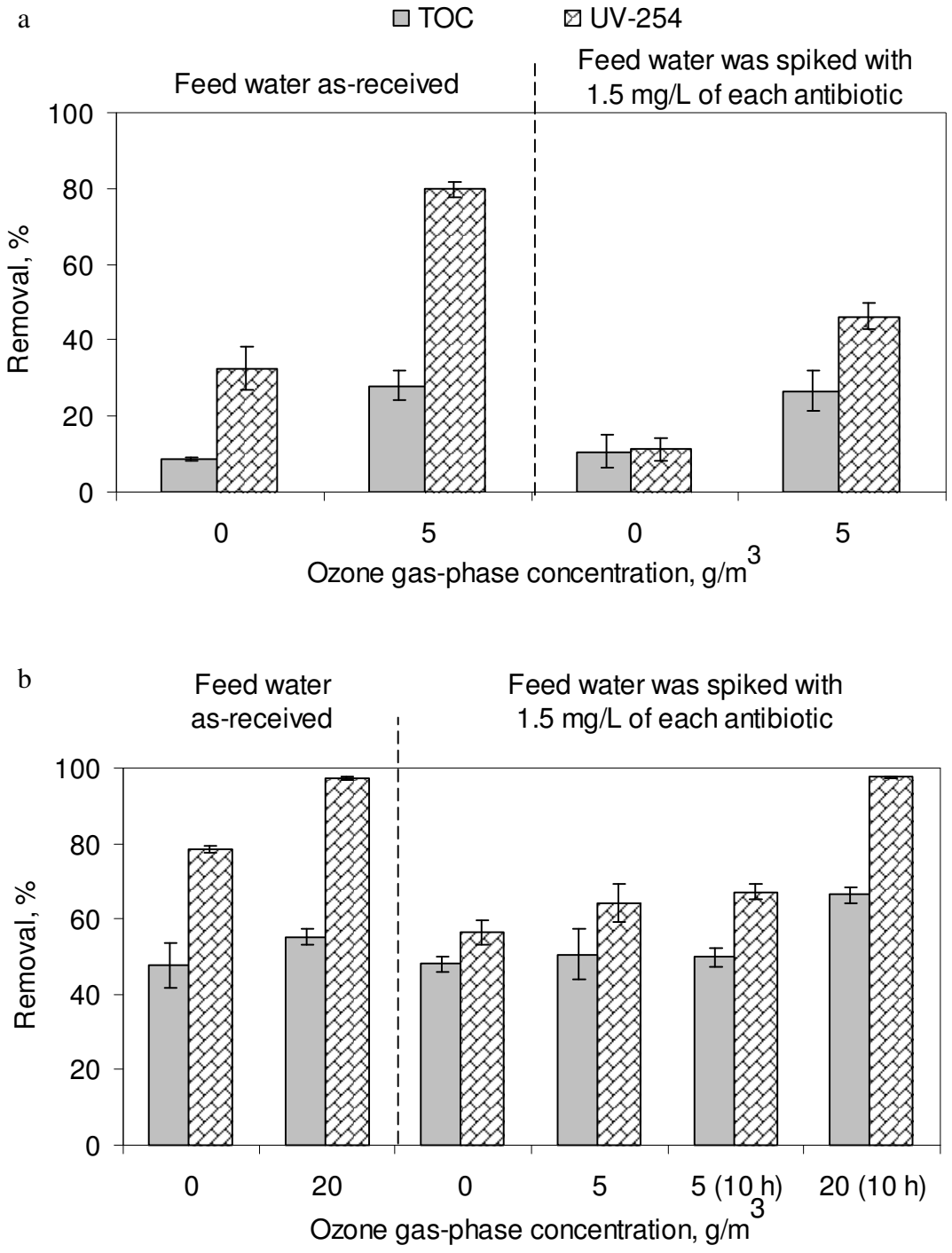

Figure 4.6. Effect of ozone gas-phase concentration on TOC and UV-254 removal from Lake Huron (a) and LL (b) waters. Conditions: 1 kDa uncoated membrane; TMP = 2.1±0.1 bar, cross flow velocity = 0.55±0.05 m/s, ozone gas flow rate 40 mL/min.

a

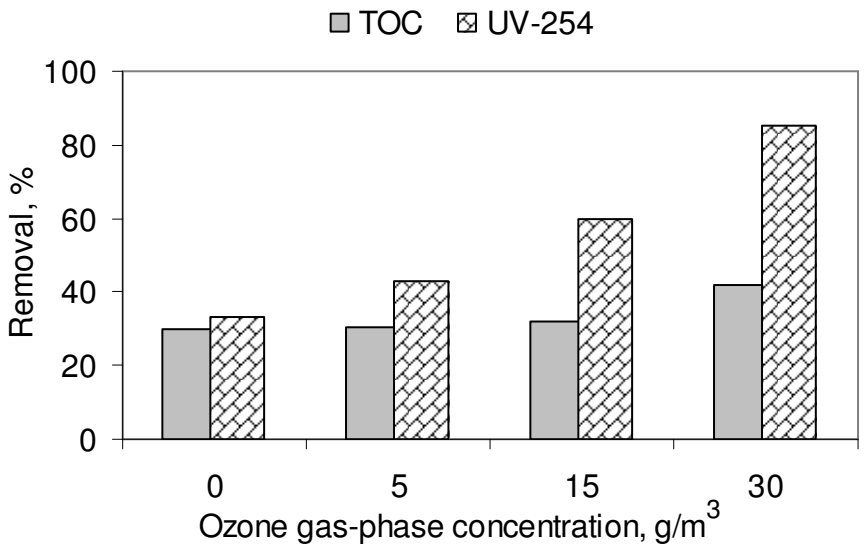

b

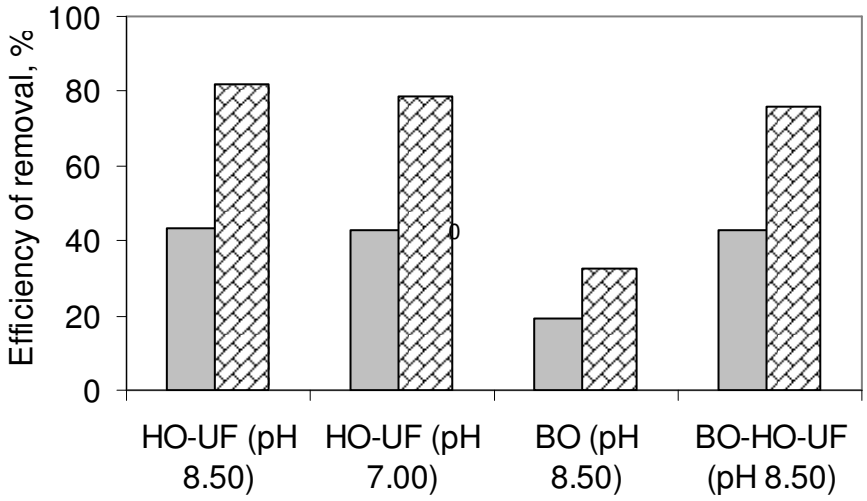

Figure 4.7. Effect of the treatment type on TOC and UV-254 removal from Huron River water (a - feed water spiked with 1.5 mg/L of each antibiotic, b - as-received water). HO-UF (pH 8.50) - hybrid ozonation-membrane filtration at 30 g/m^3 of gas-phase ozone and pH 8.50; HO-UF (pH 7.00) - hybrid ozonation-membrane filtration at 30 g/m^3 of gas-phase ozone and pH 7.00; BO (pH 8.50) - batch ozonation at 30 g/m^3 of gas-phase ozone for 2 h and pH 8.50; BO-HO-UF (pH 8.50) - batch ozonation at 30 g/m^3 of gas-phase ozone for 2 h followed by hybrid ozonation/membrane filtration at 15 g/m^3 of gas-phase ozone and pH 8.50). Conditions: 1 kDa uncoated membrane; TMP = 2.1±0.1 bar, cross flow velocity = 0.55±0.05 m/s, ozone gas flow rate 40 mL/min. Since experiments were done once, no error bars are shown.

To investigate the effect of pre-ozonation on the water quality characteristics, Huron River water was first ozonated in a batch reactor at ozone concentration of 30 g/m^3 for 2 h, followed by 7 h of ozonation-membrane filtration at 15 g/m^3. As it can be seen from Figure 4.7b, TOC removal after ozonation-membrane filtration increased as compared to ozonation only, but did not exceed the extent of TOC removal obtained in experiments when water was treated in ozonation-membrane filtration only. The decrease in pH from 8.50 to 7.00 also did not change the extent of TOC removal during filtration of Huron River water. The monitoring of pH during the course of experiment showed that the pH increased from 7.00 to 8.30 after 3 h of ozonation-membrane filtration. This means that a significant part of this experiment was actually conducted at pH which was similar to pH of the unadjusted water. On the contrary, Karnik et al. [82] reported that when pH of LL water was reduced from 8.2 to 7.00, significant increase in the dissolved organic carbon removal was achieved on 5 and 15 kDa membranes (from 35 to 40% and from 46 to >95%, accordingly). However, the direct comparison of these two studies is difficult because of different membrane pore size and the water matrixes.

The extent of the UV-254 removal was greater than that of TOC for all waters regardless the treatment type or applied ozone dosage (Figures 4.6 and 4.7). Consistently with the TOC removal, the removal of the UV-254 absorbing compounds followed this order Lake Huron water < Huron River water < LL water. The efficiency of the UV-254 removal was greater with hybrid ozonation-membrane filtration as compared to membrane filtration only and increased with an increase in the applied ozone dose for both Huron River and LL waters. This is consistent with the findings by Karnik et al [82], who suggested that the removal of the UV-254

compounds during ozonation-membrane filtration water was predominantly due to their ozonation and not due to the filtration itself.

4.3.5. The removal of disinfection byproducts in a hybrid ozonation-membrane filtration

The removal of DBPs precursors in a hybrid ozonation-membrane filtration was evaluated. The TTHMs and HAAs formation potential of the permeate was compared to that obtained using the feed water with conditions that simulate DBPs formation in the distribution system. As it is seen in Figures 4.8-4.10, the applied treatments significantly decreased the DBPs formation potential in all three waters tested. In all but one case the ozonation-membrane filtration resulted in statistically significant reduction (at 95% CI) of TTHMs and HAA as compared to conventional membrane filtration (see Table 4.6). The greatest removal of TTHMs (77.65±2.42%) and HAAs (51.87±9.98%) was achieved during ozonation-membrane filtration of LL water. The increase in DBPs removal efficiency during catalytic membrane oxidation is consistent with the previous studies on ozonation-membrane filtration of LL water [82, 102]. The smallest percentage of TTHMs removal during ozonation-membrane filtration was observed for Lake Huron water (11.20±1.23%) as compared to Huron River (64.32%) and LL waters (77.65±2.42 %) (Table 4.6). The removal of DBPs formation potential increases in the following order: Lake Huron water < Huron River < LL water and is consistent with TOC and UV-254 removal from studied waters. Surprisingly, ozonation-membrane filtration of as-received Lake Huron water did not result in a statistically significant improvement of TTHMs removal as compared to that of conventional membrane filtration (11.49±0.20 and 11.20±1.23%, respectively). On the contrarily, the TTHMs formation potential of this water spiked with the model pharmaceuticals decreased by 34.66±1.00% as compared to 45.89±0.76% decrease observed during membrane

filtration only. This may be explained as follows: the oxidation of organic material on the surface of ceramic membrane during catalytic ozonation is usually resulted in two processes: (1) the formation of lower weight molecular compounds, which could freely pass through the membrane, and (2) the mineralization of organic carbon to CO_2 and water. The low TOC removal observed during ozonation-membrane filtration of Lake Huron water (Figure 4.5a) suggests that the ozonation-membrane filtration facilitated the formation of smaller organic molecules, which react with chlorine to form THHMs. As a consequence, this process would not lead to the removal of any appreciable amount of THHM precursors. Since the ozonation-membrane filtration facilitates the removal of model pharmaceuticals below their detection limit (Figure 4.3), the overall THHMs removal efficiency would be higher as compared to non-spiked water.

The percentage of TTHM precursor removal during ozonation-membrane filtration was greater as compared to that of HAA precursor removal for Huron River and LL waters. This is consistent with the results by Chen et al. [102] who observed the reduction in the TTHM and HAA formation potentials (68 and 38% accordingly) upon the ozonation of the Huron River water. The authors suggested that the different degrees of removal were due to different reaction rates of TTHMs and HAAs precursors with ozone and/or ·OH radicals.

As seen in Figure 4.9, when the pH of Huron River water was decreased from 8.50 to 7.00, it did not effect its DBPs formation potential. Similarly, batch ozonation followed by the ozonation-membrane filtration only slightly increased the DBPs formation potential of this water.

In this study, the EPA regulatory standards for THHMs (80 µg/L) and HAA (60 µg/L) were met during the ozonation-membrane filtration of Lake Huron water. Although the concentrations of TTHMs and HAAs in as-received Lake Huron water were originally less than the corresponding EPA limits, they were further decreased as a result of the hybrid ozonation-membrane filtration. This is significant achievement since these two waters are used as a drinking water sources in Michigan. Although the HAAs regulatory limit was not met in the case of LL water, the efficiency of the hybrid ozonation-membrane filtration system in removing TTHMs precursors from this water points to the need for future research to optimize the systems parameters so that both regulatory standards can be met.

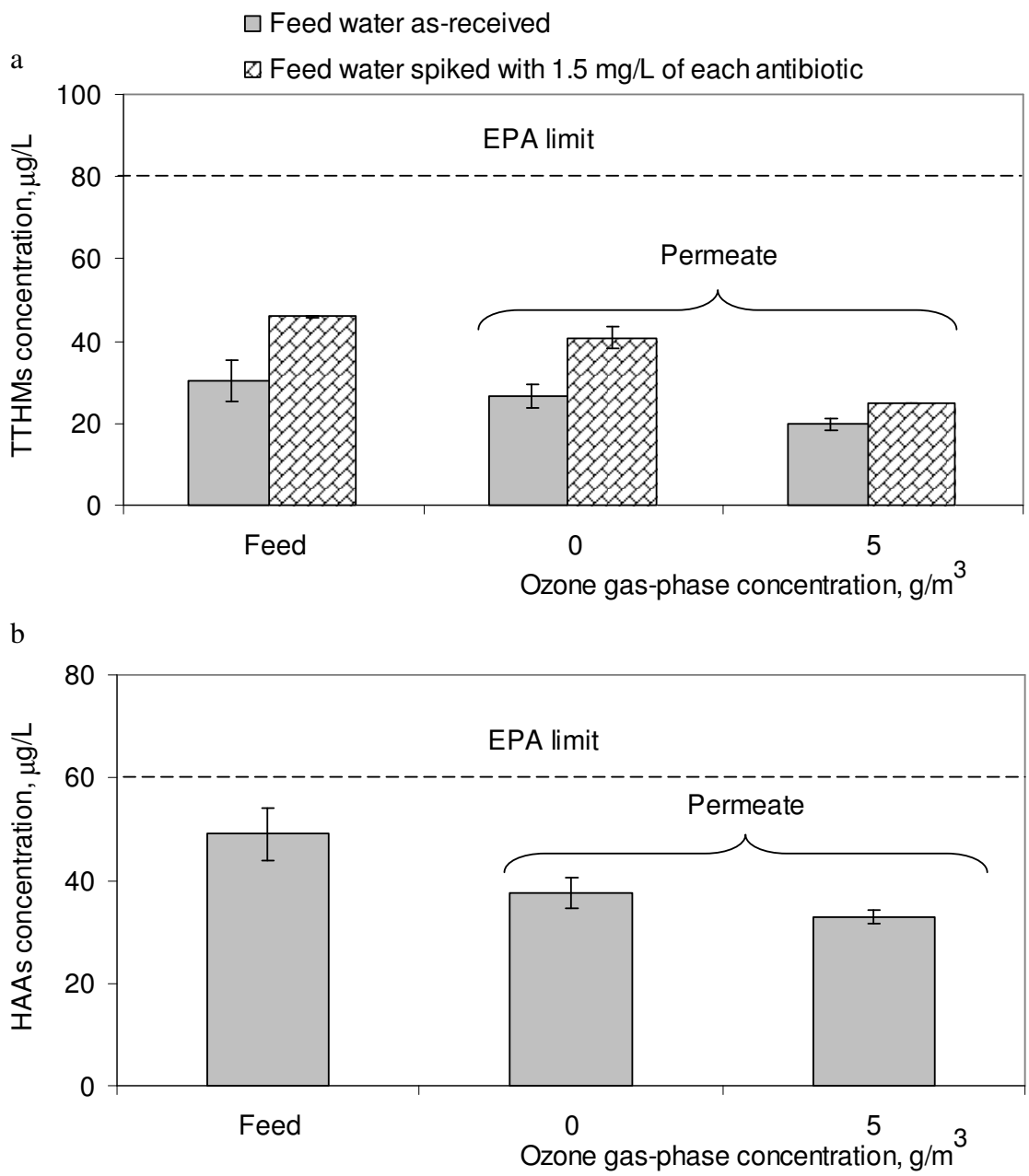

Figure 4.8. Effect of ozone gas-phase concentration on DBPs removal (a - TTHMs, b - HAA) during hybrid ozonation-membrane filtration of Lake Huron water. Conditions: 1 kDa uncoated membrane; TMP = 2.1±0.1 bar, cross flow velocity = 0.55±0.05 m/s, ozone gas flow rate 40 mL/min.

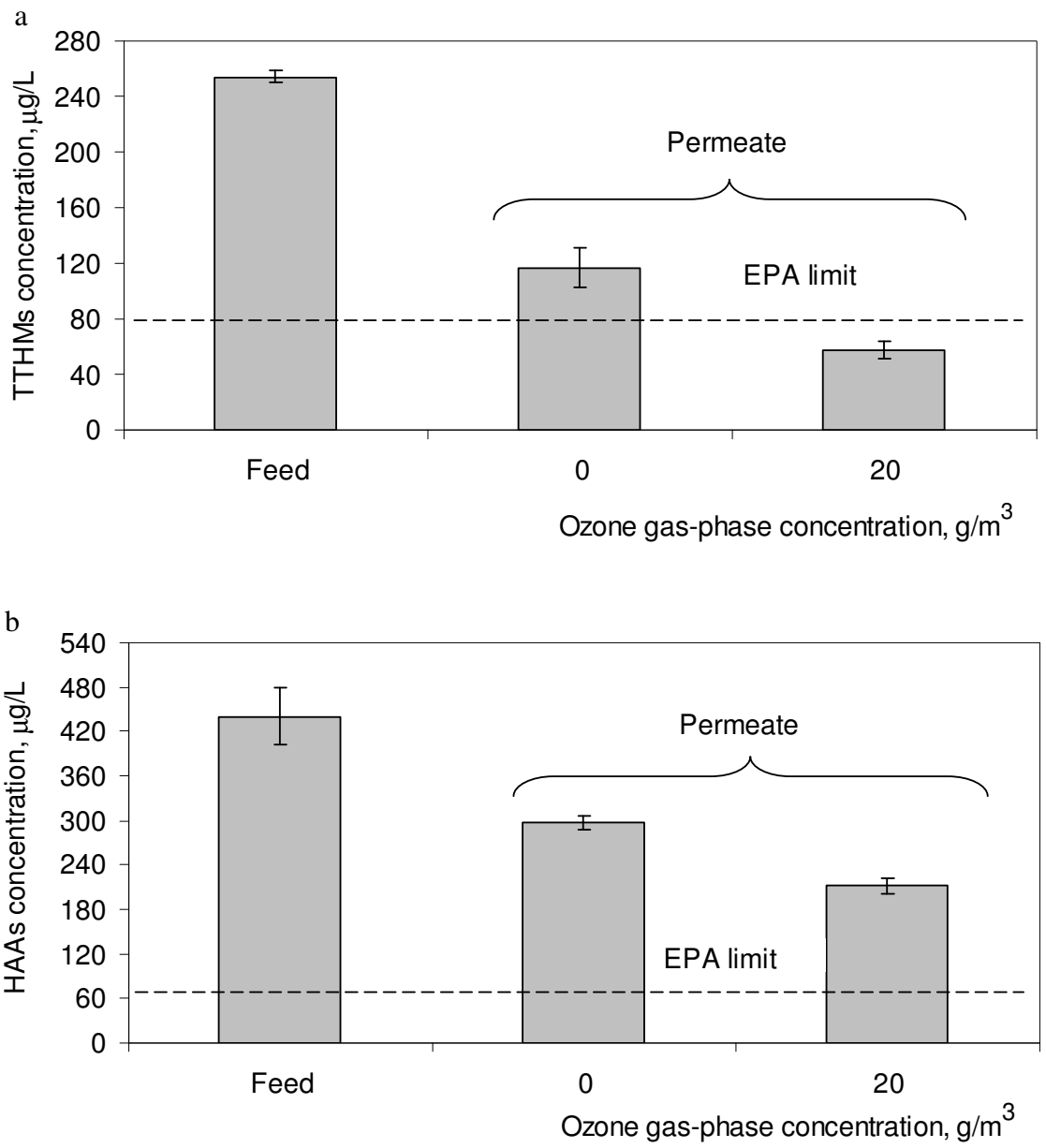

Figure 4.9. Effect of ozone gas-phase concentration on DBPs removal (a - TTHMs, b - HAA) during hybrid ozonation-membrane filtration of Lake Lansing water. Conditions: 1 kDa uncoated membrane; TMP = 2.1±0.1 bar, cross flow velocity = 0.55±0.05 m/s, ozone gas flow rate 40 mL/min.

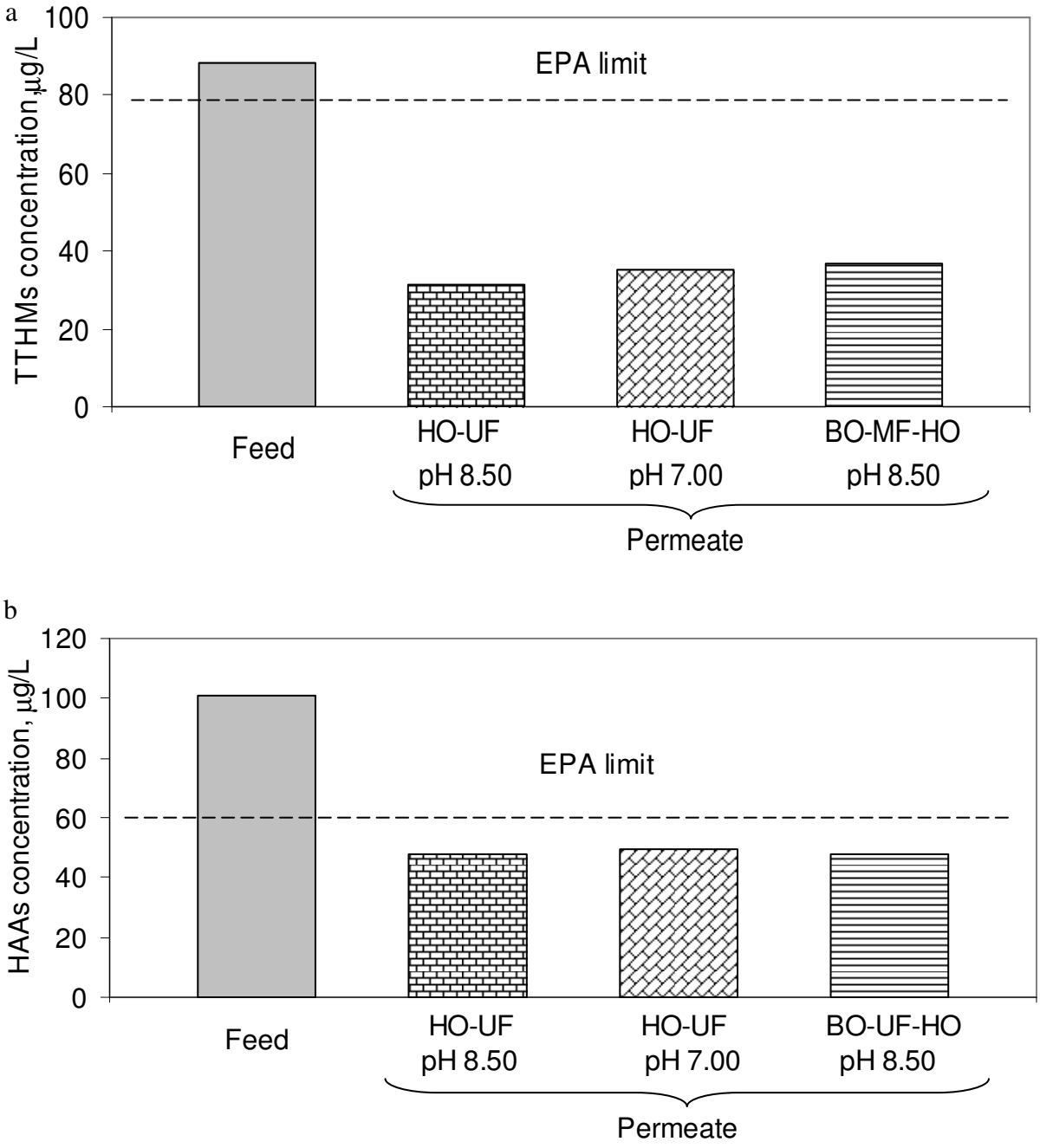

Figure 4.10. Effect of treatment type on disinfection by-products removal from Huron River water (HO-UF - hybrid ozonation-membrane filtration at 30 g/m^3 of gas-phase ozone and pH 8.50; HO-UF - hybrid ozonation-membrane filtration at 30 g/m^3 of gas-phase ozone and pH 7.00; BO-HO-UF - batch ozonation at 30 g/m^3 of gas-phase ozone for 2 h followed by hybrid ozonation/membrane filtration at 15 g/m^3 of gas-phase ozone and pH 8.50). Conditions: 1 kDa uncoated membrane; TMP = 2.1±0.1 bar, cross flow velocity = 0.55±0.05 m/s, ozone gas flow rate 40 mL/min. Since experiments were done once, no error bars are shown.

Table 4.7. The percentage of TTHMs and HAAs removal as a function of water type and treatment type.

DBPs type	Lake Huron water				LL water		*Huron River water		
	Ozone gas-phase concentration, g/m^3								
	0	5	0 (feed spiked with 1.5 mg/L of each antibiotic)	5 (feed spiked with 1.5 mg/L of each antibiotic)	0	20	30 (pH 8.50)	30 (pH 7.70)	**
TTHMs	11.49±0.20	11.20±1.23	34.66±1.00	45.89±0.76	54.86±5.42	77.65±2.42	64.32	60.16	58.69
HAAs	23.48±0.23	32.98±0.28	***n/a	***n/a	32.54±1.80	51.87±9.98	52.54	50.59	52.65

* - experiments were done once

** - batch ozonation at 30 g/m^3 of gas-phase ozone for 2 h followed by ozonation/membrane filtration at 15 g/m^3 of gas-phase ozone and pH 8.5.

*** - non available.

BIBLIOGRAPHY

BIBLIOGRAPHY

1. Webb, S.; Ternes, T.; Gibert, M.; Olejniczak, K. Indirect human exposure to pharmaceuticals via drinking water. *Toxicology Letters* (2003), **142**:3, 157-167.

2. Kummerer, K. The presence of pharmaceuticals in the environment due to human use – present knowledge and future challenges. *Journal of Environmental Management* (2009), 1-13.

3. Kummerer, K. Antibiotics in the aquatic environment - A review - Part 1. *Chemosphere* (2009), **75**, 417-434.

4. Klavarioti, M.; Mantzavinos, D.; Kassinos, D. Removal of residual pharmaceuticals from aqueous systems by advanced oxidation processes. *Environment International* (2009), **35**:2, 402-417.

5. Mompelat, S.; Le Bot, B.; Thomas, O. Occurrence and fate of pharmaceutical products and by-products, from resource to drinking water. *Environment International* (2009), **35**:5, 803-814.

6. Santos, L.H.M.L.M.; Araújo, A.N.; Fachini, A.; Pena, A.; Delerue-Matos, C.; Montenegro, M.C.B.S.M. Ecotoxicological aspects related to the presence of pharmaceuticals in the aquatic environment. *Journal of Hazardous Materials* (2010), **175**:1-3, 45-95.

7. Heberer, T.; Reddersen, K.; Mechlinski, A. From municipal sewage to drinking water: fate and removal of pharmaceutical residues in the aquatic environment in urban areas. *Water Science and Technology* (2002), **46**, 81-88.

8. Kolpin, D.W.; Furlong, E.T.; Meyer, M.T.; Thurman, E.M.; Zaugg, S.D.; Barber, L.B.; Buxton, H.T. Pharmaceuticals, hormones, and other organic wastewater contaminants in U.S. streams, 1999–2000: A national reconnaissance. *Environmetal Science and Technology* (2002), **36**:6, 1202-1211.

9. Oaks, J.L.; Gilbert, M.; Virani, M.Z.; Watson, R.T.; Meteyer, C.U.; Rideout, B.A.; Shivaprasad, H.L.; Ahmed, S.; Chaudhry, M.J.I.; Arshad, M.; Mahmood, S.; Ali, A.; Khan, A.A. Diclofenac residues as the cause of vulture population decline in Pakistan. *Nature* (2004), **427**:6975, 630-633.

10. Nash, J.P.; Kime, D.E.; Van der Ven, L.T.; Wester, P.W.; Brion, F.; Maack, G.; Stahlschmidt-Allner, P.; Tyler, C.R. Long-term exposure to environmental concentrations of the pharmaceutical ethinylestradiol causes reproductive failure in fish. *Environmental Health Perspectives* (2004), **112**:17, 1725-1733.

11. Pawlowski, S.; van Aerle, R.; Tyler, C.R.; Braunbeck, T. Effects of 17-alpha-ethinylestradiol in a fathead minnow (Pimephales promelas) gonadal recrudescence assay. *Ecotoxicology and Environmental Safety* (2004), **57**:3, 330-345.

12. Fenske, M.; Maack, G.; Schafers, C.; Segner, H. An environmentally relevant concentration of estrogen induces arrest of male gonad development in zebrafish, Danio rerio. . *Environmental Toxicology and Chemistry* (2005), **24**:5, 1088-1098.

13. Pascoe, D.; Karntanut, W.; Muller, C.T. Do pharmaceuticals affect freshwater invertebrates?Astudy with the cnidarian Hydra vulgaris. *Chemosphere* (2003), **51**:6, 521-528.

14. Kummerer, K.; Al-Ahmad, A. The cancer risk for humans related to cyclophoshamide and ifosfamide excretions emitted into surface water via hospital effluents. *Cancer Detection and Prevention* (1998), **22**:Supplement 1, 136.

15. Sengelov, G.; Halling-Sorensen, B.; Aarestrup, F.M. Susceptibility of *Escherichia coli* and *Enterococcus faecium* isolated from pigs and broiler chickens to tetracycline degradation products and distribution of tetracycline resistance determinants in E. coli from food animals. *Veterinary Microbiology* (2003), **95**:1-1, 91-101.

16. Cleuvers, M. Mixture toxicity of the anti-inflammatory drugs diclofenac, ibuprofen, naproxen, and acetylsalicylic acid. *Ecotoxicology and Environmental Safety* (2004), **59**:3, 309-315.

17. Halling-Sorensen, B.; Lykkeberg, A.; Ingerslev, F.; Blackwell, P.; Tjornelund, J. Characterisation of the abiotic degradation pathways of oxytetracyclines in soil interstitial water using LC–MS–MS. *Chemosphere* (2003), **50**:10, 1331-1342.

18. Webb, S.F., *A data-based perspective on the environmental risk assessment of human pharmaceuticals III - Indirect human exposure*, in *Pharmaceuticals in the Environment*, K. Kummerer, Editor. 2001, Springer: Berlin. 221-230.

19. EMEA, *Note for Guidance on Environmental Risk Assessment of medicinal Products for Human Use, CPMS/SWP/4447/draft*. 2005, The European Agency for Evaluation of Medicinal Products (EMEA), London.

20. FDA-CDER, *Guidance for Industry-Environmental Assessment of Human drugs and biological applications, Revision 1*. 1998, FDA Centre for Drug Evaluation and Research, Rockville.

21. Perez, S.; Eichhorn, P.; Aga, D.S. Evaluating the biodegradability of sulfamethazine, sulfamethoxazole, sulfathiazole and trimethoprim at different stages of sewage treatment. *Environmental Toxicology and Chemistry* (2005), **24**, 1361-1367.

22. Miao, X.-S.; Yang, J.-J.; Metcalfe, C.D. Carbamazepine and Its Metabolites in Wastewater and in Biosolids in a Municipal Wastewater Treatment Plant. *Environmental Science & Technology* (2005), **39**:19, 7469-7475.

23. Batt, A.L.; Bruce, I.B.; Aga, D.S. Evaluating the vulnerability of surface waters to antibiotic contamination from varying wastewater treatment plant discharges. *Environmental Pollution* (2006), **142**, 295-302.

24. Watkinson, A.J.; Murby, E.J.; Costanzo, S.D. Removal of antibiotics in conventional and advanced wastewater treatment: Implications for environmental discharge and wastewater recycling. *Water Research* (2007), **41**, 4164-4176.

25. Li, D.; Yang, M.; Hu, J.; Ren, L.; Zhang, Y.; Li, K. Determination and fate of oxytetracycline and related compounds in oxytetracycline production wastewater and the receiving river. *Environmental Toxicology and Chemistry* (2008), **27**:1, 80-86.

26. Qiting, J.; Xiheng, Z. Combination process of anaerobic digestion and ozonation technology for treating wastewater from antibiotic production. *Water Treatment* (1988), **3**, 285-291.

27. Thomas, K.V.; Dye, C.; Schlabach, M.; Langford, K.H. Source to sink tracking of selected human pharmaceuticals from two Oslo city hospitals and a wastewater treatment works. *Journal of Environmental Monitoring* (2007), **9**, 1410-1418.

28. Brown, K.D.; Kulis, J.; Thomson, B.; Chapman, T.H.; Mawhinney, D.B. Occurrence of antibiotics in hospital, residential, and dairy effluent, municipal wastewater, and the Rio Grande in New Mexico. *Science of the Total Environment* (2006), **366**, 772-83.

29. Focazio, M.J.; Kolpin, D.W.; Barnes, K.K.; Furlong, E.T.; Meyer, M.T.; Zaugg, S.D.; Barber, L.B.; Thurman, M.E. A national reconnaissance for pharmaceuticals and other organic wastewater contaminants in the United States - II) Untreated drinking water sources. *Science of the Total Environment* (2008), **402**:2-3, 201-216.

30. Ashton, D.; Hilton, M.; Thomas, K.V. Investigating the environmental transport of human pharmaceuticals to streams in the United Kingdom. *Science of the Total Environment* (2004), **333**, 167-184.

31. Thomas, K.V.; Hilton, M.J. The occurrence of selected human pharmaceutical compounds in UK estuaries. *Marine Pollution Bulletin* (2004), **49**:5/6, 436-444.

32. Alder, A.C.; McArdell, C.S.; Golet, E.M.; Ibric, S.; Molnar, E.; Nipales, N.S.; Giger, W., *Occurrence and fate of fluoroquinolone, macrolide and sulfonamide antibiotics during wastewater treatment and in ambient waters in Switzerland*, in *Pharmaceuticals and Personal Care Products in the Environment: Scientific and Regulatory Issues*, C.G. Daughton and T.L. Jones-Lepp, Editors. 2001, American Chemical Society: Washington, DC. 39-54.

33. Ternes, T.A.; Meisenheimer, M.; McDowell, D.; Sacher, F.; Brauch, H.-J.; Haist-Gulde, B.; Preuss, G.; Wilme, U.; Zulei-Seibert, N. Removal of pharmaceuticals during drinking water treatment *Environmetal Science and Technology* (2002), **36**:17, 3855-3863.

34. Holm, J.V.; Ruegge, K.; Bjerg, P.L.; Christensen, T.H. Occurrence and distribution of pharmaceutical organic compounds in the groundwater downgradient of a landfill (Grindsted, Denmark). *Environmental Science & Technology* (1995), **29**:5, 1415-1420.

35. Costanzo, S.D.; Murby, J.; Bates, J. Ecosystem response to antibiotics entering the aquatic environment. *Marine Pollution Bulletin* (2005), **51**, 218-223.

36. Stumpf, M.; Ternes, T.A.; Wilken, R.-D.; Silvana Vianna Rodrgues Baumann, W. Polar drug residues in sewage and natural waters in the state of Rio de Janeiro, Brazil. *Science of the Total Environment* (1999), **225**:1/2, 135-141.

37. Kim, S.D.; Cho, J.; Kim, I.S.; Vanderford, B.J.; Snyder, S.A. Occurrence and removal of pharmaceuticals and endocrine disruptors in South Korean surface, drinking, and waste waters. *Water Research* (2007), **41**:5, 1013-1021.

38. Heberer, T.; Stan, H.J. Determination of clofibric acid and N-(Phelylsulfonyl)-sacrosine in sewage, river and drinking water. *International Journal of Analytical Chemistry* (1997), **67**, 113-124.

39. Farre, M.L.; Ferrer, I.; Ginebreda, A.; Figueras, M.; Olivella, L.; Tirapu, L.; Vilanova, M.; Barcelo, D. Determination of drugs in surface water and wastewater samples by liquid chromatography–mass spectrometry: methods and preliminary results including toxicity studies with Vibrio fischeri. *Journal of Chromatography A* (2001), **938**:1/2, 187-197.

40. Christian, T.; Schneider, R.J.; Farber, H.A.; Skutlarek, D.; Meyer, M.T.; Goldbach, H.E. Determination of antibiotic residues in manure, soil, and surface waters. *Acta Hydrochimica Et Hydrobiologica* (2003), **31**:1, 36-44.

41. Hirsch, R.; Ternes, T.; Haberer, K.; Kratz, K.L. Occurrence of antibiotics in the aquatic environment. *Science of the Total Environment* (1999), **225**, 109-118.

42. Calamari, D.; Zuccato, E.; Castiglioni, S.; Bagnati, R.; Fanelli, R. Strategic of therapeutic drugs in the rivers Po and Lambro in Northern Italy. *Environmental Science & Technology* (2003), **37**, 1241-1248.

43. Sacher, F.; Gabriel, S.; Metzinger, M.; Stretz, A.; Wenz, M.; Lange, F.T.; Brauch, H.J.; Blankenhorn, I. Arzneimittelwirkstoffe im Grundwasser – Ergebnisse eines Monitoring-Programms in Baden-Württemberg (Active pharmaceutical ingredients in ground water – the results of a monitoring program in Baden-Württemberg (Germany)). *Vom Wasser* (2002), **99**, 183-196.

44. Thaker, P.D. Pharmaceutical data elude researchers. *Environmental Science & Technology* (2005), **39**:9, 193A-194A.

45. Westerhoff, P.; Yoon, Y.; Snyder, S.A.; Wert, E. Fate of endocrine-disruptor, pharmaceutical, and personal care product chemicals during simulated drinking water treatment processes. *Environmetal Science and Technology* (2005), **39**, 6649-6663.

46. Massmann, G.; Dunnbier, U.; Heberer, T.; Taure, T. Behaviour and redox sensitivity of pharmaceutical residues during bank filtration - ivestigation of residues of phenazone-type analgesics. *Chemosphere* (2008), **71**, 1476-1485.

47. Zuehlke, S.; Duennbier, U.; Heberer, T. Investigation of the behavior and metabolizm of pharmaceutical residues during purification of contaminated ground water used for drinking water supply. *Chemosphere* (2007), **69**, 1673-1680.

48. Kimura, K.; Amy, G.; Drewes, J.E.; Heberer, T.; Kim, T.-U.; Watanabe, Y. Rejection of organic micropollutants (disinfection by-products, endocrine disrupting compounds, and pharmaceutically active compounds) by NF/RO membranes. *Journal of Membrane Science* (2003), **227**, 113-121.

49. Yoon, Y.; Westerhoff, P.; Snyder, S.A.; Wert, E.C.; Yoon, J. Removal of endocrine disrupting compounds and pharmaceuticals by nanofiltration and ultrafiltration membranes. *Desalination* (2007), **202**, 16-23.

50. Kimura, K.; Toshima, S.; Amy, G.; Watanabe, Y. Rejection of neutral endocrine disrupting compounds (EDCs) and pharmaceutical active compounds (PhACs) by RO membranes. *Journal of Membrane Science* (2004), **245**, 71-78.

51. Chang, S.; Waite, T.D.; Schfer, A.I.; Fane, A.G. Adsorption of the endocrine-active compound estrone on microfiltration hollow fiber membranes. *Environmetal Science and Technology* (2003), **37**:14, 3158-3163.

52. Schfer, A.I.; Nghiem, L.D.; Waite, T.D. Removal of the natural hormone estrone from aqueous solutions using nanofiltration and reverse osmosis. *Environmetal Science and Technology* (2003), **37**:1, 182-188.

53. Koyuncu, I.; Arikan, O.A.; Wiesner, M.R.; Rice, C. Removal of hormones and antibiotics by nanofiltration membranes. *Journal of Membrane Science* (2008), **309**, 94-101.

54. Nghiem, L.D.; Manis, A.; Soldenhoff, K.; Schäfer, A.I. Estrogenic hormone removal from wastewater using NF/RO membranes. *Journal of Membrane Science* (2004), **242**, 37-45.

55. Schafer, A.I.; NMastrup, M.; Lund Jensen, R. Particle interactions and removal of trace contaminants from water and wastewater. *Desalination* (2002), **147**, 243-250.

56. Comerton, A.M.; Andrews, R.C.; Bagley, D.M.; Yang, P. Membrane adsorption of endocrine disrupting compounds and pharmaceutically active compounds. *Journal of Membrane Science* (2007), **303**, 267-277.

57. Comerton, A.M.; Andrews, R.C.; Bagley, D.M.; Haoc, C. The rejection of endocrine disrupting and pharmaceutically active compounds by NF and RO membranes as a function of compound and water matrix properties. *Journal of Membrane Science* (2008), **313**, 323-335.

58. Schafer, A.I.; Nghiem, L.D.; Waite, T.D. Removal of the natural hormone estrone from aqueous solutions using nanofiltration and reverse osmosis. *Environmetal Science and Technology* (2003), **37**:1, 182-188.

59. Urase, T.; Sato, K. The effect of deterioration of nanofiltration membrane on retention of pharmaceuticals. *Desalination* (2007), **202**, 385-391.

60. Radjenovic, J.; Petrovic, M.; Ventura, F.; Barcelo, D. Rejection of pharmaceuticals in nanofiltration and reverse osmosis membrane drinking water treatment. *Water Research* (2008), **42**, 3601-3610.

61. Nghiem, L.D.; A.I., S.; Waite, T.D. Adsorption of estrone on nanofiltrationand reverse osmosis membranes in water and wastewater treatment. *Water Science and Technology* (2002), **46**:4-5, 265-272.

62. Nghiem, L.D.; Schfer, A.I.; Elimelech, M. Pharmaceutical retention mechanisms by nanofiltration membranes *Environmetal Science and Technology* (2005), **39**:19, 7698-7705.

63. Ngiem, L.; Schafer, A.; Elimelech, M. Removal of natural hormones by nanofiltration membranes: measuring, modelling and mechanisms. *Environmental Science & Technology* (2004), **39**, 1888-1896.

64. Nghiem, L.D.; Schifer*, A.I.; Waite, T.D. Adsorptive interactions between membranes and trace contaminants. *Desalination* (2002), **147**, 269-274.

65. Nghiem, L.; Schafer, A.; Elimelech, M. Removal of natural hormones by nanofiltration membranes: measuring, modelling and mechanisms. *Environmental Science & Technology* (2004), **39**, 1888-1896.

66. Maskaoui, K.; Hibberd, A.; Zhou, J.L. Assessment of the interaction between aquatic colloids and pharmaceuticals facilitated by cross-flow ultrafiltration. *Environmetal Science and Technology* (2007), **41**:23, 8038-8043.

67. Crittenden, J.C. Water treatment: principles and design. 2 ed. 2005, Hoboken, NJ: Wiley.

68. von Gunten, U. Review. Ozonation of drinking water: Part I. Oxidation kinetics and product formation. *Water Research* (2003), **37**, 1443-1467.

69. von Gunten, U. Review. Ozonation of drinkingwater: Part II. Disinfection and by-product formation in presence of bromide, iodide or chlorine. *Water Research* (2003), **37**, 1469-1487.

70. von Gunten, U. The basics of oxidants in water treatment. Part B: ozone reactions. *Water Science and Technology* (2007), **55**:12, 25-29.

71. Ozone in water treatment: Application and Engineering. 2 ed, ed. B. Langilas. 1991, USA: Lewis Publishers.

72. Broséus, R.; Vincent, S.; Aboulfadl, K.; Daneshvar, A.; Sauvé, S.; Barbeau, B.; Prévost, M. Ozone oxidation of pharmaceuticals, endocrine disruptors and pesticides during drinking water treatment. *Water Research* (2009), **43**:18, 4707-4717.

73. Ternes, T.A.; Stuber, J.; Herrmann, N.; McDowell, D.; Ried, A.; Kampmann, M.; Teiser, B. Ozonation: a tool for removal of pharmaceuticals, contrast media and musk fragrances from wastewater? *Water Research* (2003), **37**, 1976-1982.

74. Dodd, M.C.; Kohler, H.-P.; von Gunten, U. Oxidation of antibacterial compounds by ozone and hydroxyl radical: elimination of biological activity during aqueous ozonation process. *Environmetal Science and Technology* (2009), **43**, 2498-2503.

75. Li, K.; Yediler, A.; Yang, M.; Schulte-Hostede, S.; Wong, M.H. Ozonation of oxytetracycline and toxicological assessment of its oxidation by-products. *Chemosphere* (2008), **72**, 473-478.

76. Beltran, F.J.; Rivas, F.J.; Acedo, B. Atrazine removal by ozonation processes in surface waters. *Journal of Environmental Science and Health B* (1999), **34**, 449-468.

77. Li, L.; Zhu, W.; Zhang, P.; Chen, Z.; Han, W. Photocatalytic oxidation and ozonation of catechol over carbon-black-modified nano-TiO2 thin films supported on Al sheet. *Water Research* (2003), **37**, 3646-3651.

78. Ernst, M.; Lurot, F.; Schrotter, J.-C. Catalytic ozonation of refractory organic model compounds in aqueous solution by aluminum oxide. *Applied Catalysis B: Environmental* (2004), **47**:1, 15-25.

79. Skoumal, M.; Cabot, P.-L.; centellas, F.; Arias, C.; Rodrigez, R.M.; Garrido, J.A.; Brillas, E. Mineralization of paracetamol by ozonation catalysed with Fe^{2+}, Cu^{2+} and UVA light. *Applied Catalysis B: Environmental* (2006), **66**, 228-240.

80. Kasprzyk-Hordern, B.; Raczyk-Stanislawiak, U.; Swietlik, J.; Nawrocki, J. Catalytic ozonation of natural organic matter on alumina. *Applied Catalysis B: Environmental* (2006), **62**:3-4, 345-358.

81. Parisheva, Z.; Litcheva, P. 2007. *Oxidation Communication* (2007), **30**:1, 165-171.

82. Karnik, B.S.; Davies, S.H.; M.J., B.; S.J., M. The effects of combined ozonation and filtration on disinfection by-product formation. *Water Research* (2005), **39**, 2839-2850.

83. Kim, J.; Davies, S.H.R.; Baumann, M.J.; Tarabara, V.V.; Masten, S.J. Effect of ozone dosage and hydrodynamic conditions on the permeate flux in a hybrid ozonation-ceramic ultrafiltration system treating natural waters. *Journal of Membrane Science* (2007), **311**, 165-172.

84. Tsuru, T. Inorganic porous membranes for liquid phase separation. *Separation and Purification Technology* (2001), **30**:2, 191-200.

85. Mulder, M. Basic Principles of Membrane Technology. 2nd ed. 2003, Netherlands: Kluwer Academic Publishers.

86. Karnik, B.S.; Davies, S.H.R.; Baumann, M.J.; Masten, S.J. Fabrication of catalytic membranes for the treatment of drinking water using combined ozonation and ultrafiltration. *Environmental Science and Technology* (2005), **39**:19, 7656-7661.

87. Karnik, B.S.; Davies, S.H.R.; Chen, K.C.; Jaglowski, D.R.; Baumann, M.J.; Masten, S.J. Effect of ozonation on the permeate flux of nanocrystalline ceramic membranes. *Water Research* (2005), **39**, 728-734.

88. Shlitcher, B.; Mavrov, V.; Chimel, H. Study of a hybrid process combining ozonation and microfiltration/ultrafiltration for drinking water production from surface water *Desalination* (2004), **168**, 307-317.

89. Karnik, B.S.; Davis, S.H.R.; Baumann, M.J.; Masten, S.J. Use of salicylic acid as a model compound to investigate hydroxyl radical reaction in ozonation–membrane filtration hybrid processes. *Environmental Engineering Science* (2007), **24**:6, 1-9.

90. Hoigné, J. The Handbook of Environmental Chemistry: Quality and Treatment of Drinking Water (Part II), ed. J. Hrubec. 1998, Berlin: Springer.

91. Naydenov, A.; Mehandjiev, D. Complete oxidation of benzene on manganese dioxide by ozone. *Applied Catalysis A: General* (1993), **97**, 17-22.

92. Castle, S.S.; Enna, S.J.; David, B.B., *Dicloxacillin*, in *xPharm: The Comprehensive Pharmacology Reference*. 2007, Elsevier: New York. 1-5.

93. Castle, S.S.; Enna, S.J.; David, B.B., *Ceftazidime*, in *xPharm: The Comprehensive Pharmacology Reference*. 2007, Elsevier: New York. 1-5.

94. Clesceri, L.S.; Greenberg, A.E.; Eaton, A.D. Standard Methods for Examinations of Water and Wastewater. 20th ed. 1998: American Public health association.

95. Determination of haloacetic acids and dalapon in drinking water by liquid-liquid microextraction, derivatization, and gas chromatography with electron capture detection. Vol. 815-B-03-002. 2003: US EPA.

96. Lyman, W.J.; Reehl, W.F.; Rosenblatt, D.H. Handbook of chemical property estimation methods. 1990, Washington, DC: American Chemical Society.

97. *EPI Suite software*, US EPA: www.epa.gov.

98. Nyström, M.; Ruohomäki, K.; Kaipia, L. Humic acid as a fouling agent in filtration. *Desalination* (1996), **106**:1-3, 79-87.

99. Agbekodo, K.M.; Legube, B.; Dard, S. Atrazine and simazine removal mechanisms by nanofiltration: influence of natural organic matter concentration. *Water Research* (2996), **30**:11, 2535-2542.

100. Kurt-Karakus, P.B.; Muir, D.C.G.; Bidleman, T.F.; Small, J.; Backus, S.; Dove, A. Metolachlor and atrazine in the Great Lakes. *Environmental Science and Technology* (2010), **44**:12, 4678-4684.

101. Yavich, A.A.; Lee, K.-H.; Chen, K.-C.; Pape, L.; Masten, S.J. Evaluation of biodegradability of NOM after ozonation. *Water Research* (2004), **38**:12, 2839-2846.

102. Chen, K.C., *Ozonation, ultrafiltration, and biofiltration for the control of NOM and DBP in drinking water*. 2003, Michigan State University: East Lansing.

CHAPTER 5

CONCLUSIONS

The epigenetic toxicity of dispersed single-walled carbon nanotubes (SWCNTs) was evaluated for the first time using a gap junctional intercellular communication assay (GJIC) with WB-F344 rat liver epithelial cells resulting in no inhibition by SWCNTs non-covalently functionalized using gum Arabic (GA), PVP (polyvinylpyrrolidone), amylose, and natural organic matter (NOM). There were no cytotoxic effects of these SWCNTs suspensions on either the prokaryotic, bacterial (*E. coli*), or eukaryotic (WB-F344 rat liver epithelial) cell types. Only when the dispersant itself was toxic, no losses of cell viability were observed. Bacterial CFU counts or neutral red uptake was affected only by SWCNTs dispersed using Triton X-100, which was cytotoxic in the absence of SWCNT (vehicle control II). The results suggest a strong dependence of the toxicity of SWCNT suspensions on the toxicity of the dispersing agent and point to the potential of non-covalent functionalization with non-toxic dispersants as a method for the preparation of aqueous suspensions of biocompatible CNTs.

Our research demonstrates that the physicochemical properties of nC$_{60}$ aggregates, such as ζ - potential and surface functionality, were altered as a result of ozonation and chlorination. Sequential ozonation/chlorination of nC$_{60}$ suspensions has led to a more profound decrease in the ζ – potential, as compared to that observed when nC$_{60}$ was subjected to ozonation alone. The formation of C-Cl bonds on the surface of chlorinated nC$_{60}$ suggests the ability of this nanomaterial to manifest itself as a precursor for chlorinated carbon-based disinfection by-

products and thus, be a potential health hazard. This is an important finding as it is known that the chlorination of carbon-rich natural organic matter can result in the formation of a wide range of toxic halogenated compounds. However, neither cytotoxic effects to *E.coli* and WB-F344 rat liver epithelial cells (exposure times 3 and 24 h) nor GJIC inhibition (exposure times 30 min and 24 h) were detected for as-prepared nC_{60} and their oxidized by-products at the nC_{60} concentration range studied.

This study demonstrated that under appropriate operating conditions, ozonation-ceramic membrane filtration could significantly improve the quality of waters with very different characteristics and reduce membrane fouling as compared to conventional filtration only. The permeate flux recovery was strongly affected by the water matrix constituents such as TOC and alkalinity. While the higher flux decline was observed from water with a higher TOC content, a greater flux recovery was observed from water with lower alkalinity. The former was attributed to the presence of carbonate ions which act as $^{\cdot}OH$ radical scavengers and to increase the ozone demand of the feed water. The concentration of model pharmaceuticals (dicloxacilline and ceftazidime) in the permeate was reduced to below the detection limits as a result of ozonation-membrane filtration in all three waters studied. Significant reductions in TOC, UV-254 absorbing compounds and DBP formation potential was also achieved. The EPA regulatory limit for TTHMs (80 µg/L) was met for all three waters. The concentration of HAAs compounds was reduced to below its regulatory limit of 60 µg/L in the Lake Huron and Huron River waters.

CHAPTER 6

RECOMMENDATIONS FOR FUTURE WORK

Surface characterization studies of sequentially ozonated/chlorinated nC$_{60}$ should be performed to validate the results obtained by our XPS. For example, infrared (IR) or Raman spectroscopy could be used as techniques have already been used to study the surface functionality of fullerenes [1]. Transmission electron microscopy (TEM) studies of the oxidized nC$_{60}$ aggregates should also be performed to gain a better understanding of the morphology of the formed particles.

Two model pharmaceuticals were successfully removed from surface waters as a result of the applied treatment. It was also shown that concentrations of disinfection by-products (TTHMs and HAAs) were significantly reduced below the EPA limits. However, given that tested pharmaceuticals contain various types of nitrogenous moieties (azo, amino, heterocyclic, etc) in their structure, a range of nitrogenous disinfection by-products (NDBPs) could be formed upon their reaction with ozone. NDBPs (e.g., halonitromethanes, cyanogen chloride, haloacetonitriles and haloamides) [2-6] were recently added to the U.S. EPA's Contaminant Candidate List [7]. N-nitrosodimethylamine (NDMA), a highly toxic compound, which has been found in municipal drinking waters [8], is formed during chlorination/chloramination [8, 9] and ozonation [10, 11] of natural water as a result of reaction of the oxidants with natural [8, 9] and synthetic [8, 10] organic constituents of the water. Halonitromethanes and haloacetonitriles were also found to be potent toxicants at concentrations three orders of magnitude smaller than that of US EPA-regulated trichloromethanes [5, 12]. Although NDMA is not regulated at the national level in any

country, California (USA) and Ontario (Canada) have set a public health goal and provisional maximum allowable concentration of NDMA at < 3 ng/L [13] and 9 ng/L [14], respectively. As many US drinking water utilities are switching from chlorination to chloramination [5] to comply with the Stage 2 Disinfectants/Disinfection Byproducts Rule, the concern with the formation of N-DBPs will further increase in importance. Therefore, this work should be completed by a comprehensive identification and quantification of the NDBPs formed as a result of ozonation of model pharmaceuticals. This will allow identification of the reaction pathways and aid in assesing the efficiency of the removal of organic molecules with structures, similar to the compounds used in this study.

BIBLIOGRAPHY

BIBLIOGRAPHY

1. Scharff, P.; Risch, K.; Carta-Abelmann, L.; Dmytruk, I.M.; Bilyi, M.M.; Golub, O.A.; Khavryuchenko, A.V.; Buzaneva, E.V.; Aksenov, V.L.; Avdeev, M.V.; Prylutskyy, Y.I. Structure of C_{60} in water: spectroscopic data. *Carbon* (2004), **42**, 1203-1206.

2. Mitch, W.A.; Schreiber, I.M. Degradation of Tertiary Alkylamines during Chlorination/Chloramination: Implications for Formation of Aldehydes, Nitriles, Halonitroalkanes, and Nitrosamines *Environmental Science and Technology* (2008), **42**:13, 4811-4817.

3. Krasner, S.W.; Weinberg, H.S.; Richardson, S.D.; Pastor, S.J.; Chinn, R.; Sclimenti, M.J.; Onstad, G.D.; Thruston Jr., A.D. The occurrence of a new generation of disinfection by-products. *Environmental Science and Technology* (2006), **40**, 7175–7185.

4. Weinberg, H.S.; Krasner, S.W.; Richardson, S.D.; Jr., A.D.T., *The occurrence of disinfection by-products (DBPs) of health concern in drinking water: results of a nationwide DBP occurrence study*, EPA/600/R02/068, Editor. 2002.

5. Plewa, M.J.; Muellner, M.G.; Richardson, S.D.; Fasano, F.; Buettner, K.M.; Woo, Y.-T.; McKague, A.B.; Wagner, E.D. Occurrence, synthesis, and mammalian cell cytotoxicity and cenotoxicity of haloacetamides: an emerging class of nitrogenous drinking water disinfection byproducts. *Environmental Science and Technology* (2008), **42**:3, 955-961.

6. Plewa, M.J.; Wagner, E.D.; Jazwierska, P.; Richardson, S.D.; Chen, P.H.; McKague, A.B. Halonitromethane drinking water disinfection byproducts: chemical characterization and mammalian cell cytotoxicity and genotoxicity. *Environmental Science and Technology* (2004), **38**, 62–68.

7. *US EPA, Contaminant Candidate List 3 (CCL 3)*. 2009, www.epa.gov/OGWDW/ccl/ccl3.html.

8. Gerecke, A.C.; Sedlak, D.L. Precursors of N-nitrosodimethylamine in natural waters. *Environmental Science and Technology* (2003), **37**, 1331–1336.

9. Lee, C.; Schmidt, C.; Yoon, J.; von Gunten, U. Oxidation of N-nitrosodimethylamine (NDMA) precursors with ozone and chlorine dioxide: kinetics and effect on NDMA formation potential. *Environmental Science and Technology* (2007), **41**, 2056–2063.

10. Andrzejewski, P.; Kasprzyk-Hordern, B.; Nawrocki, J. N-Nitrosodimethylamine (NDMA) formation during ozonation of dimethylamine containing water. *Water Research* (2008), **42**, 863-870.

11. Schmidt, C.K.; Brauch, H.J. N,N-Dimethylsulfamide as precursor for N-nitrosodimethylamine (NDMA) formation upon ozonation and its fate during drinking water treatment. *Environmental Science and Technology* (2008), **42**, 6340-6346.

12. Muellner, M.G.; Wagner, E.D.; McCalla, K.; Richardson, S.D.; Woo, Y.T.; Plewa, M.J. Haloacetonitriles vs. regulated haloacetic acids: are nitrogen-containing DBPs more toxic. *Environ. Sci. Technol.* (2007), **41**, 645–651.

13. *NDMA and other nitrosamines - drinking water issues. California Department of Public Health*. 2008, www.cdph.ca.gov/CERTLIC/DRINKINGWATER/Pages/NDMA.aspxN.

14. *Technical support document for Ontario Drinking Water Standards, objectives and guidelines. Ministry of the Environment of Ontario*. 2009, www.ene.gov.on.ca/envision/techdocs/4449e.htmN.

15. Fortner, J.D.; Kim, D.-I.; Boyd, A.M.; Falkner, J.C.; Moran, S.; Colvin, V.L.; Huges, J.B.; Kim, J.-H. Reaction of water-stable C_{60} aggregates with ozone. *Environmental Science and Technology* (2007), **41**, 7497-7502.

16. Castle, S.S.; Enna, S.J.; David, B.B., *Dicloxacillin*, in *xPharm: The Comprehensive Pharmacology Reference*. 2007, Elsevier: New York. 1-5.

17. Castle, S.S.; Enna, S.J.; David, B.B., *Ceftazidime*, in *xPharm: The Comprehensive Pharmacology Reference*. 2007, Elsevier: New York. 1-5.

18. Lyman, W.J.; Reehl, W.F.; Rosenblatt, D.H. Handbook of chemical property estimation methods. 1990, Washington, DC: American Chemical Society.

19. *EPI Suite software*, US EPA: www.epa.gov.

APPENDICES

APPENDIX A

Effective diameter and particle size distribution of nC_{60} aggregates

Stable nC_{60} suspensions were obtained, with no visual signs of precipitation over three months of observation. Particle size distribution of the parental nC_{60} suspension has one peak in intensity-weighted curve as determined by dynamic light scattering measurements (Figure A1) with the corresponding effective diameter of (188.8±0.8 nm). When nC_{60} suspensions were gradually ozonated in a batch reactor, the effective diameter of 25-75% oxidized suspensions increased slightly from (194±2 nm) to (197±2 nm) and decreased to (190±2 nm) when the highest ozone dosage was applied (Figure A2a). No relationship between the degree of oxidation and number of peaks in the intensity-weighted particle size distribution was observed as the ozonation proceeded. As shown in Figure A1, particle size distribution for the nC_{60} suspensions oxidized until 50% and 75% comprised one peak, whereas small second peaks at 47.5 and 74.0 nm appeared for 25% and 90% oxidized suspensions, respectively. Fortner et al [1] reported progressive decrease in the particle size of nC_{60} aggregates when the ozone CT value increased, likely due to disintegration of the derivatized nC_{60}. This is in agreement with our findings. Indeed, after ozonation derivatized nC_{60} aggregates would comprise a mixture of the as-prepared nC_{60} (which were detected by the dynamic light scattering technique) and its products (which we attributed to small peaks appeared in particle size distribution for 25% and 75% ozonated samples). Also, if disintegration with formation of molecular fullerene has occurred, the detection limit of Zeta Pals would not allow for its detection.

As it is shown in Figure A2a, when nC$_{60}$ suspensions were subjected to chlorination only and the sequential ozonation/chlorination procedure, it also did not lead to significant changes in the effective diameter of nC$_{60}$ aggregates, with suspensions chlorinated according to scheme 2B exhibiting slightly higher effective diameters as compared to that chlorinated according to scheme 2A. In a former case, effective diameter slightly increased from (194±1 nm) for chlorinated only suspension to (206± 2 nm) for 75% ozonated/chlorinated nC$_{60}$ suspensions and then decreased to (202 ± 2 nm) for 90% ozonated/chlorinated nC$_{60}$ suspensions. In a latter case, mean aggregate size gradually increased from (195±1 nm) for chlorinated only suspension to (202±2 nm) for 90% ozonated/chlorinated nC$_{60}$ suspensions. Second peak (approximately half of the intensity of the main peak) has appeared in the particle size distribution for suspensions consequently ozonated at 25 and 75 % and then chlorinated at chlorine dose of 6.8 mg (Cl_2)/L and allowed to react for 10 min (Figure A2). As opposite to the ozonated only suspensions, in this case second peaks corresponded to larger aggregates (355 and 420 nm, accordingly). One possible explanation to this is that derivatized nC$_{60}$ aggregates formed under these particular treatment, promoted aggregation of nC$_{60}$, thus favors formation of the less stable suspensions. However, nC$_{60}$ suspensions generated during treatment Scheme 2B, were found to be more stable, comprising of one peak (Figure A1). An additional peak of a smaller diameter (46.2 nm) observed for 75 % ozonated/chlorinated nC$_{60}$ suspensions could be attributed to byproducts from nC$_{60}$ ozonation.

Table A1. 10^{th} and 90^{th} percentiles of the intensity-weighted particle sizes of nC_{60} aggregates.

Ozonated only nC_{60} aggregates					
Degree of oxidation	*0*	*25*	*50*	*75*	*90*
d_{10}	159.6	184.9	133.4	154.9	186.3
d_{90}	208.2	245.7	316.2	238.3	222.1
nC_{60} aggregates ozonated and then chlorinated at a chlorine dose of 6.8 mg (Cl_2)/L and allowed to react for 10 min					
d_{10}	193.6	369.4	196.2	420	157.2
d_{90}	244.1	148.1	200	146.2	335.6
nC_{60} aggregates ozonated and then chlorinated at a chlorine dose of 6.8 mg (Cl_2)/L and allowed to react for 10 min					
d_{10}	161.9	163.7	153.8	193.6	170.6
d_{90}	260.6	203.5	215.7	240.1	265.4

Table A2. 10^{th} and 90^{th} percentiles of the number-weighted particle sizes of nC_{60} aggregates.

Ozonated only nC_{60} aggregates					
Degree of oxidation	*0*	*25*	*50*	*75*	*90*
d_{10}	151.3	44.2	100.0	134.1	70.8
d_{90}	204.6	51	177.8	206.4	80.8
nC_{60} aggregates ozonated and then chlorinated at a chlorine dose of 6.8 mg (Cl_2)/L and allowed to react for 10 min					
d_{10}	38.2	166.9	197.5	208.22	157.2
d_{90}	44.6	148.1	201.3	146.2	335.6
nC_{60} aggregates ozonated and then chlorinated at a chlorine dose of 6.8 mg (Cl_2)/L and allowed to react for 10 min					
d_{10}	138.2	152.3	153.8	43.0	162.4
d_{90}	222.4	202.08	215.7	49.7	234.8

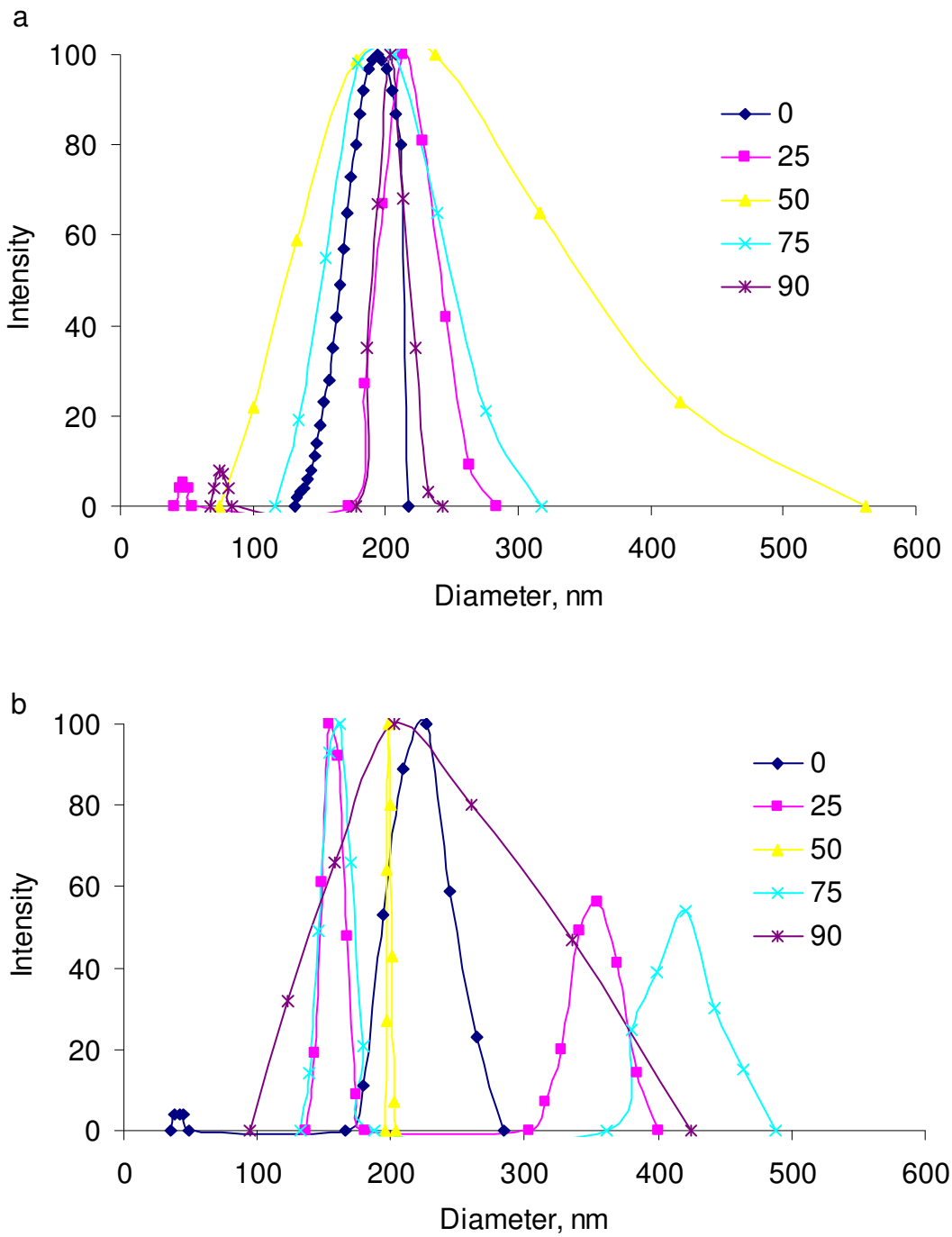

Figure A1. Intensity-weighted particle size distribution of nC$_{60}$ aggregates: (a) ozonated until the absorbance at 346 nm has decreased by 25, 50, 75 or 90%; (b) ozonated and then chlorinated at chlorine dose of 6.8 mg (Cl_2)/L and allowed to react for 10 min; (c) ozonated and then chlorinated at initial chlorine dose of 68 mg (Cl_2)/L and allowed to react for 10 min.

Figure A1 (cont'd).

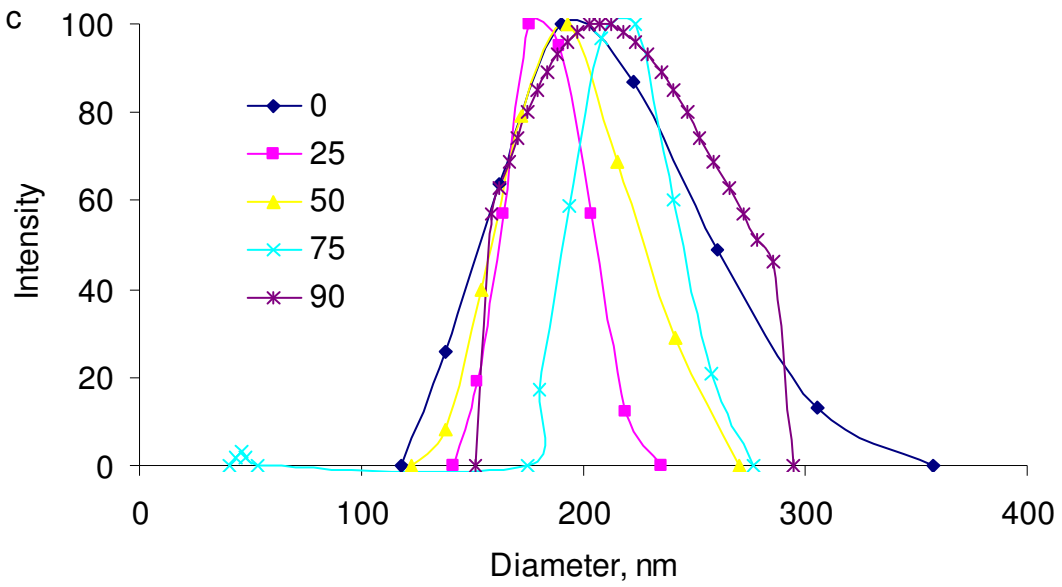

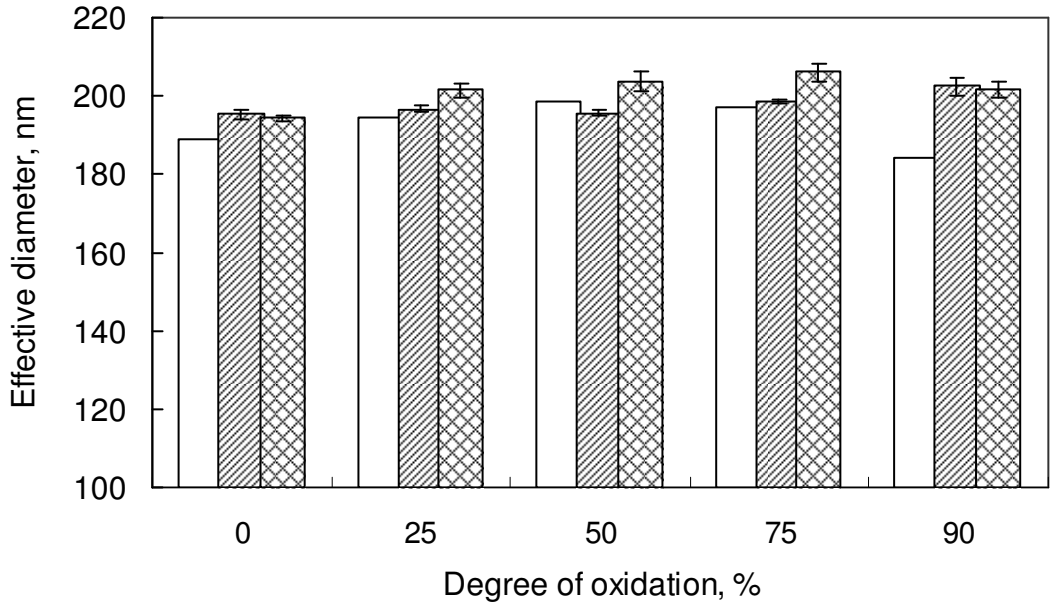

Figure A2. Effective diameter of nC$_{60}$ aggregates. Open bars correspond to suspensions ozonated until the absorbance at 346 nm has decreased by 25, 50, 75 or 90%; hatched bars correspond to suspensions ozonated and then chlorinated at a chlorine dose of 6.8 mg (Cl_2)/L and allowed to react for 10 min; cross-hatched bars correspond to suspensions ozonated and then chlorinated at a chlorine dose of 68 mg (Cl_2)/L and allowed to react for 10 min. Degree of oxidation is measured as a % decrease in the absorbance at 346 nm upon treatment with ozone.

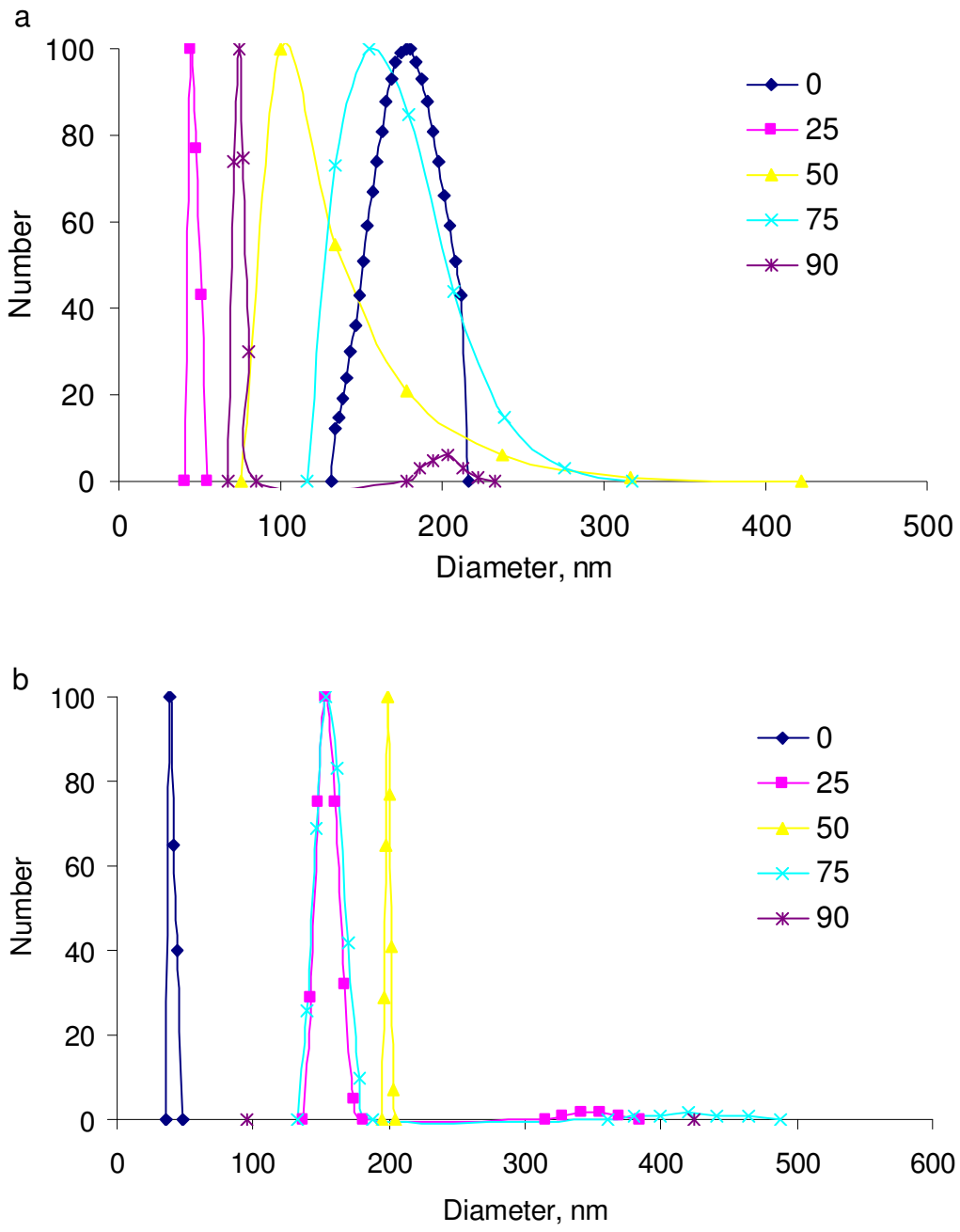

Figure A3. Number-weighted particle size distribution of nC$_{60}$ aggregates: (a) ozonated until the absorbance at 346 nm has decreased by 25, 50, 75 or 90%; (b) ozonated and then chlorinated at chlorine dose of 6.8 mg (Cl_2)/L and allowed to react for 10 min; (c) ozonated and then chlorinated at initial chlorine dose of 68 mg (Cl_2)/L and allowed to react for 10 min.

Figure A3 (cont'd).

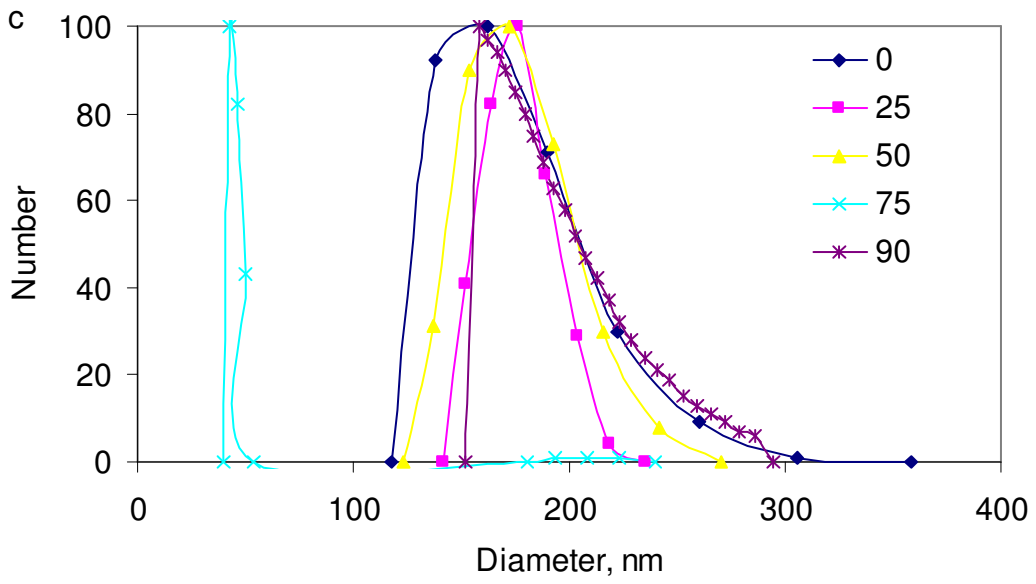

APPENDIX B

Removal of acetaminophen, diclofenac and mefenamic acid by hybrid ozonation-ceramic membrane filtration with 5kDa-20-500 manganese oxide coated ceramic membrane

Lake Lansing water was spiked with aliquot of freshly prepared stock of acetaminophen, diclofenac and mefenamic acid stock solutions to result in 1.5 mg/L of each pharmaceutical and subjected to ozonation-membrane filtration experiments with 5kDa-20-500 manganese oxide coated ceramic membrane with 0 and 10 g/m^3 of gas-phase ozone in a system which was described in details in Chapter 4. The details of membrane coating technique can be found elsewhere [2]. The operating conditions are shown in Table B1.

Table B1. Operating conditions of the hybrid ozonation-membrane filtration system.

Ozonation	
Ozone gas-phase concentration (mg/L):	10±0.5
Volumetric ozone-gas flow rate (mL/min):	10±0.5
Ozone inlet pressure (bar):	2.5±0.1
Membrane filtration	
TMP (bar):	2.1±0.1
Volumetric cross-flow rate (mL/min):	0.80±0.05
Temp. (^{o}C):	23±1
Feed volume (L):	1

The concentration of pharmaceuticals in the feed and permeate was measured by HPLC. The system consisted of Perkin Elmer Instruments (PEI) (Shelton, CT) Binary LC 250 pump, PEI Diode Array detector 235C, PEI series 200 autosampler and Discovery C18 HPLC column (25

cm x 4.6 mm, 5 µm) (Supelco, Bellefonte, PA). The HPLC operating conditions are listed in Table B2. The characteristics of these antibiotics are presented in Table B3.

Table B2. HPLC operating conditions.

Parameter	Acetominophen	Diclofenac	Mefenamic acid
Mobile phase	15% acetonitrile and 85% of 0.1% H_3PO_4	50% acetonitrile and 50% of 0.1% H_3PO_4	50% acetonitrile and 50% of 0.1% H_3PO_4
Flow rate (mL/min)	1	1	1
Detection wavelength (nm)	220	280	280
Injection volume (µL)	100	130	130
Retention time (min)	3.6	11.5	15.8
Run time (min)	6.5	25	25

The % removal of model pharmaceuticals in Lake Lansing water as a function of ozone dose is shown in Figure B1. The efficiency of pharmaceuticals removal was higher during ozonation-membrane filtration as compared to conventional filtration for all tested pharmaceuticals. The 99.90% removal of acetominophen, diclofenac and mefenamic acid was achieved at 10 g/m^3 of gas-phase ozone, while only 3.60, 10.88 and 13.15% of acetominophen, diclofenac and mefenamic acid were removed during conventional filtration with 5-20-50 ceramic membrane.

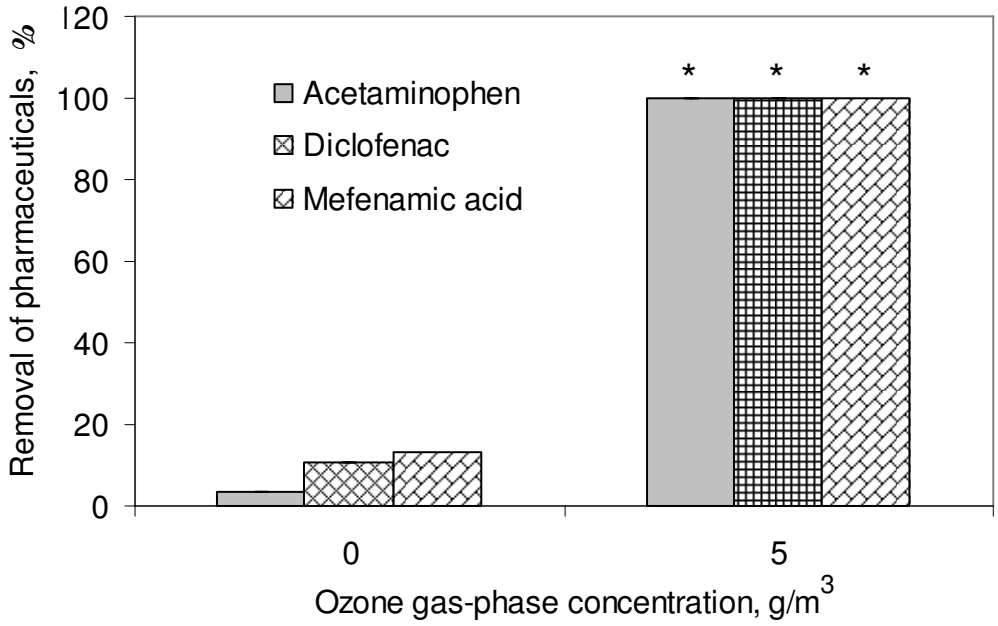

Figure B1. Effect of ozone gas-phase concentration on the removal of acetaminophen, diclofenac and mefenamic acid during hybrid ozonation-membrane filtration.

Table B3.Selected characteristics of acetaminophen, diclofenac and mefenafic acid.

Common name	Acetaminophen	Diclofenac	Mefenamic acid
Type	Non-steroidal anti-inflammatory drug	Non-steroidal anti-inflammatory drug	Non-steroidal anti-inflammatory drug
MW, g/mole	$C_8H_9NO_2$	$C_{14}H_{11}Cl_2NO_2$	$C_{15}H_{15}NO_2$
	151	296	241
[1]$\log K_{ow}$	0.46	4.51	5.12
[1]Water solubility at 25 ^{o}C, mg/L	3.035E+004	4.52	1.12
[1]Estimated % in effluent after Sewage Treatment	1.86	56.55	81.16

[1][3]

APPENDIX C

Elsevier license terms and conditions

This is a License Agreement between Alla Alpatova ("You") and Elsevier ("Elsevier") provided by Copyright Clearance Center ("CCC"). The license consists of your order details, the terms and conditions provided by Elsevier, and the payment terms and conditions.

Supplier	Elsevier Limited The Boulevard,Langford Lane Kidlington,Oxford,OX5 1GB,UK
Registered Company Number	1982084
Customer name	Alla Alpatova
Customer address	814L Cherry Lane East lansing, MI 48823
License number	2561310426845
License date	Dec 03, 2010
Licensed content publisher	Elsevier
Licensed content publication	Water Research
Licensed content title	Single-walled carbon nanotubes dispersed in aqueous media via non-covalent functionalization: Effect of dispersant on the stability, cytotoxicity, and epigenetic toxicity of nanotube suspensions
Licensed content author	Alla L. Alpatova, Wenqian Shan, Pavel Babica, Brad L. Upham, Adam R. Rogensues, Susan J. Masten, Edward Drown, Amar K. Mohanty, Evangelyn C. Alocilja, Volodymyr V. Tarabara
Licensed content date	January 2010
Licensed content volume number	44
Licensed content issue number	2
Number of pages	16
Start Page	505
End Page	520

Type of Use	reuse in a thesis/dissertation
Portion	full article
Format	both print and electronic
Are you the author of this Elsevier article?	Yes
Will you be translating?	No
Order reference number	
Title of your thesis/dissertation	Emerging contaminants: their availability, toxicity and removal by hybrid ozonation-membrane filtration
Expected completion date	Dec 2010
Estimated size (number of pages)	215

BIBLIOGRAPHY

BIBLIOGRAPHY

1. Fortner, J.D.; Kim, D.-I.; Boyd, A.M.; Falkner, J.C.; Moran, S.; Colvin, V.L.; Huges, J.B.; Kim, J.-H. Reaction of water-stable C_{60} aggregates with ozone. *Environmental Science and Technology* (2007), **41**, 7497-7502.

2. Corneal, L.M., *The use of MnO_2 coated ceramic membranes for combined catalytic ozonation and ultrafiltration for the control of natural organic matter (NOM) in drinking water*. 2010, PhD Dissertation, Michigan State University: East Lansing.

3. *EPI Suite software*, US EPA: www.epa.gov.